AEROSPACE NUCLEAR SAFETY

RESEARCH REPORT

RE-ENTRY FLIGHT DEMONSTRATION NO. 1 (RFD-1): OPTICAL DATA AND FUEL-ELEMENT EXPERIMENT

Department 7410

SC-RR-64-516
TID-4500 (35th Edition)
AEROSPACE SAFETY

SANDIA CORPORATION

PRIME CONTRACTOR TO THE
UNITED STATES ATOMIC
ENERGY COMMISSION
ALBUQUERQUE, NEW MEXICO
LIVERMORE, CALIFORNIA

TID-4500 (35th Edition)
AEROSPACE SAFETY

SC-RR-64-516

RE-ENTRY FLIGHT DEMONSTRATION NO. 1 (RFD-1): OPTICAL DATA AND FUEL-ELEMENT EXPERIMENT

Prepared By	Checked By	Approved By
I. B. White	H. E. Hansen - 7411	V. E. Blake - 7410
M. M. Robertson	I. B. White - 7411	Don B. Shuster - 7400
B. W. Marshall	A. J. Clark - 7412	
J. A. Allensworth	A. E. Bentz - 7413	
H. L. Ivy		

ABSTRACT

This report on the RFD-1 optical data and external fuel-element experiment includes a description of the instruments and test components used, a presentation of the data obtained, an explanation of the methods of data reduction employed, and a statement of the conclusions derived. It covers the theory, design, qualification tests, flight-test data, and results of the external fuel-element experiment. Also presented is a theoretical analysis of observed versus predicted ablation times and altitudes for the external fuel elements. In addition, this report presents recommendations for improvements to data acquisition and reduction methods in future, similar flight tests.

October 1964

ACKNOWLEDGMENT

In the acknowledgments carried in SC-RR-64-501 (listed in the Foreword), Sandia Corporation Department 7410, Aerospace Nuclear Safety Department, gratefully acknowledges the outstanding support of a large number of Sandia Corporation departments and outside agencies without whose help the RFD-1 flight and subsequent analysis could not have been performed. In addition to the support provided by these groups to the overall RFD-1 program, the authors would like to acknowledge the following Sandia Corporation departments who have contributed outstanding support to the work presented in this report:

Department Number	Department Name
1110	Materials and Process Department I
7220	Test Range Department
7240	Test Support Department
7620	Programming Department

Outside agencies who have contributed to the work presented in this report are acknowledged by specific references to their support throughout the text.

Issued by Sandia Corporation,
a prime contractor to the
United States Atomic Energy Commission

Printed in USA. Price $4.00. Available from the Clearinghouse for Federal Scientific and Technical Information, National Bureau of Standards, U. S. Department of Commerce, Springfield, Virginia

FOREWORD

Nuclear power supplies designed for use in space vehicles must incorporate safety features to preclude significant radiation hazards to the earth's population during orbital-decay re-entries or in the event of aborted missions. Sandia Corporation, a prime nuclear-weapon contractor to the AEC, has been authorized by the AEC Division of Reactor Development to act as the prime contractor for the independent safety evaluation of aerospace nuclear power systems. The Aerospace Nuclear Safety Program at Sandia includes research and development studies, ground testing, flight testing, system analysis, and independent safety assessment.

Re-entry Flight Demonstration Number One (RFD-1) was the first re-entry flight test conducted under this program since its inception in March 1962. The SNAP-10A (systems for nuclear auxiliary power) reactor, designed and constructed by Atomics International (AI), was selected for RFD-1 because of its proposed early use as a nuclear auxiliary power supply for earth satellites. An inert version of the SNAP-10A was flown on RFD-1 to determine the effectiveness of the safety design. The simulated reactor was mounted on a re-entry vehicle (RV) which was placed into the required trajectory by a four-stage Scout missile launched from the National Aeronautics and Space Administration (NASA) Wallops Station, Wallops, Island, Va.

Sandia carried out its assignment in the Aerospace Nuclear Safety Program by performing the following tasks:

1. Design of the flight-test experiment and the configuration of the simulated test reactor (STR), in cooperation with AI.
2. Study of the capabilities of the Scout launch vehicle, and recommendation of a trajectory which would assure that the desired information would be obtained.
3. Design of the RV and the telemetry (TM) system, and coordination of interface problems with AI, NASA, and Ling-Temco-Vought Corporation.
4. Theoretical predictions of flight-test outcomes.
5. Preparation of documents on support requirements for the Atlantic Missile Range (AMR) and the NASA Wallops and Bermuda stations.
6. Provision of complementary downrange instrumentation for the collection of TM and optical data.
7. Management of flight-implementation activities.
8. Data reduction and analysis.
9. Comparison of flight-test results with theoretical calculations.

The following Sandia Corporation reports, together with the present volume, comprise the final documentation of RFD-1:

Report No.	Title
SC-RR-64-501	Re-entry Flight Demonstration Number One (RFD-1): Final Flight-Test Plan
SC-RR-64-502	Re-entry Flight Demonstration Number One (RFD-1): Data Book
SC-RR-64-510	Re-entry Flight Demonstration Number One (RFD-1): Comparison of the Preflight and Observed Trajectories
SC-RR-64-511	Re-entry Flight Demonstration Number One (RFD-1): Design, Development, and Performance of the Re-entry Vehicle
SC-RR-64-515	Re-entry Flight Demonstration Number One (RFD-1): Preflight Disassembly Analysis and Observed Disassembly of the Simulated SNAP-10A Reactor
SC-RR-64-517	Re-entry Flight Demonstration Number One (RFD-1): Atmospheric Sciences Support

TABLE OF CONTENTS

LIST OF ILLUSTRATIONS

LIST OF ILLUSTRATIONS (cont.)

LIST OF ILLUSTRATIONS (cont.)

LIST OF TABLES

LIST OF ABBREVIATIONS

RFD-1	Re-entry Flight Demonstration Number One
AI	Atomics International
SNAP	Systems for Nuclear Auxiliary Power
RV	Re-entry Vehicle
NASA	National Aeronautics and Space Administration
STR	Simulated Test Reactor
TM	Telemetry
AMR	Atlantic Missile Range
UZrH	Uranium-Zirconium Hydride
AFSWC	Air Force Special Weapons Command
TACODA	Target Coordinate Data
TRSS	Time-Resolved Streak Spectrograph
BRT	Bermuda Range Time
W/C_DA	Ballistic Coefficient
RS	Re-entry System

RE-ENTRY FLIGHT DEMONSTRATION NO. 1 (RFD-1): OPTICAL DATA AND FUEL-ELEMENT EXPERIMENT

SECTION I -- INTRODUCTION AND SUMMARY

Introduction

SNAP-10A is a 500-watt electrical power supply designed for use in space vehicles. Heat to operate the power supply is provided by a 30-kw nuclear reactor. After normal operation of the SNAP-10A in space, the reactor fuel elements will contain long-lived fission products. These products could pose a radiation hazard if a space vehicle carrying a SNAP-10A reactor were to re-enter the earth's atmosphere before they had decayed to a relatively harmless level. Since the orbital life of a space vehicle cannot be predicted with surety before launch, the possibility of re-entry at any time after launch must be considered. It is therefore necessary to ensure that the reactor fuel elements will be disposed of in such a manner that no radiation hazard will result. One method proposed to ensure safe disposal is to use re-entry heating to disassemble the reactor and burn up the fuel elements thus exposed; atmospheric diffusion and high-altitude winds would then disperse the resulting debris widely enough so that no radiation hazard would be posed.

In May 1963, Sandia conducted the RFD-1 flight test to investigate the effectiveness of this method. A flight test was necessary because it is not possible to exactly simulate the orbital-decay re-entry environment in laboratory experiments. The main objectives of RFD-1 were to evaluate reactor disassembly and fuel-element burnup (particle size and dispersion are being investigated separately). Other objectives included the confirmation of analytical techniques for predicting re-entry phenomena, and the development of optical and electronic instrumentation for use in future flight tests.

In the fuel-element experiment, four groups of simulated fuel elements, or rods, were simultaneously ejected from the RFD-1 RV early in re-entry. Each rod consisted essentially of a core of tracer material surrounded by a uranium-zirconium-hydride (UZrH) wall, with the UZrH in turn covered by a 15-mil cladding of Hastelloy N. During re-entry, the times and altitudes of rod burnup were optically recorded, using spectrographic analysis to identify each group of rods, and the results were compared with the computed heat inputs for the RFD-1 trajectory.

This report presents the conclusions drawn concerning the data recorded and the probable fate of the groups of fuel rods. It also presents recommendations, drawn on the basis of these conclusions, for modifications and refinements to existing instrumentation and to present methods of data acquisition and reduction for application in future flight tests.

Summary

Re-entry of the RV, the reactor, and the simulated tracer-loaded fuel rods was photographed with 61 cameras, including plate, spectral, and framing types. Twenty cameras were located at High Point, Bermuda, and forty-one were airborne in aircraft provided by NASA and the Air Force Special Weapons Command (AFSWC).

Many of the films were underexposed because of the distances involved and the effects of atmospheric attenuation. However, much information was extracted from the films and other records obtained, permitting valid conclusions to be drawn about the re-entry events and the degree to which the test objectives were achieved. Data from the plate, spectral, and framing cameras were reduced by individual type, and all the results were then correlated to confirm agreement of the conclusions.

The re-entry was first visible 325.40 seconds after launch, when the RV was at an altitude of 266,000 feet. Melting and disassembly of the reactor were evident on all the films which viewed its re-entry. Information on these observations was used in the analysis of reactor disassembly (see SC-RR-64-515).

All of the rods for the fuel-element experiment were 1.25 inches in diameter and 12.25 inches long. The tracer materials and UZrH wall thicknesses for each group of rods were as follows:

Group	UZrH Wall Thickness (in.)	Tracer
1	0.101	Strontium
2	0.184	Barium
3	0.306	Silver
4	0.406	Gold

The strontium-loaded rods were visible from 342.27 seconds after launch (220,100 feet) to 363.32 seconds (161,400 feet). It is believed that they were completely consumed at this altitude. Theoretical predictions based on laboratory data indicated that, for the heat inputs from the RFD-1 trajectory, complete burnup should have occurred at 364.30 seconds (158,000 feet). This close agreement was within the accuracy expected of the RFD-1 test.

The barium-loaded rods were visible from 348.00 seconds (205,200 feet) to 371.50 seconds (142,000 feet), at which time they are believed to have been completely consumed. Again, theoretical predictions agreed closely with the flight-test results; predicted burnup was at 374.60 seconds (135,000 feet).

The trails of the silver- and gold-loaded rods were identified, but no evidence of the silver or gold tracers was found on any of the films. Presumably, neither of these rod groups ablated enough to expose the tracers. This was as predicted in both the preflight and postflight analyses of the test.

SECTION II -- DESCRIPTION OF THE TEST PROGRAM

SC-RR-64-501 describes the complete flight-test plan as it was drawn up before the test. The discussion in this section will also cover the flight-test plan, but it will be more general in the areas of the RV, the reactor, and the trajectories, and more specific in the areas of the optical instrumentation, the optical data, and the fuel-element experiment.

SNAP-10A System

Figure 1 shows the SNAP-10A. A comprehensive discussion of the system appears in SC-RR-64-515; the principal system components are:

1. A core vessel housing 37 UZrH fuel elements which provide heat to operate the system.
2. Four beryllium reflectors to control the nuclear reaction.
3. A conical radiator which houses the thermoelectric conversion elements and also houses the tubes which carry a eutectic mixture of sodium and potassium (NaK-78) used to transfer heat from the reactor core to the thermoelectric junctions.
4. A pump to circulate the NaK-78 through the system.

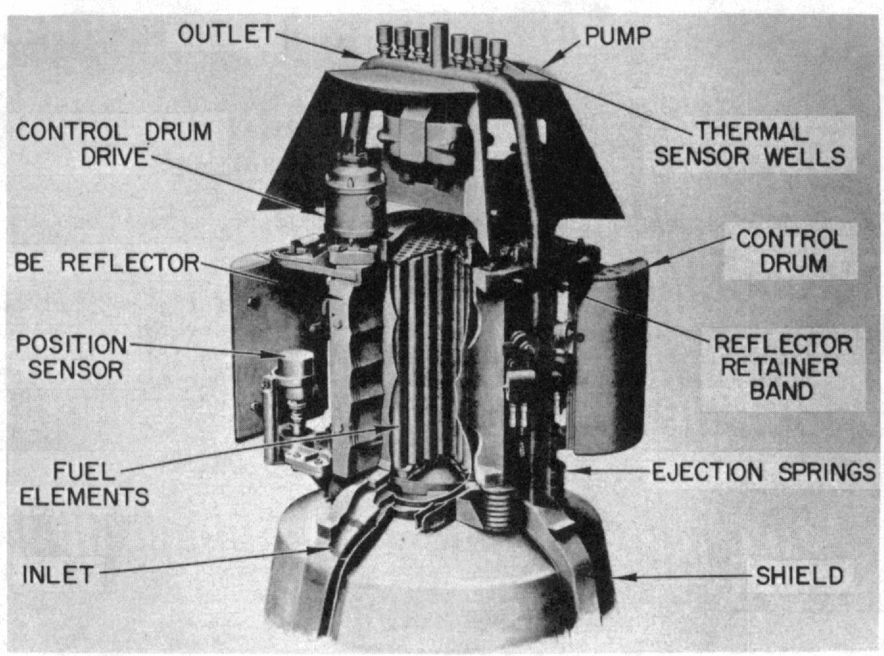

Figure 1. SNAP-10A reactor

The proposed design of the SNAP-10A includes features to promote disassembly of the reactor under re-entry heating, and consequent exposure of the rods. The steps in disassembly (Figure 2) are:

1. Melting of fusible links in a band which holds the reflectors in place on the reactor, and subsequent separation of the band.
2. Spring ejection of the reflectors.
3. Burn-off of the NaK pump.
4. Melting of the lip weld which holds the lid of the reactor core vessel in place, and subsequent separation of the lid.
5. Expulsion of the fuel elements from the core vessel through the effects of aerodynamic drag forces on the reactor.

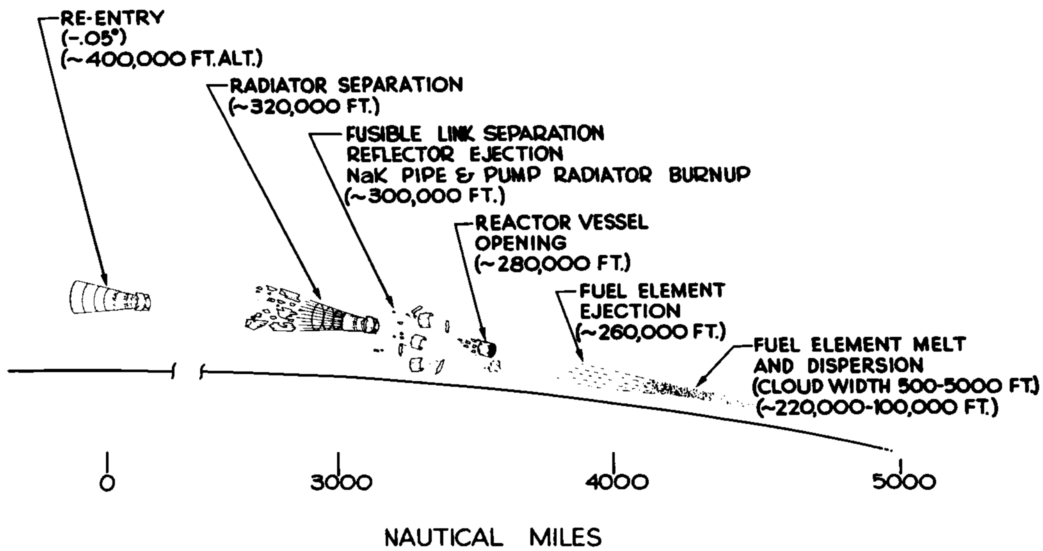

Figure 2. SNAP-10A desired orbital-decay re-entry sequence

If this sequence of events results in exposure of the rods at an altitude sufficiently high, the rods will be subjected to considerable aerodynamic heating. Assuming the requisite heat input, the rods will melt, ablate into small particles, and disperse in the atmosphere over a wide area. If adequate dilution of the particles containing fission products is achieved, their potential for offering a radiation hazard will be eliminated.

Test Objectives

Reactor Disassembly

One objective of RFD-1 was to provide information on the disassembly sequence of the SNAP-10A so that the current design could be evaluated. Because of the payload limitation of the Scout launch vehicle, some deviations from the actual SNAP-10A design were required in the STR to reduce its weight; these included the substitution of lighter, aluminum reflectors for the beryllium reflectors actually used in the SNAP-10A, and omission of the fuel elements from inside the reactor core vessel, as well as other, minor changes. It is not expected that these deviations affected the results of the experiment appreciably. Reactor disassembly is covered comprehensively in SC-RR-64-515.

Fuel-Element Ablation

Knowledge of the response of UZrH to an environment of re-entry into the atmosphere is very limited. Calculations indicate that, in an orbital-decay re-entry, aerodynamic heating alone may be insufficient to assure complete ablation of the fuel elements. However, the available heat input could be augmented by the exothermic chemical reactions of UZrH with the re-entry atmosphere. Conversely, if a hard oxide layer is formed on the surface of UZrH fuel elements, as it frequently does on specimens heat-tested in the laboratory, this phenomenon may retard ablation. Since exact simulation of the re-entry environment is not possible in laboratory experiments, it was decided to investigate the ablation of UZrH fuel elements on RFD-1.

The objectives of the fuel-element experiment were:

1. To obtain data, for UZrH in general and the SNAP-10A fuel rods in particular, on ablation rate and on the volume consumed by burnup during re-entry.
2. To confirm theoretical calculations and laboratory data pertaining to re-entry ablation.
3. To evaluate optical instrumentation and data-reduction techniques for use in future flight tests.

Complete ablation of the re-entering fuel elements is not absolute proof that radiation hazards will be eliminated, since adequate dispersion of the resulting debris in the atmosphere is also necessary. However, the collection of ablation particles was not compatible with the other objectives of RFD-1, so future flight tests may be required for this purpose. Both analytical and laboratory investigations of particle sizes and dispersion are currently under way.

Fuel-Element Experiment

Concept

The experimental concept was to simultaneously eject four groups of three tracer-loaded, simulated fuel rods each from the RFD-1 RV early in re-entry, and record their burnup with spectral, plate, and motion-picture cameras. In normal operation, of course, the fuel rods would be carried within the reactor core vessel, and released as a consequence of reactor disassembly. For RFD-1, however, the rods were ejected from an external mounting, since calculations indicated that melting of the lip weld securing the core-vessel cover, which must separate from the vessel before the rods can be released, would occur too late in the trajectory for the rods to be exposed to the desired maximum heating.

The construction of the tracer-loaded rods, with varying thicknesses of UZrH surrounding the tracer material, has already been noted. Since all the rods should follow the same trajectory and therefore experience essentially the same heating, the UZrH should ablate away first from the group with the thinnest UZrH wall, exposing the tracer material contained in that group. The tracer element should then flare, emitting radiation characteristic of that particular material. Because of the different wall thickness of UZrH in the four groups, each tracer element should flare at a different time and altitude. Comparison between the volume of UZrH consumed and the calculated heating for the trajectory should then provide indications of the rate and volume of ablation versus re-entry heating.

Fuel-Rod Design

Figure 3 shows a cutaway view of a normal SNAP-10A fuel element. Figures 4 through 7 are cutaways of the tracer-loaded, simulated fuel rods used for the RFD-1 fuel-element experiment. Configurations of the tracer-loaded rods were dictated largely by the physical and mechanical properties of the materials included. Since UZrH is extremely brittle, the minimum wall thickness that would be machined without fracturing the rod was 0.100 inch. Conversely, it was surmised that a minimum of 0.300 cubic inch of tracer material would be necessary to permit spectral observation at ranges of 100 to 200 miles. The void required to accommodate this amount of tracer material and its insulation limited the maximum wall thickness of UZrH to 0.406 inch. One group of rods was made with the minimum thickness, and one group with the maximum; wall thicknesses of the remaining two groups were spaced about equally between these extremes. Wall thicknesses for the four groups were 0.101, 0.184, 0.306, and 0.406 inch, resulting in volume ratios of 1.00, 1.65, 2.45, and 2.92, respectively. Since predictions indicated that only a small volume of fuel element would be consumed during the RFD-1 re-entry, these ratios were considered to be near optimum. Table I lists the weights and volumes of principal materials in each group of rods, and Figure 8 shows the 12 tracer-loaded rods flown on RFD-1.

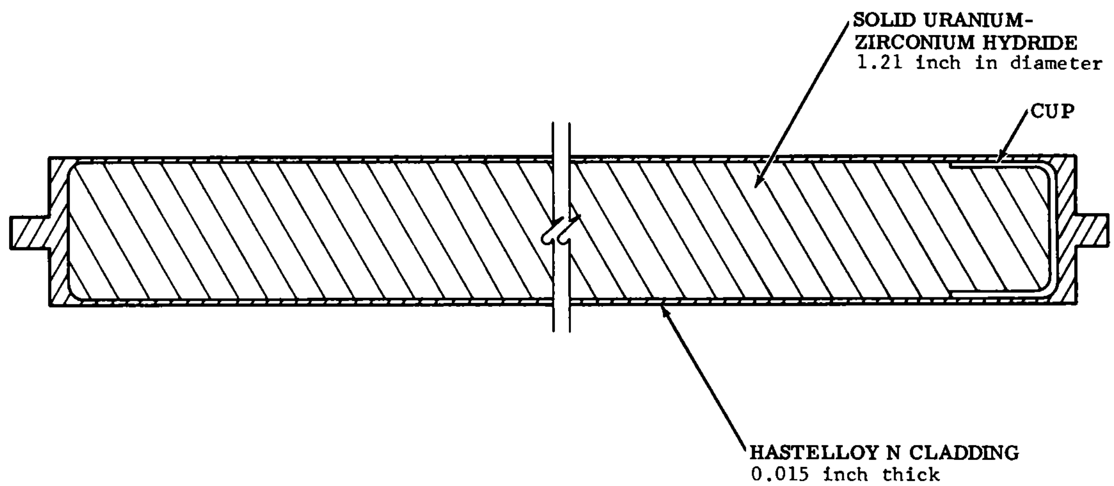

Figure 3. SNAP-10A fuel rod

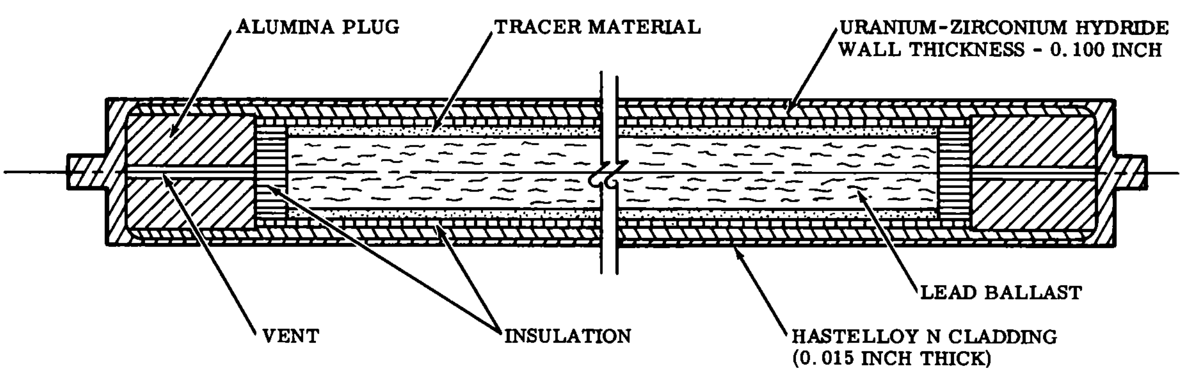

Figure 4. SNAP-10A fuel rod with strontium tracer

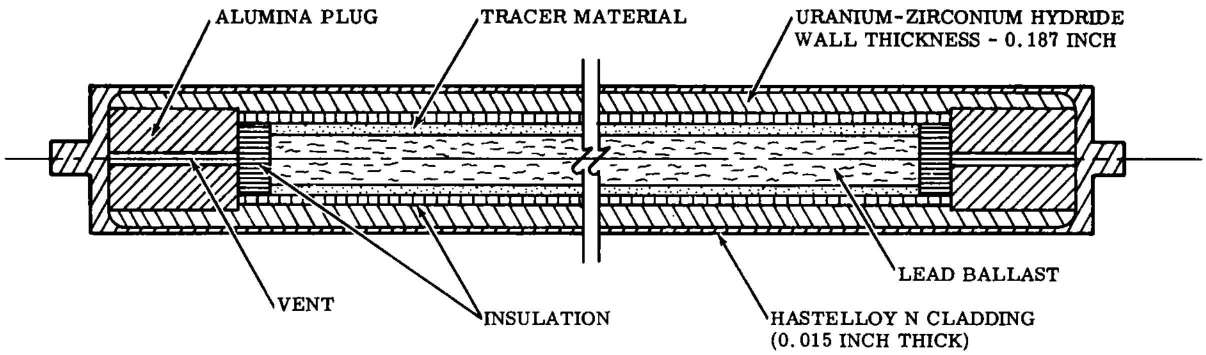

Figure 5. SNAP-10A fuel rod with barium tracer

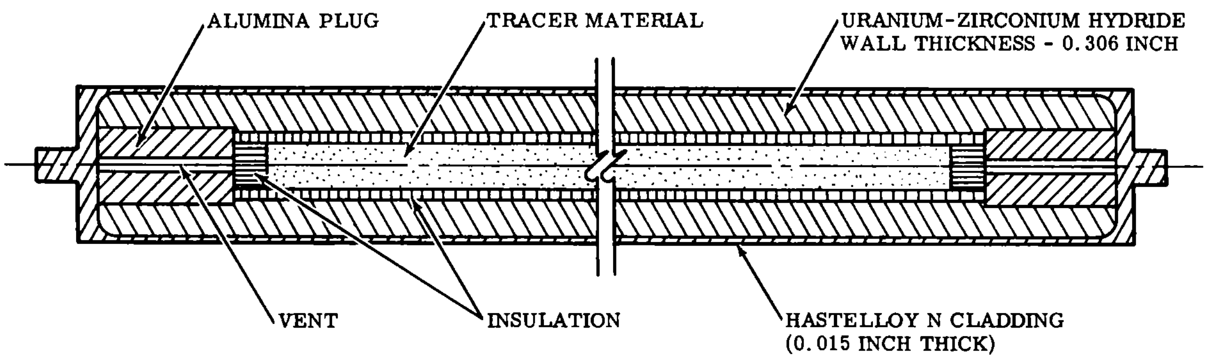

Figure 6. SNAP-10A fuel rod with silver tracer

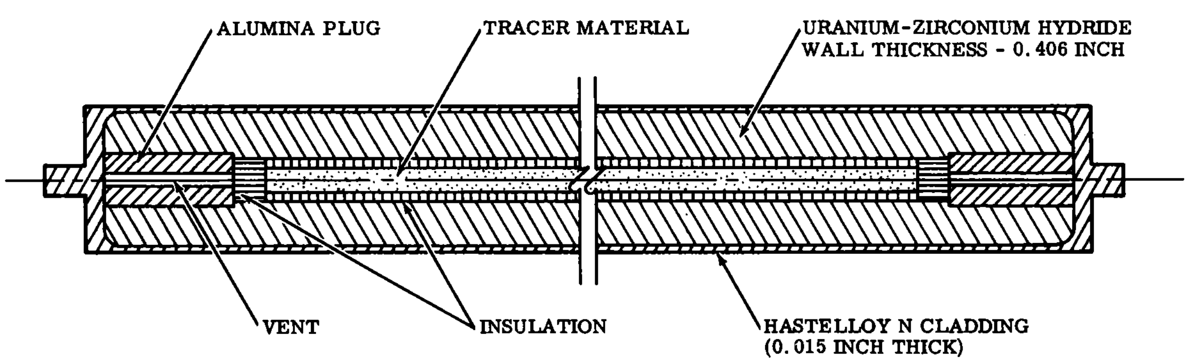

Figure 7. SNAP-10A fuel rod with gold tracer

TABLE I

RFD-1 Tracer-Loaded Fuel Rods

Group No.	Tracer			UZrH		Cladding		Lead Ballast		Total Weight (lb)	Ballistic Coefficient, W/C_DA (lb/ft^2)
	Material	Weight (lb)	Volume (in.^{3})	Weight (lb)	Volume (in.^{3})	Weight (lb)	Volume (in.^{3})	Weight (lb)	Volume (in.^{3})		
1	Strontium	0.205	1.965	0.955	4.30	0.336	0.982	1.040	2.550	*2.812	43.70
2	Barium	0.217	1.526	1.543	7.10	0.325	0.982	0.577	1.394	*2.864	44.40
3	Silver	0.426	1.132	2.311	10.59	0.326	0.982	--	--	*3.160	49.10
4	Gold	0.203	0.287	2.731	12.25	0.327	0.982	--	--	*3.294	51.10
SNAP-10A	--	--	--	3.140	14.17	0.329	0.982	--	--	3.469	53.90

*Includes insulation and alumina end plugs.

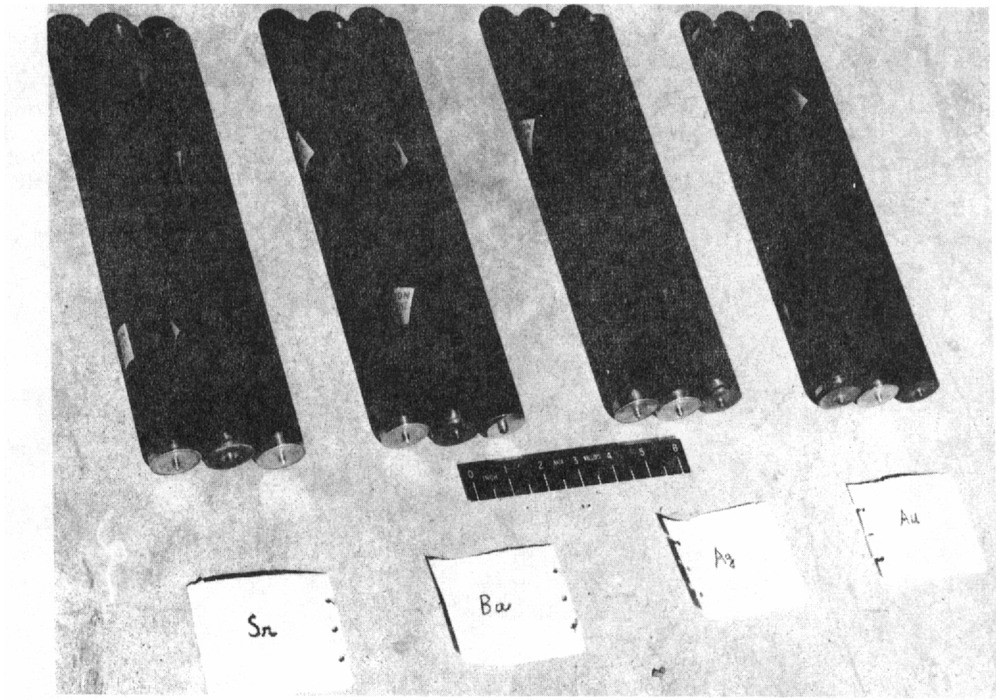

Figure 8. Full complement of tracer-loaded fuel rods for RFD-1 external fuel-element experiment

The four tracer elements, strontium, barium, silver, and gold, were selected because of their intense and easily identified spectral characteristics. (Figures 35, 36, 37, and 38 show the wave lengths and intensities of the various tracers.)

Calculations indicated that insulation would be necessary to delay melting of the tracers as long as possible during ablation of the fuel elements. Insulation would also help to maintain the pressure of the tracer vapor at a low level. (A high pressure would have ruptured the rod walls and exposed the tracers, giving a premature indication of ablation.) Fiberfrax insulation (51% AlO_3, 47% SiO_2) was used because of its high melting point (3300°F) and relatively good insulating properties. In addition to the insulation, a small vent hole was provided in each end of the rod to ensure against pressure build-up.

To ensure that all of the fuel rods received essentially the same heat input, it was necessary that they follow essentially the same trajectory. This meant that all 12 rods had to have a nearly identical W/C_DA. Since the density of strontium and barium is much lower than that of silver, gold, and UZrH, lead ballast was inserted into the centers of the rods containing strontium and barium tracers.

The brittleness of UZrH made it impossible to machine screw threads in the fuel elements for end plugs to contain the tracers. Accordingly, after the tracers and insulation had been inserted into the rods, alumina ceramic was sprayed into the ends to form a plug.

Hastelloy N cladding with a thin, internal coating of ceramic barrier material, as used on the actual SNAP-10A fuel rods, was included on the experimental fuel rods. Preflight calculations indicated that, since this cladding is only 0.015 inch thick, it would melt away early in the re-entry.

Fuel-Rod Mounting and Ejection

The 12 tracer-loaded fuel-rods were mounted externally on the RV in four groups of 3 rods each, with each group 90 degrees from the next (Figure 9). The mounting brackets were designed to release all 12 rods simultaneously 282 seconds after launch, at an altitude of 350,000 feet. Release was effected by detonating explosive bolts, which were initiated by signals programmed through a timer in the RFD-1 TM system. Immediately after rod release, the wires which held the mounting brackets in place were severed by an explosively actuated cutter, permitting all the bracket hardware to fall free of the RV.

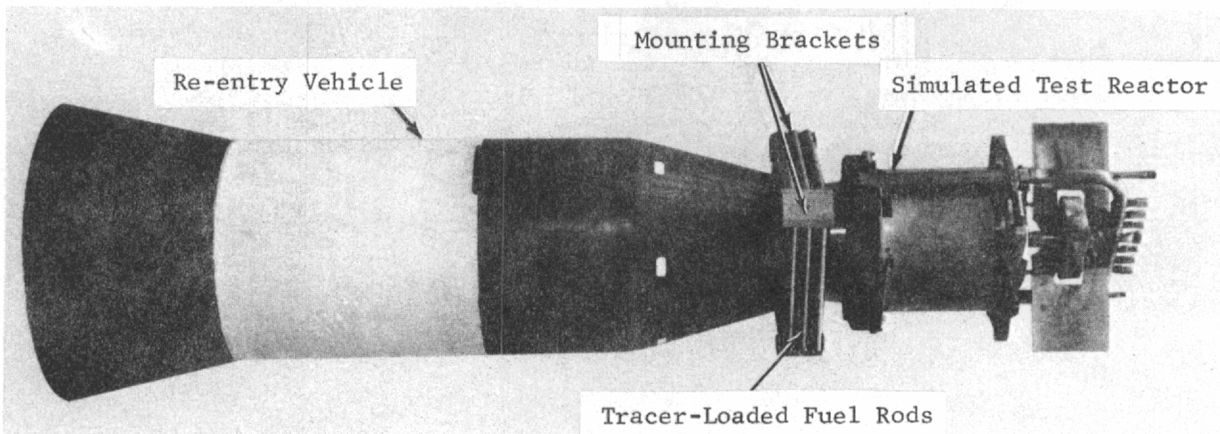

Figure 9. RFD-1 re-entry vehicle

Structural and Functional Tests

Before the RFD-1 flight test, a series of qualification tests was conducted on both the RV and the fuel rods. Tests concerning the fuel rods are described briefly below.

Shock, Vibration, Acceleration, and Balance -- The RV was subjected to sinusoidal and random vibration, linear acceleration, shock, and a test for spin balance. In each of these tests, a set of the experimental fuel rods was mounted on the RV. The rods, which were radiographed before and after testing, suffered no observable detrimental effects as a result of any of the tests.

Ejection -- During development of the fuel-rod brackets, a series of tests was conducted to monitor their performance. Dummy fuel rods were mounted in the brackets, which were in turn mounted on a simulated RV cone (Figure 10A). This assembly was spun at the predicted RV spin rate of 150 rpm. The explosive bolts were then detonated, releasing the entire bracket mechanism and the dummy fuel rods. As a result of centrifugal force, the fuel rods and bracket components accelerated away from the simulated RV cone. Cameras mounted above the assembly photographed the entire sequence of events (Figure 10B). On the basis of comparison between distance traveled and time (both measured from the film), a history of ejection velocity and of the direction in which the fuel rods and brackets traveled was determined. This information was used in trajectory predictions, both before and after the flight test.

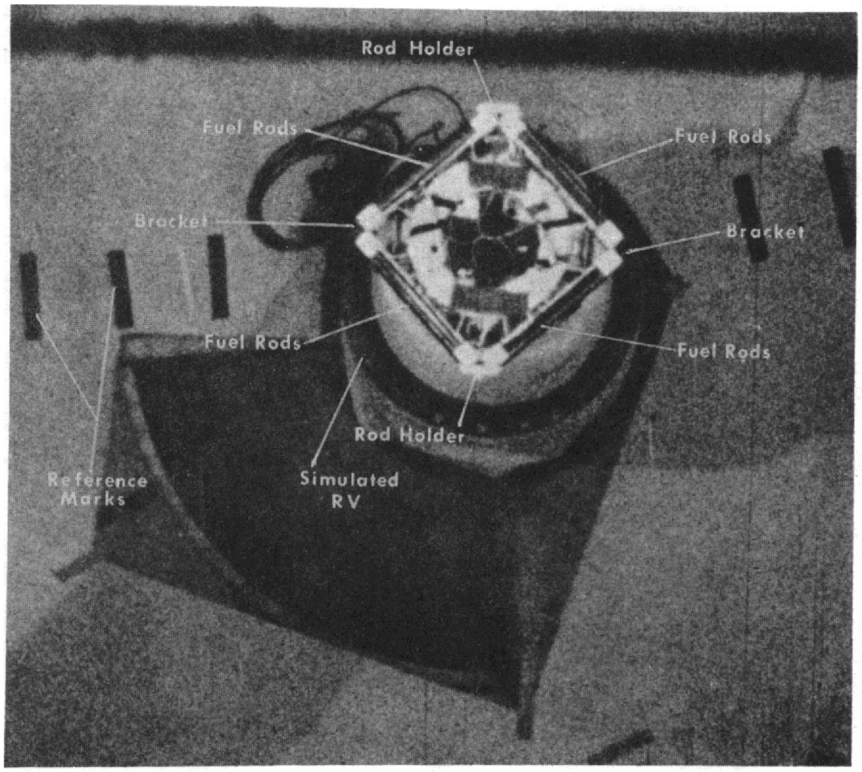

(A) Before ejection

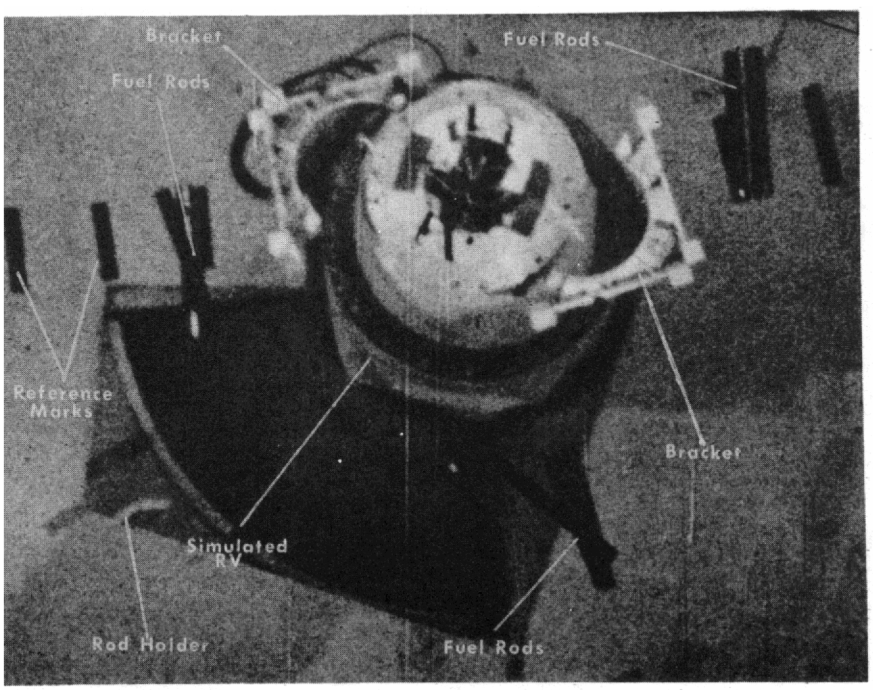

(B) At ejection

Figure 10. Ejection test of fuel rods for RFD-1 external fuel-element experiment

Qualification and Ablation Tests

The tracer-loaded fuel rods were extensively modified from the normal SNAP-10A fuel elements, giving the rods physical properties quite different from those of the normal fuel elements. Machining the cavities for the tracer materials reduced the strength of the rods, and inclusion of the tracer materials and insulation disrupted the normal heat-transfer pattern of the UZrH fuel element. In addition, an internal pressure build-up caused by tracer vapor was possible. Since the possible consequences of these deviations were not obvious, a series of tests was conducted in a 1-megawatt, electric-arc tunnel. Two-inch-long test specimens simulating the experimental designs and materials except for length and deletion of the external cladding were subjected to the predicted re-entry heat input pressure and enthalpy. Figure 11 is a cutaway view of a typical test specimen. (Specimens of actual SNAP-10A fuel elements were also tested for comparison.) The support rod was inserted in a rotating mechanism and rotated about its longitudinal axis at 2.4 rps. This procedure simulated the tumbling re-entry of a cylinder as closely as was possible, and distributed the heating around the cylinder circumference.

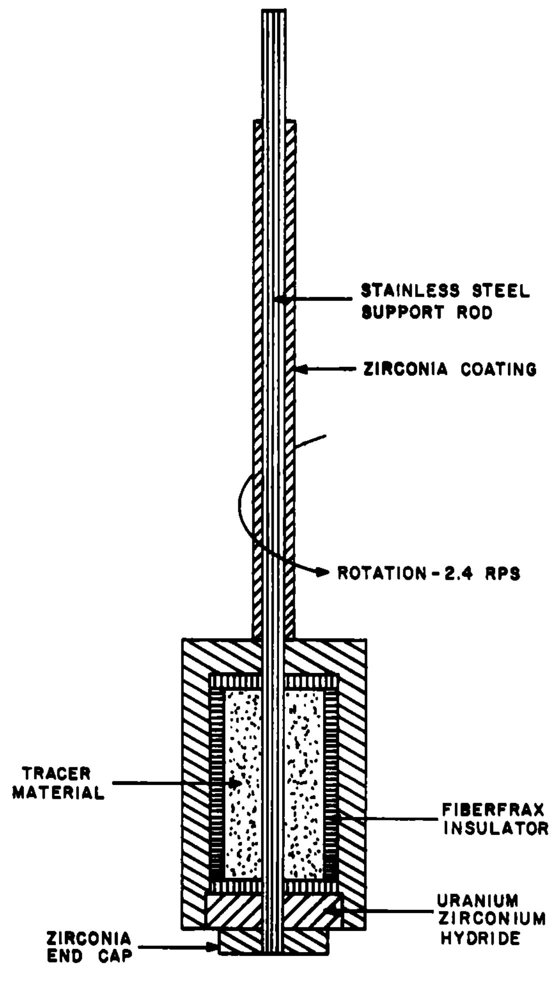

Figure 11. Tracer-loaded fuel-rod specimen for tests in the electric-arc tunnel

The objectives of these tests were:

1. To ascertain the structural integrity of the tracer-loaded fuel rods under the RFD-1 re-entry environment.

2. To observe the mode of fuel-rod ablation and tracer exposure.

3. To establish factors to be used in interpreting the flight-test data, including extrapolation from experimental to actual (SNAP-10A) fuel-element ablation, and extrapolation from the RFD-1 trajectory to an orbital-decay trajectory.

4. To verify and record the spectral characteristics of the tracer materials.

5. To test the operation of the spectral and event cameras to be used in the test flight.

Figures 12A and 12B show typical tests. Figure 12A shows fuel-rod ablation and the flare of the strontium tracer. Figure 12B shows the flare from the barium tracer. The marked difference in color of the two flares may be seen in color photoprints on file in Sandia Division 7411. This phenomenon was used to aid in identifying the fuel elements during data evaluation. Results of the tests and the conclusions derived were:

1. Design of the specimens was acceptable, although minor modifications to the end caps were shown to be necessary. No serious structural defects were observed.

2. The mode of fuel-rod ablation and tracer exposure was not uniform. In all cases, the UZrH developed "hot spots" and ablated at these hot areas. This was especially true where flaws such as scratches or cracks were present in the UZrH; eventually a hole (or holes) would ablate through the UZrH in the flawed area and expose the tracer material. As ablation continued, the tracer would flare through the holes in a pulsating pattern (depending on its orientation relative to the jet).

   Some of this problem of nonuniform ablation was caused by attenuation of the jet temperature from the center to the outer circumference. It was surmised that during re-entry, heating would be more evenly distributed over the entire surface of the fuel rod, and that these effects would therefore be somewhat reduced. Ideally, all of the UZrH would have ablated away before the tracers were exposed. Since this was not possible, the observed mode of tracer exposure was considered in interpretation of the RFD-1 data.

3. Little difference was noted between the BTU/lb required to ablate the test specimens and that required to ablate solid SNAP-10A fuel elements. Inclusion of the tracer materials and insulation appeared to have a negligible effect on the total ablation of the rods.

4. The record of spectral characteristics of the tracers was satisfactory. These films were used for comparison with the flight-test films to evaluate results.

The heat inputs and pressure required to ablate the fuel elements were used for both preflight predictions and postflight analysis. (See Section IV of this report, and also SCDR 124-63, RFD-1 Fuel Rod Qualification Tests - Phase I, which presents details of the tests described above, including methods of analysis and results.)

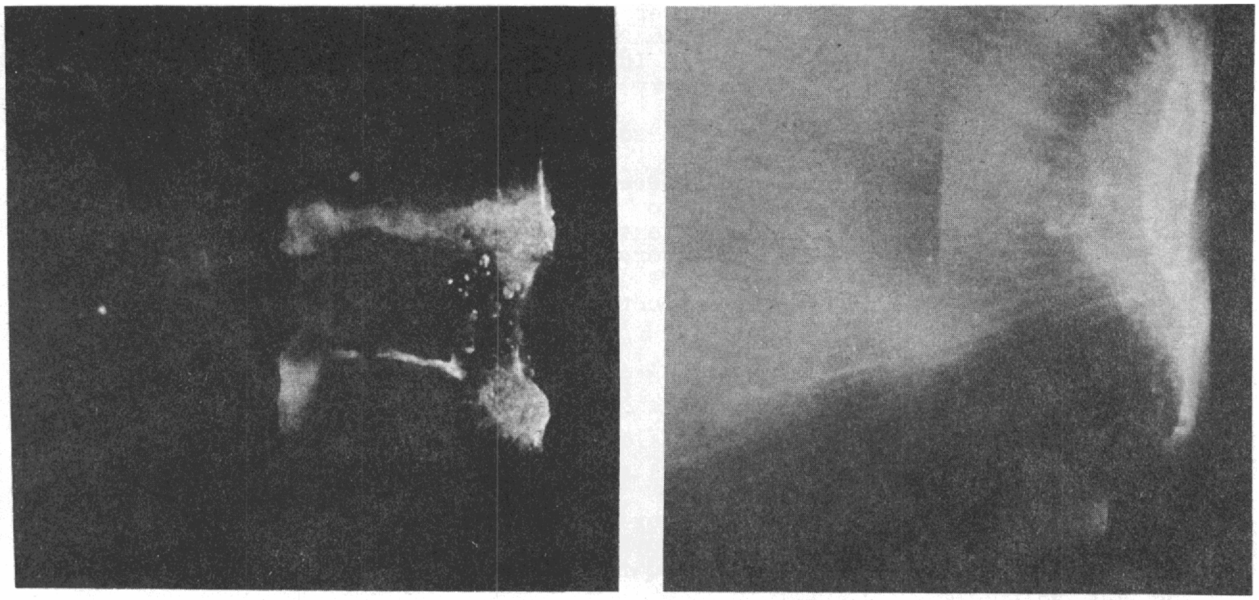

(A) Strontium-loaded UZrH test (B) Barium-loaded UZrH test

Figure 12. RFD-1 fuel-rod ablation and qualification tests in electric-arc tunnel

Preflight Predictions

Data from fuel-rod qualification tests conducted in the hyperthermal tunnel were used as the basis for calculating predictions of burnup in the flight test. Since the tunnel can produce only a constant-flow condition (as opposed to the pulse profile of heating generated in an actual re-entry), the predictions were made from considerations of total heat input. Justification for this type of analysis is the fact that present computer programs are not able to describe adequately the real effects of surface oxidation, combustion, and hydrogen diffusion on rod heating and temperature response. Work to develop such a program is in progress, but in the meantime only gross effects can be considered.

The SNAP-000439 theoretical trajectory and heating curve was used as the basis for the preflight predictions. This theoretical trajectory assumed a higher re-entry velocity than that achieved in the flight test, and therefore produced higher heat-input conditions than the actual RFD-1 trajectory. By means of the analysis described in detail later in this report (Section IV, pp. 114-126), the following predictions of burnup altitudes were made:

Tracer	Predicted Burnup Altitude
Strontium	166,000 to 177,000 feet
Barium	126,000 to 145,000 feet
Silver	Tracer not exposed
Gold	Tracer not exposed

Seven aircraft, three ships, and two ground stations adjacent to the flight path and in the impact area were used for data acquisition during the test. Figure 13 shows their locations relative to the re-entry flight path.

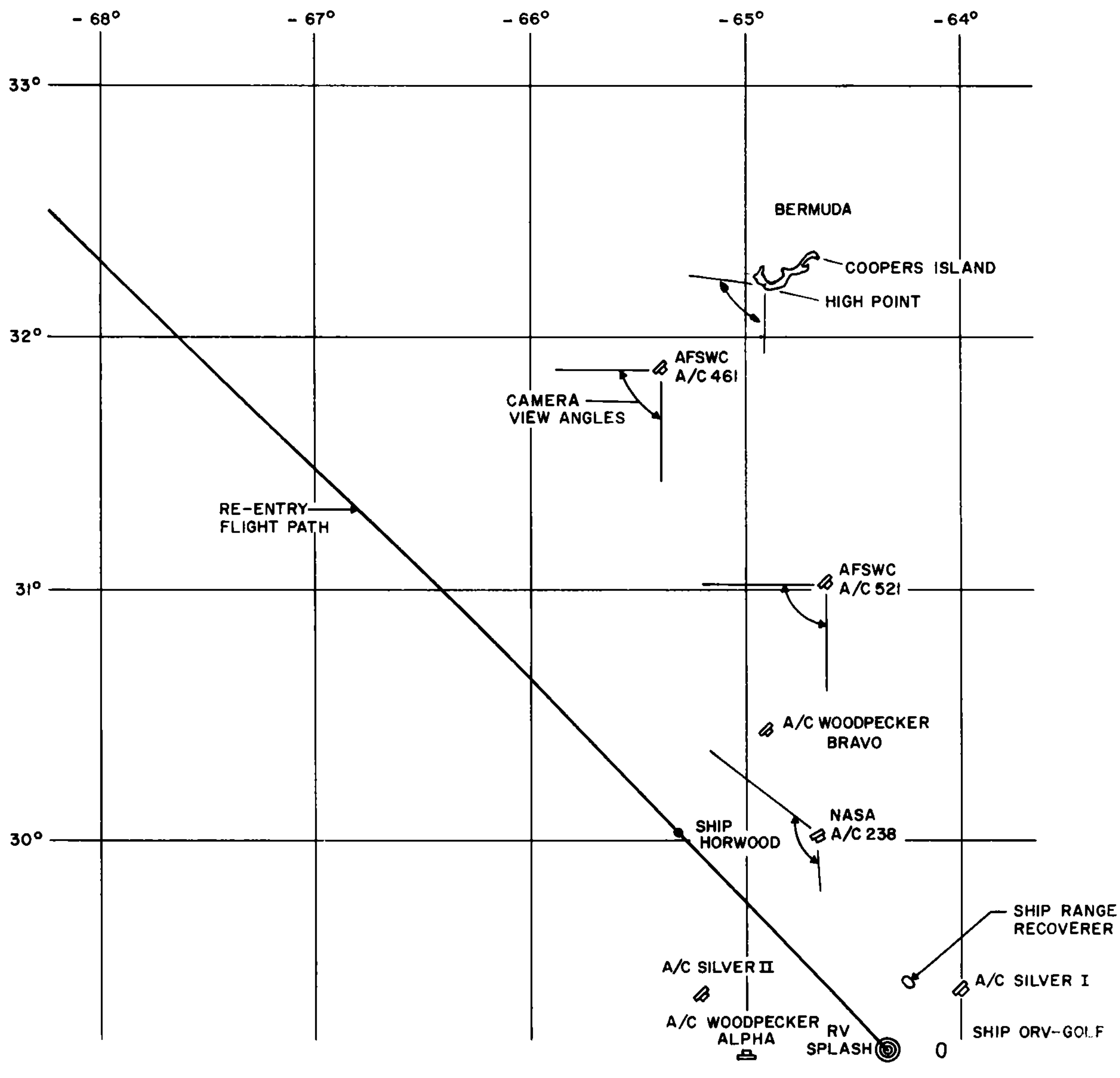

Figure 13. RFD-1 re-entry flight path and locations of downrange instrument stations

The intended function of the ships was to record TM data and to recover the RV and the remains of the STR after impact. Four of the aircraft were equipped to receive TM data from the RV (a presentation of the TM data is included in SC-RR-64-502, SC-RR-64-511, and SC-RR-64-515). Four of the aircraft were also equipped to receive the SARAH beacon transmitted from the RV after impact to assist in recovery. Three aircraft were employed as airborne platforms for the optical instrumentation.

The ground station at Cooper's Island was headquarters for RFD-1 operations at Bermuda. This was also the location of the NASA FPS-16 radar, which tracked the RV C-band beacon and recorded its trajectory. High Point, Bermuda, was the only ground-based camera station.

Optical Instrumentation

Twenty ground-based and 41 airborne cameras photographed the re-entry. The reasons for using both ground-based and airborne cameras were:

1. In the event of any major breakdown, such as electrical power failure, at least partial coverage of the re-entry was still possible.
2. The closeness of the aircraft to the re-entry flight path was not limited. Since re-entry closer to Bermuda than 90 nautical miles was not allowed, ground-camera slant ranges were restricted to at least that distance.
3. The effects of atmospheric attenuation were reduced by the 10,000-foot altitude of the aircraft cameras.
4. Because of their large light-gathering systems, many of the ground-based cameras could not be installed in aircraft.
5. Ground-based cameras are more stable and are not subject to aircraft vibrations. These two factors are important in reduction of the data.

Ground-Based Cameras

All ground-based cameras were stationed at High Point (Figures 14 and 15), on the south coast of Bermuda. High Point is 125 feet above sea level, with an unobstructed view of the re-entry flight path. The facilities there were essentially self-sustaining. Auxiliary equipment included:

1. Diesel-electric generators, 65 and 45 KVA.
2. A power-distribution system capable of converting to generator or commercial power.
3. An operations building.
4. A photo trailer for loading cameras and developing film.
5. A transportainer to house recording and TACODA (a parallax-compensating computer) equipment.
6. Two transportainers for spare parts.
7. A storage building.

Table II lists the films and the mechanical features of the cameras used at High Point to record the RFD-1 re-entry. The TACODA (target coordinate data) system used to control the tracking of certain of the cameras during part of the trajectory is described briefly below, followed by descriptions of the optical instrumentation at High Point.

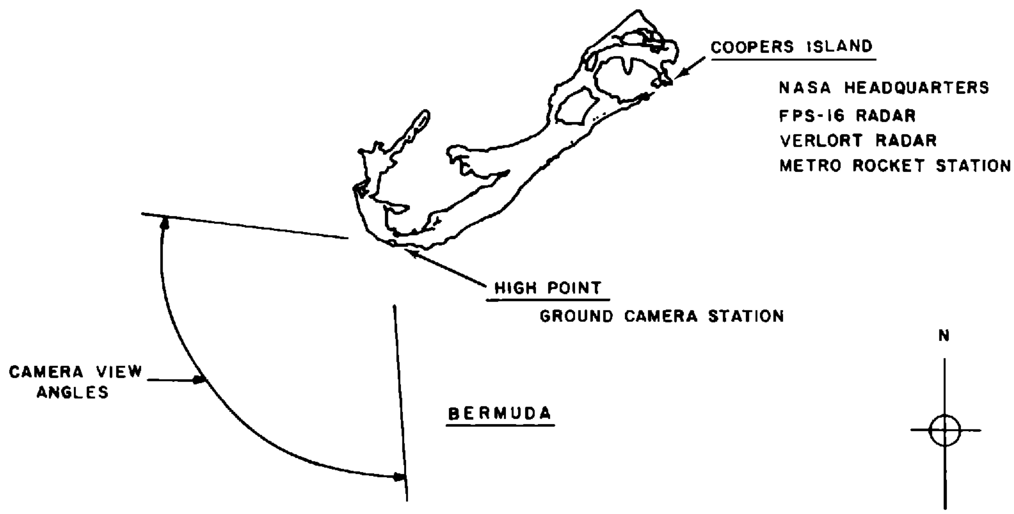

Figure 14. Bermuda ground stations

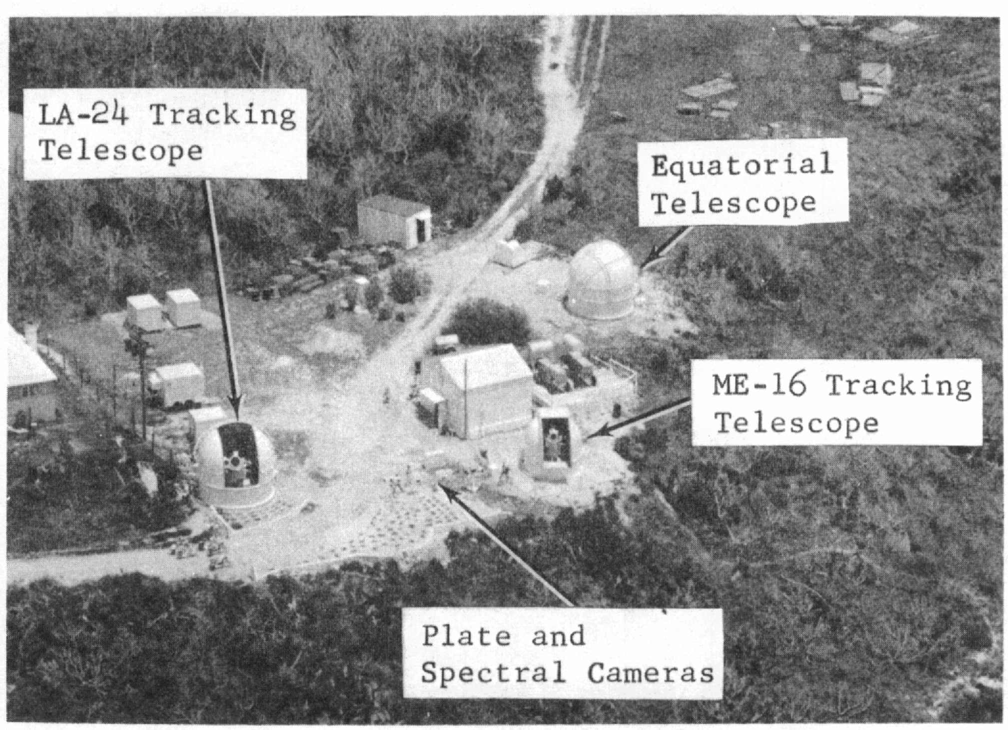

Figure 15. Camera station at High Point, Bermuda

TABLE II

High Point Cameras

			Lens					
Camera No.	Description	Grating or Filter	Focal Length (in.)	Aperture	Field of View	Film	Sampling Rate	Illustration
ME-16-1	Photosonics 70-mm motion-picture camera	None	117.5	f/7.0	1.1 x 1.1°	Super Anscochrome	90 frames/sec	Figure 16
ME-16-2	Mitchell 35-mm motion-picture camera	None	18	f/3.0	3.4 x 2.3°	Super Anscochrome	96 frames/sec	Figure 16
ME-16-3	Mitchell 35-mm motion-picture camera	None	2	f/2.0	27.0 x 20.0°	Super Anscochrome	96 frames/sec	Figure 16
LA-24-1	K-37 time-resolved streak spectrograph	Bausch and Lomb 600-lines/mm grating	117.5	f/5.0	0°27' wide	Tri-X Aerecon	3/16 in./sec	Figure 17
LA-24-2	Photometer	Filter wheel with 24 special interference filters	12-in. dia. cassigrainian	--	0°24' wide	None	Filter wheel turning 600 rpm	Figure 17
LA-24-3	Mitchell 35-mm motion-picture camera	None	40	f/5.7	1.5 x 1.0°	Super Anscochrome	96 frames/sec	Figure 17
P-1, P-2, and P-3	K-37 plate cameras	None	12	f/2.5	53.0 x 45.2°	10 x 12-in. glass plates with Kodak 103-F emulsion	Continuous	Not shown
T-1, T-2, and T-3	K-37 plate trajectory cameras	None	12	f/2.5	53.0 x 45.2°	10 x 12-in. glass plates with Kodak 103-F emulsion	Chopped: open 7 sec closed 2 sec; repeat	Figure 19
S-1 through S-6	K-37 plate spectrographs	Bausch and Lomb 600-lines/mm grating	12	f/2.5	53.0 x 45.2°	10 x 12-in. glass plates with Kodak 103-F emulsion	Continuous	Figure 18
C-1	Photosonics 70-mm cinespectrograph	Bausch and Lomb 600-lines/mm grating	4	f/1.9	30 x 30°	Kodak Linagraph Shellburst	10 frames/sec	Figure 20
H-1 (hand held)	Bell and Howell 16-mm motion-picture camera	None	6	f/2.5	4.0 x 2.8°	Super Anscochrome	126 frames/sec	Not shown

TACODA -- TACODA is a parallax-compensating computer system through which the tracking mounts for High Point optical instruments were slaved to the FPS-16 radar at Cooper's Island. Operation is as follows:

1. Well before re-entry began, the FPS-16 made the initial Bermuda acquisition of the RV, picking up and automatically tracking the C-band beacon.

2. Position data from the FPS-16 were fed to the TACODA, which was located at High Point, through a land telephone-line link from Cooper's Island. From these data, the TACODA computed the changing azimuths and elevations for the tracking mounts, compensating for the parallax introduced by the 12-mile separation between the FPS-16 and the mounts.

3. Signals reflecting these azimuths and elevations were continually transmitted from the TACODA to the drive systems for the mounts, which then automatically tracked the not-yet visible RV.

4. When the tracking-mount operators at High Point sighted the RV, first through 5.6-power and then through 32-power telescopes, they switched to manual control. This was done because objects other than the RV required tracking, and because visual tracking is more accurate than radar once an object is sighted.

During the RFD-1 flight, the TACODA system functioned perfectly, guiding the tracking mounts to the RV before it was visible to the operators through their tracking scopes.

ME-16 Tracking Mount -- The entire ME-16 mount and protective dome (Figure 16) is motorized to rotate 360 degrees in azimuth and 90 degrees in elevation. Three cameras were included on the mount for RFD-1 coverage. The main optics, contained in the large center tube, were connected to a 70-mm Photosonics 10-B high-speed motion-picture camera. Light from the re-entry was collected by a Newtonian telescope 16 inches in diameter and 117.5 inches in focal length, and focused on a parabolic mirror at the rear of the tube. This mirror reflected the light via two flat-angled mirrors to a focus on the film plane of the camera. A rotating prism and shutter system in the camera directed the image onto the film. Each rotation of the prism recorded one frame on the film. With a film frame rate of 90 frames/sec, this camera is capable of pulling 1700 feet in 100 seconds.

The remaining two cameras were 35-mm Mitchell shutter-operated framing cameras with focal lengths of 18 and 2 inches, respectively. They were not connected to the Newtonian telescope in the main optics. A timing code received from the Bermuda Range Time (BRT) transmitter was recorded on the film edges by a neon lamp.

LA-24 Tracking Telescope -- This tracking mount operates similarly to the ME-16. However it mounted different instrumentation.

The large center tube shown in Figure 17 housed a parabolic mirror 24 inches in diameter with a focal length of 117.5 inches. The light from the re-entry was reflected from this mirror and brought to a focus at the focal point of an Aero-ektar 12-inch f.l. (focal length) lens. On leaving this lens, the light rays (which were parallel) passed through a 600-lines/mm grating. After diffraction by the grating, the light was brought to another focus on the film plane of the camera by a second 12-inch-f.l., f/2.5 lens. The 9-inch wide film was pulled perpendicular to the dispersion of the grating at 3/16 inch per second. From the resulting spectral record and the time code recorded on the edge of the film, it was possible to determine when spectrally distinct events occurred.

The smaller tube on the left in Figure 17 housed the photometer, consisting of a 12-inch cassigrainian system for gathering light which was then passed through 24 narrow band-pass filters. These filters, approximately 10 Å at half width, were centered on predetermined spectral lines of the tracer materials: strontium, barium, silver, and gold. Two spectral lines per tracer were chosen as the lines which, for that material, had the best chance of being detected. The probable relative intensities of lines and interfering lines were considered in this choice.

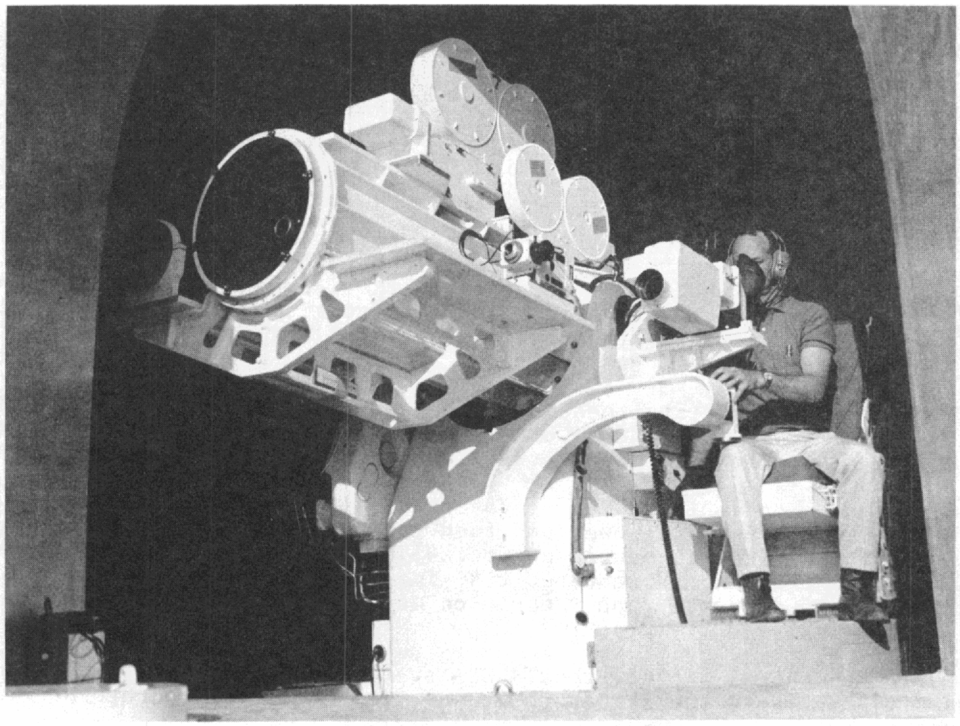

Figure 16. ME-16 tracking telescope

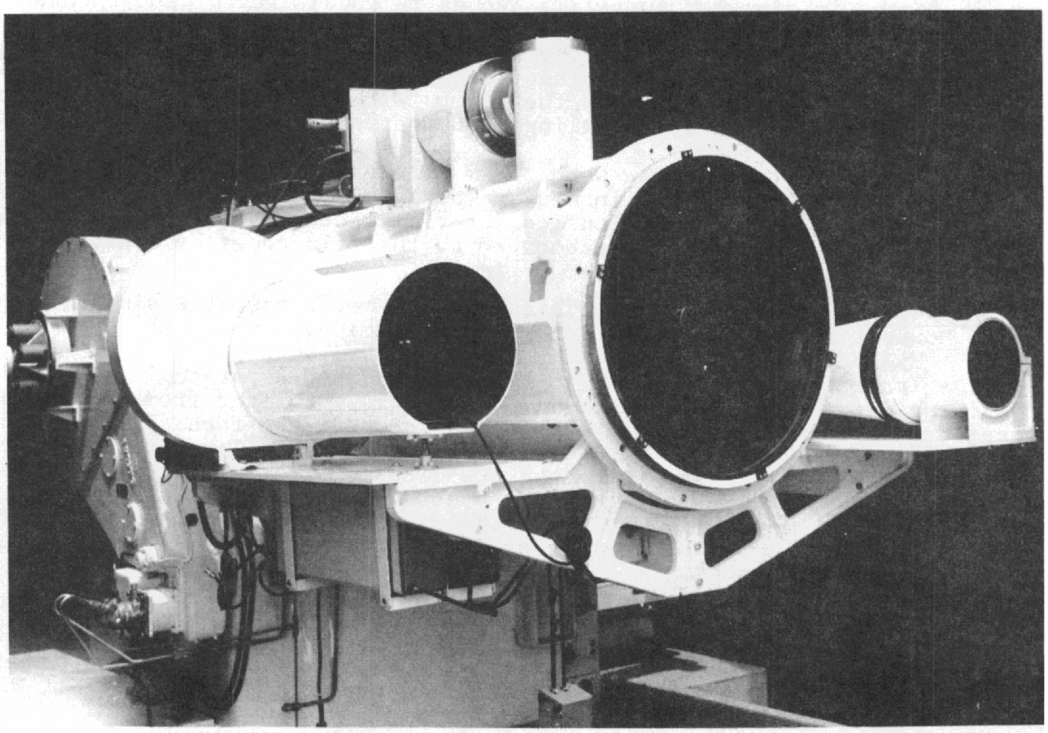

Figure 17. LA-24 tracking telescope

To distinguish between spectral line radiation and overall intensity fluctuations, background filters were used to monitor the background radiation 50 Å on each side of the spectral line of interest. The filters were mounted around the periphery of a disc which was spun at 600 rpm to provide 0.1-second time resolution for each wavelength monitored.

The radiation transmitted through each filter as it passed the opening in the lens system was detected by a dry-ice-cooled RCA-C-7265 fourteen-stage photomultiplier tube, which had a sensitivity of 3000 amps/lumen and a usable signal range of from 5×10^{-13} to 2×10^{-8} lumens. This tube transmitted an electrical pulse of measured intensity to a C.E.C. oscillograph. Time was recorded on the oscillograph simultaneously with the photometer pulses, making it possible to determine the elements flaring during the re-entry and the times of their appearances.

The shelf on the right in Figure 17 supported a Sandia-designed 40-inch-f.l., f/6.8 lens mounted with a high-speed 35-mm Mitchell motion-picture camera. This camera provided high-magnification, slow-motion movies of objects and events recorded by the streak spectrograph and photometer.

Plate Cameras -- The plate cameras were essentially continuous-exposure cameras. The optics were war-surplus Kodak Aeroektar 12-inch-f.l., f/2.5 aerial-mapping lenses; the camera bodies were cast by Sandia. The film, located at the rear of the housing, consisted of a 10 x 12-inch glass film plate coated with Kodak 103-F film emulsion. Images of the re-entry objects were focused on the film plate by the lenses. The lens shutter was an iris-type diaphragm which was kept open so that the film was continuously exposed during re-entry. The re-entry was recorded as a series of streaks across the film. Three cameras oriented at different angles were required to record the entire re-entry.

Spectrographic Plate Cameras -- These cameras (Figure 18) were similar to the plate cameras. However, a Bausch and Lomb 600-lines/mm transmission-diffraction grating blazed at 5500 Å was attached to the front of each lens. Light from the re-entry objects was separated, as it passed through the grating, into spectral groupings characteristic of the radiation from the elements comprising the different materials in the RS. This light was then focused onto the film plane by the lens. Two arrays of three cameras each were used. One group was oriented at a high elevation angle and the other at a lower elevation angle to assure coverage of the entire re-entry envelope.

Chopped Trajectory Plate Cameras -- These cameras (Figure 19) used lens systems and glass film plates similar to those in the plate and spectrographic plate cameras. The shutter system, located in the cylindrical housing, was operated by an electrically actuated spring. A pre-set timing mechanism opened the shutter for 7 seconds and then closed it for 2 seconds. This sequence continued during the entire re-entry, causing the re-entry trails on the film to be interrupted at these intervals. The times of openings and closing were also recorded on the C.E.C. oscillograph. Comparison of the times with

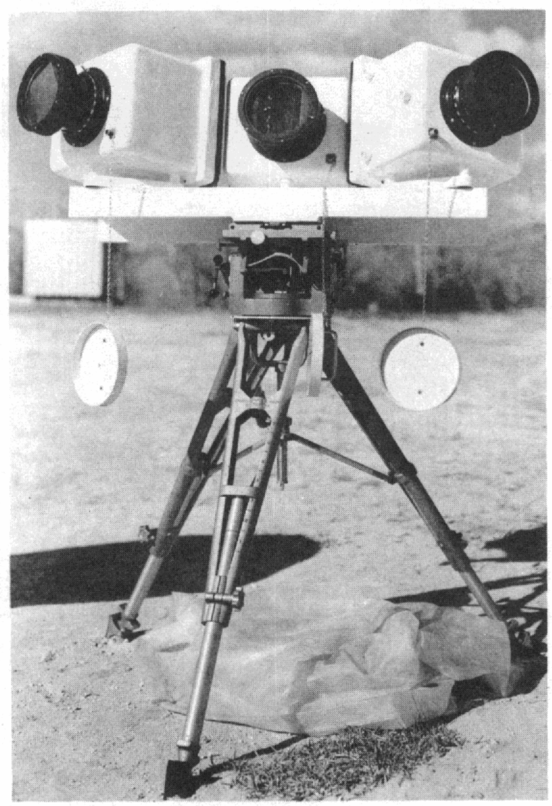

Figure 18. Spectrographic plate cameras

the measured and theoretical trajectories furnished a history of altitude, range, and velocity for the various objects (this is discussed in Section IV, pp. 41-134).

Cinespectrograph -- This instrument (Figure 20) was hand-tracked and operated. It was equipped with a 4-inch-f.l., f/1.9 lens and a Bausch and Lomb 600-lines/mm transmission grating, and provided ten 70-mm spectral pictures per second.

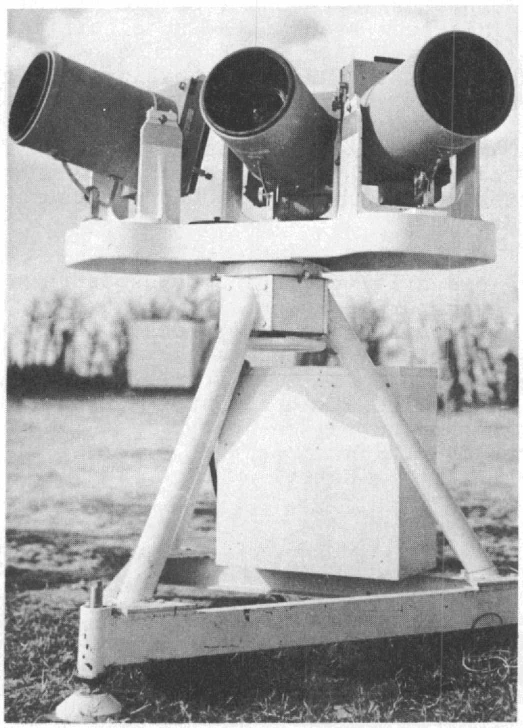

Figure 19. Chopped trajectory plate cameras

Figure 20. Cinespectrograph

Airborne Cameras

Three aircraft, one DC-4 and two C-54's, supported RFD-1 camera operations. Their locations during the re-entry were as shown in Figure 13.

The DC-4 was furnished and outfitted by NASA's Langley Research Center, Hampton, Virginia. It was designated NASA-238. Although this aircraft was not included in the formal RFD-1 plan, films from its cameras furnished much of the data used for evaluation of the re-entry events. Table III lists the cameras used on this plane to photograph the RFD-1 re-entry.

The two C-54's and their flight crews were furnished by AFSWC, Kirtland AFB, Albuquerque, New Mexico. Sandia instrumented these planes with cameras and TM-receiving equipment. AFSWC installed additional cameras for experimentation, documentary films, and re-entry analysis. These aircraft were designated AFSWC-461 and

TABLE III

NASA Airborne Cameras

			Lens					
Camera No.	Description	Grating	Type	Focal Length (in.)	Aperture	Field of View	Film	Sampling Rate
AC-37	KG-24 spectral camera	600 lines/mm	Aeroektar	7	f/2.5	40.0 x 40.0°	Royal-X Pan black-and-white	Continuous
AC-84	KG-24 spectral camera	75 lines/mm	Aeroektar	7	f/2.5	40.0 x 40.0°	Royal-X Pan black-and-white	Continuous
AC-85	KG-24 spectral camera	400 lines/mm	Aeroektar	7	f/2.5	40.0 x 40.0°	Royal-X Pan black-and-white	Continuous
AC-36, AC-38, AC-80, AC-86	KG-24 plate cameras	None	Aeroektar	7	f/2.5	40.0 x 40.0°	Royal-X Pan black-and-white	Continuous
AC-1	RC-5 plate trajectory camera	None	Avigon	6	f/2.6	73.0 x 73.0°	Royal-X Pan black-and-white	Chopped: open 0.25 sec, closed 0.25 sec; repeat
AC-101	Flight Research 35-mm motion-picture camera	None	Bell and Howell Eyemax	10	f/4.5	5.6 x 4.2°	Royal-X Pan black-and-white	10 frames/sec
113	Cine Kodak 16-mm motion-picture camera	None	Kodak Anastigmat	2	f/2.0	10.4 x 8.3°	Ektachrome ER color	16 frames/sec

AFSWC-521. Figure 21 shows the bank of Sandia cameras carried in AFSWC-521. Included were a streak spectrograph, a photometer, a 16-mm motion-picture camera, and three K-24 spectral cameras; the optical instrumentation in AFSWC-461 was essentially the same, although the photometer was omitted. Figure 22 shows the locations of cameras carried in the AFSWC aircraft, and Table IV lists these cameras. The major cameras in these planes are described briefly below.

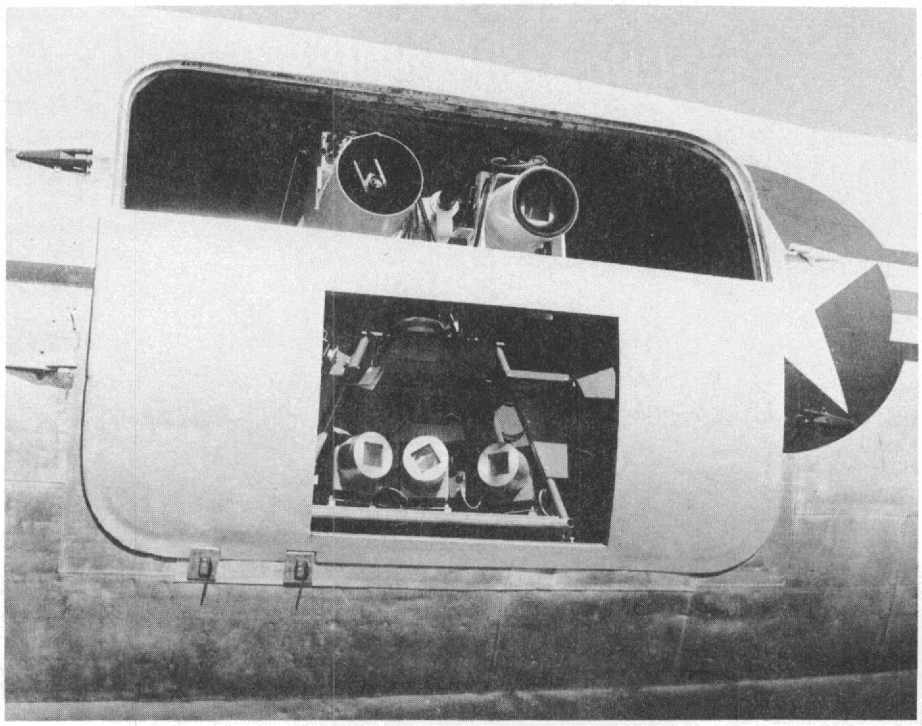

Figure 21. Sandia airborne cameras

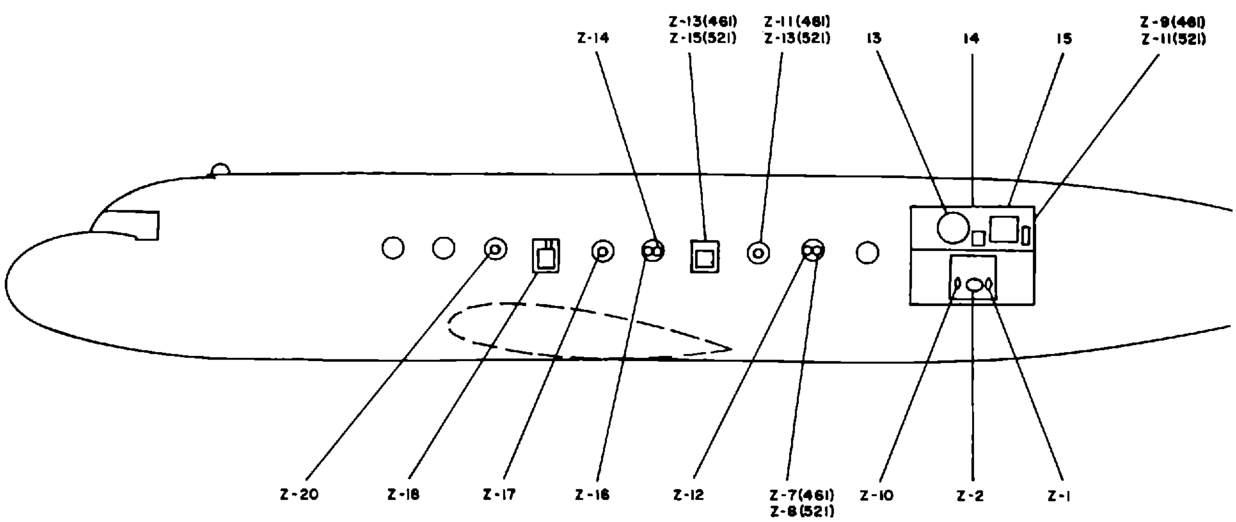

Figure 22. Optical instrumentation in AFSWC Aircraft 461 and 521 (refer to Table III)

TABLE IV

Airborne Cameras, AFSWC Aircraft 461 and 521

Camera No.	Aircraft	Description	Grating or Filter	Lens: Type	Lens: Focal Length (in.)	Lens: Aperture	Lens: Field of View	Type	ASA Speed	Camera Capacity (ft)	Sampling Rate
13	461, 521	Photometer	Filter wheel with 24 special interference filters	12-in.-dia. mirror	--	--	0°24'	--	--	--	Filter wheel turning 600 rpm
14	461, 521	Milliken DBM-5 16-mm motion-picture camera	None	--	6	f/2.5	4.0 x 2.8°	Super Anscochrome	160	1200	400 frames/sec
15	521, 521	General Electric aircraft-type K-37 time-resolved streak spectrograph	Bausch and Lomb 600-lines/mm grating	Aeroektar	12	f/2.5	3 x 42°	Tri-X Aerecon	200	--	3/16-in./sec
Z-13 Z-15	461 521	Hulcher Model 100 70-mm motion-picture camera	Bausch and Lomb 600-lines/mm grating	Aeroektar	7	f/2.5	18 x 18°	DuPont 140	320	400	20 frames/sec
Z-9	461	Milliken DBM-5 16-mm motion-picture camera	None	Raptar	2	f/2.5	11.7 x 8.4°	Ansco Ultraspeed color	500	400	128 frames/sec
Z-11	521	Milliken DBM-5 16-mm motion-picture camera	None	Angenieux	3	f/2.5	7.5 x 5.4°	Ansco Ultraspeed color	500	400	128 frames/sec
Z-20	461, 521	Aerosonics ballistic camera	None	Metrogon	6	f/6.3	67 x 79°	RXP 8 x 10 in.	1250	One plate	Random chop: 0.04-0.065 sec
Z-18	461, 521	Mitchell Model B 35-mm motion-picture camera	None	Baltar	6	f/2.5	6.9 x 9.2°	RXP	1250	1000	96 frames/sec
Z-11 Z-13	461 521	General Electric aircraft-type K-37	None	Aeroektar	12	f/2.5	42 x 42°	RXP	650	75	1.25 sec (461) 0.5 sec (521)
Z-17	461, 521	Avco-Everett ballistic camera	None	Metrogon	6	f/6.3	67 x 79°	RXP 8 x 10 in.	1250	One plate	Random chop: 0.04-0.065 sec
Z-16	461, 521	Aerosonics ballistic camera	None	Metrogon	6	f/6.3	67 x 79°	RXP 8 x 10 in.	1250	One plate	Random chop: 0.04-0.065 sec
Z-12	461, 521	Eastman Kodak K-24	None	Aeroektar	7	f/2.5	39 x 39°	RXP	650	56	0.5 sec, 4-sec cycle
Z-14	461, 521	Eastman Kodak K-24	None	Aeroektar	7	f/2.5	39 x 39°	RXP	650	56	0.5 sec, 4-sec cycle
Z-7 Z-8	461 521	Eastman Kodak K-24	None	Aeroektar	7	f/2.5	39 x 39°	Tri-X	200	56	0.5 sec, 4-sec cycle
Z-10	461, 521	Eastman Kodak K-24	Bausch and Lomb 600-lines/mm grating	Aeroektar	7	f/4.0	39 x 39°	RXP	650	56	2.5 sec, 4-sec cycle
Z-2	461, 521	Eastman Kodak K-24	Bausch and Lomb 600-lines/mm	Aeroektar	7	f/5.6	39 x 39°	RXP	650	56	2.5 sec, 4-sec cycle
Z-1	461, 521	Eastman Kodak K-24	Bausch and Lomb 600-lines/mm grating	Aeroektar	7	f/2.5	39 x 39°	RXP	650	56	2.5 sec, 4-sec cycle

Time-Resolved Streak Spectrograph -- This instrument was similar to the TRSS in the LA-24, but employed a refracting system for light gathering in lieu of a reflecting telescope.

Sampling Photometer -- The photometer was the same as the one mounted on the LA-24.

K-24 Spectral Cameras -- These cameras were fitted with 7-inch-f.l., f/2.5 Aeroektar lenses. A 300-lines/mm diffraction grating was included to produce spectral films. These cameras furnished one 5-1/2-inch-wide photo per second.

Description of the Re-entry

Since optical coverage was one of the primary methods employed to record RFD-1 events, it was imperative that no clouds or haze be present between High Point and the expected flight path at re-entry. After numerous delays caused by such adverse weather conditions, the Scout missile bearing RFD-1 was launched at 04-38-14 Zulu time on May 22, 1963. Impact of the re-entry vehicle and reactor into the ocean occurred approximately 500 seconds later.

Trajectory

Before the flight, trajectories were computed for the RV, the fourth-stage motor, the simulated fuel rods, and the reflectors. They were computed for the nominal, 2-σ low steep, and 2-σ high shallow re-entry conditions. These are discussed in SC-RR-64-510. Figure 23 shows the envelope of computed azimuths and elevations for the RV and fuel-rod trajectories, referenced to High Point; the actual RFD-1 RV trajectory is superimposed for comparison. The actual trajectory was somewhat high and shallow compared with the predicted nominal trajectory. This was actually better from the standpoint of optical data acquisition, since the re-entry path remained above the ocean haze for a longer time.

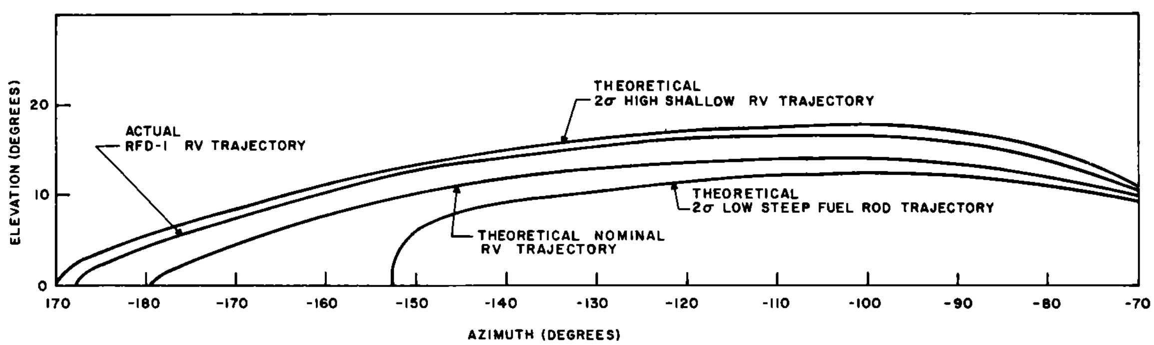

Figure 23. Envelope of RFD-1 re-entry trajectories

Events

In the nominal trajectory, re-entry was predicted to be visible 325 seconds after launch, at an altitude of 240,000 feet. For the possible steep or shallow re-entry trajectories, the times at which the RV would reach this altitude were 309 and 343 seconds, respectively. It was decided to uncap the plate cameras at 240 seconds, since they were used essentially for time exposures. However, because of limitations on film footage, the motion-picture cameras required a more exact starting time, and were therefore started upon command from the NASA FPS-16 radar plot board when the re-entry vehicle reached an altitude of 270,000 feet. This occurred at 324 seconds in the actual flight.

The actual re-entry flight path was as shown in Figure 13. The times of re-entry, of separation of the fourth-stage motor and the simulated fuel rods, and of all events and sequences in general were very close to those which had been predicted.

Data Obtained

Almost all of the optical instrumentation functioned satisfactorily during the re-entry. Performance was less than satisfactory in three instances: (1) one ground-based and two aircraft cameras did not operate, (2) timing did not record on several films, and (3) many of the films were underexposed to varying degrees as a result of the distances involved and of atmospheric attenuation. However, the data obtained were ample to permit satisfactory reduction for investigation of the test objectives. Table V is a listing of all optical instruments included in the test, showing the amount and quality of data obtained from each.

TABLE V

RFD-1 Photographic Data

High Point Plate Cameras

Camera No.	Objects Photographed	Remarks
P-1	4th-stage motor and early portion of bracket trajectories	Good data; clear.
P-2	All objects; center portion of re-entry	Good data; slightly out of focus and somewhat underexposed.
P-3	Reactor burnup during final portion of re-entry	Good data; slightly underexposed.
T-1	Same as P-1 but time chopped	Badly fogged due to light leak; furnished valuable information on 4th-stage timing.
T-2	Same as P-2 but time chopped	Excellent exposure; good resolution; used entensively in data analysis.
T-3	Same as P-3 but time chopped	Excellent exposure; good resolution; used extensively in data analysis.

High Point Spectral Cameras

S-1	4th-stage motor and early portion of bracket trajectories	Spectra off plate; not usable.
S-2	All objects; center portion of re-entry	Faint but good data.
S-3	Reactor burnup during final portion of re-entry	Zero order not sharp, but first-order spectra clear.
S-4	Same as S-1	Zero order first-order spectra not sharp due to poor focus and underexposure.

High Point Spectral Cameras (cont.)

Camera No.	Objects Photographed	Remarks
S-5	Same as S-2	Fainter than S-2; valuable information on strontium flares obtained.
S-6	Same as S-3	Good focus; zero order sharp; spectra less distinct.
LA-24 TRSS	Mistracked (tracked 4th-stage motor)	Very good spectral data; elements of 4th stage clear.
LA-24 Photometer	Mistracked (tracked 4th-stage motor)	Good record; confirmed LA-24 TRSS.
LA-24-3	Mistracked (tracked 4th-stage motor)	Camera malfunction; no film record.
Cinespectrograph	Re-entry vehicle	Badly underexposed; not usable.

High Point Framing Cameras

Camera No.	Objects Photographed	Remarks
ME-16-1	Experimental fuel rods	Underexposed; few faint objects visible; not usable.
ME-16-2	Experimental fuel rods	Good film; RV, fuel-rod flares, and brackets visible; color of flares used to identify tracers.
ME-16-3	Experimental fuel rods	Badly underexposed; not used.
H-1	Re-entry vehicle	Faint record of RV; not used.

AFSWC Aircraft 521 Plate Cameras

Camera No.	Objects Photographed	Remarks
Z-20, Z-17, Z-16, Z-14, Z-13, Z-12, and Z-8	Entire re-entry	Severe vibration; poor resolution; not used in data analysis.

AFSWC Aircraft 521 Spectral Cameras

Camera No.	Objects Photographed	Remarks
Z-10	Entire re-entry	Fair focus; underexposed; RV, fuel-rod, and bracket spectra faintly visible.
Z-2	Re-entry vehicle	Faint spectra.
Z-1	Re-entry vehicle	Sharp focus; vibration apparent; clear spectra of RV.
Z-15	Experimental fuel rods	Underexposed; not usable.
13	Experimental fuel rods	No data; mistrack due to narrow field of view.
15	RV and fuel rods	RV, fuel-rod, and bracket spectra identified; good timing.

AFSWC Aircraft 521 Framing Cameras

Camera No.	Objects Photographed	Remarks
Z-18	Re-entry vehicle	Underexposed; no data.
14	Experimental fuel rods	Faint objects visible; not used in data analysis.

AFSWC Aircraft 521 Framing Cameras (cont.)

Camera No.	Objects Photographed	Remarks
Z-11	Re-entry vehicle	Underexposed; no data.

AFSWC Aircraft 461 Plate Cameras

Camera No.	Objects Photographed	Remarks
Z-20, Z-17, Z-16, Z-12, Z-7, Z-14, and Z-11	Entire re-entry	Severe vibration; poor resolution; not used in data analysis.

AFSWC Aircraft 461 Spectral Cameras

Camera No.	Objects Photographed	Remarks
Z-10, Z-2, and Z-1	Entire re-entry	No data; possibly due to camera orientation.
Z-13	Experimental fuel rods	Underexposed; not usable.
15	RV and fuel rods	RV, fuel-rod, and bracket spectra visible; no timing.

AFSWC Aircraft 461 Framing Cameras

Camera No.	Objects Photographed	Remarks
Z-18	Re-entry vehicle	Underexposed; no data.
14	Experimental fuel rods	Mistrack; no data.
Z-9	Re-entry vehicle	Underexposed; no data.

NASA Aircraft 238 Plate Cameras

Camera No.	Objects Photographed	Remarks
AC-38, AC-36, AC-80, and AC-86	Entire re-entry	Good clear film; use limited due to lack of timing and information on aircraft orientation.
AC-1	Entire re-entry	Good timing; no detail resolution; used for time only.

NASA Aircraft 238 Spectral Cameras

Camera No.	Objects Photographed	Remarks
AC-85	Entire re-entry	Excellent film; RV, fuel-rod flares, and 4th-stage motor very clear.
AC-37	Entire re-entry	Slightly out of focus; RV spectra visible.
AC-84	Entire re-entry	Only second-order spectra visible; RV, brackets, and 4th-stage motor identified.

NASA Aircraft 238 Framing Cameras

Camera No.	Objects Photographed	Remarks
AC-101	Entire re-entry	Excellent film; shows RV, fuel rods, and brackets; good timing; used extensively in data analysis.
AC-113	Entire re-entry	Good film; fuel-rod flare colors confirmed identification of tracers.

SECTION IV -- DATA EVALUATION

Reduction of the films from RFD-1 was not straightfoward. Reasons for the difficulties encountered were:

1. The majority of the motion-picture and spectrographic films were underexposed. This was caused by atmospheric attenuation, a too-fast film-frame rate, and the relatively great distance of the cameras from the re-entry.

2. Superposition of the 16 groups of re-entry objects on the plate films made it difficult to distinguish individual objects with certainty.

3. Timing chops on the plate-camera films were too long to allow accurate connection of re-entry streaks across the chops. In addition, the time between chops was too long to permit precise event/time correlation.

In spite of these problems, much usable information was extracted from the films and records. It will be presented in this section.

Methods of Analysis

Because a number of different kinds of films and records were obtained from RFD-1, it was necessary to reduce the data from each type of camera (plate, spectral, and framing) separately and then to correlate the results. The procedures included in reduction were:

1. Calibration of the Sandia plate-camera films from the star background, and establishment of lines of sight for each re-entry object.

2. Replotting, on an expanded scale, the trajectories from the plate cameras. This allowed separation of the individual streaks for identification as described in Item 3, below.

3. Construction of a re-entry picture of all the objects, based on the theoretical trajectory program described by J. A. Allensworth in The TTA Generalized Rigid Body Theoretical Trajectory Program for Digital Computer, SC-TM-64-526. This picture was then compared with the plates replotted as described in 2, above. Comparison between the theoretical and observed re-entry patterns confirmed identification of many of the objects.

4. Investigation of the spectrographic films. Spectral characteristics of the various re-entry objects were compared with the spectra recorded on the films. Times of occurrence of events were recorded for comparison with the other data.

5. Tabulation of motion-picture film events versus time. Timing marks on the film allowed a precise record of event time. Information from these films was used to confirm data from the preceding steps and to provide exact timing for them.

6. Correlation of all records. Throughout the process of data reduction, the data from each individual film and record were continuously compared with data from the others to confirm tentative findings. When all the separate analyses were completed, a compilation of all the data was made to assure agreement and to allow a synthesis of the entire re-entry sequence.

Time

Since time was the only initially known quantity recorded on each film and record, it was used as the common base for the identification and comparison of events. WWV time, broadcast from Station WWV, Washington, D.C., was recorded on the C.E.C. oscillograph. BRT, generated at Cooper's Island, was synchronized with the WWV time. BRT was transmitted via cable to all ground cameras and was radioed to the aircraft cameras. This time was recorded on the film edges by neon lamps as a serial decimal code. The NASA aircraft generated its own binary time-code, which was also synchronized with WWV time. All times on the films were measurable to 0.01 second.

Detailed discussion of the data reduction procedure and results follows.

Plate-Camera Data

Sixteen groups of objects were re-entering the atmosphere during the re-entry phase of RFD-1. Table VI lists their physical characteristics.

TABLE VI

Physical Characteristics of RFD-1

Item	Weight (lb)	W/C_DA (lb/ft^2)
RV-reactor	*532.9 to 330.0	*372.00 to 248.35
4th-stage motor	67.0	14.0
Strontium-loaded fuel rods (ea)	2.812	43.7
Barium-loaded fuel rods (ea)	2.864	44.4
Silver-loaded fuel rods (ea)	3.160	49.1
Gold-loaded fuel rods (ea)	3.294	51.1
Brackets 1 and 2 (ea)	4.23	6.43
Rod holders 1 and 2 (ea)	0.25	2.0
Reflectors 1 and 2 (ea)	7.80	8.69
Reflector springs 1-4 (ea)	0.50	12.0

*Variation is due to ejection of fourth-stage motor, fuel rods, brackets, holders, reflectors, and springs, and to disassembly of the reactor.

In spite of a large variation in W/C_DA, all the objects (except the fourth-stage rocket motor, which was retro-rocketed away from the flight path) followed very nearly the same trajectory. They were, however, displaced in time. On the plate-camera films, the continuous procession of re-entry objects appeared as a series of superimposed streaks (see Figures 24 and 25). Except for the RV and the fourth-stage motor, which were obvious, the various items could not be identified from

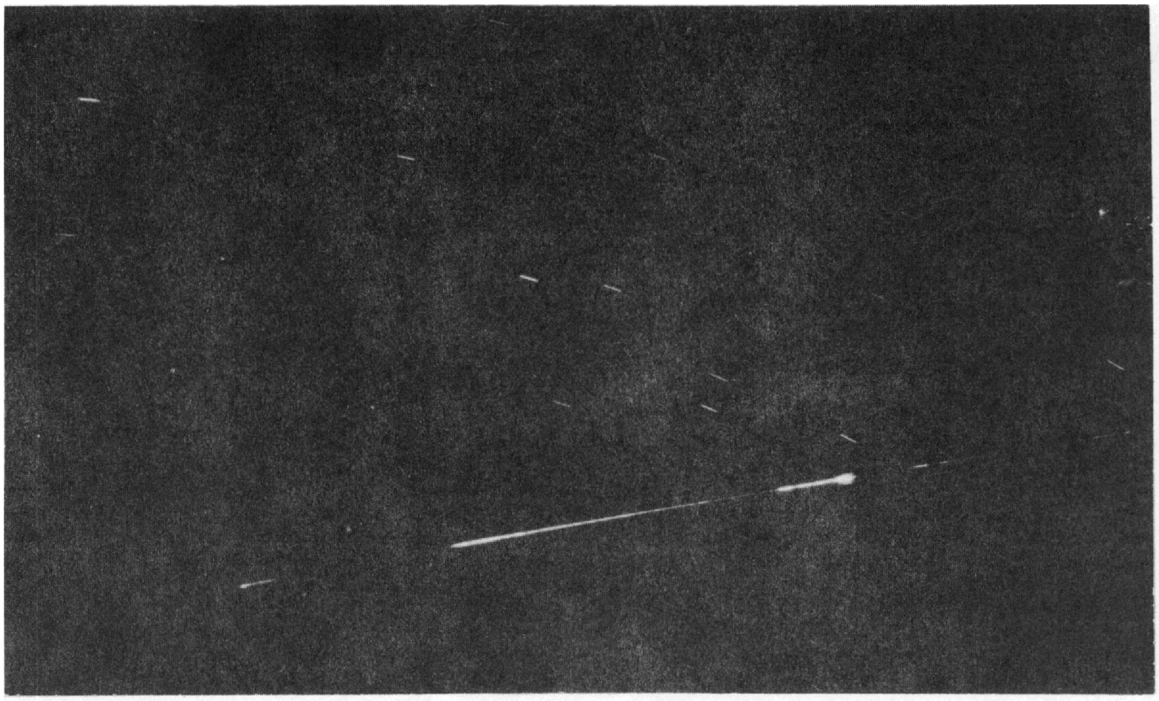

Figure 24. RFD-1 re-entry (from Sandia Plate Camera P-3)
(0.1 inch ≈ 7800 feet)

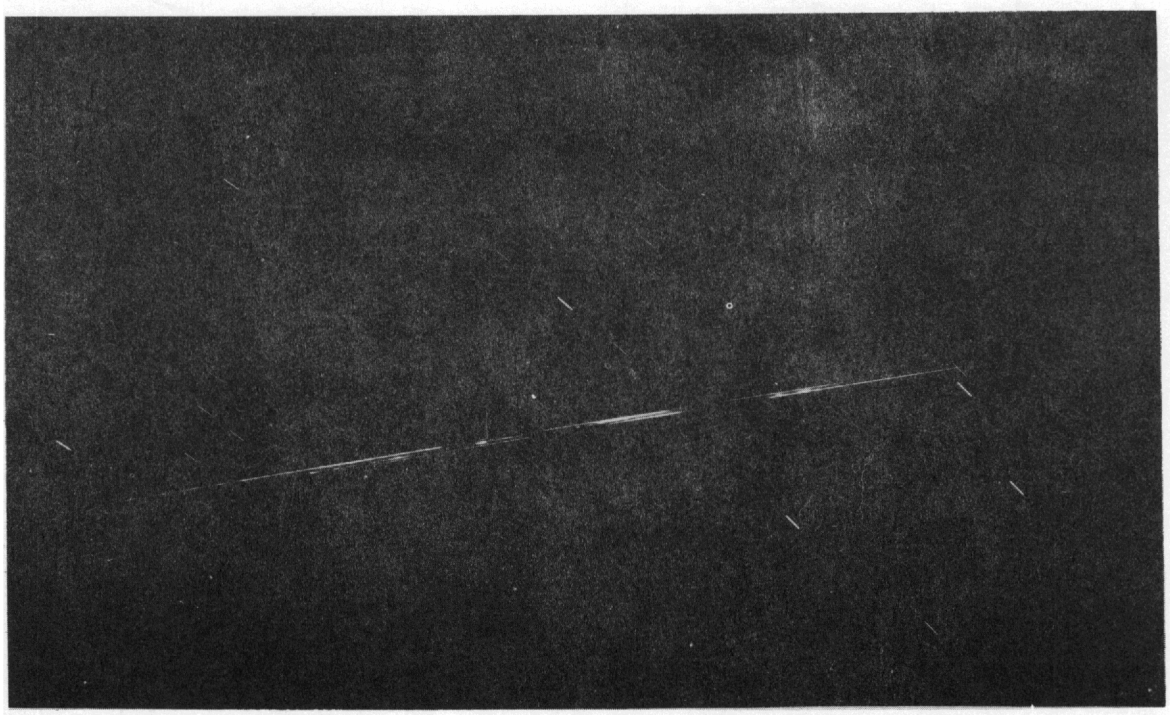

Figure 25. RFD-1 re-entry (from Sandia Plate Camera T-2)
(0.1 inch ≈ 7800 feet)

mere visual inspection. Comparison of the calculated trajectories with those measured from the plate-camera films was made in an effort to:

1. Identify individual re-entry objects, especially the four groups of tracer-loaded fuel rods.

2. Furnish a history of altitudes and velocities versus time. This information was needed for the computation of heat inputs to the RV and fuel rods, and for the location of observed events (disassembly of the RV and exposure of the fuel-rod tracers) in space.

3. Correlate the FPS-16 radar and the plate-camera data.

Camera Calibration

On each plate film, at least 11 star images distributed over the region of interest were selected and measured on a Mann comparator. The directions corresponding to those images were established from data given in Boss', General Catalogue of 33,342 Stars for the Epoch 1950, and from WWV timing recorded on the C.E.C. oscillograph during the re-entry flight. Apparent lines of sight to the selected stars were obtained by applying the atmospheric-refraction corrections in Manual of Geodetic Astronomy. Figure 26 illustrates the phenomena of atmospheric refraction and apparent lines of sight. The refractions were adjusted to High Point surface temperature and pressure.

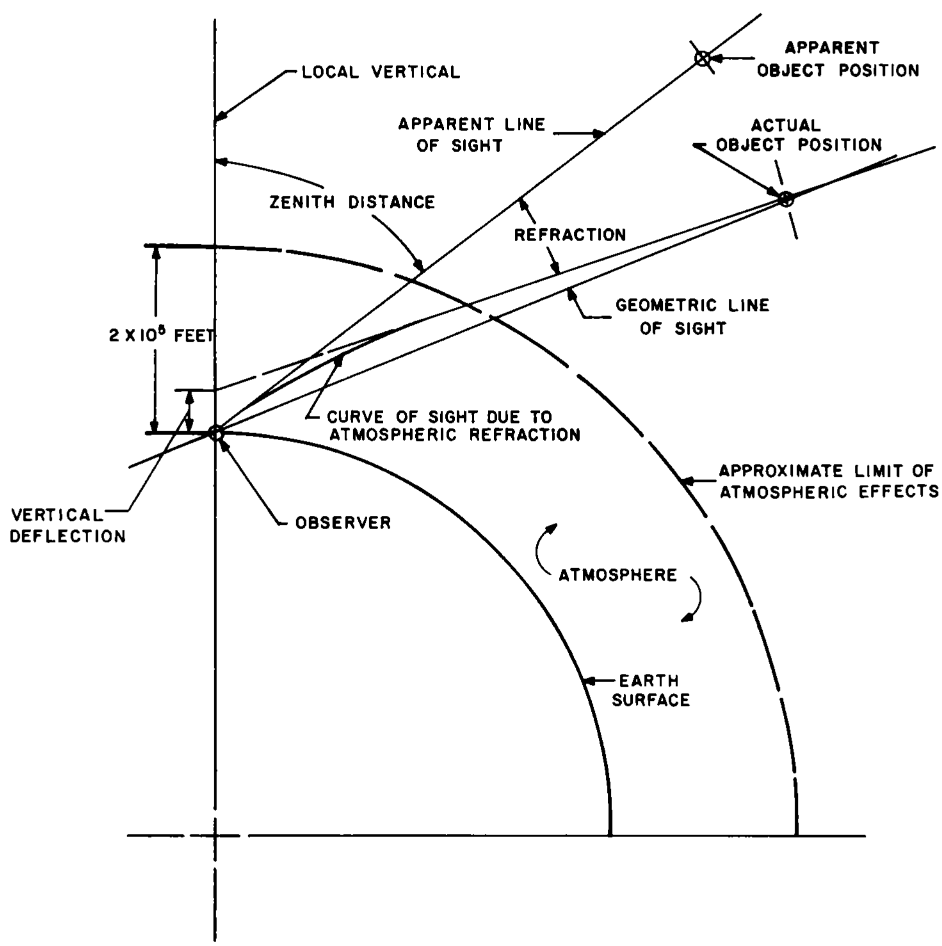

Figure 26. Atmospheric refraction

For each camera, (1) direction of the optical axis, (2) plate coordinates of the intersection between the optical axis and the film emulsion, (3) image distance, (4) orientation of the plate coordinate system, and (5) radial-distortion coefficients were determined by minimizing the sum of the squares of the distances between predicted and measured star images (Figure 27). Those distances appeared to be randomly distributed about zero, with a standard deviation of less than 0.00020 inch in each coordinate. Since 12-inch lenses were used, a probable relative error of no greater than 3.4 seconds of arc is indicated. The effects of plate-surface irregularities and tangential distortion are quite small and were therefore disregarded.

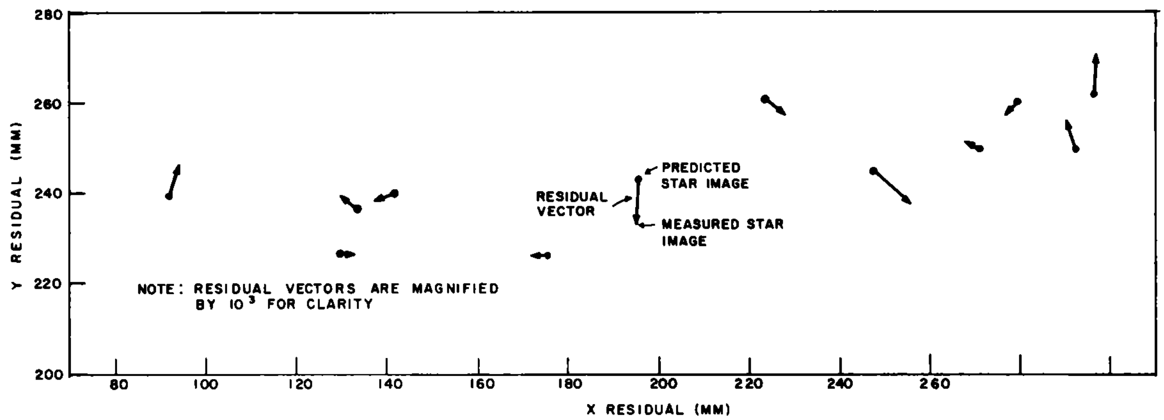

Figure 27. Calibration for Plate Camera T-2, predicted versus measured star images

Since the points on the plate-film re-entry trails were less distinct than the star images, and since photographic emulsion distorts images that are very close together, the data points may be in error by a significantly larger amount. Comparison of two lines of sight to the same object, as determined by two different cameras, indicates that a bias error as large as 30 seconds of arc may be present. No estimate of the error in atmospheric-refraction correction can be made because no independent data are available for comparison. However, it is reasonable to assume that no line of sight is in error by as much as 2 minutes of arc. Also, the relative error between two lines determined from the same camera plate is less than 1/2 minute of arc. The 1/2 minute of arc represents a distance of 100 feet in the trajectory and 0.0018 inch on the plate films (Figures 24 and 25).

Plate-Film Measurements

To compare the plate-film data with the theoretical trajectories, it was necessary to convert plate-film data and trajectories to a common coordinate system. The quantities selected for comparison were azimuth and elevation of the re-entry objects as viewed from the camera stations at High Point. These quantities were chosen to facilitate the use of existing computer programs. (After the data from RFD-1 had been reduced, a computer program was formulated to predict the plate coordinates of successive images of a moving object, given position and camera calibration parameters. That program will be used on future flight tests.)

Measurements of the plate-camera films to allow conversion of the re-entry trail's apparent lines of sight to azimuths and elevations were made with a Mann comparator. This instrument includes a 40-power microscope for measuring coordinates on two perpendicular axes. Scale resolution is 1/2 micron. Measurement limitation due to the plate-film resolution was approximately 5 microns. This represents 12 feet in the trajectory and 0.000197 inch on the plate-camera films.

The flares and other points of special interest on the image of each re-entry trail were measured and recorded. The nondescript portions of the image trails were described by a series of points at 0.040-inch intervals. Each point was converted to an apparent line of sight and a large-scale graph (10 inches per degree) of apparent elevation angle versus azimuth was constructed.

Theoretical Trajectories

Theoretical trajectories were computed on the Control Data 1604 computer, using the program described in SC-TM-64-526, The TTA Generalized Rigid Body Theoretical Trajectory Program for Digital Computer.

RV Theoretical Versus Radar Trajectories

Differences in measured trajectories of the 16 re-entry objects were small. The maximum vertical separation of the highest and lowest object was 3600 feet. To compute trajectories accurate enough for comparison with the plate-film data, it was essential first to establish agreement with a known trajectory. The NASA FPS-16 radar had provided this trajectory. During re-entry, the FPS-16 tracked the RV C-band beacon from 167 seconds (450,000 feet) to 360 seconds (168,800 feet). Raw data from this track were corrected for the effects of atmospheric refraction. Resulting geometric azimuths, elevations, and slant ranges were used to calculate the geometric coordinates of the RV relative to the radar station. No smoothing was used in the process. An estimate of the initial position, velocity, and re-entry angle of the RV was made from corrected radar data. Using these initial conditions, a trajectory for the RV was computed to obtain theoretical coordinates relative to the radar station. Aerodynamic drag on the RV was calculated on the basis of TM from the flight test and the characteristics predicted for the RV during re-entry. Drag characteristics of the RV changed during re-entry as a consequence of generator disassembly (Figure 28).

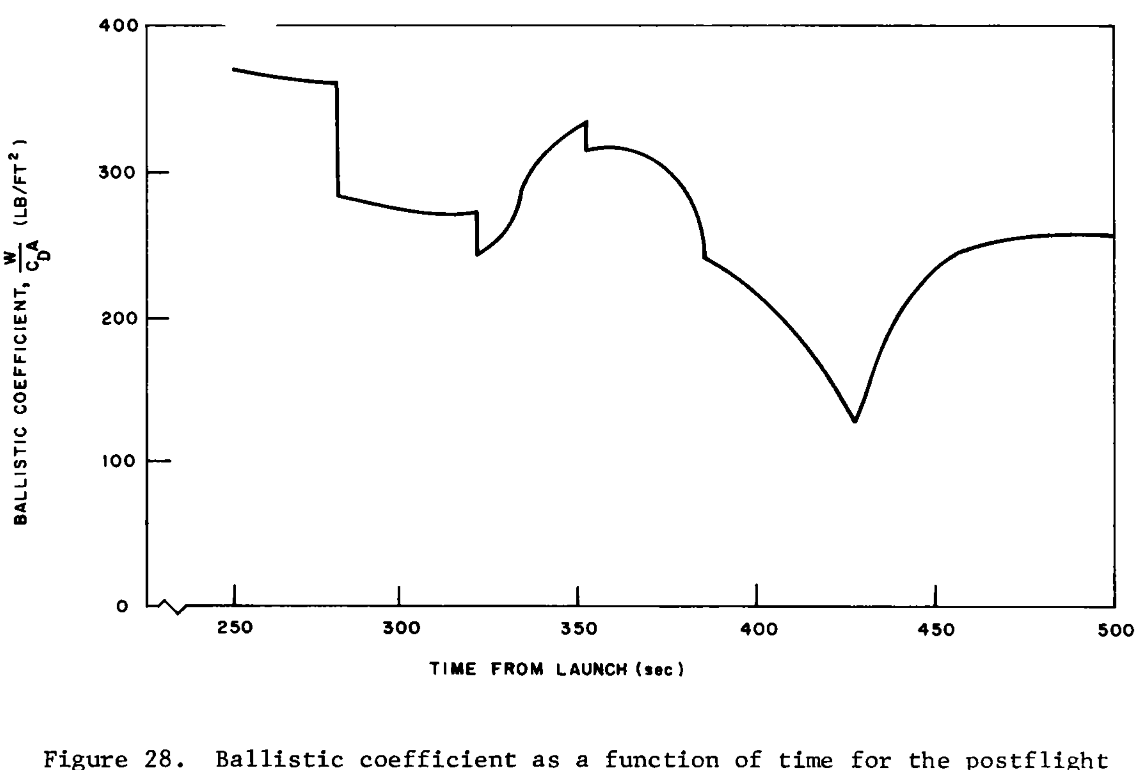

Figure 28. Ballistic coefficient as a function of time for the postflight theoretical calculation of re-entry trajectory

The standard 1959 ARDC atmosphere was used to define density, temperature. and pressure. This agreed closely with the measurements discussed in SC-RR-64-517.

The difference between the radar and theoretical values was determined for each coordinate. The resulting differences were then plotted as a function of time, and a straight line was fitted to the plot. The slope of the straight line was taken to be the correction in initial value of the corresponding velocity, while the intercept at the initial time was applied as the correction to the coordinate. The trajectory was then repeated, using the corrected values. This iterative procedure was continued until coordinate deviations were randomly dispersed about zero. The matching was based upon the points every 5 seconds from 259.4 to 349.4 seconds. In this range, only five points (259.4, 264.4, 269.4, 329.4, and 344.4 seconds) exceeded 250 feet (Figure 29). The disagreement between the radar and theoretical RV trajectories is within the expected accuracy of the radar.

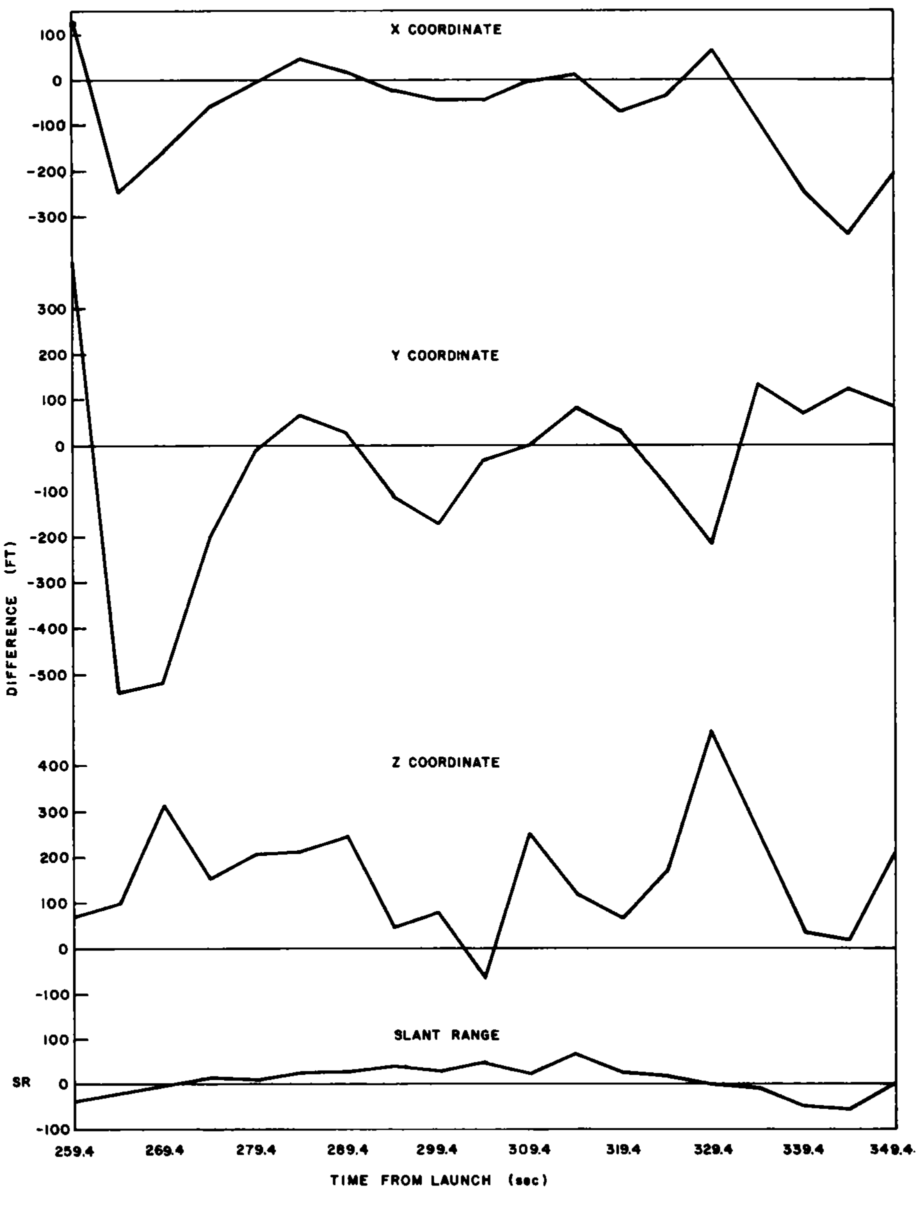

Figure 29. Coordinate distances between radar-observed and theoretical trajectories

Theoretical Versus Measured Trajectories

With agreement between the radar data and the theoretical RV trajectory established, a comparison of this trajectory with the plate-film trajectory was made. Coordinates from the theoretical RV trajectory were used to compute apparent azimuths and elevations relative to the camera locations at High Point. Those lines agreed with the corresponding lines computed from the plate-camera data to within 1.5 minutes of arc (300 feet) from 338 to 392 seconds. Deviation in time, measured from plate-camera chops, from the theoretically computed time at common azimuths and elevations did not exceed 0.25 second at any point. Since the radar lost contact with the RV C-band beacon at 360.00 seconds (168,000 feet), the theoretical trajectory from this point to impact was used to define that portion of the RV flight path.

The close agreement of the RV theoretical trajectory with both radar and plate-camera films indicated that this method was adequate for identification of the remaining re-entry objects. Theoretical trajectories were then computed for all the re-entry objects. The initial conditions for the various re-entry items were taken from the RV trajectory at the time of their ejection from the RV. Times of ejection were recorded during the flight from telemetered switches. These ejection times are shown in Table VII. The direction of ejection of each item was calculated from the telemetered orientation of the RV as measured by a roll-stabilized, free-gyro system. Orientation of the RV and components at launch is shown in Figure 30A. Orientation and ejection directions and velocities for the fuel rods, brackets, and holders is shown in Figure 30B. Ejection velocities and relative directions were measured during the preflight tests discussed in Section II.

TABLE VII

RFD-1 Ejection Times

Time from Launch (sec)	Items Ejected
282.09	12 experimental fuel rods 2 fuel-rod brackets 2 fuel-rod holders
322.94	2 reflectors 4 reflector springs 1 reflector band

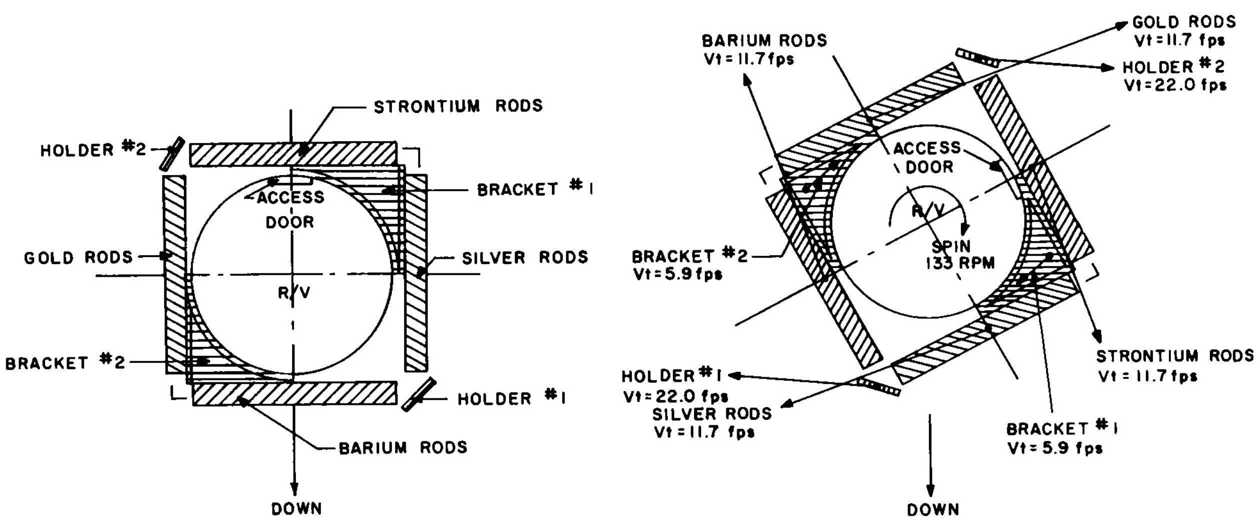

A. Orientation at launch B. Orientation at ejection

Figure 30. Ejection velocities for components ejected in the external fuel-rod experiment

In each case, the resulting ejection velocity and direction were applied as a perturbation of the initial conditions taken from the RV. Theoretical trajectories for each re-entry item are presented in Tables VIII through XX. A large scale graph similar to the graph of the measured trajectories described on page 46 was then constructed. However, an overlay combining both measured and computed trajectories proved too cumbersome for practical presentation. Figures 31 and 32 present similar information at a greatly distorted scale. The abscissa represents the azimuth of each object. The ordinate scale, however, represents the variation in elevation of each object from the RV. The advantages of this method of presentation are:

1. It allows expansion of the vertical scale, which provides more separation between individual objects.

2. The differential effect of drag and ejection conditions can be seen more readily, since, in differential plotting of the vertical scale, only the relative curvature of the various trajectories is apparent.

3. The entire trajectory is brought within the span of vision as a result of contracting the horizontal scale. This has a twofold effect: (a) it accentuates the differential behavior of the object, and (b) it facilitates reconstruction of the curves from their disconnected line segments.

4. The combination of differential plotting and contraction of the horizontal scale makes possible comparison between the behavior of the objects relative to one another as recorded in the optical data and their behavior relative to one another as predicted by the theoretical trajectory. Consequently, correlation of the two types of data can be established by both the position and shape of the resulting curve. This eliminates the confusion which would be created by a slight translation of the entire system of streaks in the vertical direction.

Comparison of the measured and theoretical trajectories shown in Figures 31 and 32 revealed the following:

1. The actual re-entry patterns of 13 of the 15 re-entry objects agreed with the patterns predicted for them. The plotted theoretical trajectories paralleled the plotted trails taken from Sandia Plate Cameras T-2 and P-2 for the major portion of the re-entry. During the latter part of the trajectories, most measured objects fell slightly lower than the theoretical trajectories, as a result of ablation and the associated reduction in W/C_DA. Each group of three fuel rods was considered to be visible as one object. Also, considering their angles of ejection, it was assumed that two reflector springs appeared as one object. The two fuel-rod holders did not follow any of the predicted trajectories, but rather re-entered at a much steeper angle.

2. The average deviation in elevation between the measured and theoretical trajectories was within 2 minutes of arc (400 feet) for all the objects except the fuel-rod holders. This is within the overall accuracy of the optical system and measurements. The extremely low W/C_DA of the fuel-rod holders caused them to decrease in velocity before a high temperature was reached. It is possible that they impacted intact.

The correlation between actual and predicted trajectories and the identification of objects is considered valid in spite of the deviation in elevation. Small inaccuracies in the W/C_DA, or perturbations in initial conditions, could cause such deviations; in addition, the limitations in accuracy of the optical system (mentioned above) contributed.

TABLE VIII

RFD-1 RV Re-entry Trajectory

TTA7622 38-64 SNAP 000635 091263 RV RFD-1 ATMOS= THEORETICAL ARDC 1959 ATMOSPHERE
CONTROLSNAP 000635 DATA-A=SNAP POSTDATA DATA-B=RFDA REFRACTION DATA-C= DATA-D=
OBSERVER 32.3467=LAT -64.6538=LONG 0.0000=ORNT 64=ELEV -64484=X . -36074=Y. -0=Z

RLTMA	RLTMB	RLTMC	WT	VI	GAMMAI	TAUI	AREA	CD	STAX	STAY	STAZ	VT	GAMMA	TAU
259.400	16953.	.00000	372.	20865.00	-5.30500	-40.09	1.0	1.00	-64484.	-36074.	-.47000	19901.9	-5.5625	-42.488

TIME	HITE	LAT	LONG	VT	GAMMA	TAU	Q	QC	DQC	AT	RANGE	SR	AZM	ELOBS
259.40	416756	34.29	-70.51	19902	-5.56	-42.5	.0029386	.00000	.622	.09	1.968-8	1942244	-65.121	9.764
260.00	415597	34.27	-70.48	19904	-5.58	-42.5	.0030322	.37603	.632	.09	1.91687	1931215	-65.248	9.814
262.00	411704	34.19	-70.39	19910	-5.64	-42.6	.0033467	1.6717	.664	.09	8.30804	1894512	-65.683	9.986
264.00	407769	34.12	-70.29	19916	-5.70	-42.6	.0037479	3.0348	.703	.09	14.7016	1857907	-66.136	10.16
266.00	403791	34.05	-70.20	19922	-5.76	-42.7	.0042179	4.4837	.746	.10	21.0977	1821409	-66.607	10.34
268.00	399770	33.98	-70.10	19928	-5.82	-42.8	.0047076	6.0179	.788	.10	27.4963	1785024	-67.099	10.52
270.00	395706	33.90	-70.01	19935	-5.88	-42.8	.0054409	7.6509	.848	.10	33.8975	1748761	-67.612	10.70
272.00	391599	33.83	-69.92	19941	-5.94	-42.9	.0061827	9.4032	.904	.10	40.3012	1712628	-68.147	10.89
274.00	387449	33.76	-69.82	19947	-6.00	-42.9	.0072157	11.281	.977	.10	46.7075	1676634	-68.707	11.07
276.00	383256	33.68	-69.73	19954	-6.06	-43.0	.0084398	13.314	1.06	.10	53.1164	1640791	-69.291	11.27
278.00	379020	33.61	-69.64	19961	-6.12	-43.1	.0098873	15.514	1.14	.10	59.5279	1605109	-69.903	11.46
280.00	374741	33.54	-69.54	19967	-6.18	-43.1	.0120544	17.918	1.26	.10	65.9422	1569601	-70.544	11.66
282.00	370420	33.47	-69.45	19974	-6.24	-43.2	.0142462	20.558	1.37	.10	72.3591	1534279	-71.215	11.87
282.00	370420	33.47	-69.45	19974	-6.24	-43.2	.0142462	20.558	1.37	.10	72.3591	1534279	-71.215	11.87
283.05	368134	33.43	-69.40	19977	-6.27	-43.2	.0162680	22.052	1.47	.10	75.7291	1515815	-71.580	11.97
284.00	366055	33.39	-69.35	19981	-6.30	-43.2	.0182836	23.490	1.56	.11	78.7788	1499159	-71.919	12.07
286.00	361648	33.32	-69.26	19988	-6.36	-43.3	.0225621	26.780	1.73	.11	85.2012	1464255	-72.658	12.28
288.00	357198	33.24	-69.17	19994	-6.42	-43.4	.0300778	30.496	2.00	.11	91.6264	1429585	-73.435	12.50
290.00	352704	33.17	-69.08	20001	-6.48	-43.4	.0395716	34.787	2.30	.11	98.0545	1395169	-74.252	12.72
292.00	348168	33.10	-68.98	20008	-6.54	-43.5	.0508641	39.683	2.60	.11	104.485	1361026	-75.111	12.94
294.00	343589	33.02	-68.89	20016	-6.60	-43.5	.0648070	45.222	2.94	.11	110.919	1327179	-76.017	13.16
296.00	338967	32.95	-68.80	20023	-6.66	-43.6	.0814053	51.454	3.30	.11	117.356	1293652	-76.971	13.39
298.00	334302	32.87	-68.71	20030	-6.72	-43.6	.1069719	58.510	3.78	.11	123.795	1260474	-77.978	13.62
300.00	329594	32.80	-68.61	20037	-6.78	-43.7	.1347200	66.537	4.24	.11	130.238	1227673	-79.042	13.85
302.00	324843	32.73	-68.52	20045	-6.84	-43.8	.1832004	75.692	4.95	.11	136.684	1195283	-80.166	14.09
304.00	320050	32.65	-68.43	20052	-6.90	-43.8	.2321904	86.233	5.58	.11	143.132	1163339	-81.355	14.33
306.00	315213	32.58	-68.34	20059	-6.96	-43.9	.3273402	98.363	6.62	.12	149.584	1131881	-82.614	14.57
308.00	310334	32.50	-66.25	20067	-7.01	-43.9	.4239551	112.55	7.54	.12	156.038	1100952	-83.947	14.81
310.00	305411	32.43	-68.15	20075	-7.07	-44.0	.6145020	129.07	9.08	.12	162.496	1070600	-85.359	15.05
312.00	300446	32.35	-68.06	20082	-7.13	-44.0	.8138161	148.64	10.5	.12	168.957	1040878	-86.857	15.29
314.00	295438	32.28	-67.97	20090	-7.19	-44.1	1.154503	171.46	12.5	.12	175.421	1011843	-88.446	15.52
316.00	290387	32.20	-67.88	20097	-7.25	-44.2	1.512359	198.22	14.3	.12	181.888	983558.	-90.131	15.75
318.00	285293	32.13	-67.79	20105	-7.31	-44.2	2.152600	229.36	17.0	.12	188.358	956091.	-91.919	15.97
320.00	280156	32.05	-67.70	20112	-7.37	-44.3	2.822259	265.95	19.5	.11	194.831	929517.	-93.815	16.19
322.00	274977	31.98	-67.61	20119	-7.43	-44.3	4.052048	308.61	23.4	.11	201.308	903919.	-95.825	16.38
322.00	274977	31.98	-67.61	20119	-7.43	-44.3	4.052048	308.61	23.4	.11	201.308	903919.	-95.825	16.38
323.05	272240	31.94	-67.56	20123	-7.46	-44.4	4.711488	334.13	25.2	.11	204.709	890899.	-96.928	16.48
324.00	269755	31.90	-67.52	20126	-7.49	-44.4	5.355993	358.88	26.9	.10	207.787	879382.	-97.954	16.57
326.00	264490	31.82	-67.43	20133	-7.54	-44.4	7.593666	417.81	32.0	.10	214.269	856001.	-100.21	16.73
328.00	259183	31.75	-67.34	20139	-7.60	-44.5	10.01221	486.70	36.8	.09	220.754	833877.	-102.59	16.86
330.00	253833	31.67	-67.24	20144	-7.66	-44.6	13.34066	565.82	42.5	.08	227.242	813113.	-105.09	16.97
332.00	248441	31.60	-67.15	20149	-7.72	-44.6	17.18985	656.51	48.2	.07	233.732	793820.	-107.73	17.04
334.00	243008	31.52	-67.06	20153	-7.78	-44.7	22.29097	759.49	54.9	.05	240.224	776108.	-110.49	17.07
336.00	237532	31.44	-66.97	20156	-7.84	-44.7	28.51603	876.43	62.1	.04	246.718	760092.	-113.38	17.05
338.00	232016	31.37	-66.88	20158	-7.89	-44.8	36.11852	1008.3	69.9	.02	253.214	745883.	-116.38	16.98
340.00	226458	31.29	-66.79	20158	-7.95	-44.8	45.87754	1156.7	78.7	-.01	259.710	733586.	-119.49	16.85
342.00	220859	31.21	-66.70	20157	-8.01	-44.9	56.90381	1323.1	87.6	-.04	266.208	723301.	-122.68	16.66
344.00	215221	31.14	-66.62	20153	-8.07	-44.9	71.78121	1508.7	98.3	-.08	272.705	715115.	-125.95	16.41
346.00	209543	31.06	-66.53	20146	-8.13	-45.0	87.88757	1715.8	109.	-.13	279.201	709100.	-129.27	16.09
348.00	203826	30.98	-66.44	20136	-8.19	-45.0	109.5006	1945.3	121.	-.19	285.695	705311.	-132.63	15.71

TTA7622 3B-64 SNAP 000635 091263 RV RFD-1 ATMOS= THEORETICAL ARDC 1959 ATMOSPHERE
CONTROLSNAP 000635 DATA-A=SNAP POSTDATA DATA-B=RFDA REFRACTION DATA-C= DATA-D=
OBSERVER 32.3467=LAT -64.6538=LONG 0.0000=ORNT 64=ELEV -64484=X . -36074=Y. -0=Z

RLTMA	RLTMB	RLTMC	WT	VI	GAMMAI	TAUI	AREA	CD	STAX	STAY	STAZ	VT	GAMMA	TAU
350.000	17044.	90.600	334.	21066.70	-7.87537	-42.52	1.0	1.00	-64484.	-36074.	-.47000	20121.2	-8.2480	-45.089

TIME	HITE	LAT	LONG	VT	GAMMA	TAU	Q	QC	DOC	AT	RANGE	SR	AZM	ELOBS
350.00	198071	30.91	-66.35	20121	-8.25	-45.1	133.0103	2199.7	133.	-.26	292.186	703781.	-135.99	15.26
352.00	192281	30.83	-66.26	20102	-8.31	-45.1	162.2690	2479.5	147.	-.34	298.673	704519.	-139.34	14.75
352.95	189518	30.79	-66.22	20091	-8.34	-45.2	177.6681	2622.1	153.	-.39	301.752	705661.	-140.91	14.49
354.00	186455	30.75	-66.17	20076	-8.37	-45.2	196.7944	2787.2	161.	-.48	305.153	707512.	-142.64	14.19
354.00	186455	30.75	-66.17	20076	-8.37	-45.2	196.7944	2787.2	161.	-.48	305.153	707512.	-142.64	14.19
356.00	180596	30.68	-66.08	20041	-8.43	-45.2	237.2375	3124.6	176.	-.61	311.624	712721.	-145.89	13.59
358.00	174707	30.60	-65.99	19998	-8.49	-45.3	285.6854	3492.9	192.	-.76	318.083	720085.	-149.06	12.95
360.00	168790	30.52	-65.91	19942	-8.55	-45.3	352.8237	3897.0	212.	-.97	324.527	729519.	-152.12	12.28
362.00	162849	30.45	-65.82	19872	-8.61	-45.4	434.9779	4343.2	234.	-1.2	330.952	740921.	-155.08	11.59
364.00	156888	30.37	-65.73	19783	-8.68	-45.5	535.4437	4833.8	257.	-1.5	337.352	754169.	-157.91	10.89
366.00	150913	30.29	-65.65	19671	-8.74	-45.5	666.8348	5373.4	283.	-2.0	343.720	769127.	-160.61	10.18
368.00	144932	30.22	-65.56	19527	-8.81	-45.6	834.7765	5967.8	312.	-2.5	350.047	785642.	-163.17	9.483
370.00	138954	30.14	-65.48	19342	-8.88	-45.6	1052.351	6621.9	343.	-3.2	356.323	803547.	-165.59	8.795
372.00	132994	30.07	-65.39	19106	-8.95	-45.6	1322.710	7338.6	374.	-4.1	362.531	822656.	-167.87	8.123
374.00	127068	30.00	-65.31	18805	-9.03	-45.7	1654.128	8117.0	404.	-5.2	368.654	842769.	-170.00	7.475
376.00	121196	29.92	-65.23	18426	-9.11	-45.7	2053.002	8952.3	431.	-6.6	374.667	863661.	-171.99	6.851
378.00	115405	29.85	-65.15	17952	-9.20	-45.8	2521.264	9835.2	451.	-8.2	380.543	885088.	-173.83	6.257
380.00	109725	29.79	-65.08	17363	-9.30	-45.8	3060.520	10750.	462.	-10.	386.249	906778.	-175.53	5.696
382.00	104196	29.72	-65.00	16635	-9.41	-45.9	3651.478	11675.	460.	-12.	391.742	928430.	-177.09	5.172
384.00	98862.	29.66	-64.93	15757	-9.53	-45.9	4236.731	12580.	441.	-15.	396.976	949711.	-178.50	4.684
384.00	98862.	29.66	-64.93	15757	-9.53	-45.9	4236.731	12580.	441.	-15.	396.976	949711.	-178.50	4.684
386.00	93779.	29.60	-64.87	14665	-9.68	-46.0	4709.089	13424.	398.	-19.	401.894	970250.	-179.77	4.238
386.00	93779.	29.60	-64.87	14665	-9.68	-46.0	4709.089	13424.	398.	-19.	401.894	970250.	-179.77	4.238
388.00	89023.	29.54	-64.81	13376	-9.85	-46.0	4964.476	14160.	336.	-21.	406.422	989590.	179.11	3.836
390.00	84633.	29.49	-64.75	12032	-10.1	-46.0	5002.519	14764.	268.	-21.	410.522	1007438	178.14	3.479
392.00	80620.	29.45	-64.70	10694	-10.3	-46.1	4829.191	15236.	204.	-20.	414.186	1023643	177.30	3.165
394.00	76979.	29.41	-64.66	9413.	-10.6	-46.1	4473.167	15589.	150.	-19.	417.425	1038154	176.58	2.883
396.00	73687.	29.38	-64.62	8238.	-10.9	-46.1	4005.149	15842.	106.	-17.	420.264	1051010	175.96	2.636
398.00	70711.	29.35	-64.59	7183.	-11.4	-46.1	3501.301	16021.	73.9	-15.	422.741	1062326	175.44	2.419
400.00	68014.	29.32	-64.56	6258.	-11.8	-46.2	3033.858	16145.	51.2	-13.	424.896	1072243	174.99	2.228
402.00	65559.	29.30	-64.54	5453.	-12.4	-46.2	2578.359	16230.	35.1	-12.	426.770	1080917	174.61	2.058
404.00	63312.	29.28	-64.52	4757.	-13.1	-46.2	2193.452	16288.	24.1	-10.	428.400	1088497	174.29	1.906
406.00	61242.	29.26	-64.50	4158.	-13.9	-46.2	1847.210	16328.	16.6	-8.6	429.820	1095121	174.01	1.770
408.00	59321.	29.25	-64.48	3647.	-14.7	-46.2	1555.371	16356.	11.5	-7.3	431.058	1100916	173.76	1.646
410.00	57525.	29.23	-64.47	3209.	-15.7	-46.2	1316.865	16375.	8.01	-6.3	432.142	1105995	173.56	1.532
412.00	55834.	29.22	-64.45	2831.	-16.9	-46.2	1107.247	16389.	5.61	-5.5	433.091	1110453	173.37	1.428
414.00	54234.	29.21	-64.44	2500.	-18.2	-46.2	932.7173	16398.	3.94	-4.8	433.924	1114367	173.22	1.330
416.00	52713.	29.20	-64.43	2212.	-19.6	-46.3	787.4406	16405.	2.78	-4.2	434.655	1117800	173.08	1.240
418.00	51260.	29.20	-64.43	1960.	-21.2	-46.3	661.4588	16409.	1.97	-3.6	435.296	1120809	172.96	1.154
420.00	49868.	29.19	-64.42	1741.	-23.1	-46.3	555.5404	16413.	1.40	-3.2	435.858	1123445	172.85	1.074
422.00	48529.	29.18	-64.41	1552.	-25.1	-46.3	473.0873	16415.	1.01	-2.7	436.351	1125754	172.76	.9977
424.00	47234.	29.18	-64.41	1389.	-27.3	-46.3	403.6531	16417.	.733	-2.3	436.783	1127777	172.68	.9250
426.00	45977.	29.17	-64.40	1250.	-29.7	-46.3	345.9218	16418.	.540	-2.0	437.164	1129549	172.61	.8552
428.00	44753.	29.17	-64.40	1130.	-32.4	-46.3	298.9566	16419.	.404	-1.7	437.498	1131102	172.55	.7880
428.00	44753.	29.17	-64.40	1130.	-32.4	-46.3	298.9566	16419.	.404	-1.7	437.498	1131102	172.55	.7880
430.00	43554.	29.17	-64.39	1035.	-35.2	-46.3	267.0602	16420.	.316	-1.2	437.793	1132466	172.49	.7229
432.00	42362.	29.16	-64.39	967.3	-38.1	-46.3	247.1199	16420.	.263	-.90	438.057	1133679	172.45	.6587
434.00	41162.	29.16	-64.39	917.6	-41.1	-46.3	235.0100	16421.	.229	-.66	438.295	1134769	172.40	.5947
436.00	39947.	29.16	-64.38	881.2	-44.1	-46.3	228.6340	16421.	.207	-.48	438.513	1135758	172.36	.5303
438.00	38709.	29.15	-64.38	853.8	-47.0	-46.3	228.2804	16422.	.193	-.38	438.712	1136660	172.33	.4652

TABLE IX

RFD-1 Strontium-Loaded Rod Trajectory

```
TTA7622 3B-64  8804 SNP 627 SR WHITE 040964 ED                            ATMOS= THEORETICAL ARDC 1959 ATMOSPHERE
CONTROLJIM AUG 28       DATA-A=                    DATA-B=RFDA REFRACTION  DATA-C=                    DATA-D=
OBSERVER    32.3467=LAT   -64.6538=LONG    0.0000=ORNT        64=ELEV      -64484=X .    -36074=Y.        -0=Z
   WT    CD  AREA       VI    GAMMAI        TAUI          LAT   LONG       VT    GAMMA      TAU
 43.7  1.00  1.00  20933. -5.98290 -40.74000  33.467000 -69.45  19974. -6.2713 -43.183
```

TIME	HITE	LAT	LONG	VT	GAMMA	TAU	Q	QC	DQC	AT	RANGE	SR	AZM	ELOBS
282.00	370528	33.47	-69.45	19974	-6.27	-43.2	.014192	.00000	1.37	.10	.000000	1535275	-71.203	11.86
284.00	366143	33.39	-69.36	19981	-6.33	-43.2	.018199	2.9205	1.55	.11	6.41933	1500149	-71.906	12.07
286.00	361715	33.32	-69.26	19988	-6.39	-43.3	.022497	6.2072	1.73	.11	12.8414	1465240	-72.645	12.28
288.00	357244	33.25	-69.17	19995	-6.45	-43.4	.029980	9.8960	2.00	.11	19.2663	1430564	-73.421	12.49
290.00	352730	33.17	-69.08	20002	-6.51	-43.4	.039517	14.182	2.29	.11	25.6940	1396141	-74.237	12.70
292.00	348174	33.10	-68.99	20009	-6.57	-43.5	.050847	19.076	2.60	.11	32.1246	1361991	-75.095	12.92
294.00	343574	33.02	-68.89	20016	-6.63	-43.5	.064852	24.615	2.94	.11	38.5580	1328136	-76.000	13.15
296.00	338932	32.95	-68.80	20023	-6.69	-43.6	.081598	30.853	3.30	.11	44.9943	1294602	-76.953	13.37
298.00	334246	32.88	-68.71	20030	-6.75	-43.7	.107276	37.917	3.79	.11	51.4335	1261415	-77.959	13.60
300.00	329518	32.80	-68.62	20037	-6.81	-43.7	.135494	45.961	4.26	.11	57.8757	1228606	-79.022	13.84
302.00	324747	32.73	-68.52	20044	-6.87	-43.8	.184178	55.142	4.96	.11	64.3208	1196206	-80.144	14.07
304.00	319933	32.65	-68.43	20051	-6.93	-43.8	.234012	65.716	5.60	.11	70.7689	1164252	-81.332	14.31
306.00	315076	32.58	-68.34	20059	-6.98	-43.9	.330023	77.895	6.65	.11	77.2199	1132783	-82.589	14.55
308.00	310176	32.50	-68.25	20066	-7.04	-43.9	.427012	92.136	7.57	.11	83.6738	1101843	-83.920	14.79
310.00	305233	32.43	-68.16	20073	-7.10	-44.0	.621498	108.73	9.13	.10	90.1307	1071479	-85.331	15.02
312.00	300248	32.35	-68.07	20079	-7.16	-44.1	.821508	128.40	10.5	.10	96.5904	1041745	-86.826	15.26
314.00	295220	32.28	-67.97	20086	-7.22	-44.1	1.16940	151.33	12.5	.09	103.053	1012698	-88.412	15.49
316.00	290150	32.20	-67.88	20092	-7.28	-44.2	1.52825	178.24	14.3	.09	109.518	984400.	-90.095	15.72
318.00	285037	32.13	-67.79	20097	-7.34	-44.2	2.18416	209.55	17.1	.07	115.986	956922.	-91.879	15.94
320.00	279882	32.05	-67.70	20101	-7.40	-44.3	2.86784	246.38	19.6	.06	122.456	930338.	-93.771	16.15
322.00	274685	31.98	-67.61	20104	-7.46	-44.3	4.11599	289.32	23.5	.03	128.927	904730.	-95.777	16.35
324.00	269446	31.90	-67.52	20105	-7.52	-44.4	5.47528	340.03	27.1		135.401	880186.	-97.900	16.53
326.00	264167	31.83	-67.43	20104	-7.57	-44.4	7.70853	399.10	32.2	-.05	141.875	856801.	-100.15	16.69
328.00	258847	31.75	-67.34	20099	-7.63	-44.5	10.1801	468.26	36.9	-.10	148.348	834676.	-102.52	16.82
330.00	253488	31.67	-67.25	20090	-7.69	-44.6	13.4820	547.53	42.5	-.18	154.820	813916.	-105.01	16.93
332.00	248091	31.60	-67.16	20076	-7.75	-44.6	17.3910	638.08	48.1	-.27	161.290	794631.	-107.64	16.99
334.00	242657	31.52	-67.07	20055	-7.81	-44.7	22.4003	740.57	54.5	-.38	167.754	776933.	-110.38	17.02
336.00	237188	31.45	-66.98	20026	-7.87	-44.7	28.6175	856.31	61.4	-.52	174.211	760932.	-113.25	17.00
338.00	231687	31.37	-66.89	19988	-7.93	-44.8	35.9556	986.09	68.5	-.69	180.658	746735.	-116.22	16.93
340.00	226156	31.29	-66.80	19937	-7.99	-44.8	45.4564	1130.9	76.5	-.90	187.091	734442.	-119.29	16.81
342.00	220599	31.22	-66.71	19871	-8.06	-44.9	55.8020	1291.7	84.2	-1.1	193.507	724142.	-122.43	16.62
344.00	215019	31.14	-66.62	19788	-8.12	-44.9	69.7436	1468.8	93.2	-1.5	199.899	715908.	-125.64	16.37
346.00	209422	31.07	-66.54	19683	-8.18	-45.0	84.3376	1663.4	101.	-1.8	206.261	709791.	-128.89	16.06
348.00	203813	30.99	-66.45	19555	-8.25	-45.0	103.320	1875.0	110.	-2.2	212.587	705819.	-132.15	15.69
350.00	198200	30.92	-66.36	19397	-8.32	-45.1	123.045	2104.1	118.	-2.7	218.868	703991.	-135.40	15.26
352.00	192590	30.85	-66.28	19208	-8.39	-45.1	146.610	2349.1	127.	-3.2	225.093	704273.	-138.62	14.78
354.00	186992	30.77	-66.20	18983	-8.47	-45.2	172.900	2609.6	134.	-3.8	231.252	706600.	-141.77	14.26
356.00	181416	30.70	-66.11	18717	-8.54	-45.2	201.720	2884.0	140.	-4.5	237.332	710876.	-144.84	13.70
358.00	175874	30.63	-66.03	18406	-8.63	-45.3	233.034	3169.8	145.	-5.2	243.319	716972.	-147.80	13.11
360.00	170379	30.56	-65.95	18045	-8.71	-45.3	272.155	3465.7	150.	-6.1	249.199	724731.	-150.63	12.50
362.00	164945	30.49	-65.87	17622	-8.81	-45.4	315.791	3770.4	154.	-7.1	254.952	733969.	-153.33	11.88
364.00	159591	30.42	-65.80	17133	-8.91	-45.4	362.915	4080.1	155.	-8.2	260.559	744478.	-155.87	11.27
366.00	154336	30.36	-65.72	16572	-9.02	-45.5	412.725	4389.9	154.	-9.3	265.996	756029.	-158.26	10.66
368.00	149202	30.30	-65.65	15934	-9.15	-45.5	468.670	4695.3	151.	-11.	271.239	768379.	-160.47	10.06
370.00	144214	30.24	-65.58	15213	-9.28	-45.6	523.298	4991.0	144.	-12.	276.263	781272.	-162.52	9.494
372.00	139395	30.18	-65.52	14416	-9.43	-45.6	573.085	5270.3	134.	-13.	281.041	794448.	-164.40	8.951
374.00	134769	30.13	-65.46	13551	-9.61	-45.6	614.089	5526.9	122.	-14.	285.550	807657.	-166.10	8.439
376.00	130356	30.08	-65.40	12634	-9.80	-45.7	644.620	5756.3	107.	-15.	289.770	820667.	-167.64	7.962
378.00	126173	30.03	-65.35	11681	-10.0	-45.7	662.458	5955.6	91.9	-15.	293.687	833274.	-169.03	7.522
380.00	122231	29.99	-65.30	10713	-10.3	-45.7	664.116	6123.9	76.3	-15.	297.292	845308.	-170.26	7.116

TTA7622 38-64 8804 SNP 627 SR WHITE 040964 ED ATMOS= THEORETICAL ARDC 1959 ATMOSPHERE
CONTROLJIM AUG 28 DATA-A= DATA-B=RFDA REFRACTION DATA-C= DATA-D=
OBSERVER 32.3467=LAT -64.6538=LONG 0.0000=ORNT 64=ELEV -64484=X . -36074=Y. -0=Z

WT	CD	AREA	VI	GAMMAI	TAUI	LAT	LONG	VT	GAMMA	TAU
43.7	1.00	1.00	10713.	-9.60165	-40.58021	29.946427	-65.26	9755.9	-10.553	-45.759

TIME	HITE	LAT	LONG	VT	GAMMA	TAU	Q	QC	DOC	AT	RANGE	SR	AZM	ELOBS
382.00	118534	29.95	-65.26	9756.	-10.6	-45.8	649.019	6261.8	61.7	-15.	300.584	856641.	-171.35	6.746
384.00	115081	29.91	-65.22	8833.	-10.9	-45.8	618.467	6371.8	48.6	-14.	303.570	867192.	-172.32	6.409
386.00	111863	29.88	-65.18	7956.	-11.3	-45.8	585.059	6458.0	37.8	-13.	306.265	876920.	-173.17	6.104
388.00	108867	29.85	-65.15	7141.	-11.7	-45.8	540.865	6524.1	28.8	-12.	308.684	885817.	-173.91	5.827
390.00	106078	29.82	-65.12	6392.	-12.2	-45.9	493.434	6574.3	21.7	-11.	310.849	893902.	-174.56	5.576
392.00	103477	29.80	-65.09	5713.	-12.7	-45.9	446.723	6611.8	16.2	-10.	312.782	901214.	-175.14	5.349
394.00	101046	29.78	-65.07	5104.	-13.3	-45.9	399.761	6639.8	12.0	-8.9	314.506	907803.	-175.64	5.141
396.00	98766.	29.76	-65.05	4563.	-14.0	-45.9	357.036	6660.6	8.92	-7.9	316.042	913726.	-176.08	4.951
398.00	96619.	29.74	-65.03	4082.	-14.8	-45.9	317.507	6676.0	6.62	-7.0	317.412	919045.	-176.47	4.777
400.00	94588.	29.73	-65.02	3659.	-15.7	-45.9	280.659	6687.4	4.92	-6.2	318.633	923817.	-176.81	4.615
402.00	92657.	29.72	-65.00	3287.	-16.7	-45.9	250.528	6695.9	3.69	-5.4	319.725	928098.	-177.11	4.465
404.00	90813.	29.71	-64.99	2958.	-17.8	-46.0	221.578	6702.3	2.77	-4.8	320.701	931940.	-177.38	4.324
406.00	89043.	29.69	-64.98	2670.	-19.0	-46.0	197.592	6707.2	2.09	-4.2	321.575	935387.	-177.62	4.193
408.00	87338.	29.69	-64.97	2416.	-20.3	-46.0	176.903	6710.8	1.60	-3.7	322.359	938484.	-177.83	4.068
410.00	85687.	29.68	-64.96	2193.	-21.8	-46.0	157.753	6713.6	1.23	-3.2	323.063	941265.	-178.02	3.950
412.00	84083.	29.67	-64.95	1997.	-23.4	-46.0	141.986	6715.8	.951	-2.9	323.697	943766.	-178.19	3.836
414.00	82519.	29.66	-64.94	1824.	-25.1	-46.0	128.443	6717.5	.744	-2.5	324.267	946016.	-178.34	3.728
416.00	80989.	29.66	-64.94	1672.	-26.9	-46.0	116.120	6718.8	.587	-2.2	324.782	948040.	-178.47	3.624
418.00	79487.	29.65	-64.93	1539.	-28.9	-46.0	105.675	6719.8	.468	-1.9	325.247	949863.	-178.60	3.523
420.00	78009.	29.65	-64.92	1422.	-31.1	-46.0	97.1806	6720.7	.379	-1.7	325.667	951503.	-178.71	3.425
422.00	76551.	29.64	-64.92	1318.	-33.3	-46.0	89.4882	6721.4	.309	-1.5	326.047	952980.	-178.81	3.330
424.00	75112.	29.64	-64.91	1228.	-35.7	-46.0	82.6937	6721.9	.255	-1.3	326.391	954310.	-178.90	3.237
426.00	73688.	29.63	-64.91	1148.	-38.1	-46.0	77.7998	6722.4	.214	-1.2	326.703	955506.	-178.98	3.146
428.00	72278.	29.63	-64.91	1077.	-40.6	-46.0	73.3671	6722.8	.181	-1.0	326.985	956580.	-179.05	3.055
430.00	70881.	29.63	-64.90	1015.	-43.2	-46.0	69.3894	6723.1	.155	-.91	327.241	957544.	-179.12	2.966
432.00	69497.	29.62	-64.90	960.0	-45.8	-46.0	66.2328	6723.4	.134	-.80	327.472	958407.	-179.17	2.878
434.00	68126.	29.62	-64.90	911.1	-48.5	-46.0	63.9510	6723.7	.118	-.72	327.681	959179.	-179.23	2.791
436.00	66768.	29.62	-64.89	867.3	-51.1	-46.0	61.8103	6723.9	.104	-.64	327.869	959866.	-179.28	2.706
438.00	65425.	29.62	-64.89	828.4	-53.8	-46.0	59.8581	6724.1	.093	-.57	328.039	960476.	-179.32	2.623
440.00	64096.	29.62	-64.69	793.5	-56.3	-46.0	58.6625	6724.3	.084	-.51	328.192	961017.	-179.36	2.540
442.00	62784.	29.61	-64.89	761.8	-58.8	-46.0	57.7234	6724.4	.076	-.47	328.329	961493.	-179.39	2.460
444.00	61489.	29.61	-64.89	732.9	-61.3	-46.0	56.7530	6724.6	.070	-.43	328.451	961910.	-179.43	2.380
446.00	60214.	29.61	-64.88	706.6	-63.6	-46.0	55.8125	6724.7	.064	-.39	328.561	962274.	-179.45	2.302
448.00	58958.	29.61	-64.88	682.5	-65.8	-46.0	55.5052	6724.8	.059	-.36	328.659	962589.	-179.48	2.226
450.00	57723.	29.61	-64.88	659.8	-68.0	-46.0	55.1482	6724.9	.055	-.34	328.745	962861.	-179.50	2.151
452.00	56512.	29.61	-64.88	638.6	-70.0	-45.9	54.6710	6725.0	.051	-.32	328.822	963093.	-179.52	2.077
454.00	55323.	29.61	-64.88	618.9	-71.9	-45.9	54.1213	6725.1	.047	-.29	328.890	963289.	-179.54	2.005
456.00	54159.	29.61	-64.88	600.4	-73.6	-45.9	53.9862	6725.2	.044	-.28	328.949	963454.	-179.55	1.935
458.00	53019.	29.61	-64.88	582.6	-75.3	-45.9	53.8407	6725.3	.041	-.27	329.002	963590.	-179.57	1.867
460.00	51905.	29.60	-64.88	565.6	-76.8	-45.8	53.5011	6725.4	.039	-.25	329.047	963701.	-179.58	1.800
462.00	50816.	29.60	-64.88	549.6	-78.2	-45.8	53.0531	6725.5	.036	-.24	329.087	963789.	-179.59	1.734
464.00	49753.	29.60	-64.88	534.5	-79.5	-45.7	52.6783	6725.5	.034	-.23	329.122	963858.	-179.60	1.671
466.00	48714.	29.60	-64.88	520.0	-80.7	-45.7	52.6229	6725.6	.032	-.22	329.152	963910.	-179.61	1.609
468.00	47700.	29.60	-64.88	505.9	-81.8	-45.6	52.3622	6725.7	.030	-.21	329.178	963947.	-179.61	1.548
470.00	46711.	29.60	-64.88	492.5	-82.8	-45.6	51.9747	6725.7	.028	-.20	329.200	963971.	-179.62	1.489
472.00	45745.	29.60	-64.88	479.8	-83.6	-45.5	51.5179	6725.8	.027	-.19	329.220	963984.	-179.62	1.431
474.00	44803.	29.60	-64.68	467.9	-84.4	-45.4	51.1291	6725.8	.025	-.18	329.236	963988.	-179.63	1.375
476.00	43883.	29.60	-64.88	456.4	-85.1	-45.3	51.0469	6725.9	.024	-.17	329.250	963984.	-179.63	1.320
478.00	42984.	29.60	-64.88	445.2	-85.8	-45.2	50.7993	6725.9	.022	-.17	329.262	963974.	-179.63	1.267
480.00	42107.	29.60	-64.88	434.5	-86.3	-45.0	50.4538	6726.0	.021	-.16	329.272	963958.	-179.64	1.215

TABLE X

RFD-1 Barium-Loaded Rod Trajectory

TTA7622 38-64 8805 SNP 628 BA WHITE 040964 ED ATMOS= THEORETICAL ARDC 1959 ATMOSPHERE
CONTROLJIM AUG 28 DATA-A= DATA-B=RFDA REFRACTION DATA-C= DATA-D=
OBSFRVER 32.3467=LAT -64.6538=LONG 0.0000=ORNT 64=ELEV -64484=X . -36074=Y. -0=Z

WT	CD	AREA	VI	GAMMAI	TAUI	LAT	LONG	VT	GAMMA	TAU
44.4	1.00	1.00	20933.	-5.92350	-40.74000	33.467000	-69.45	19974.	-6.2090	-43.183

TIME	HITE	LAT	LONG	VT	GAMMA	TAU	Q	QC	DQC	AT	RANGE	SR	AZM	ELOBS
282.00	370528	33.47	-69.45	19974	-6.21	-43.2	.014192	.00000	1.37	.10	.000000	1535275	-71.203	11.86
284.00	366186	33.39	-69.36	19981	-6.27	-43.2	.018157	2.9185	1.55	.10	6.42002	1500157	-71.906	12.07
286.00	361801	33.32	-69.26	19987	-6.33	-43.3	.022413	6.2000	1.73	.11	12.8428	1465256	-72.645	12.28
288.00	357374	33.25	-69.17	19994	-6.39	-43.4	.029706	9.8743	1.99	.11	19.2683	1430590	-73.421	12.49
290.00	352903	33.17	-69.08	20001	-6.45	-43.4	.039151	14.140	2.28	.11	25.6967	1396176	-74.237	12.71
292.00	348390	33.10	-68.99	20008	-6.51	-43.5	.050190	19.007	2.59	.11	32.1278	1362035	-75.096	12.93
294.00	343833	33.02	-68.89	20015	-6.57	-43.5	.064062	24.510	2.92	.11	38.5618	1328191	-76.000	13.16
296.00	339234	32.95	-68.80	20022	-6.63	-43.6	.079940	30.698	3.27	.11	44.9986	1294667	-76.954	13.39
298.00	334592	32.88	-68.71	20029	-6.69	-43.7	.105378	37.692	3.75	.11	51.4384	1261492	-77.960	13.62
300.00	329907	32.80	-68.62	20036	-6.75	-43.7	.131524	45.644	4.19	.11	57.8810	1228693	-79.023	13.86
302.00	325179	32.73	-68.52	20043	-6.80	-43.8	.179760	54.697	4.90	.11	64.3266	1196305	-80.146	14.09
304.00	320409	32.65	-68.43	20051	-6.86	-43.8	.228502	65.146	5.53	.11	70.7751	1164364	-81.333	14.33
306.00	315595	32.58	-68.34	20058	-6.92	-43.9	.319748	77.158	6.55	.11	77.2265	1132908	-82.590	14.57
308.00	310739	32.50	-68.25	20065	-6.98	-43.9	.415864	91.187	7.47	.11	83.6808	1101981	-83.922	14.81
310.00	305839	32.43	-68.16	20072	-7.04	-44.0	.597196	107.51	8.95	.10	90.1381	1071631	-85.332	15.06
312.00	300897	32.35	-68.07	20078	-7.10	-44.1	.795433	126.82	10.3	.10	96.5982	1041911	-86.828	15.29
314.00	295913	32.28	-67.97	20085	-7.16	-44.1	1.12039	149.33	12.3	.10	103.061	1012878	-88.415	15.53
316.00	290886	32.20	-67.88	20091	-7.22	-44.2	1.47612	175.71	14.1	.09	109.527	984596.	-90.097	15.76
318.00	285816	32.13	-67.79	20096	-7.28	-44.2	2.08276	206.40	16.7	.08	115.995	957133.	-91.882	15.99
320.00	280705	32.05	-67.70	20100	-7.34	-44.3	2.74774	242.39	19.2	.06	122.465	930564.	-93.774	16.20
322.00	275551	31.98	-67.61	20104	-7.39	-44.3	3.90795	284.34	22.9	.04	128.937	904971.	-95.780	16.40
324.00	270355	31.90	-67.52	20105	-7.45	-44.4	5.15557	333.65	26.3		135.411	880443.	-97.904	16.58
326.00	265119	31.83	-67.43	20104	-7.51	-44.4	7.30598	391.04	31.3	-.04	141.886	857073.	-100.15	16.75
328.00	259842	31.75	-67.34	20100	-7.57	-44.5	9.56607	458.27	35.8	-.09	148.360	834963.	-102.52	16.89
330.00	254526	31.67	-67.25	20093	-7.63	-44.6	12.8441	535.35	41.5	-.16	154.834	814217.	-105.02	16.99
332.00	249171	31.60	-67.16	20080	-7.69	-44.6	16.3928	623.60	46.7	-.24	161.304	794945.	-107.64	17.07
334.00	243779	31.52	-67.07	20061	-7.75	-44.7	21.3714	723.40	53.2	-.35	167.771	777259.	-110.39	17.10
336.00	238351	31.45	-66.98	20035	-7.81	-44.7	27.0590	836.37	59.7	-.48	174.231	761269.	-113.25	17.09
338.00	232891	31.37	-66.89	19999	-7.87	-44.8	34.3648	962.97	67.0	-.64	180.682	747082.	-116.23	17.02
340.00	227399	31.29	-66.80	19952	-7.93	-44.8	43.1243	1104.6	74.7	-.84	187.120	734799.	-119.30	16.90
342.00	221880	31.22	-66.71	19890	-7.99	-44.9	53.4523	1261.8	82.5	-1.1	193.541	724510.	-122.45	16.72
344.00	216337	31.14	-66.62	19813	-8.06	-44.9	66.3978	1435.4	91.2	-1.4	199.941	716286.	-125.66	16.47
346.00	210776	31.07	-66.54	19715	-8.12	-45.0	80.4559	1625.9	99.3	-1.7	206.313	710182.	-128.92	16.17
348.00	205200	30.99	-66.45	19595	-8.19	-45.0	98.7581	1833.5	109.	-2.1	212.651	706227.	-132.19	15.80
350.00	199617	30.92	-66.36	19447	-8.25	-45.1	117.389	2058.6	116.	-2.5	218.947	704421.	-135.45	15.37
352.00	194035	30.84	-66.28	19270	-8.33	-45.1	140.259	2299.5	125.	-3.0	225.191	704735.	-138.67	14.90
354.00	188460	30.77	-66.19	19058	-8.40	-45.2	165.896	2556.5	132.	-3.6	231.372	707107.	-141.83	14.37
356.00	182904	30.70	-66.11	18807	-8.48	-45.2	194.156	2828.1	139.	-4.2	237.479	711443.	-144.91	13.81
358.00	177377	30.63	-66.03	18513	-8.56	-45.3	224.942	3111.9	145.	-4.9	243.499	717619.	-147.88	13.22
360.00	171891	30.56	-65.95	18170	-8.64	-45.3	261.928	3406.5	150.	-5.8	249.417	725482.	-150.74	12.61
362.00	166461	30.49	-65.87	17769	-8.74	-45.4	304.868	3710.5	154.	-6.7	255.215	734854.	-153.45	11.99
364.00	161103	30.42	-65.79	17304	-8.84	-45.4	350.922	4021.0	156.	-7.8	260.873	745529.	-156.01	11.37
366.00	155836	30.36	-65.72	16771	-8.94	-45.5	399.203	4333.0	156.	-8.8	266.371	757286.	-158.42	10.75
368.00	150682	30.29	-65.65	16163	-9.06	-45.5	454.119	4642.0	153.	-10.	271.684	769885.	-160.66	10.15
370.00	145661	30.23	-65.58	15475	-9.19	-45.6	509.955	4943.5	148.	-11.	276.788	783075.	-162.73	9.574
372.00	140800	30.17	-65.51	14707	-9.34	-45.6	562.825	5230.9	139.	-13.	281.656	796598.	-164.63	9.024
374.00	136122	30.12	-65.45	13867	-9.50	-45.6	609.116	5497.9	127.	-14.	286.264	810202.	-166.37	8.503
376.00	131648	30.07	-65.39	12968	-9.69	-45.7	645.001	5739.3	114.	-14.	290.590	823648.	-167.94	8.016
378.00	127397	30.02	-65.34	12026	-9.90	-45.7	667.069	5951.3	98.2	-15.	294.618	836722.	-169.35	7.566
380.00	123381	29.97	-65.29	11064	-10.1	-45.7	672.880	6131.8	82.4	-15.	298.336	849245.	-170.61	7.151

TTA7622 3B-64 8805 SNP 628 BA WHITE 040964 ED ATMOS= THEORETICAL ARDC 1959 ATMOSPHERE

CONTROLJIM AUG 28 DATA-A= DATA-B=RFDA REFRACTION DATA-C= DATA-D=

OBSERVER 32.3467=LAT -64.6538=LONG 0.0000=ORNT 64=ELEV -64484=X . -36074=Y. -0=Z

WT	CD	AREA	VI	GAMMAI	TAUI	LAT	LONG	VT	GAMMA	TAU
44.4	1.00	1.00	11063.	-9.50080	-40.75242	29.932550	-65.24	10107.	-10.409	-45.767

TIME	HITE	LAT	LONG	VT	GAMMA	TAU	Q	QC	DQC	AT	RANGE	SR	AZM	ELOBS
382.00	119608	29.93	-65.24	10107	-10.4	-45.8	661.351	6281.3	67.2	-15.	301.743	861081.	-171.73	6.772
384.00	116076	29.90	-65.20	9174.	-10.7	-45.8	640.340	6401.9	53.7	-14.	304.842	872137.	-172.72	6.426
386.00	112780	29.86	-65.16	8280.	-11.1	-45.8	607.819	6497.3	41.9	-14.	307.645	882359.	-173.59	6.113
388.00	109710	29.83	-65.13	7443.	-11.5	-45.8	562.819	6571.0	32.1	-12.	310.167	891727.	-174.36	5.828
390.00	106852	29.80	-65.10	6670.	-11.9	-45.9	519.194	6627.2	24.3	-11.	312.427	900256.	-175.03	5.570
392.00	104187	29.78	-65.07	5968.	-12.5	-45.9	470.188	6669.5	18.2	-10.	314.447	907980.	-175.62	5.337
394.00	101697	29.76	-65.05	5334.	-13.0	-45.9	423.837	6701.1	13.6	-9.3	316.249	914948.	-176.14	5.125
396.00	99365.	29.74	-65.03	4767.	-13.7	-45.9	377.730	6724.6	10.1	-8.3	317.856	921216.	-176.59	4.930
398.00	97171.	29.72	-65.01	4265.	-14.5	-45.9	337.704	6742.0	7.50	-7.4	319.289	926846.	-176.99	4.752
400.00	95099.	29.71	-64.99	3821.	-15.3	-45.9	297.829	6755.0	5.56	-6.4	320.567	931899.	-177.34	4.587
402.00	93131.	29.69	-64.98	3430.	-16.2	-46.0	266.406	6764.6	4.17	-5.7	321.709	936432.	-177.65	4.434
404.00	91256.	29.68	-64.96	3084.	-17.3	-46.0	236.057	6771.9	3.12	-5.0	322.730	940498.	-177.93	4.292
406.00	89459.	29.67	-64.95	2782.	-18.5	-46.0	209.615	6777.3	2.36	-4.4	323.643	944148.	-178.17	4.158
408.00	87730.	29.66	-64.94	2515.	-19.7	-46.0	187.959	6781.4	1.80	-3.9	324.463	947425.	-178.39	4.032
410.00	86059.	29.65	-64.93	2280.	-21.1	-46.0	167.623	6784.6	1.37	-3.4	325.198	950368.	-178.58	3.912
412.00	84437.	29.64	-64.92	2074.	-22.7	-46.0	150.216	6787.0	1.06	-3.0	325.859	953014.	-178.76	3.798
414.00	82858.	29.64	-64.91	1892.	-24.4	-46.0	135.882	6788.9	.828	-2.7	326.455	955394.	-178.91	3.689
416.00	81315.	29.63	-64.91	1732.	-26.2	-46.0	122.723	6790.3	.651	-2.3	326.992	957535.	-179.05	3.585
418.00	79801.	29.62	-64.90	1592.	-28.1	-46.0	111.200	6791.5	.517	-2.0	327.477	959462.	-179.18	3.484
420.00	78314.	29.62	-64.89	1469.	-30.2	-46.0	102.155	6792.4	.416	-1.8	327.915	961198.	-179.29	3.386
422.00	76848.	29.61	-64.89	1360.	-32.4	-46.0	93.9077	6793.2	.338	-1.6	328.311	962760.	-179.39	3.291
424.00	75401.	29.61	-64.88	1264.	-34.7	-46.0	86.5942	6793.8	.278	-1.4	328.669	964168.	-179.48	3.198
426.00	73970.	29.61	-64.88	1180.	-37.1	-46.0	81.0559	6794.3	.232	-1.2	328.994	965434.	-179.56	3.106
428.00	72554.	29.60	-64.88	1106.	-39.6	-46.0	76.3110	6794.7	.195	-1.1	329.288	966573.	-179.64	3.016
430.00	71151.	29.60	-64.87	1040.	-42.1	-46.0	72.0289	6795.1	.166	-.96	329.555	967595.	-179.71	2.927
432.00	69761.	29.60	-64.87	982.6	-44.8	-46.0	68.4152	6795.4	.143	-.84	329.796	968511.	-179.77	2.839
434.00	68384.	29.59	-64.87	931.3	-47.4	-46.0	65.9672	6795.6	.126	-.75	330.014	969332.	-179.82	2.753
436.00	67020.	29.59	-64.86	885.3	-50.0	-46.0	63.6574	6795.9	.111	-.67	330.211	970063.	-179.87	2.668
438.00	65669.	29.59	-64.86	844.5	-52.7	-46.0	61.5537	6796.1	.098	-.60	330.388	970714.	-179.92	2.585
440.00	64334.	29.59	-64.86	808.1	-55.3	-46.0	60.0890	6796.3	.088	-.54	330.548	971292.	-179.96	2.503
442.00	63014.	29.59	-64.86	775.0	-57.8	-46.0	59.0836	6796.4	.080	-.49	330.691	971802.	-179.99	2.422
444.00	61711.	29.58	-64.85	744.9	-60.3	-46.0	58.0506	6796.6	.073	-.44	330.820	972250.	179.98	2.343
446.00	60427.	29.58	-64.85	717.6	-62.6	-46.0	57.0429	6796.7	.067	-.40	330.935	972642.	179.95	2.265
448.00	59162.	29.58	-64.85	692.7	-64.9	-46.0	56.5722	6796.9	.061	-.37	331.037	972983.	179.92	2.189
450.00	57918.	29.58	-64.85	669.4	-67.1	-46.0	56.2283	6797.0	.057	-.35	331.129	973277.	179.90	2.114
452.00	56696.	29.58	-64.85	647.5	-69.2	-46.0	55.7374	6797.1	.053	-.33	331.209	973530.	179.88	2.040
454.00	55497.	29.58	-64.85	627.2	-71.1	-45.9	55.1712	6797.2	.049	-.30	331.281	973745.	179.86	1.969
456.00	54322.	29.58	-64.85	608.3	-72.9	-45.9	54.9435	6797.3	.046	-.29	331.344	973926.	179.85	1.899
458.00	53172.	29.58	-64.85	590.1	-74.6	-45.9	54.8236	6797.4	.043	-.27	331.399	974077.	179.83	1.830
460.00	52047.	29.58	-64.85	572.8	-76.2	-45.9	54.5022	6797.5	.040	-.26	331.447	974201.	179.82	1.763
462.00	50947.	29.58	-64.85	556.4	-77.6	-45.8	54.0559	6797.5	.037	-.24	331.490	974301.	179.81	1.698
464.00	49872.	29.58	-64.85	541.0	-79.0	-45.8	53.6161	6797.6	.035	-.23	331.527	974380.	179.80	1.634
466.00	48823.	29.57	-64.85	526.2	-80.2	-45.7	53.5891	6797.7	.033	-.23	331.558	974441.	179.79	1.572
468.00	47798.	29.57	-64.84	511.9	-81.3	-45.7	53.3455	6797.7	.031	-.22	331.586	974486.	179.78	1.511
470.00	46799.	29.57	-64.84	498.1	-82.4	-45.6	52.9613	6797.8	.029	-.21	331.610	974517.	179.78	1.452
472.00	45823.	29.57	-64.84	485.2	-83.3	-45.5	52.4996	6797.9	.028	-.19	331.630	974536.	179.77	1.395
474.00	44871.	29.57	-64.84	473.0	-84.1	-45.5	52.0680	6797.9	.026	-.18	331.648	974545.	179.77	1.339
476.00	43941.	29.57	-64.84	461.3	-84.8	-45.3	51.9972	6798.0	.025	-.18	331.663	974545.	179.77	1.284
478.00	43033.	29.57	-64.84	449.9	-85.5	-45.2	51.7531	6798.0	.023	-.17	331.676	974539.	179.76	1.230
480.00	42147.	29.57	-64.84	438.9	-86.1	-45.1	51.4019	6798.1	.022	-.16	331.687	974526.	179.76	1.178

TABLE XI

RFD-1 Silver-Loaded Rod Trajectory

```
TTA7622 38-64  8806 SNP 629 AG WHITE 040964 ED                          ATMOS= THEORETICAL ARDC 1959 ATMOSPHERE
CONTROLJIM AUG 28        DATA-A=                 DATA-B=RFDA REFRACTION  DATA-C=                   DATA-D=
OBSERVER    32.3467=LAT   -64.6538=LONG    0.0000=ORNT          64=ELEV      -64484=X .    -36074=Y.        -0=Z
   WT     CD  AREA        VI    GAMMAI         TAUI          LAT    LONG       VT    GAMMA      TAU
  49.1  1.00  1.00   20933. -5.96460 -40.74000  33.467000 -69.45  19974. -6.2521 -43.183
```

TIME	HITE	LAT	LONG	VT	GAMMA	TAU	Q	QC	DQC	AT	RANGE	SR	AZM	ELOBS
282.00	370528	33.47	-69.45	19974	-6.25	-43.2	.014192	.00000	1.37	.10	.000000	1535275	-71.203	11.86
284.00	366156	33.39	-69.36	19981	-6.31	-43.2	.018186	2.9198	1.55	.10	6.41954	1500152	-71.906	12.07
286.00	361742	33.32	-69.26	19988	-6.37	-43.3	.022471	6.2049	1.73	.11	12.8418	1465245	-72.645	12.28
288.00	357284	33.25	-69.17	19994	-6.43	-43.4	.029896	9.8893	1.99	.11	19.2669	1430572	-73.421	12.49
290.00	352784	33.17	-69.08	20001	-6.49	-43.4	.039404	14.169	2.29	.11	25.6948	1396152	-74.237	12.71
292.00	348240	33.10	-68.99	20008	-6.55	-43.5	.050645	19.055	2.60	.11	32.1256	1362005	-75.095	12.93
294.00	343654	33.02	-68.89	20015	-6.61	-43.5	.064609	24.583	2.94	.11	38.5592	1328153	-76.000	13.15
296.00	339025	32.95	-68.80	20023	-6.67	-43.6	.081088	30.805	3.29	.11	44.9957	1294622	-76.953	13.38
298.00	334353	32.88	-68.71	20030	-6.73	-43.7	.106692	37.848	3.78	.11	51.4351	1261439	-77.960	13.61
300.00	329638	32.80	-68.62	20037	-6.79	-43.7	.134272	45.864	4.24	.11	57.8774	1228632	-79.022	13.84
302.00	324880	32.73	-68.52	20044	-6.85	-43.8	.182820	55.005	4.95	.11	64.3227	1196236	-80.145	14.08
304.00	320079	32.65	-68.43	20051	-6.91	-43.8	.231874	65.537	5.57	.11	70.7709	1164285	-81.332	14.32
306.00	315236	32.58	-68.34	20058	-6.97	-43.9	.326865	77.658	6.62	.11	77.2221	1132820	-82.589	14.56
308.00	310349	32.50	-68.25	20066	-7.02	-43.9	.423591	91.835	7.54	.11	83.6762	1101884	-83.921	14.79
310.00	305420	32.43	-68.16	20073	-7.08	-44.0	.614038	108.35	9.08	.11	90.1333	1071525	-85.331	15.03
312.00	300448	32.35	-68.07	20079	-7.14	-44.1	.813520	127.91	10.5	.10	96.5933	1041794	-86.827	15.27
314.00	295433	32.28	-67.97	20086	-7.20	-44.1	1.15440	150.71	12.5	.10	103.056	1012751	-88.413	15.50
316.00	290376	32.20	-67.88	20092	-7.26	-44.2	1.51235	177.46	14.3	.09	109.522	984457.	-90.096	15.73
318.00	285276	32.13	-67.79	20098	-7.32	-44.2	2.15324	208.59	17.0	.08	115.990	956982.	-91.880	15.95
320.00	280134	32.05	-67.70	20102	-7.38	-44.3	2.82238	245.14	19.5	.07	122.460	930401.	-93.773	16.17
322.00	274950	31.98	-67.61	20106	-7.44	-44.3	4.05304	287.75	23.4	.04	128.933	904796.	-95.778	16.36
324.00	269724	31.90	-67.52	20108	-7.50	-44.4	5.35900	338.02	26.8	.02	135.407	880254.	-97.902	16.55
326.00	264457	31.83	-67.43	20106	-7.56	-44.4	7.58847	396.54	31.9	-.03	141.882	856871.	-100.15	16.71
328.00	259150	31.75	-67.34	20105	-7.61	-44.5	9.99830	465.18	36.6	-.08	148.357	834747.	-102.52	16.84
330.00	253803	31.67	-67.25	20098	-7.67	-44.6	13.2977	543.86	42.2	-.14	154.832	813987.	-105.02	16.95
332.00	248417	31.60	-67.16	20086	-7.73	-44.6	17.1057	633.84	47.8	-.22	161.304	794700.	-107.64	17.02
334.00	242993	31.52	-67.07	20069	-7.79	-44.7	22.1191	735.70	54.2	-.32	167.772	776999.	-110.39	17.05
336.00	237534	31.45	-66.98	20045	-7.85	-44.7	28.2001	850.88	61.0	-.44	174.235	760994.	-113.26	17.03
338.00	232041	31.37	-66.89	20012	-7.91	-44.8	35.5631	980.10	68.3	-.59	180.689	746794.	-116.23	16.96
340.00	226516	31.29	-66.80	19966	-7.97	-44.8	44.9036	1124.5	76.3	-.78	187.132	734498.	-119.30	16.83
342.00	220963	31.22	-66.71	19911	-8.04	-44.9	55.3276	1285.1	84.2	-.99	193.559	724197.	-122.46	16.65
344.00	215385	31.14	-66.62	19839	-8.10	-44.9	69.1229	1462.3	93.3	-1.3	199.966	715966.	-125.68	16.40
346.00	209787	31.07	-66.54	19748	-8.16	-45.0	83.5568	1657.3	102.	-1.6	206.347	709859.	-128.93	16.09
348.00	204174	30.99	-66.45	19635	-8.23	-45.0	102.870	1869.8	111.	-2.0	212.696	705908.	-132.21	15.72
350.00	198551	30.92	-66.36	19496	-8.29	-45.1	122.740	2100.8	120.	-2.4	219.006	704114.	-135.48	15.29
352.00	192926	30.84	-66.28	19329	-8.36	-45.1	146.754	2348.7	128.	-2.8	225.267	704452.	-138.71	14.81
354.00	187308	30.77	-66.19	19129	-8.44	-45.2	173.760	2613.6	136.	-3.4	231.469	706862.	-141.88	14.28
356.00	181704	30.70	-66.11	18891	-8.51	-45.2	203.647	2894.0	144.	-4.0	237.601	711254.	-144.97	13.71
358.00	176127	30.63	-66.03	18613	-8.59	-45.3	236.459	3188.0	150.	-4.7	243.650	717507.	-147.96	13.12
360.00	170586	30.55	-65.95	18286	-8.68	-45.3	277.537	3494.3	156.	-5.5	249.602	725472.	-150.82	12.50
362.00	165098	30.49	-65.87	17902	-8.77	-45.4	324.138	3812.3	161.	-6.5	255.441	734973.	-153.55	11.88
364.00	159678	30.42	-65.79	17454	-8.86	-45.4	375.357	4138.4	164.	-7.5	261.145	745808.	-156.13	11.25
366.00	154346	30.35	-65.71	16936	-8.97	-45.5	430.873	4468.2	165.	-8.6	266.693	757754.	-158.56	10.63
368.00	149124	30.29	-65.64	16340	-9.09	-45.5	494.591	4797.1	164.	-9.9	272.061	770571.	-160.81	10.02
370.00	144034	30.23	-65.57	15660	-9.21	-45.6	558.909	5120.1	159.	-11.	277.224	784006.	-162.90	9.440
372.00	139102	30.17	-65.51	14897	-9.36	-45.6	620.152	5429.4	150.	-12.	282.153	797795.	-164.82	8.884
374.00	134355	30.11	-65.44	14059	-9.52	-45.6	673.888	5718.2	138.	-14.	286.823	811679.	-166.57	8.358
376.00	129813	30.06	-65.38	13158	-9.70	-45.7	715.377	5980.1	123.	-14.	291.211	825415.	-168.16	7.867
378.00	125496	30.01	-65.33	12211	-9.90	-45.7	744.039	6210.7	107.	-15.	295.299	838782.	-169.58	7.412
380.00	121419	29.96	-65.28	11237	-10.1	-45.7	756.484	6408.2	90.3	-15.	299.075	851594.	-170.86	6.993

TTA7622 3B-64 8806 SNP 629 AG WHITE 040964 ED ATMOS= THEORETICAL ARDC 1959 ATMOSPHERE
CONTROLJIM AUG 28 DATA-A= DATA-B=RFDA REFRACTION DATA-C= DATA D=
OBSERVER 32.3467=LAT -64.6538=LONG 0.0000=ORNT 64=ELEV -64484=X . -36074=Y. -0=Z

WT	CD	AREA	VI	GAMMAI	TAUI	LAT	LONG	VT	GAMMA	TAU
49.1	1.00	1.00	11214.	-9.50453	-40.82507	29.923072	-65.23	10259.	-10.399	-45.772

TIME	HITE	LAT	LONG	VT	GAMMA	TAU	Q	QC	DQC	AT	RANGE	SR	AZM	ELOBS
382.00	117590	29.92	-65.23	10259	-10.4	-45.8	749.641	6572.3	73.9	-15.	302.535	863701.	-171.99	6.610
384.00	114010	29.89	-65.19	9304.	-10.7	-45.8	723.595	6704.8	58.8	-15.	305.680	875002.	-172.98	6.263
386.00	110675	29.85	-65.15	8391.	-11.1	-45.8	685.068	6809.1	45.8	-14.	308.522	885441.	-173.86	5.948
388.00	107573	29.82	-65.12	7534.	-11.4	-45.8	640.758	6889.6	35.1	-13.	311.077	895000.	-174.63	5.662
390.00	104689	29.79	-65.09	6743.	-11.9	-45.9	584.615	6950.9	26.4	-12.	313.363	903691.	-175.31	5.404
392.00	102005	29.77	-65.06	6023.	-12.4	-45.9	532.849	6996.9	19.8	-11.	315.404	911550.	-175.90	5.171
394.00	99503.	29.75	-65.04	5376.	-13.0	-45.9	476.798	7031.1	14.7	-9.5	317.223	918628.	-176.41	4.959
396.00	97162.	29.73	-65.01	4798.	-13.7	-45.9	427.492	7056.4	10.9	-8.5	318.842	924988.	-176.87	4.765
398.00	94963.	29.71	-64.99	4286.	-14.4	-45.9	377.121	7075.2	8.01	-7.4	320.283	930691.	-177.27	4.587
400.00	92890.	29.69	-64.98	3835.	-15.2	-46.0	337.090	7089.0	5.96	-6.6	321.568	935802.	-177.62	4.424
402.00	90925.	29.68	-64.96	3436.	-16.2	-46.0	297.509	7099.3	4.42	-5.8	322.713	940380.	-177.93	4.272
404.00	89053.	29.67	-64.95	3087.	-17.2	-46.0	264.033	7107.0	3.31	-5.1	323.735	944481.	-178.20	4.131
406.00	87262.	29.66	-64.94	2780.	-18.4	-46.0	235.120	7112.7	2.49	-4.5	324.649	948157.	-178.44	3.999
408.00	85540.	29.65	-64.93	2511.	-19.7	-46.0	208.215	7117.1	1.88	-3.9	325.468	951453.	-178.66	3.874
410.00	83877.	29.64	-64.92	2275.	-21.1	-46.0	186.303	7120.4	1.44	-3.4	326.202	954412.	-178.85	3.756
412.00	82264.	29.63	-64.91	2067.	-22.6	-46.0	167.045	7122.9	1.11	-3.0	326.862	957070.	-179.02	3.644
414.00	80693.	29.62	-64.90	1885.	-24.3	-46.0	149.627	7124.9	.862	-2.6	327.456	959459.	-179.17	3.536
416.00	79157.	29.62	-64.89	1726.	-26.1	-46.0	135.247	7126.4	.678	-2.3	327.991	961608.	-179.31	3.433
418.00	77651.	29.61	-64.89	1586.	-28.1	-46.0	123.070	7127.6	.539	-2.0	328.474	963543.	-179.43	3.334
420.00	76169.	29.61	-64.88	1463.	-30.2	-46.0	112.147	7128.6	.433	-1.8	328.911	965285.	-179.54	3.237
422.00	74709.	29.60	-64.87	1356.	-32.4	-46.0	102.862	7129.4	.352	-1.6	329.306	966854.	-179.64	3.142
424.00	73267.	29.60	-64.87	1261.	-34.7	-46.0	95.8014	7130.0	.290	-1.4	329.663	968268.	-179.73	3.049
426.00	71840.	29.59	-64.87	1177.	-37.1	-46.1	89.3570	7130.5	.242	-1.2	329.987	969540.	-179.81	2.957
428.00	70427.	29.59	-64.86	1103.	-39.6	-46.1	83.6278	7131.0	.204	-1.1	330.281	970685.	-179.89	2.867
430.00	69027.	29.59	-64.86	1038.	-42.2	-46.1	79.4012	7131.3	.174	-.95	330.546	971713.	-179.95	2.778
432.00	67639.	29.58	-64.86	980.7	-44.8	-46.1	75.8630	7131.7	.150	-.85	330.787	972636.	179.98	2.691
434.00	66264.	29.58	-64.85	929.4	-47.4	-46.1	72.6193	7132.0	.131	-.75	331.004	973461.	179.93	2.606
436.00	64902.	29.58	-64.85	884.1	-50.1	-46.0	69.8093	7132.2	.115	-.66	331.201	974198.	179.88	2.522
438.00	63552.	29.58	-64.85	843.7	-52.7	-46.0	68.1754	7132.4	.103	-.60	331.378	974854.	179.84	2.439
440.00	62218.	29.57	-64.85	807.1	-55.3	-46.0	66.5601	7132.6	.093	-.54	331.537	975437.	179.80	2.357
442.00	60899.	29.57	-64.84	774.2	-57.8	-46.0	65.0326	7132.8	.084	-.48	331.681	975951.	179.76	2.277
444.00	59596.	29.57	-64.84	744.6	-60.3	-46.0	63.8968	7132.9	.076	-.44	331.809	976404.	179.73	2.198
446.00	58312.	29.57	-64.84	717.4	-62.7	-46.0	63.3450	7133.1	.070	-.41	331.924	976800.	179.70	2.121
448.00	57048.	29.57	-64.84	692.2	-65.0	-46.0	62.6585	7133.2	.065	-.37	332.026	977145.	179.68	2.045
450.00	55804.	29.57	-64.84	668.9	-67.1	-46.0	61.9127	7133.4	.060	-.34	332.117	977444.	179.65	1.970
452.00	54582.	29.57	-64.84	647.5	-69.2	-46.0	61.4107	7133.5	.055	-.32	332.198	977700.	179.63	1.897
454.00	53384.	29.57	-64.84	627.3	-71.1	-45.9	61.2862	7133.6	.052	-.31	332.269	977918.	179.62	1.826
456.00	52209.	29.57	-64.83	608.0	-72.9	-45.9	60.9357	7133.7	.048	-.29	332.332	978103.	179.60	1.756
458.00	51059.	29.56	-64.83	589.8	-74.6	-45.9	60.4472	7133.8	.045	-.27	332.387	978257.	179.59	1.688
460.00	49934.	29.56	-64.83	572.8	-76.2	-45.9	59.9183	7133.9	.042	-.25	332.436	978384.	179.58	1.621
462.00	48834.	29.56	-64.83	556.6	-77.7	-45.8	59.9360	7133.9	.040	-.25	332.478	978487.	179.56	1.556
464.00	47759.	29.56	-64.83	540.9	-79.0	-45.8	59.6779	7134.0	.037	-.24	332.515	978569.	179.56	1.493
466.00	46710.	29.56	-64.83	525.8	-80.2	-45.7	59.2591	7134.1	.035	-.22	332.546	978633.	179.55	1.431
468.00	45686.	29.56	-64.83	511.7	-81.4	-45.7	58.7422	7134.2	.033	-.21	332.574	978680.	179.54	1.371
470.00	44686.	29.56	-64.83	498.3	-82.4	-45.6	58.3551	7134.2	.031	-.20	332.598	978714.	179.53	1.312
472.00	43710.	29.56	-64.83	485.4	-83.3	-45.5	58.2496	7134.3	.029	-.20	332.618	978736.	179.53	1.255
474.00	42758.	29.56	-64.83	472.8	-84.1	-45.5	57.9393	7134.3	.027	-.19	332.636	978747.	179.53	1.199
476.00	41829.	29.56	-64.83	460.9	-84.9	-45.4	57.5115	7134.4	.026	-.18	332.651	978749.	179.52	1.144
478.00	40921.	29.56	-64.83	449.6	-85.5	-45.2	57.0233	7134.4	.024	-.17	332.664	978745.	179.52	1.091
480.00	40035.	29.56	-64.83	439.0	-86.1	-45.1	56.5115	7134.5	.023	-.16	332.675	978734.	179.52	1.039

TABLE XII

RFD-1 Gold-Loaded Rod Trajectory

TTA7622 38-64 8807 SNP 630 AU WHITE 040964 ED ATMOS= THEORETICAL ARDC 1959 ATMOSPHERE
CONTROLJIM AUG 28 DATA-A= DATA-B=RFDA REFRACTION DATA-C= DATA-D=
OBSERVER 32.3467=LAT -64.6538=LONG 0.0000=ORNT 64=ELEV -64484=X . -36074=Y. -0=Z

WT	CD	AREA	VI	GAMMAI	TAUI	LAT	LONG	VT	GAMMA	TAU
51.1	1.00	1.00	20933.	-5.94180	-40.74000	33.467000	-69.45	19974.	-6.2282	-43.183

TIME	HITE	LAT	LONG	VI	GAMMA	TAU	Q	QC	DQC	AT	RANGE	SR	AZM	ELOBS
282.00	370528	33.47	-69.45	19974	-6.23	-43.2	.014192	.00000	1.37	.10	.000000	1535275	-71.203	11.86
284.00	366173	33.39	-69.36	19981	-6.29	-43.2	.018170	2.9191	1.55	.10	6.41981	1500155	-71.906	12.07
286.00	361775	33.32	-69.26	19987	-6.35	-43.3	.022439	6.2022	1.73	.11	12.8424	1465251	-72.645	12.28
288.00	357334	33.25	-69.17	19994	-6.41	-43.4	.029790	9.8810	1.99	.11	19.2677	1430582	-73.421	12.49
290.00	352850	33.17	-69.08	20001	-6.47	-43.4	.039264	14.153	2.29	.11	25.6959	1396165	-74.237	12.71
292.00	348323	33.10	-68.99	20008	-6.53	-43.5	.050392	19.029	2.59	.11	32.1268	1362022	-75.096	12.93
294.00	343754	33.02	-68.89	20015	-6.59	-43.5	.064306	24.543	2.93	.11	38.5607	1328174	-76.000	13.16
296.00	339141	32.95	-68.80	20022	-6.65	-43.6	.080452	30.746	3.28	.11	44.9974	1294647	-76.954	13.38
298.00	334486	32.88	-68.71	20030	-6.70	-43.7	.105964	37.762	3.76	.11	51.4370	1261466	-77.960	13.62
300.00	329787	32.80	-68.62	20037	-6.76	-43.7	.132748	45.743	4.21	.11	57.8795	1228666	-79.022	13.85
302.00	325046	32.73	-68.52	20044	-6.82	-43.8	.181124	54.835	4.92	.11	64.3249	1196274	-80.145	14.09
304.00	320262	32.65	-68.43	20051	-6.88	-43.8	.230006	65.321	5.55	.11	70.7733	1164328	-81.333	14.33
306.00	315435	32.58	-68.34	20058	-6.94	-43.9	.322924	77.382	6.58	.11	77.2247	1132868	-82.590	14.56
308.00	310565	32.50	-68.25	20065	-7.00	-43.9	.419315	91.478	7.50	.11	83.6790	1101937	-83.921	14.81
310.00	305652	32.43	-68.16	20072	-7.06	-44.0	.604717	107.89	9.01	.11	90.1362	1071582	-85.332	15.05
312.00	300697	32.35	-68.07	20079	-7.12	-44.1	.803523	127.31	10.4	.10	96.5964	1041857	-86.828	15.28
314.00	295699	32.28	-67.97	20086	-7.18	-44.1	1.13561	149.95	12.4	.10	103.059	1012819	-88.414	15.52
316.00	290658	32.20	-67.88	20092	-7.24	-44.2	1.49237	176.50	14.2	.09	109.525	984531.	-90.097	15.75
318.00	285575	32.13	-67.79	20098	-7.30	-44.2	2.11440	207.39	16.9	.08	115.993	957062.	-91.881	15.97
320.00	280450	32.05	-67.70	20102	-7.35	-44.3	2.78140	243.64	19.3	.07	122.464	930486.	-93.774	16.18
322.00	275282	31.98	-67.61	20106	-7.41	-44.3	3.97345	285.89	23.1	.05	128.937	904887.	-95.780	16.38
324.00	270073	31.90	-67.52	20109	-7.47	-44.4	5.22516	335.60	26.5	.02	135.411	880351.	-97.904	16.57
326.00	264822	31.83	-67.43	20109	-7.53	-44.4	7.43487	393.45	31.6	-.02	141.887	856972.	-100.15	16.73
328.00	259531	31.75	-67.34	20106	-7.59	-44.5	9.76428	461.36	36.2	-.06	148.363	834852.	-102.52	16.87
330.00	254200	31.67	-67.25	20100	-7.65	-44.6	13.0557	539.22	41.8	-.13	154.839	814097.	-105.02	16.97
332.00	248829	31.60	-67.16	20090	-7.71	-44.6	16.7276	628.35	47.3	-.20	161.312	794814.	-107.65	17.05
334.00	243421	31.52	-67.07	20074	-7.77	-44.7	21.7324	729.22	53.8	-.29	167.782	777116.	-110.39	17.08
336.00	237977	31.45	-66.98	20052	-7.83	-44.7	27.6161	843.40	60.4	-.41	174.247	761114.	-113.26	17.06
338.00	232498	31.37	-66.89	20021	-7.89	-44.8	34.9750	971.51	67.8	-.55	180.704	746915.	-116.24	16.99
340.00	226988	31.29	-66.80	19980	-7.95	-44.8	44.0463	1114.9	75.7	-.73	187.150	734622.	-119.31	16.87
342.00	221448	31.22	-66.71	19927	-8.01	-44.9	54.4837	1274.2	83.7	-.93	193.582	724324.	-122.47	16.69
344.00	215882	31.14	-66.62	19859	-8.07	-44.9	67.9337	1450.4	92.7	-1.2	199.995	716097.	-125.69	16.44
346.00	210294	31.07	-66.54	19774	-8.14	-45.0	82.2149	1644.2	101.	-1.5	206.384	709996.	-128.95	16.13
348.00	204690	30.99	-66.45	19668	-8.20	-45.0	101.342	1855.7	111.	-1.8	212.743	706055.	-132.23	15.76
350.00	199074	30.92	-66.36	19537	-8.27	-45.1	120.906	2086.0	119.	-2.2	219.065	704278.	-135.51	15.33
352.00	193454	30.84	-66.28	19379	-8.34	-45.1	144.813	2333.3	128.	-2.7	225.340	704639.	-138.75	14.85
354.00	187838	30.77	-66.19	19189	-8.41	-45.2	171.792	2598.2	137.	-3.2	231.560	707084.	-141.93	14.32
356.00	182233	30.70	-66.11	18964	-8.48	-45.2	201.773	2879.3	144.	-3.8	237.714	711525.	-145.03	13.75
358.00	176651	30.62	-66.02	18698	-8.56	-45.3	234.803	3174.7	151.	-4.4	243.789	717843.	-148.03	13.15
360.00	171102	30.55	-65.94	18387	-8.65	-45.3	275.718	3483.4	158.	-5.2	249.772	725893.	-150.90	12.54
362.00	165601	30.48	-65.86	18021	-8.73	-45.4	322.944	3804.7	163.	-6.2	255.646	735504.	-153.65	11.91
364.00	160163	30.41	-65.79	17592	-8.83	-45.4	374.412	4135.4	167.	-7.2	261.391	746475.	-156.24	11.28
366.00	154807	30.35	-65.71	17095	-8.93	-45.5	430.338	4471.0	168.	-8.3	266.988	758590.	-158.68	10.65
368.00	149554	30.28	-65.64	16523	-9.05	-45.5	496.291	4807.5	168.	-9.6	272.412	771612.	-160.96	10.04
370.00	144426	30.22	-65.57	15865	-9.17	-45.6	563.793	5139.8	164.	-11.	277.637	785288.	-163.07	9.451
372.00	139450	30.16	-65.50	15124	-9.31	-45.6	629.226	5460.5	156.	-12.	282.637	799356.	-165.01	8.888
374.00	134651	30.10	-65.43	14304	-9.46	-45.6	688.078	5762.1	145.	-13.	287.383	813556.	-166.78	8.355
376.00	130052	30.05	-65.37	13417	-9.64	-45.7	735.687	6037.9	130.	-14.	291.853	827639.	-168.39	7.857
378.00	125674	30.00	-65.32	12478	-9.83	-45.7	771.409	6282.9	114.	-15.	296.027	841379.	-169.83	7.395
380.00	121533	29.95	-65.27	11504	-10.1	-45.7	789.097	6494.3	97.0	-15.	299.891	854577.	-171.13	6.969

TTA7622 38-64 8807 SNP 630 AU WHITE 040964 ED ATMOS= THEORETICAL ARDC 1959 ATMOSPHERE

CONTROLJIM AUG 28 DATA-A= DATA-B=RFDA REFRACTION DATA-C= DATA-D=

OBSERVER 32.3467=LAT -64.6538=LONG 0.0000=ORNT 64=ELEV -64484=X . -36074=Y. -0=Z

WT	CD	AREA	VI	GAMMAI	TAUI	LAT	LONG	VT	GAMMA	TAU
51.1	1.00	1.00	11476.	-9.44760	-40.94391	29.912276	-65.22	10521.	-10.314	-45.778

TIME	HITE	LAT	LONG	VT	GAMMA	TAU	Q	QC	DQC	AT	RANGE	SR	AZM	ELOBS
382.00	117640	29.91	-65.22	10521	-10.3	-45.8	786.644	6671.2	79.9	-15.	303.437	867076.	-172.27	6.580
384.00	113997	29.87	-65.18	9555.	-10.6	-45.8	763.672	6814.9	64.0	-15.	306.666	878763.	-173.29	6.226
386.00	110602	29.84	-65.14	8627.	-10.9	-45.8	726.344	6928.6	50.1	-14.	309.587	889576.	-174.18	5.905
388.00	107443	29.81	-65.10	7751.	-11.3	-45.9	682.380	7016.8	38.6	-13.	312.215	899488.	-174.97	5.614
390.00	104508	29.78	-65.07	6940.	-11.8	-45.9	625.191	7084.1	29.1	-12.	314.569	908508.	-175.66	5.353
392.00	101778	29.75	-65.04	6199.	-12.3	-45.9	570.402	7134.7	21.8	-11.	316.671	916667.	-176.26	5.116
394.00	99235.	29.73	-65.02	5532.	-12.8	-45.9	512.200	7172.3	16.2	-9.8	318.544	924018.	-176.79	4.900
396.00	96858.	29.71	-65.00	4935.	-13.5	-45.9	458.845	7200.3	12.0	-8.7	320.211	930621.	-177.25	4.704
398.00	94630.	29.69	-64.98	4406.	-14.2	-45.9	405.960	7220.9	8.82	-7.7	321.694	936540.	-177.65	4.524
400.00	92531.	29.68	-64.96	3938.	-15.0	-46.0	362.040	7236.1	6.54	-6.8	323.015	941843.	-178.01	4.359
402.00	90544.	29.66	-64.94	3527.	-15.9	-46.0	318.903	7247.4	4.84	-6.0	324.192	946590.	-178.32	4.206
404.00	88654.	29.65	-64.93	3167.	-16.9	-46.0	283.832	7255.8	3.62	-5.3	325.243	950842.	-178.60	4.064
406.00	86848.	29.64	-64.92	2849.	-18.1	-46.0	251.952	7262.1	2.72	-4.6	326.182	954652.	-178.84	3.932
408.00	85114.	29.63	-64.91	2571.	-19.3	-46.0	222.567	7266.8	2.05	-4.0	327.022	958066.	-179.06	3.807
410.00	83440.	29.62	-64.90	2327.	-20.7	-46.0	199.523	7270.4	1.57	-3.6	327.775	961129.	-179.25	3.688
412.00	81818.	29.61	-64.89	2113.	-22.2	-46.0	178.302	7273.2	1.20	-3.1	328.452	963880.	-179.43	3.576
414.00	80240.	29.60	-64.88	1926.	-23.9	-46.0	159.273	7275.3	.931	-2.7	329.060	966352.	-179.58	3.469
416.00	78698.	29.60	-64.87	1762.	-25.7	-46.0	144.182	7276.9	.731	-2.4	329.609	968576.	-179.72	3.366
418.00	77187.	29.59	-64.86	1617.	-27.6	-46.0	130.761	7278.2	.579	-2.1	330.104	970578.	-179.84	3.266
420.00	75702.	29.59	-64.86	1491.	-29.6	-46.1	118.833	7279.3	.464	-1.8	330.551	972381.	-179.96	3.169
422.00	74238.	29.58	-64.85	1380.	-31.8	-46.1	109.257	7280.1	.376	-1.6	330.955	974005.	179.94	3.074
424.00	72792.	29.58	-64.85	1282.	-34.1	-46.1	101.397	7280.8	.310	-1.4	331.322	975468.	179.85	2.981
426.00	71362.	29.57	-64.84	1196.	-36.5	-46.1	94.2903	7281.4	.257	-1.3	331.653	976786.	179.77	2.889
428.00	69947.	29.57	-64.84	1120.	-39.0	-46.1	88.0607	7281.8	.216	-1.1	331.954	977972.	179.70	2.799
430.00	68544.	29.57	-64.84	1054.	-41.5	-46.1	83.7586	7282.2	.184	-.98	332.226	979038.	179.63	2.711
432.00	67153.	29.56	-64.83	994.0	-44.1	-46.1	79.7462	7282.6	.159	-.87	332.473	979995.	179.57	2.625
434.00	65775.	29.56	-64.83	941.4	-46.8	-46.1	76.1382	7282.9	.138	-.77	332.695	980852.	179.51	2.539
436.00	64409.	29.56	-64.83	894.9	-49.4	-46.1	73.4033	7283.1	.121	-.68	332.897	981618.	179.46	2.456
438.00	63057.	29.56	-64.82	853.2	-52.1	-46.1	71.4504	7283.4	.108	-.61	333.079	982301.	179.42	2.373
440.00	61718.	29.55	-64.82	815.7	-54.7	-46.1	69.5767	7283.6	.097	-.55	333.242	982907.	179.38	2.292
442.00	60395.	29.55	-64.82	782.1	-57.2	-46.0	67.8392	7283.7	.087	-.49	333.389	983444.	179.34	2.212
444.00	59088.	29.55	-64.82	751.8	-59.7	-46.0	66.8887	7283.9	.080	-.45	333.521	983917.	179.31	2.133
446.00	57799.	29.55	-64.82	723.9	-62.1	-46.0	66.1413	7284.1	.073	-.41	333.639	984332.	179.28	2.056
448.00	56530.	29.55	-64.82	698.2	-64.4	-46.0	65.2968	7284.2	.067	-.38	333.745	984693.	179.26	1.980
450.00	55281.	29.55	-64.81	674.7	-66.6	-46.0	64.4313	7284.3	.062	-.35	333.838	985007.	179.23	1.906
452.00	54053.	29.55	-64.81	652.9	-68.7	-46.0	64.1822	7284.5	.058	-.33	333.921	985277.	179.21	1.833
454.00	52848.	29.55	-64.81	632.2	-70.7	-46.0	63.9178	7284.6	.054	-.31	333.995	985509.	179.19	1.762
456.00	51667.	29.54	-64.81	612.6	-72.5	-45.9	63.4514	7284.7	.050	-.29	334.060	985704.	179.18	1.692
458.00	50511.	29.54	-64.81	594.3	-74.2	-45.9	62.8793	7284.8	.047	-.27	334.117	985869.	179.16	1.624
460.00	49380.	29.54	-64.81	577.1	-75.8	-45.9	62.6355	7284.9	.044	-.26	334.167	986005.	179.15	1.558
462.00	48273.	29.54	-64.81	560.6	-77.3	-45.9	62.5176	7284.9	.041	-.25	334.211	986116.	179.14	1.493
464.00	47192.	29.54	-64.81	544.6	-78.7	-45.8	62.1643	7285.0	.038	-.24	334.249	986205.	179.13	1.430
466.00	46137.	29.54	-64.81	529.5	-79.9	-45.8	61.6636	7285.1	.036	-.23	334.282	986275.	179.12	1.368
468.00	45106.	29.54	-64.81	515.3	-81.1	-45.7	61.0921	7285.2	.034	-.21	334.310	986329.	179.12	1.308
470.00	44100.	29.54	-64.81	501.8	-82.1	-45.6	61.0220	7285.2	.032	-.21	334.335	986367.	179.11	1.249
472.00	43118.	29.54	-64.81	488.5	-83.1	-45.6	60.7693	7285.3	.030	-.20	334.356	986393.	179.11	1.192
474.00	42160.	29.54	-64.81	475.8	-83.9	-45.5	60.3630	7285.4	.028	-.19	334.374	986408.	179.10	1.136
476.00	41225.	29.54	-64.81	463.8	-84.7	-45.4	59.8640	7285.4	.027	-.18	334.390	986414.	179.10	1.082
478.00	40313.	29.54	-64.81	452.5	-85.4	-45.3	59.3233	7285.5	.025	-.17	334.403	986413.	179.09	1.029
480.00	39421.	29.54	-64.81	441.8	-86.0	-45.2	59.0249	7285.5	.024	-.16	334.415	986404.	179.09	.9767

TABLE XIII

RFD-1 Bracket No. 1 Trajectory

```
TTA7622 38-64  SNAP    000631  091263  BR1                                         ATMOS= THEORETICAL ARDC 1959 ATMOSPHERE
CONTROLJIM AUG 28         DATA-A=                       DATA-B=RFDA REFRACTION  DATA-C=                     DATA-D=
OBSERVER    32.3467=LAT   -64.6538=LONG     0.0000=ORNT           64=ELEV      -64484=X .     -36074=Y.          -0=Z
   WT     CD  AREA        VI    GAMMAI         TAUI          LAT   LONG       VT    GAMMA      TAU
 6.43  1.00  1.00  20933. -5.96380 -40.74000  33.467000 -69.45  19974. -6.2513 -43.183
```

TIME	HITE	LAT	LONG	VI	GAMMA	TAU	Q	QC	DQC	AI	RANGE	SR	AZM	ELOBS
282.00	370528	33.47	-69.45	19974	-6.25	-43.2	.014192	.00000	1.37	.10	.000000	1535275	-71.203	11.86
284.00	366157	33.39	-69.36	19981	-6.31	-43.2	.018185	2.9198	1.55	.10	6.41953	1500152	-71.906	12.07
286.00	361743	33.32	-69.26	19987	-6.37	-43.3	.022470	6.2047	1.73	.10	12.8418	1465246	-72.645	12.28
288.00	357286	33.25	-69.17	19994	-6.43	-43.4	.029890	9.8886	1.99	.10	19.2667	1430574	-73.421	12.49
290.00	352786	33.17	-69.08	20001	-6.49	-43.4	.039395	14.167	2.29	.10	25.6944	1396155	-74.237	12.71
292.00	348244	33.10	-68.99	20007	-6.55	-43.5	.050628	19.052	2.60	.10	32.1249	1362009	-75.095	12.93
294.00	343658	33.02	-68.89	20014	-6.61	-43.5	.064585	24.578	2.93	.10	38.5580	1328160	-76.000	13.15
296.00	339030	32.95	-68.80	20020	-6.67	-43.6	.081040	30.798	3.29	.10	44.9938	1294633	-76.953	13.38
298.00	334359	32.88	-68.71	20027	-6.73	-43.7	.106623	37.836	3.77	.10	51.4324	1261454	-77.959	13.61
300.00	329646	32.80	-68.62	20033	-6.79	-43.7	.134136	45.846	4.23	.09	57.8735	1228653	-79.021	13.84
302.00	324889	32.73	-68.52	20039	-6.85	-43.8	.182622	54.978	4.94	.09	64.3172	1196265	-80.144	14.08
304.00	320090	32.65	-68.43	20044	-6.91	-43.8	.231588	65.496	5.56	.08	70.7634	1164324	-81.331	14.32
306.00	315249	32.58	-68.34	20049	-6.97	-43.9	.326276	77.597	6.61	.07	77.2118	1132872	-82.587	14.56
308.00	310366	32.50	-68.25	20053	-7.02	-43.9	.422711	91.743	7.52	.05	83.6623	1101952	-83.918	14.79
310.00	305440	32.43	-68.16	20055	-7.08	-44.0	.612152	108.21	9.05	.02	90.1145	1071614	-85.327	15.03
312.00	300473	32.35	-68.07	20056	-7.14	-44.1	.810589	127.69	10.4		96.5679	1041912	-86.821	15.27
314.00	295465	32.28	-67.97	20054	-7.20	-44.1	1.14846	150.38	12.4	-.06	103.022	1012904	-88.405	15.50
316.00	290417	32.20	-67.88	20048	-7.26	-44.2	1.50292	176.95	14.2	-.11	109.475	984659.	-90.083	15.73
318.00	285329	32.13	-67.79	20038	-7.32	-44.2	2.13378	207.78	16.8	-.21	115.927	957246.	-91.863	15.95
320.00	280203	32.05	-67.70	20022	-7.38	-44.3	2.79095	243.88	19.2	-.31	122.375	930746.	-93.747	16.16
322.00	275041	31.98	-67.61	19996	-7.44	-44.3	3.98746	285.77	22.9	-.49	128.817	905244.	-95.742	16.36
324.00	269845	31.90	-67.52	19959	-7.50	-44.4	5.22935	334.85	26.1	-.69	135.249	880835.	-97.849	16.54
326.00	264619	31.83	-67.43	19904	-7.56	-44.4	7.36877	391.49	30.8	-1.0	141.668	857620.	-100.07	16.70
328.00	259367	31.75	-67.34	19828	-7.63	-44.5	9.59420	457.22	34.8	-1.4	148.066	835705.	-102.41	16.83
330.00	254096	31.68	-67.25	19726	-7.69	-44.6	12.6351	531.46	39.5	-1.8	154.437	815202.	-104.86	16.94
332.00	248812	31.60	-67.17	19591	-7.76	-44.6	15.9226	614.76	43.7	-2.3	160.770	796219.	-107.42	17.01
334.00	243525	31.53	-67.08	19420	-7.82	-44.7	20.2480	706.71	48.3	-3.0	167.054	778861.	-110.08	17.04
336.00	238243	31.46	-66.99	19202	-7.89	-44.7	24.9926	807.53	52.4	-3.8	173.277	763226.	-112.82	17.03
338.00	232981	31.38	-66.91	18933	-7.97	-44.8	30.6905	916.24	56.3	-4.6	179.422	749394.	-115.64	16.97
340.00	227751	31.31	-66.82	18604	-8.05	-44.8	36.9062	1032.1	59.4	-5.6	185.471	737424.	-118.50	16.86
342.00	222569	31.24	-66.74	18210	-8.13	-44.9	43.6943	1153.4	61.7	-6.7	191.403	727348.	-121.39	16.70
344.00	217454	31.18	-66.66	17746	-8.22	-44.9	50.8777	1278.3	63.0	-7.8	197.198	719164.	-124.28	16.49
346.00	212423	31.11	-66.58	17211	-8.32	-45.0	57.9921	1404.5	62.9	-8.9	202.832	712828.	-127.13	16.24
348.00	207494	31.04	-66.51	16604	-8.43	-45.0	64.9909	1529.3	61.7	-10.	208.282	708259.	-129.93	15.94
350.00	202687	30.98	-66.44	15931	-8.56	-45.1	71.2519	1650.2	59.0	-11.	213.525	705337.	-132.64	15.61
352.00	198019	30.92	-66.37	15202	-8.69	-45.1	76.0699	1764.6	55.1	-12.	218.542	703909.	-135.24	15.25
354.00	193503	30.87	-66.30	14430	-8.84	-45.1	80.1517	1870.5	50.6	-12.	223.315	703798.	-137.70	14.87
356.00	189150	30.81	-66.24	13623	-9.01	-45.2	82.7602	1966.6	45.4	-13.	227.833	704811.	-140.03	14.48
358.00	184969	30.76	-66.18	12798	-9.20	-45.2	83.8080	2052.0	39.9	-13.	232.087	706751.	-142.19	14.09
360.00	180964	30.72	-66.13	11969	-9.41	-45.2	83.6683	2126.4	34.5	-13.	236.072	709427.	-144.21	13.69
362.00	177138	30.67	-66.08	11149	-9.65	-45.3	82.2071	2190.3	29.4	-13.	239.790	712662.	-146.06	13.30
364.00	173488	30.63	-66.03	10347	-9.91	-45.3	80.1402	2244.3	24.7	-12.	243.245	716294.	-147.76	12.93
366.00	170011	30.59	-65.99	9569.	-10.2	-45.3	77.4720	2289.5	20.5	-12.	246.444	720183.	-149.31	12.56
368.00	166702	30.56	-65.95	8819.	-10.5	-45.4	74.4706	2326.8	16.9	-11.	249.394	724209.	-150.72	12.21
370.00	163556	30.52	-65.91	8105.	-10.9	-45.4	70.4838	2357.3	13.7	-11.	252.107	728273.	-152.00	11.88
372.00	160566	30.50	-65.88	7434.	-11.3	-45.4	65.9658	2381.9	11.0	-10.	254.595	732296.	-153.16	11.56
374.00	157721	30.47	-65.85	6809.	-11.8	-45.4	61.5438	2401.6	8.79	-9.4	256.872	736219.	-154.21	11.26
376.00	155010	30.44	-65.82	6230.	-12.3	-45.5	56.6537	2417.3	6.97	-8.6	258.953	739999.	-155.15	10.98
378.00	152424	30.42	-65.79	5697.	-12.8	-45.5	52.7776	2429.8	5.55	-8.0	260.853	743607.	-156.00	10.72
380.00	149953	30.40	-65.77	5205.	-13.4	-45.5	48.3857	2439.7	4.37	-7.3	262.586	747022.	-156.77	10.47

1TA7622 3B-64 SNAP 000631 091263 BR1 ATMOS= THEORETICAL ARDC 1959 ATMOSPHERE
CONTROLJIM AUG 28 DATA-A= DATA-B=RFDA REFRACTION DATA-C= DATA-D=
OBSERVER 32.3467=LAT -64.6538=LONG 0.0000=ORNT 64=ELEV -64484=X . -36074=Y. -0=Z

WT	CD	AREA	VI	GAMMAI	TAUI	LAT	LONG	VT	GAMMA	TAU
6.43	1.00	1.00	5739.4	-11.6414	-35.81627	30.381217	-65.75	4754.4	-14.098	-45.510

TIME	HITE	LAT	LONG	VI	GAMMA	TAU	Q	QC	DQC	AI	RANGE	SR	AZM	ELOBS
382.00	147587	30.38	-65.75	4754.	-14.1	-45.5	44.6528	2447.5	3.46	-6.7	264.166	750233.	-157.46	10.23
384.00	145318	30.36	-65.73	4343.	-14.8	-45.5	40.6894	2453.6	2.72	-6.1	265.604	753235.	-158.08	10.01
386.00	143135	30.35	-65.71	3970.	-15.7	-45.5	37.3336	2458.5	2.15	-5.5	266.913	756029.	-158.65	9.794
388.00	141031	30.33	-65.70	3631.	-16.5	-45.6	33.9938	2462.3	1.69	-5.0	268.106	758619.	-159.15	9.592
390.00	138998	30.32	-65.68	3324.	-17.5	-45.6	31.0217	2465.3	1.33	-4.5	269.192	761011.	-159.61	9.401
392.00	137028	30.31	-65.67	3047.	-18.6	-45.6	28.3530	2467.7	1.06	-4.1	270.181	763217.	-160.03	9.218
394.00	135114	30.30	-65.66	2797.	-19.7	-45.6	25.7658	2469.5	.839	-3.7	271.083	765244.	-160.40	9.044
396.00	133251	30.29	-65.64	2572.	-21.0	-45.6	23.7029	2471.0	.672	-3.3	271.906	767103.	-160.74	8.876
398.00	131431	30.28	-65.63	2368.	-22.3	-45.6	21.7019	2472.2	.538	-3.0	272.656	768806.	-161.05	8.715
400.00	129652	30.27	-65.62	2185.	-23.8	-45.6	19.8816	2473.2	.433	-2.7	273.341	770362.	-161.33	8.559
402.00	127907	30.26	-65.62	2020.	-25.3	-45.6	18.4087	2474.0	.352	-2.4	273.966	771781.	-161.59	8.409
404.00	126195	30.26	-65.61	1871.	-27.0	-45.6	16.9834	2474.6	.287	-2.2	274.537	773073.	-161.82	8.264
406.00	124511	30.25	-65.60	1737.	-28.7	-45.6	15.7283	2475.1	.235	-2.0	275.059	774246.	-162.03	8.122
408.00	122852	30.25	-65.60	1617.	-30.6	-45.6	14.7115	2475.6	.195	-1.8	275.536	775310.	-162.22	7.985
410.00	121217	30.24	-65.59	1508.	-32.6	-45.6	13.7310	2475.9	.162	-1.6	275.971	776271.	-162.40	7.852
412.00	119604	30.24	-65.58	1410.	-34.6	-45.7	12.6683	2476.2	.136	-1.4	276.368	777139.	-162.56	7.721
414.00	118011	30.23	-65.58	1322.	-36.8	-45.7	12.2015	2476.5	.115	-1.3	276.731	777918.	-162.70	7.594
416.00	116437	30.23	-65.57	1242.	-39.0	-45.7	11.5515	2476.7	.098	-1.2	277.062	778617.	-162.83	7.469
418.00	114883	30.22	-65.57	1170.	-41.3	-45.7	10.9553	2476.9	.084	-1.1	277.364	779240.	-162.95	7.346
420.00	113347	30.22	-65.57	1106.	-43.7	-45.7	10.5517	2477.0	.073	-.96	277.639	779794.	-163.06	7.226
422.00	111830	30.22	-65.56	1047.	-46.1	-45.7	10.1433	2477.2	.064	-.87	277.889	780284.	-163.16	7.108
424.00	110332	30.21	-65.56	994.0	-48.5	-45.7	9.75271	2477.3	.056	-.78	278.116	780714.	-163.25	6.993
426.00	108854	30.21	-65.56	946.3	-50.9	-45.7	9.50225	2477.4	.049	-.71	278.322	781089.	-163.33	6.880
428.00	107396	30.21	-65.56	902.5	-53.3	-45.7	9.27074	2477.5	.044	-.65	278.508	781413.	-163.40	6.769
430.00	105960	30.21	-65.55	862.7	-55.7	-45.6	9.03507	2477.6	.040	-.59	278.676	781691.	-163.47	6.660
432.00	104547	30.21	-65.55	826.5	-58.0	-45.6	8.84984	2477.6	.036	-.54	278.828	781927.	-163.53	6.554
434.00	103156	30.20	-65.55	793.2	-60.3	-45.6	8.74669	2477.7	.032	-.50	278.964	782123.	-163.58	6.450
436.00	101791	30.20	-65.55	762.1	-62.5	-45.6	8.61703	2477.8	.030	-.46	279.086	782284.	-163.63	6.348
438.00	100451	30.20	-65.55	733.6	-64.7	-45.6	8.47580	2477.8	.027	-.42	279.195	782413.	-163.67	6.248
440.00	99138.	30.20	-65.54	707.2	-66.8	-45.6	8.41245	2477.9	.025	-.40	279.293	782512.	-163.71	6.151
442.00	97852.	30.20	-65.54	682.2	-68.7	-45.6	8.35916	2477.9	.023	-.38	279.379	782586.	-163.74	6.056
444.00	96595.	30.20	-65.54	658.7	-70.6	-45.6	8.27491	2478.0	.021	-.35	279.456	782636.	-163.77	5.963
446.00	95367.	30.20	-65.54	636.7	-72.4	-45.5	8.17353	2478.0	.020	-.33	279.523	782665.	-163.80	5.873
448.00	94167.	30.20	-65.54	616.1	-74.1	-45.5	8.14195	2478.0	.018	-.31	279.583	782676.	-163.82	5.785
450.00	92997.	30.20	-65.54	596.3	-75.6	-45.5	8.10788	2478.1	.017	-.30	279.635	782671.	-163.84	5.699
452.00	91857.	30.20	-65.54	577.4	-77.1	-45.5	8.04018	2478.1	.016	-.28	279.681	782652.	-163.86	5.616
454.00	90746.	30.20	-65.54	559.6	-78.4	-45.4	7.95371	2478.1	.015	-.26	279.721	782620.	-163.88	5.535
456.00	89664.	30.20	-65.54	542.9	-79.7	-45.4	7.88981	2478.2	.014	-.25	279.755	782579.	-163.89	5.456
458.00	88610.	30.19	-65.54	526.8	-80.8	-45.3	7.87446	2478.2	.013	-.24	279.785	782529.	-163.90	5.380
460.00	87584.	30.19	-65.54	511.2	-81.9	-45.3	7.82291	2478.2	.012	-.23	279.811	782471.	-163.91	5.306
462.00	86585.	30.19	-65.54	496.5	-82.8	-45.2	7.75047	2478.3	.011	-.22	279.834	782407.	-163.92	5.233
464.00	85613.	30.19	-65.54	482.6	-83.7	-45.1	7.66733	2478.3	.010	-.21	279.853	782339.	-163.93	5.163
466.00	84666.	30.19	-65.54	469.6	-84.5	-45.0	7.60521	2478.3	.010	-.19	279.869	782266.	-163.94	5.095
468.00	83743.	30.19	-65.54	457.1	-85.2	-44.9	7.57635	2478.3	.009	-.19	279.883	782191.	-163.94	5.028
470.00	82844.	30.19	-65.54	445.1	-85.8	-44.8	7.52388	2478.3	.009	-.18	279.895	782113.	-163.95	4.963
472.00	81967.	30.19	-65.54	433.7	-86.4	-44.7	7.45949	2478.3	.008	-.17	279.905	782034.	-163.95	4.899
474.00	81112.	30.19	-65.54	423.1	-86.8	-44.5	7.39019	2478.4	.008	-.16	279.914	781954.	-163.95	4.838
476.00	80277.	30.19	-65.54	413.1	-87.3	-44.3	7.32016	2478.4	.007	-.15	279.921	781873.	-163.96	4.777
478.00	79461.	30.19	-65.54	403.8	-87.7	-44.1	7.28416	2478.4	.007	-.14	279.927	781792.	-163.96	4.718
480.00	78663.	30.19	-65.54	394.8	-88.0	-43.8	7.25442	2478.4	.007	-.14	279.932	781711.	-163.96	4.661

TABLE XIV

RFD-1 Bracket No. 2 Trajectory

TTA7622 3B-64 SNAP 000632 091263 BR2 ATMOS= THEORETICAL ARDC 1959 ATMOSPHERE
CONTROLJIM AUG 28 DATA-A= DATA-B=RFDA REFRACTION DATA-C= DATA-D=
OBSERVER 32.3467=LAT -64.6538=LONG 0.0000=ORNT 64=ELEV -64484=X . -36074=Y. -0=Z

WT	CD	AREA	VI	GAMMAI	TAUI	LAT	LONG	VT	GAMMA	TAU
6.43	1.00	1.00	20933.	-5.94260	-40.74000	33.467000	-69.45	19974.	-6.2290	-43.183

TIME	HITE	LAT	LONG	VT	GAMMA	TAU	Q	QC	DQC	AT	RANGE	SR	AZM	ELOBS
282.00	370528	33.47	-69.45	19974	-6.23	-43.2	.014192	.00000	1.37	.10	.000000	1535275	-71.203	11.86
284.00	366172	33.39	-69.36	19981	-6.29	-43.2	.018170	2.9191	1.55	.10	6.41978	1500155	-71.906	12.07
286.00	361774	33.32	-69.26	19987	-6.35	-43.3	.022440	6.2021	1.73	.10	12.8423	1465252	-72.645	12.28
288.00	357332	33.25	-69.17	19994	-6.41	-43.4	.029792	9.8809	1.99	.10	19.2675	1430583	-73.421	12.49
290.00	352848	33.17	-69.08	20000	-6.47	-43.4	.039265	14.152	2.29	.10	25.6954	1396167	-74.237	12.71
292.00	348321	33.10	-68.99	20007	-6.53	-43.5	.050394	19.028	2.59	.10	32.1260	1362025	-75.096	12.93
294.00	343751	33.02	-68.89	20014	-6.59	-43.5	.064303	24.541	2.93	.10	38.5593	1328180	-76.000	13.16
296.00	339138	32.95	-68.80	20020	-6.65	-43.6	.080448	30.743	3.28	.10	44.9954	1294656	-76.953	13.38
298.00	334483	32.88	-68.71	20026	-6.71	-43.7	.105946	37.756	3.76	.10	51.4341	1261481	-77.959	13.62
300.00	329784	32.80	-68.62	20032	-6.77	-43.7	.132720	45.733	4.21	.09	57.8754	1228685	-79.022	13.85
302.00	325044	32.73	-68.52	20038	-6.82	-43.8	.181047	54.819	4.92	.09	64.3193	1196300	-80.144	14.09
304.00	320260	32.65	-68.43	20044	-6.88	-43.8	.229853	65.295	5.54	.08	70.7656	1164364	-81.331	14.32
306.00	315434	32.58	-68.34	20048	-6.94	-43.9	.322616	77.340	6.57	.07	77.2142	1132916	-82.588	14.56
308.00	310566	32.50	-68.25	20052	-7.00	-43.9	.418743	91.411	7.48	.05	83.6649	1102001	-83.918	14.80
310.00	305656	32.43	-68.16	20055	-7.06	-44.0	.603507	107.78	8.98	.02	90.1173	1071666	-85.328	15.04
312.00	300705	32.35	-68.07	20056	-7.12	-44.1	.801329	127.13	10.3		96.5708	1041970	-86.822	15.28
314.00	295712	32.28	-67.97	20054	-7.18	-44.1	1.13108	149.68	12.3	-.06	103.025	1012968	-88.405	15.52
316.00	290679	32.20	-67.88	20049	-7.24	-44.2	1.48449	176.05	14.1	-.11	109.479	984727.	-90.084	15.75
318.00	285607	32.13	-67.79	20039	-7.30	-44.2	2.09801	206.67	16.7	-.20	115.930	957319.	-91.864	15.97
320.00	280496	32.05	-67.70	20023	-7.36	-44.3	2.75339	242.49	19.1	-.30	122.379	930823.	-93.748	16.18
322.00	275349	31.98	-67.61	19998	-7.42	-44.3	3.91481	284.07	22.7	-.48	128.822	905326.	-95.743	16.38
324.00	270168	31.90	-67.52	19961	-7.48	-44.4	5.12605	332.68	25.8	-.67	135.255	880920.	-97.851	16.56
326.00	264956	31.83	-67.43	19908	-7.54	-44.4	7.23112	388.79	30.5	-1.0	141.675	857708.	-100.07	16.72
328.00	259719	31.75	-67.34	19833	-7.60	-44.5	9.38716	453.89	34.5	-1.3	148.074	835795.	-102.41	16.86
330.00	254462	31.68	-67.25	19733	-7.67	-44.6	12.4263	527.45	39.2	-1.8	154.447	815292.	-104.87	16.96
332.00	249191	31.60	-67.17	19601	-7.73	-44.6	15.6025	610.08	43.3	-2.3	160.783	796308.	-107.43	17.04
334.00	243916	31.53	-67.08	19433	-7.80	-44.7	19.9341	701.30	48.0	-3.0	167.071	778949.	-110.09	17.07
336.00	238645	31.46	-66.99	19219	-7.87	-44.7	24.5325	801.45	52.0	-3.7	173.299	763311.	-112.83	17.06
338.00	233393	31.38	-66.91	18954	-7.95	-44.8	30.2575	909.49	56.0	-4.6	179.450	749476.	-115.65	17.00
340.00	228171	31.31	-66.82	18630	-8.02	-44.8	36.3017	1024.8	59.1	-5.5	185.506	737503.	-118.52	16.89
342.00	222997	31.24	-66.74	18242	-8.11	-44.9	43.1579	1145.6	61.6	-6.6	191.449	727427.	-121.42	16.73
344.00	217887	31.17	-66.66	17784	-8.20	-44.9	50.1647	1270.2	62.8	-7.7	197.255	719244.	-124.31	16.52
346.00	212858	31.11	-66.58	17255	-8.30	-45.0	57.4108	1396.3	63.0	-8.8	202.903	712914.	-127.17	16.27
348.00	207931	31.04	-66.51	16655	-8.41	-45.0	64.2562	1521.2	61.7	-9.9	208.368	708357.	-129.97	15.97
350.00	203123	30.98	-66.44	15989	-8.53	-45.1	70.7250	1642.4	59.3	-11.	213.629	705454.	-132.69	15.64
352.00	198452	30.92	-66.37	15265	-8.66	-45.1	75.5163	1757.4	55.4	-12.	218.665	704053.	-135.30	15.28
354.00	193930	30.86	-66.30	14498	-8.81	-45.1	79.6859	1863.9	51.0	-12.	223.460	703977.	-137.78	14.90
356.00	189571	30.81	-66.24	13695	-8.98	-45.2	82.3991	1960.7	45.8	-13.	228.001	705033.	-140.11	14.51
358.00	185381	30.76	-66.18	12873	-9.17	-45.2	83.7013	2047.0	40.4	-13.	232.278	707026.	-142.29	14.12
360.00	181367	30.71	-66.13	12044	-9.38	-45.2	83.6629	2122.5	35.0	-13.	236.288	709763.	-144.31	13.72
362.00	177531	30.67	-66.08	11223	-9.61	-45.3	82.2734	2187.3	29.8	-13.	240.031	713064.	-146.18	13.33
364.00	173870	30.63	-66.03	10421	-9.87	-45.3	80.1284	2242.1	25.1	-12.	243.510	716767.	-147.89	12.95
366.00	170381	30.59	-65.98	9642.	-10.2	-45.3	77.6962	2288.0	20.9	-12.	246.733	720731.	-149.45	12.58
368.00	167061	30.55	-65.94	8890.	-10.5	-45.4	74.7141	2326.0	17.2	-11.	249.707	724834.	-150.87	12.23
370.00	163904	30.52	-65.91	8173.	-10.9	-45.4	70.7374	2357.1	14.0	-11.	252.442	728976.	-152.16	11.89
372.00	160902	30.49	-65.87	7499.	-11.3	-45.4	66.3613	2382.2	11.2	-10.	254.952	733076.	-153.33	11.58
374.00	158045	30.46	-65.84	6870.	-11.7	-45.4	61.9037	2402.4	8.99	-9.4	257.250	737075.	-154.38	11.28
376.00	155324	30.44	-65.81	6287.	-12.2	-45.5	57.0903	2418.5	7.13	-8.7	259.350	740928.	-155.33	10.99
378.00	152728	30.42	-65.79	5750.	-12.7	-45.5	53.1148	2431.2	5.68	-8.0	261.268	744607.	-156.18	10.72
380.00	150247	30.39	-65.76	5254.	-13.3	-45.5	48.7613	2441.3	4.48	-7.4	263.018	748090.	-156.96	10.47

TTA7622 3B-64 SNAP 000632 091263 RR2 ATMOS= THEORETICAL ARDC 1959 ATMOSPHERE
CONTROLJIM AUG 28 DATA-A= DATA-B=RFDA REFRACTION DATA-C= DATA-D=
OBSERVER 32.3467=LAT -64.6538=LONG 0.0000=ORNT 64=ELEV -64484=X . -36074=Y. -0=Z

WT	CD	AREA	VI	GAMMAI	TAUI	LAT	LONG	VT	GAMMA	TAU
6.43	1.00	1.00	5785.2	-11.5934	-35.89760	30.375891	-65.74	4800.6	-14.015	-45.513

TIME	HITE	LAT	LONG	VI	GAMMA	TAU	Q	QC	DQC	AT	RANGE	SR	AZM	ELOBS
382.00	147872	30.38	-65.74	4801.	-14.0	-45.5	44.9983	2449.3	3.54	-6.8	264.613	751365.	-157.65	10.23
384.00	145594	30.36	-65.72	4386.	-14.7	-45.5	41.0616	2455.6	2.79	-6.1	266.065	754427.	-158.28	10.01
386.00	143404	30.34	-65.70	4009.	-15.6	-45.5	37.6366	2460.6	2.20	-5.6	267.388	757277.	-158.85	9.795
388.00	141293	30.33	-65.69	3666.	-16.4	-45.6	34.3149	2464.5	1.73	-5.1	268.593	759920.	-159.36	9.592
390.00	139253	30.32	-65.67	3357.	-17.4	-45.6	31.2749	2467.6	1.37	-4.6	269.690	762362.	-159.82	9.400
392.00	137276	30.30	-65.66	3077.	-18.4	-45.6	28.6186	2470.0	1.09	-4.1	270.690	764613.	-160.24	9.217
394.00	135356	30.29	-65.65	2824.	-19.6	-45.6	26.0274	2471.9	.861	-3.7	271.602	766683.	-160.62	9.041
396.00	133487	30.28	-65.64	2597.	-20.8	-45.6	23.9084	2473.5	.689	-3.4	272.433	768582.	-160.96	8.873
398.00	131663	30.27	-65.63	2391.	-22.2	-45.6	21.9075	2474.7	.552	-3.0	273.191	770321.	-161.27	8.711
400.00	129879	30.27	-65.62	2206.	-23.6	-45.6	20.0368	2475.7	.444	-2.7	273.883	771910.	-161.55	8.556
402.00	128130	30.26	-65.61	2039.	-25.1	-45.6	18.5680	2476.5	.361	-2.5	274.516	773360.	-161.81	8.405
404.00	126414	30.25	-65.60	1888.	-26.8	-45.6	17.1381	2477.2	.294	-2.2	275.093	774681.	-162.04	8.259
406.00	124726	30.24	-65.59	1753.	-28.5	-45.6	15.8422	2477.7	.241	-2.0	275.620	775880.	-162.26	8.117
408.00	123064	30.24	-65.59	1631.	-30.4	-45.6	14.8277	2478.1	.199	-1.8	276.102	776968.	-162.45	7.980
410.00	121425	30.23	-65.58	1520.	-32.4	-45.7	13.8424	2478.5	.166	-1.6	276.542	777953.	-162.62	7.846
412.00	119809	30.23	-65.58	1421.	-34.4	-45.7	12.9468	2478.8	.139	-1.5	276.944	778841.	-162.78	7.715
414.00	118213	30.22	-65.57	1332.	-36.5	-45.7	12.2822	2479.0	.117	-1.3	277.311	779640.	-162.93	7.588
416.00	116637	30.22	-65.57	1251.	-38.8	-45.7	11.6289	2479.3	.100	-1.2	277.646	780356.	-163.06	7.462
418.00	115060	30.22	-65.56	1179.	-41.0	-45.7	11.0146	2479.4	.085	-1.1	277.951	780996.	-163.18	7.340
420.00	113541	30.21	-65.56	1113.	-43.4	-45.7	10.6028	2479.6	.074	-.97	278.229	781565.	-163.29	7.220
422.00	112021	30.21	-65.56	1054.	-45.8	-45.7	10.1940	2479.7	.065	-.88	278.482	782068.	-163.39	7.102
424.00	110520	30.21	-65.55	1000.	-48.2	-45.7	9.80095	2479.9	.057	-.79	278.712	782510.	-163.48	6.986
426.00	109039	30.21	-65.55	952.0	-50.6	-45.7	9.52903	2480.0	.050	-.72	278.920	782897.	-163.56	6.873
428.00	107579	30.20	-65.55	907.8	-53.0	-45.7	9.30141	2480.1	.045	-.66	279.109	783232.	-163.64	6.762
430.00	106139	30.20	-65.54	867.5	-55.4	-45.7	9.06516	2480.1	.040	-.59	279.279	783520.	-163.71	6.653
432.00	104723	30.20	-65.54	830.9	-57.7	-45.6	8.86180	2480.2	.036	-.54	279.433	783764.	-163.77	6.547
434.00	103329	30.20	-65.54	797.3	-60.0	-45.6	8.76275	2480.3	.033	-.50	279.571	783968.	-163.82	6.443
436.00	101960	30.20	-65.54	766.0	-62.3	-45.6	8.63562	2480.4	.030	-.47	279.694	784137.	-163.87	6.341
438.00	100617	30.19	-65.54	737.1	-64.4	-45.6	8.49512	2480.4	.027	-.43	279.805	784272.	-163.91	6.241
440.00	99301.	30.19	-65.54	710.4	-66.5	-45.6	8.41626	2480.5	.025	-.40	279.904	784377.	-163.95	6.144
442.00	98011.	30.19	-65.54	685.3	-68.5	-45.6	8.36856	2480.5	.023	-.38	279.992	784456.	-163.98	6.049
444.00	96750.	30.19	-65.53	661.6	-70.4	-45.6	8.28775	2480.6	.021	-.35	280.069	784511.	-164.01	5.956
446.00	95518.	30.19	-65.53	639.4	-72.2	-45.5	8.18749	2480.6	.020	-.33	280.138	784544.	-164.04	5.865
448.00	94315.	30.19	-65.53	618.6	-73.9	-45.5	8.14229	2480.6	.018	-.31	280.199	784559.	-164.06	5.777
450.00	93141.	30.19	-65.53	598.7	-75.4	-45.5	8.11439	2480.7	.017	-.30	280.252	784557.	-164.08	5.692
452.00	91997.	30.19	-65.53	579.7	-76.9	-45.5	8.05056	2480.7	.016	-.29	280.298	784541.	-164.10	5.608
454.00	90883.	30.19	-65.53	561.7	-78.3	-45.4	7.96542	2480.7	.015	-.27	280.339	784512.	-164.12	5.527
456.00	89797.	30.19	-65.53	544.9	-79.5	-45.4	7.88994	2480.8	.014	-.25	280.374	784473.	-164.13	5.449
458.00	88739.	30.19	-65.53	528.6	-80.7	-45.3	7.87941	2480.8	.013	-.25	280.404	784425.	-164.14	5.372
460.00	87710.	30.19	-65.53	513.2	-81.7	-45.3	7.83158	2480.8	.012	-.24	280.431	784369.	-164.15	5.298
462.00	86708.	30.19	-65.53	498.3	-82.7	-45.2	7.76094	2480.8	.011	-.22	280.454	784306.	-164.16	5.225
464.00	85732.	30.19	-65.53	484.3	-83.6	-45.1	7.67852	2480.9	.011	-.21	280.473	784239.	-164.17	5.155
466.00	84782.	30.19	-65.53	471.2	-84.4	-45.0	7.60787	2480.9	.010	-.19	280.490	784168.	-164.18	5.086
468.00	83856.	30.19	-65.53	458.7	-85.1	-44.9	7.58200	2480.9	.009	-.19	280.504	784093.	-164.18	5.020
470.00	82954.	30.19	-65.53	446.6	-85.7	-44.8	7.53187	2480.9	.009	-.18	280.516	784016.	-164.19	4.954
472.00	82075.	30.19	-65.53	435.1	-86.3	-44.7	7.46839	2480.9	.008	-.17	280.527	783937.	-164.19	4.891
474.00	81217.	30.19	-65.53	424.4	-86.8	-44.5	7.39926	2481.0	.008	-.16	280.535	783858.	-164.19	4.829
476.00	80379.	30.19	-65.53	414.3	-87.2	-44.3	7.32904	2481.0	.007	-.15	280.543	783777.	-164.20	4.769
478.00	79561.	30.19	-65.53	404.9	-87.6	-44.1	7.28683	2481.0	.007	-.14	280.549	783696.	-164.20	4.710
480.00	78761.	30.19	-65.53	395.9	-88.0	-43.9	7.25907	2481.0	.007	-.14	280.554	783615.	-164.20	4.652

TABLE XV

RFD-1 Rod Holder No. 1 Trajectory

```
TTA7622 38-64   SNAP    000633  091263  H1                                ATMOS= THEORETICAL ARDC 1959 ATMOSPHERE
CONTROLJIM AUG 28        DATA-A=                 DATA-B=RFDA REFRACTION  DATA-C=                    DATA-D=
OBSERVER     32.3467=LAT    -64.6538=LONG     0.0000=ORNT         64=ELEV       -64484=X .     -36074=Y.        -0=Z
  WT     CD  AREA       VI    GAMMAI        TAUI          LAT    LONG        VT    GAMMA       TAU
 2.00  1.00  1.00  20933. -5.94880 -40.74000  33.467000 -69.45  19974. -6.2355 -43.183
```

TIME	HITE	LAT	LONG	VT	GAMMA	TAU	Q	QC	DQC	AT	RANGE	SR	AZM	ELOBS
282.00	370528	33.47	-69.45	19974	-6.24	-43.2	.014192	.00000	1.37	.10	.000000	1535275	-71.203	11.86
284.00	366168	33.39	-69.36	19980	-6.30	-43.2	.018174	2.9193	1.55	.10	6.41965	1500154	-71.906	12.07
286.00	361765	33.32	-69.26	19986	-6.36	-43.3	.022446	6.2026	1.73	.09	12.8419	1465251	-72.645	12.28
288.00	357319	33.25	-69.17	19992	-6.41	-43.4	.029816	9.8822	1.99	.09	19.2667	1430583	-73.421	12.49
290.00	352831	33.17	-69.08	19998	-6.47	-43.4	.039293	14.154	2.29	.09	25.6940	1396169	-74.237	12.71
292.00	348300	33.10	-68.99	20004	-6.53	-43.5	.050442	19.031	2.59	.08	32.1237	1362031	-75.095	12.93
294.00	343726	33.02	-68.89	20009	-6.59	-43.5	.064351	24.544	2.93	.08	38.5558	1328191	-75.999	13.15
296.00	339110	32.95	-68.80	20014	-6.65	-43.6	.080556	30.745	3.28	.07	44.9901	1294674	-76.953	13.38
298.00	334451	32.88	-68.71	20018	-6.71	-43.7	.106034	37.758	3.76	.06	51.4265	1261509	-77.958	13.61
300.00	329750	32.80	-68.62	20022	-6.77	-43.7	.132926	45.731	4.21	.05	57.8648	1228726	-79.020	13.85
302.00	325008	32.73	-68.52	20024	-6.83	-43.8	.181159	54.810	4.91	.02	64.3046	1196360	-80.142	14.08
304.00	320223	32.65	-68.43	20025	-6.89	-43.8	.229805	65.269	5.53		70.7456	1164447	-81.328	14.32
306.00	315397	32.58	-68.34	20024	-6.95	-43.9	.322556	77.285	6.55	-.04	77.1872	1133030	-82.582	14.56
308.00	310531	32.50	-68.25	20019	-7.01	-43.9	.418076	91.306	7.45	-.09	83.6286	1102154	-83.911	14.80
310.00	305624	32.43	-68.16	20011	-7.07	-44.0	.602142	107.59	8.93	-.18	90.0686	1071873	-85.317	15.04
312.00	300679	32.35	-68.07	19996	-7.13	-44.1	.797607	126.81	10.3	-.28	96.5055	1042244	-86.806	15.28
314.00	295697	32.28	-67.98	19973	-7.19	-44.1	1.12308	149.11	12.1	-.44	102.937	1013332	-88.383	15.51
316.00	290680	32.21	-67.89	19940	-7.25	-44.2	1.46834	175.11	13.8	-.61	109.360	985208.	-90.053	15.74
318.00	285631	32.13	-67.80	19891	-7.31	-44.2	2.06414	205.10	16.3	-.91	115.771	957853.	-91.818	15.96
320.00	280554	32.06	-67.71	19823	-7.38	-44.3	2.69140	239.92	18.5	-1.2	122.164	931656.	-93.684	16.17
322.00	275455	31.98	-67.62	19728	-7.44	-44.3	3.78538	279.89	21.7	-1.8	128.531	906413.	-95.651	16.36
324.00	270341	31.91	-67.53	19597	-7.50	-44.4	4.90123	325.95	24.3	-2.3	134.863	882330.	-97.719	16.54
326.00	265223	31.83	-67.44	19419	-7.57	-44.4	6.77534	378.06	28.0	-3.3	141.146	859523.	-99.887	16.70
328.00	260112	31.76	-67.35	19180	-7.64	-44.5	8.57796	436.90	30.7	-4.2	147.362	838109.	-102.15	16.83
330.00	255026	31.69	-67.27	18874	-7.72	-44.5	11.0609	501.15	33.6	-5.4	153.492	818206.	-104.49	16.94
332.00	249982	31.62	-67.18	18491	-7.80	-44.6	13.2608	570.22	35.2	-6.5	159.511	799916.	-106.90	17.01
334.00	244999	31.55	-67.10	18026	-7.88	-44.6	16.3390	642.40	37.0	-8.0	165.394	783326.	-109.37	17.04
336.00	240100	31.48	-67.02	17467	-7.98	-44.7	18.7931	716.75	37.1	-9.3	171.112	768493.	-111.86	17.04
338.00	235308	31.42	-66.95	16822	-8.08	-44.7	21.9955	790.81	37.0	-11.	176.636	755445.	-114.35	17.00
340.00	230646	31.36	-66.87	16085	-8.20	-44.8	24.1979	863.24	35.2	-12.	181.937	744166.	-116.82	16.92
342.00	226135	31.30	-66.80	15274	-8.34	-44.8	26.7058	931.65	33.1	-13.	186.989	734601.	-119.24	16.80
344.00	221795	31.24	-66.74	14399	-8.49	-44.9	28.0959	994.75	29.9	-14.	191.767	726653.	-121.57	16.65
346.00	217639	31.19	-66.67	13490	-8.66	-44.9	29.1683	1051.0	26.4	-14.	196.256	720190.	-123.81	16.48
348.00	213677	31.14	-66.62	12552	-8.85	-45.0	29.5012	1100.3	22.8	-15.	200.447	715055.	-125.92	16.28
350.00	209914	31.09	-66.56	11622	-9.07	-45.0	28.7801	1142.1	19.1	-14.	204.335	711078.	-127.90	16.07
352.00	206347	31.05	-66.51	10712	-9.32	-45.0	28.2817	1177.0	15.9	-14.	207.925	708087.	-129.75	15.85
354.00	202972	31.01	-66.47	9833.	-9.60	-45.0	26.8853	1205.6	12.9	-13.	211.225	705918.	-131.45	15.62
356.00	199782	30.97	-66.43	9008.	-9.92	-45.1	25.0291	1228.7	10.3	-12.	214.249	704417.	-133.01	15.39
358.00	196761	30.94	-66.39	8240.	-10.3	-45.1	23.3508	1247.0	8.19	-12.	217.014	703451.	-134.44	15.15
360.00	193897	30.91	-66.36	7530.	-10.7	-45.1	21.5235	1261.6	6.48	-11.	219.540	702905.	-135.75	14.93
362.00	191176	30.88	-66.32	6878.	-11.1	-45.2	19.7101	1273.2	5.10	-9.7	221.845	702682.	-136.94	14.70
364.00	188586	30.86	-66.30	6285.	-11.6	-45.2	17.9651	1282.2	4.01	-8.8	223.947	702704.	-138.03	14.48
366.00	186111	30.84	-66.27	5747.	-12.2	-45.2	16.3042	1289.4	3.15	-7.9	225.865	702907.	-139.02	14.27
368.00	183738	30.82	-66.25	5261.	-12.8	-45.2	14.7766	1295.0	2.48	-7.2	227.616	703240.	-139.91	14.06
370.00	181457	30.80	-66.22	4823.	-13.4	-45.2	13.3759	1299.4	1.96	-6.5	229.217	703662.	-140.73	13.86
372.00	179255	30.78	-66.20	4428.	-14.2	-45.2	12.0995	1302.9	1.55	-5.8	230.681	704144.	-141.48	13.66
374.00	177122	30.76	-66.18	4073.	-14.9	-45.3	10.9786	1305.6	1.23	-5.2	232.022	704660.	-142.16	13.47
376.00	175050	30.75	-66.17	3754.	-15.8	-45.3	9.93584	1307.8	.984	-4.7	233.253	705192.	-142.78	13.29
378.00	173029	30.74	-66.15	3465.	-16.7	-45.3	9.14360	1309.6	.794	-4.3	234.383	705726.	-143.35	13.11
380.00	171055	30.72	-66.14	3202.	-17.8	-45.3	8.37613	1311.0	.641	-3.9	235.421	706251.	-143.88	12.93

TTA7622 38-64 SNAP 000633 091263 H1 ATMOS= THEORETICAL ARDC 1959 ATMOSPHERE
CONTROLJIM AUG 28 DATA-A= DATA-B=RFDA REFRACTION DATA-C= DATA-D=
OBSERVER 32.3467=LAT -64.6538=LONG 0.0000=ORNT 64=ELEV -64484=X . -36074=Y. -0=Z

WT	CD	AREA	VI	GAMMAI	TAUI	LAT	LONG	VT	GAMMA	TAU
2.00	1.00	1.00	3969.6	-13.9571	-31.17274	30.711578	-66.13	2963.8	-18.848	-45.312

TIME	HITE	LAT	LONG	VT	GAMMA	TAU	Q	QC	DQC	AT	RANGE	SR	AZM	ELOBS
382.00	169121	30.71	-66.13	2964.	-18.8	-45.3	7.69490	1312.2	.521	-3.5	236.376	706758.	-144.36	12.76
384.00	167223	30.70	-66.11	2747.	-20.0	-45.3	7.09291	1313.1	.424	-3.2	237.255	707242.	-144.80	12.59
386.00	165358	30.69	-66.10	2550.	-21.3	-45.3	6.52213	1313.9	.347	-2.9	238.064	707698.	-145.20	12.43
388.00	163520	30.68	-66.09	2372.	-22.6	-45.3	6.04599	1314.5	.286	-2.6	238.809	708124.	-145.57	12.27
390.00	161707	30.67	-66.08	2210.	-24.1	-45.4	5.60440	1315.0	.236	-2.4	239.495	708517.	-145.91	12.11
392.00	159916	30.67	-66.07	2063.	-25.6	-45.4	5.19385	1315.5	.196	-2.2	240.129	708876.	-146.22	11.95
394.00	158144	30.66	-66.07	1929.	-27.2	-45.4	4.86486	1315.8	.164	-2.0	240.712	709201.	-146.51	11.80
396.00	156389	30.65	-66.06	1808.	-28.9	-45.4	4.54996	1316.1	.138	-1.8	241.251	709493.	-146.78	11.65
398.00	154651	30.65	-66.05	1697.	-30.7	-45.4	4.27105	1316.4	.117	-1.6	241.748	709751.	-147.02	11.50
400.00	152927	30.64	-66.05	1597.	-32.5	-45.4	4.06225	1316.6	.100	-1.5	242.207	709976.	-147.25	11.35
402.00	151218	30.64	-66.04	1504.	-34.5	-45.4	3.85485	1316.8	.086	-1.4	242.629	710169.	-147.45	11.21
404.00	149523	30.63	-66.04	1420.	-36.5	-45.4	3.67021	1316.9	.074	-1.2	243.018	710332.	-147.64	11.07
406.00	147842	30.63	-66.03	1343.	-38.5	-45.4	3.52516	1317.1	.064	-1.1	243.377	710465.	-147.82	10.93
408.00	146177	30.62	-66.03	1272.	-40.7	-45.4	3.37985	1317.2	.056	-1.0	243.706	710571.	-147.98	10.79
410.00	144527	30.62	-66.02	1208.	-42.8	-45.4	3.25213	1317.3	.049	-.96	244.009	710649.	-148.13	10.65
412.00	142893	30.62	-66.02	1149.	-45.0	-45.4	3.15724	1317.4	.043	-.88	244.286	710702.	-148.26	10.52
414.00	141276	30.61	-66.01	1094.	-47.3	-45.4	3.05949	1317.5	.038	-.80	244.541	710732.	-148.39	10.38
416.00	139678	30.61	-66.01	1045.	-49.5	-45.4	2.97139	1317.5	.034	-.74	244.773	710740.	-148.50	10.25
418.00	138099	30.61	-66.01	999.2	-51.8	-45.4	2.91500	1317.6	.031	-.68	244.985	710727.	-148.60	10.12
420.00	136540	30.61	-66.01	956.9	-54.0	-45.4	2.85279	1317.7	.028	-.63	245.179	710695.	-148.70	9.996
422.00	135003	30.60	-66.00	916.2	-56.2	-45.4	2.78841	1317.7	.025	-.57	245.355	710646.	-148.78	9.871
424.00	133489	30.60	-66.00	882.4	-58.4	-45.4	2.76073	1317.8	.023	-.54	245.514	710581.	-148.86	9.748
426.00	131999	30.60	-66.00	848.8	-60.5	-45.4	2.72326	1317.8	.021	-.50	245.659	710502.	-148.93	9.627
428.00	130535	30.60	-66.00	817.6	-62.6	-45.4	2.68095	1317.9	.019	-.46	245.789	710410.	-148.99	9.509
430.00	129097	30.60	-66.00	788.6	-64.6	-45.4	2.65786	1317.9	.018	-.44	245.906	710306.	-149.05	9.393
432.00	127687	30.60	-65.99	761.2	-66.5	-45.3	2.63890	1317.9	.016	-.41	246.012	710193.	-149.10	9.280
434.00	126305	30.60	-65.99	735.3	-68.3	-45.3	2.61107	1318.0	.015	-.39	246.106	710071.	-149.14	9.169
436.00	124953	30.59	-65.99	711.2	-70.1	-45.3	2.57944	1318.0	.014	-.36	246.190	709942.	-149.18	9.060
438.00	123630	30.59	-65.99	688.4	-71.8	-45.3	2.57461	1318.0	.013	-.35	246.265	709807.	-149.22	8.954
440.00	122338	30.59	-65.99	666.4	-73.4	-45.3	2.55734	1318.0	.012	-.33	246.332	709666.	-149.25	8.851
442.00	121076	30.59	-65.99	645.6	-74.9	-45.2	2.53269	1318.1	.011	-.31	246.391	709522.	-149.28	8.750
444.00	119845	30.59	-65.99	626.0	-76.3	-45.2	2.50741	1318.1	.010	-.29	246.443	709375.	-149.31	8.652
446.00	118643	30.59	-65.99	607.4	-77.6	-45.2	2.50238	1318.1	.010	-.28	246.489	709225.	-149.33	8.556
448.00	117472	30.59	-65.99	589.3	-78.9	-45.1	2.48646	1318.1	.009	-.27	246.529	709074.	-149.35	8.462
450.00	116330	30.59	-65.99	572.1	-80.0	-45.1	2.46354	1318.1	.009	-.26	246.564	708922.	-149.36	8.371
452.00	115218	30.59	-65.99	556.0	-81.0	-45.0	2.43678	1318.2	.008	-.24	246.595	708770.	-149.38	8.282
454.00	114133	30.59	-65.99	540.6	-82.0	-45.0	2.42862	1318.2	.008	-.23	246.622	708618.	-149.39	8.196
456.00	113076	30.59	-65.99	525.7	-82.9	-44.9	2.41619	1318.2	.007	-.23	246.645	708468.	-149.40	8.112
458.00	112046	30.59	-65.99	511.4	-83.7	-44.8	2.39714	1318.2	.007	-.21	246.665	708318.	-149.41	8.030
460.00	111042	30.59	-65.99	497.9	-84.4	-44.7	2.37409	1318.2	.006	-.20	246.683	708170.	-149.42	7.950
462.00	110064	30.59	-65.99	485.2	-85.1	-44.6	2.34943	1318.2	.006	-.19	246.698	708024.	-149.43	7.873
464.00	109109	30.59	-65.99	473.1	-85.7	-44.5	2.34519	1318.2	.006	-.18	246.710	707880.	-149.43	7.797
466.00	108177	30.59	-65.99	461.3	-86.2	-44.4	2.33376	1318.3	.005	-.18	246.722	707738.	-149.44	7.723
468.00	107267	30.59	-65.99	449.9	-86.7	-44.2	2.31754	1318.3	.005	-.17	246.731	707599.	-149.44	7.651
470.00	106379	30.59	-65.99	439.2	-87.1	-44.1	2.29848	1318.3	.005	-.16	246.739	707462.	-149.45	7.581
472.00	105512	30.59	-65.99	429.1	-87.5	-43.8	2.27841	1318.3	.004	-.15	246.746	707328.	-149.45	7.512
474.00	104664	30.59	-65.98	419.5	-87.9	-43.6	2.26614	1318.3	.004	-.14	246.752	707196.	-149.45	7.444
476.00	103835	30.59	-65.98	410.3	-88.2	-43.3	2.26278	1318.3	.004	-.14	246.757	707067.	-149.46	7.378
478.00	103024	30.59	-65.98	401.2	-88.4	-43.0	2.25294	1318.3	.004	-.14	246.761	706941.	-149.46	7.314
480.00	102231	30.59	-65.98	392.6	-88.6	-42.6	2.24006	1318.3	.004	-.13	246.765	706817.	-149.46	7.251

TABLE XVI

RFD-1 Rod Holder No. 2 Trajectory

TTA7622 3B-64 SNAP 000634 091263 H2 ATMOS= THEORETICAL ARDC 1959 ATMOSPHERE
CONTROLJIM AUG 28 DATA-A= DATA-B=RFDA REFRACTION DATA-C= DATA-D=
OBSERVER 32.3467=LAT -64.6538=LONG 0.0000=ORNT 64=ELEV -64484=X . -36074=Y. -0=Z

WT	CD	AREA	VI	GAMMAI	TAUI	LAT	LONG	VT	GAMMA	TAU
2.00	1.00	1.00	20933.	-5.95760	-40.74000	33.467000	-69.45	19974.	-6.2448	-43.183

TIME	HITE	LAT	LONG	VT	GAMMA	TAU	Q	QC	DQC	AT	RANGE	SR	AZM	ELOBS
282.00	370528	33.47	-69.45	19974	-6.24	-43.2	.014192	.00000	1.37	.10	.000000	1535275	-71.203	11.86
284.00	366161	33.39	-69.36	19980	-6.30	-43.2	.018180	2.9196	1.55	.10	6.41955	1500153	-71.906	12.07
286.00	361752	33.32	-69.26	19986	-6.36	-43.3	.022459	6.2036	1.73	.09	12.8417	1465249	-72.645	12.28
288.00	357300	33.25	-69.17	19993	-6.42	-43.4	.029856	9.8854	1.99	.09	19.2664	1430579	-73.421	12.49
290.00	352805	33.17	-69.08	19998	-6.48	-43.4	.039347	14.161	2.29	.09	25.6936	1396164	-74.237	12.71
292.00	348268	33.10	-68.99	20004	-6.54	-43.5	.050540	19.041	2.59	.08	32.1232	1362024	-75.095	12.93
294.00	343687	33.02	-68.89	20009	-6.60	-43.5	.064468	24.560	2.93	.08	38.5552	1328183	-75.999	13.15
296.00	339065	32.95	-68.80	20014	-6.66	-43.6	.080801	30.768	3.28	.07	44.9894	1294665	-76.952	13.38
298.00	334400	32.88	-68.71	20018	-6.72	-43.7	.106314	37.791	3.76	.06	51.4258	1261498	-77.958	13.61
300.00	329693	32.80	-68.62	20022	-6.78	-43.7	.133512	45.778	4.22	.05	57.8640	1228714	-79.020	13.84
302.00	324944	32.73	-68.52	20024	-6.84	-43.8	.181811	54.876	4.92	.02	64.3037	1196345	-80.141	14.08
304.00	320153	32.65	-68.43	20025	-6.90	-43.8	.230522	65.352	5.54		70.7447	1164431	-81.327	14.32
306.00	315320	32.58	-68.34	20024	-6.96	-43.9	.324067	77.390	6.57	-.05	77.1862	1133011	-82.582	14.56
308.00	310448	32.50	-68.25	20019	-7.02	-43.9	.419711	91.443	7.47	-.09	83.6274	1102134	-83.910	14.80
310.00	305535	32.43	-68.16	20011	-7.08	-44.0	.605699	107.77	8.96	-.18	90.0673	1071851	-85.317	15.03
312.00	300583	32.35	-68.07	19996	-7.14	-44.1	.801400	127.04	10.3	-.28	96.5041	1042220	-86.806	15.27
314.00	295595	32.28	-67.98	19973	-7.20	-44.1	1.13018	149.40	12.2	-.44	102.936	1013307	-88.383	15.50
316.00	290572	32.21	-67.89	19939	-7.26	-44.2	1.47580	175.47	13.9	-.62	109.359	985182.	-90.052	15.73
318.00	285516	32.13	-67.80	19891	-7.32	-44.2	2.07853	205.55	16.4	-.92	115.769	957926.	-91.818	15.95
320.00	280434	32.06	-67.71	19822	-7.38	-44.3	2.70627	240.48	18.5	-1.2	122.161	931628.	-93.683	16.16
322.00	275329	31.98	-67.62	19726	-7.45	-44.3	3.81385	280.56	21.7	-1.8	128.528	906384.	-95.650	16.36
324.00	270209	31.91	-67.53	19594	-7.51	-44.4	4.92989	326.76	24.4	-2.3	134.859	882302.	-97.718	16.53
326.00	265085	31.83	-67.44	19415	-7.58	-44.4	6.82672	379.03	28.1	-3.3	141.140	859496.	-99.885	16.69
328.00	259970	31.76	-67.35	19174	-7.65	-44.5	8.63289	438.05	30.7	-4.2	147.355	838085.	-102.14	16.82
330.00	254879	31.69	-67.27	18866	-7.73	-44.5	11.1317	502.44	33.7	-5.4	153.482	818185.	-104.49	16.92
332.00	249831	31.62	-67.18	18480	-7.81	-44.6	13.3643	571.69	35.3	-6.6	159.498	799901.	-106.90	16.99
334.00	244846	31.55	-67.10	18012	-7.89	-44.6	16.4288	644.01	37.0	-8.1	165.377	783316.	-109.36	17.03
336.00	239945	31.48	-67.02	17451	-7.99	-44.7	18.8844	718.40	37.1	-9.3	171.090	768490.	-111.85	17.02
338.00	235152	31.42	-66.95	16802	-8.10	-44.7	22.0934	792.47	37.0	-11.	176.609	755448.	-114.34	16.98
340.00	230490	31.36	-66.87	16062	-8.21	-44.8	24.2671	864.82	35.1	-12.	181.903	744175.	-116.80	16.90
342.00	225980	31.30	-66.80	15249	-8.35	-44.8	26.7922	933.13	33.0	-13.	186.946	734614.	-119.22	16.79
344.00	221641	31.24	-66.74	14371	-8.50	-44.9	28.1423	996.07	29.8	-14.	191.716	726669.	-121.55	16.64
346.00	217488	31.19	-66.68	13460	-8.67	-44.9	29.2259	1052.1	26.4	-14.	196.196	720205.	-123.78	16.47
348.00	213529	31.14	-66.62	12521	-8.86	-45.0	29.5137	1101.2	22.7	-15.	200.377	715067.	-125.89	16.27
350.00	209770	31.09	-66.56	11591	-9.09	-45.0	28.8074	1142.8	19.0	-14.	204.255	711085.	-127.86	16.06
352.00	206207	31.05	-66.52	10681	-9.34	-45.0	28.2662	1177.4	15.7	-14.	207.835	708085.	-129.70	15.84
354.00	202838	31.01	-66.47	9803.	-9.62	-45.0	26.8418	1205.9	12.8	-13.	211.125	705904.	-131.40	15.61
356.00	199651	30.98	-66.43	8979.	-9.94	-45.1	24.9936	1228.8	10.2	-12.	214.139	704391.	-132.96	15.38
358.00	196635	30.94	-66.39	8213.	-10.3	-45.1	23.2969	1247.0	8.12	-11.	216.895	703410.	-134.38	15.14
360.00	193775	30.91	-66.36	7505.	-10.7	-45.1	21.4726	1261.5	6.42	-11.	219.412	702847.	-135.69	14.92
362.00	191058	30.89	-66.33	6855.	-11.1	-45.1	19.6509	1272.9	5.05	-9.6	221.709	702608.	-136.87	14.69
364.00	188471	30.86	-66.30	6263.	-11.6	-45.2	17.9120	1281.9	3.97	-8.8	223.804	702613.	-137.95	14.47
366.00	185999	30.84	-66.27	5727.	-12.2	-45.2	16.2488	1289.0	3.12	-7.9	225.715	702799.	-138.94	14.26
368.00	183630	30.82	-66.25	5243.	-12.8	-45.2	14.7284	1294.5	2.46	-7.1	227.460	703116.	-139.83	14.06
370.00	181351	30.80	-66.23	4806.	-13.5	-45.2	13.3279	1298.9	1.94	-6.4	229.055	703523.	-140.65	13.85
372.00	179152	30.78	-66.21	4413.	-14.2	-45.2	12.0589	1302.3	1.53	-5.8	230.514	703989.	-141.39	13.66
374.00	177021	30.77	-66.19	4059.	-15.0	-45.3	10.9390	1305.1	1.22	-5.2	231.851	704490.	-142.07	13.47
376.00	174951	30.75	-66.17	3741.	-15.9	-45.3	9.90305	1307.3	.975	-4.7	233.077	705008.	-142.69	13.28
378.00	172932	30.74	-66.16	3454.	-16.8	-45.3	9.11501	1309.0	.787	-4.3	234.202	705528.	-143.26	13.10
380.00	170959	30.73	-66.14	3192.	-17.8	-45.3	8.34782	1310.4	.636	-3.9	235.237	706040.	-143.78	12.93

TTA7622 38-64 SNAP 000634 091263 H2 ATMOS= THEORETICAL ARDC 1959 ATMOSPHERE
CONTROLJIM AUG 28 DATA-A= DATA-B=RFDA REFRACTION DATA-C= DATA-D=
OBSERVER 32.3467=LAT -64.6538=LONG 0.0000=ORNT 64=ELEV -64484=X . -36074=Y. -0=Z

WT	CD	AREA	VI	GAMMAI	TAUI	LAT	LONG	VT	GAMMA	TAU
2.00	1.00	1.00	3960.0	-13.9810	-31.13538	30.713802	-66.13	2954.0	-18.897	-45.310

TIME	HITE	LAT	LONG	VT	GAMMA	TAU	Q	QC	DQC	AT	RANGE	SR	AZM	ELOBS
382.00	169027	30.71	-66.13	2954.	-18.9	-45.3	7.67192	1311.6	.516	-3.5	236.189	706535.	-144.26	12.76
384.00	167131	30.70	-66.12	2738.	-20.1	-45.3	7.07003	1312.5	.421	-3.2	237.064	707008.	-144.70	12.59
386.00	165266	30.69	-66.11	2542.	-21.3	-45.3	6.50034	1313.3	.344	-2.9	237.870	707453.	-145.10	12.43
388.00	163430	30.69	-66.10	2365.	-22.7	-45.3	6.02818	1313.9	.283	-2.6	238.613	707869.	-145.47	12.26
390.00	161618	30.68	-66.09	2203.	-24.1	-45.3	5.58703	1314.4	.234	-2.4	239.297	708252.	-145.81	12.11
392.00	159828	30.67	-66.08	2057.	-25.6	-45.4	5.18028	1314.8	.195	-2.2	239.928	708603.	-146.12	11.95
394.00	158057	30.66	-66.07	1924.	-27.3	-45.4	4.85112	1315.2	.163	-2.0	240.509	708920.	-146.41	11.80
396.00	156303	30.66	-66.06	1802.	-29.0	-45.4	4.53698	1315.5	.137	-1.8	241.046	709203.	-146.68	11.65
398.00	154566	30.65	-66.06	1692.	-30.7	-45.4	4.26233	1315.7	.116	-1.6	241.541	709454.	-146.92	11.50
400.00	152843	30.64	-66.05	1592.	-32.6	-45.4	4.05315	1316.0	.099	-1.5	241.998	709672.	-147.14	11.35
402.00	151134	30.64	-66.04	1500.	-34.5	-45.4	3.84578	1316.1	.085	-1.4	242.419	709860.	-147.35	11.21
404.00	149440	30.64	-66.04	1416.	-36.6	-45.4	3.66385	1316.3	.073	-1.2	242.807	710016.	-147.54	11.07
406.00	147761	30.63	-66.03	1339.	-38.6	-45.4	3.51849	1316.4	.064	-1.1	243.164	710144.	-147.72	10.93
408.00	146096	30.63	-66.03	1269.	-40.8	-45.4	3.37316	1316.6	.056	-1.0	243.492	710244.	-147.88	10.79
410.00	144447	30.62	-66.02	1205.	-42.9	-45.4	3.24780	1316.7	.049	-.95	243.793	710318.	-148.02	10.65
412.00	142814	30.62	-66.02	1146.	-45.1	-45.4	3.15258	1316.7	.043	-.88	244.070	710367.	-148.16	10.52
414.00	141199	30.62	-66.02	1092.	-47.4	-45.4	3.05473	1316.8	.038	-.80	244.323	710393.	-148.28	10.38
416.00	139601	30.61	-66.01	1042.	-49.6	-45.4	2.96871	1316.9	.034	-.73	244.554	710396.	-148.39	10.25
418.00	138023	30.61	-66.01	997.0	-51.9	-45.4	2.91191	1317.0	.031	-.68	244.766	710380.	-148.50	10.12
420.00	136465	30.61	-66.01	955.0	-54.1	-45.4	2.84950	1317.0	.028	-.62	244.958	710345.	-148.59	9.996
422.00	134930	30.61	-66.01	916.4	-56.3	-45.4	2.78689	1317.1	.025	-.57	245.133	710293.	-148.67	9.871
424.00	133417	30.61	-66.00	880.7	-58.5	-45.4	2.75850	1317.1	.023	-.54	245.292	710226.	-148.75	9.748
426.00	131928	30.60	-66.00	847.2	-60.6	-45.4	2.72106	1317.2	.021	-.50	245.436	710144.	-148.82	9.627
428.00	130465	30.60	-66.00	816.1	-62.6	-45.4	2.67862	1317.2	.019	-.46	245.566	710050.	-148.88	9.509
430.00	129029	30.60	-66.00	787.2	-64.6	-45.4	2.65702	1317.2	.018	-.44	245.682	709945.	-148.94	9.393
432.00	127620	30.60	-66.00	759.9	-66.6	-45.3	2.63761	1317.3	.016	-.41	245.787	709830.	-148.99	9.280
434.00	126240	30.60	-66.00	734.1	-68.4	-45.3	2.60944	1317.3	.015	-.39	245.881	709707.	-149.03	9.169
436.00	124890	30.60	-66.00	710.0	-70.2	-45.3	2.57923	1317.3	.014	-.36	245.965	709576.	-149.08	9.061
438.00	123568	30.60	-65.99	687.3	-71.9	-45.3	2.57377	1317.4	.013	-.35	246.040	709440.	-149.11	8.955
440.00	122277	30.60	-65.99	665.3	-73.5	-45.3	2.55611	1317.4	.012	-.33	246.106	709298.	-149.14	8.851
442.00	121017	30.60	-65.99	644.6	-75.0	-45.2	2.53122	1317.4	.011	-.31	246.164	709153.	-149.17	8.751
444.00	119787	30.59	-65.99	625.1	-76.4	-45.2	2.50720	1317.4	.010	-.29	246.216	709005.	-149.20	8.652
446.00	118587	30.59	-65.99	606.5	-77.7	-45.2	2.50164	1317.5	.010	-.28	246.262	708854.	-149.22	8.556
448.00	117417	30.59	-65.99	588.4	-78.9	-45.1	2.48532	1317.5	.009	-.27	246.302	708703.	-149.24	8.463
450.00	116277	30.59	-65.99	571.3	-80.0	-45.1	2.46219	1317.5	.009	-.26	246.337	708550.	-149.25	8.372
452.00	115166	30.59	-65.99	555.2	-81.1	-45.0	2.43534	1317.5	.008	-.24	246.367	708398.	-149.27	8.283
454.00	114083	30.59	-65.99	539.9	-82.1	-45.0	2.42829	1317.5	.007	-.23	246.394	708246.	-149.28	8.197
456.00	113027	30.59	-65.99	525.0	-82.9	-44.9	2.41541	1317.5	.007	-.22	246.417	708095.	-149.29	8.113
458.00	111998	30.59	-65.99	510.7	-83.7	-44.8	2.39610	1317.6	.007	-.21	246.437	707945.	-149.30	8.031
460.00	110996	30.59	-65.99	497.2	-84.5	-44.7	2.37297	1317.6	.006	-.20	246.454	707797.	-149.31	7.952
462.00	110018	30.59	-65.99	484.6	-85.1	-44.6	2.34826	1317.6	.006	-.19	246.469	707651.	-149.32	7.874
464.00	109064	30.59	-65.99	472.6	-85.7	-44.5	2.34501	1317.6	.006	-.18	246.482	707507.	-149.32	7.798
466.00	108133	30.59	-65.99	460.7	-86.3	-44.4	2.33319	1317.6	.005	-.18	246.493	707365.	-149.33	7.725
468.00	107225	30.59	-65.99	449.4	-86.7	-44.2	2.31678	1317.6	.005	-.17	246.502	707225.	-149.33	7.653
470.00	106338	30.59	-65.99	438.7	-87.2	-44.0	2.29761	1317.6	.005	-.16	246.510	707088.	-149.34	7.582
472.00	105472	30.59	-65.99	428.6	-87.5	-43.8	2.27750	1317.6	.004	-.15	246.517	706954.	-149.34	7.513
474.00	104625	30.59	-65.99	419.1	-87.9	-43.6	2.26614	1317.6	.004	-.14	246.523	706822.	-149.34	7.446
476.00	103796	30.59	-65.99	409.9	-88.2	-43.3	2.26242	1317.6	.004	-.14	246.528	706693.	-149.35	7.380
478.00	102986	30.59	-65.99	400.8	-88.4	-43.0	2.25240	1317.7	.004	-.14	246.532	706567.	-149.35	7.315
480.00	102193	30.59	-65.99	392.2	-88.6	-42.6	2.23940	1317.7	.004	-.13	246.536	706444.	-149.35	7.252

TABLE XVII

RFD-1 Reflector Springs No. 1 and 3 Trajectory

```
TTA7622 38-64  SNAP    000650  092463  SPR1                                             ATMOS= THEORETICAL ARDC 1959 ATMOSPHERE
CONTROLJIM AUG 28        DATA-A=                    DATA-B=RFDA REFRACTION  DATA-C=                DATA-D=
OBSERVER     32.3467=LAT   -64.6538=LONG    0.0000=ORNT          64=ELEV      -64484=X .     -36074=Y.        -0=Z
  WT    CD  AREA        VI   GAMMAI        TAUI          LAT    LONG      VT   GAMMA     TAU
 12.0  1.00  1.00  21074. -7.10000 -41.83400  31.940000 -67.56  20123. -7.4375 -44.349
```

TIME	HITE	LAT	LONG	VT	GAMMA	TAU	Q	QC	DQC	AT	RANGE	SR	AZM	ELOBS
323.00	272248	31.94	-67.56	20123	-7.44	-44.3	4.70947	.00000	25.2	-.27	.000000	890857.	-96.818	16.48
324.00	269639	31.90	-67.51	20113	-7.47	-44.4	5.39804	26.032	27.0	-.32	3.23916	878715.	-97.897	16.57
326.00	264394	31.83	-67.42	20087	-7.53	-44.4	7.59915	85.036	31.9	-.51	9.71247	855335.	-100.15	16.74
328.00	259117	31.75	-67.33	20046	-7.59	-44.5	9.96233	153.20	36.3	-.70	16.1760	833248.	-102.52	16.87
330.00	253810	31.68	-67.24	19994	-7.65	-44.5	13.1565	231.14	41.5	-.97	22.6255	812563.	-105.01	16.98
332.00	248479	31.60	-67.15	19923	-7.71	-44.6	16.7709	319.14	46.5	-1.3	29.0550	793393.	-107.62	17.05
334.00	243126	31.52	-67.07	19829	-7.77	-44.7	21.4717	417.58	52.0	-1.7	35.4592	775844.	-110.35	17.09
336.00	237760	31.45	-66.98	19708	-7.83	-44.7	26.9629	527.18	57.5	-2.1	41.8295	760024.	-113.17	17.07
338.00	232386	31.38	-66.89	19555	-7.90	-44.8	33.5103	647.78	63.1	-2.7	48.1565	746028.	-116.09	17.01
340.00	227014	31.30	-66.80	19363	-7.97	-44.8	41.3209	779.37	68.5	-3.3	54.4287	733938.	-119.08	16.89
342.00	221654	31.23	-66.72	19128	-8.04	-44.9	49.8360	921.29	73.3	-4.0	60.6328	723813.	-122.13	16.72
344.00	216317	31.16	-66.63	18843	-8.12	-44.9	60.1055	1072.5	77.9	-4.9	66.7536	715686.	-125.20	16.49
346.00	211019	31.09	-66.55	18502	-8.20	-45.0	70.2940	1231.6	81.0	-5.7	72.7740	709557.	-128.27	16.20
348.00	205772	31.02	-66.47	18102	-8.28	-45.0	82.5330	1396.3	83.7	-6.7	78.6754	705390.	-131.32	15.87
350.00	200593	30.95	-66.39	17639	-8.38	-45.1	93.4492	1564.4	84.2	-7.6	84.4380	703108.	-134.31	15.49
352.00	195499	30.88	-66.31	17116	-8.48	-45.1	105.096	1732.4	83.6	-8.6	90.0414	702598.	-137.21	15.07
354.00	190505	30.82	-66.24	16532	-8.59	-45.2	116.351	1897.9	81.6	-9.6	95.4662	703712.	-140.01	14.62
356.00	185627	30.75	-66.17	15890	-8.71	-45.2	126.556	2058.0	78.2	-10.	100.693	706271.	-142.68	14.15
358.00	180881	30.70	-66.10	15197	-8.85	-45.2	135.217	2209.7	73.4	-11.	105.703	710078.	-145.20	13.67
360.00	176279	30.64	-66.03	14462	-9.00	-45.3	142.093	2350.8	67.6	-12.	110.483	714921.	-147.57	13.19
362.00	171834	30.58	-65.97	13692	-9.17	-45.3	149.031	2480.0	61.5	-12.	115.019	720588.	-149.77	12.70
364.00	167556	30.53	-65.91	12888	-9.36	-45.4	154.254	2596.5	54.9	-13.	119.300	726869.	-151.81	12.23
366.00	163455	30.49	-65.86	12063	-9.57	-45.4	156.734	2699.5	48.0	-13.	123.317	733561.	-153.68	11.77
368.00	159537	30.44	-65.81	11233	-9.80	-45.4	156.344	2788.7	41.1	-13.	127.066	740483.	-155.39	11.33
370.00	155806	30.40	-65.76	10411	-10.1	-45.4	154.008	2864.4	34.7	-13.	130.546	747475.	-156.94	10.92
372.00	152260	30.36	-65.72	9604.	-10.4	-45.5	150.967	2927.8	28.8	-12.	133.762	754405.	-158.34	10.52
374.00	148899	30.33	-65.68	8820.	-10.7	-45.5	145.499	2980.1	23.6	-12.	136.720	761161.	-159.60	10.16
376.00	145717	30.29	-65.64	8070.	-11.1	-45.5	138.399	3022.6	19.0	-11.	139.428	767659.	-160.73	9.812
378.00	142708	30.26	-65.61	7361.	-11.5	-45.6	130.657	3056.6	15.1	-11.	141.900	773837.	-161.75	9.491
380.00	139862	30.24	-65.58	6698.	-11.9	-45.6	121.089	3083.5	11.9	-9.9	144.148	779656.	-162.65	9.194
382.00	137169	30.21	-65.55	6084.	-12.4	-45.6	112.406	3104.6	9.32	-9.2	146.188	785096.	-163.46	8.918
384.00	134617	30.19	-65.53	5522.	-13.0	-45.6	102.696	3121.1	7.23	-8.3	148.037	790147.	-164.18	8.661
386.00	132194	30.17	-65.50	5009.	-13.6	-45.6	94.0632	3133.9	5.61	-7.6	149.711	794817.	-164.83	8.421
388.00	129889	30.15	-65.48	4544.	-14.3	-45.6	84.9967	3143.7	4.32	-6.8	151.225	799115.	-165.40	8.198
390.00	127688	30.14	-65.47	4125.	-15.1	-45.7	77.4943	3151.4	3.35	-6.2	152.595	803059.	-165.92	7.990
392.00	125580	30.12	-65.45	3747.	-16.0	-45.7	69.8188	3157.3	2.59	-5.5	153.834	806570.	-166.38	7.795
394.00	123556	30.11	-65.43	3408.	-16.9	-45.7	63.3409	3161.8	2.01	-5.0	154.955	809968.	-166.79	7.611
396.00	121607	30.10	-65.42	3104.	-18.0	-45.7	57.2745	3165.4	1.56	-4.5	155.971	812978.	-167.16	7.437
398.00	119722	30.09	-65.41	2833.	-19.1	-45.7	51.6536	3168.2	1.22	-4.0	156.891	815720.	-167.50	7.272
400.00	117894	30.08	-65.40	2590.	-20.4	-45.7	47.1105	3170.3	.960	-3.6	157.725	818216.	-167.80	7.115
402.00	116117	30.07	-65.39	2372.	-21.7	-45.7	42.7217	3172.0	.757	-3.2	158.483	820487.	-168.07	6.965
404.00	114384	30.06	-65.38	2177.	-23.2	-45.7	38.9066	3173.4	.601	-2.9	159.170	822550.	-168.31	6.821
406.00	112689	30.05	-65.37	2003.	-24.7	-45.7	35.7278	3174.4	.481	-2.6	159.795	824423.	-168.53	6.683
408.00	111029	30.04	-65.36	1847.	-26.4	-45.8	32.7079	3175.3	.387	-2.3	160.363	826122.	-168.73	6.550
410.00	109399	30.04	-65.35	1708.	-28.2	-45.8	30.1271	3176.0	.314	-2.0	160.880	827661.	-168.91	6.421
412.00	107796	30.03	-65.35	1584.	-30.1	-45.8	28.0124	3176.6	.257	-1.8	161.351	829055.	-169.08	6.296
414.00	106218	30.03	-65.34	1472.	-32.2	-45.8	26.0000	3177.0	.211	-1.6	161.779	830314.	-169.23	6.174
416.00	104661	30.02	-65.34	1372.	-34.3	-45.8	24.2401	3177.4	.176	-1.5	162.168	831450.	-169.36	6.056
418.00	103124	30.02	-65.33	1283.	-36.5	-45.8	22.9087	3177.8	.148	-1.3	162.522	832473.	-169.48	5.940
420.00	101607	30.01	-65.33	1202.	-38.8	-45.8	21.6202	3178.0	.125	-1.2	162.845	833392.	-169.59	5.827

TTA7622 3B-64 SNAP 000650 092463 SPR1 ATMOS= THEORETICAL ARDC 1959 ATMOSPHERE
CONTROLJIM AUG 28 DATA-A= DATA-B=RFDA REFRACTION DATA-C= DATA-D=
OBSERVER 32.3467=LAT -64.6538=LONG 0.0000=ORNT 64=ELEV -64484=X . -36074=Y. -0=Z

WT	CD	AREA	VI	GAMMAI	TAUI	LAT	LONG	VT	GAMMA	TAU
12.0	1.00	1.00	2149.3	-20.2765	-17.59413	30.010759	-65.32	1130.4	-41.217	-45.782

TIME	HITE	LAT	LONG	VT	GAMMA	TAU	Q	QC	DQC	AT	RANGE	SR	AZM	ELOBS
422.00	100109	30.01	-65.32	1130.	-41.2	-45.8	20.4218	3178.3	.106	-1.0	163.137	834216.	-169.69	5.716
424.00	98628.	30.01	-65.32	1066.	-43.7	-45.8	19.6319	3178.5	.092	-.95	163.403	834952.	-169.78	5.607
426.00	97165.	30.00	-65.32	1008.	-46.1	-45.8	18.8602	3178.6	.080	-.86	163.644	835606.	-169.87	5.501
428.00	95721.	30.00	-65.31	955.6	-48.6	-45.8	18.1219	3178.8	.070	-.77	163.862	836186.	-169.94	5.398
430.00	94297.	30.00	-65.31	908.6	-51.1	-45.8	17.5827	3178.9	.062	-.69	164.059	836698.	-170.01	5.296
432.00	92891.	30.00	-65.31	865.9	-53.6	-45.8	17.1880	3179.0	.055	-.63	164.236	837147.	-170.07	5.197
434.00	91508.	30.00	-65.31	826.9	-56.1	-45.8	16.7710	3179.1	.049	-.57	164.396	837538.	-170.12	5.099
436.00	90146.	29.99	-65.30	791.7	-58.5	-45.8	16.3587	3179.2	.044	-.52	164.540	837876.	-170.17	5.003
438.00	88807.	29.99	-65.30	759.6	-60.9	-45.8	16.1991	3179.3	.040	-.48	164.668	838166.	-170.21	4.909
440.00	87492.	29.99	-65.30	729.5	-63.2	-45.7	16.0032	3179.4	.037	-.45	164.783	838413.	-170.25	4.818
442.00	86203.	29.99	-65.30	701.7	-65.4	-45.7	15.7707	3179.4	.033	-.41	164.885	838619.	-170.29	4.728
444.00	84940.	29.99	-65.30	676.2	-67.5	-45.7	15.5317	3179.5	.031	-.38	164.976	838790.	-170.32	4.641
446.00	83704.	29.99	-65.30	652.5	-69.5	-45.7	15.4674	3179.6	.028	-.36	165.056	838928.	-170.34	4.556
448.00	82496.	29.99	-65.30	629.9	-71.4	-45.7	15.3335	3179.6	.026	-.34	165.127	839038.	-170.37	4.473
450.00	81316.	29.99	-65.30	608.9	-73.2	-45.7	15.1624	3179.7	.024	-.31	165.189	839121.	-170.39	4.392
452.00	80165.	29.99	-65.30	589.4	-74.8	-45.6	14.9717	3179.7	.022	-.29	165.243	839182.	-170.41	4.313
454.00	79041.	29.99	-65.29	571.1	-76.4	-45.6	14.8919	3179.8	.021	-.28	165.291	839223.	-170.42	4.236
456.00	77944.	29.98	-65.29	553.7	-77.8	-45.6	14.7858	3179.8	.019	-.26	165.332	839247.	-170.44	4.162
458.00	76875.	29.98	-65.29	537.3	-79.2	-45.5	14.6442	3179.8	.018	-.24	165.368	839256.	-170.45	4.089
460.00	75833.	29.98	-65.29	522.0	-80.4	-45.5	14.4843	3179.9	.017	-.23	165.399	839251.	-170.46	4.018
462.00	74816.	29.98	-65.29	507.7	-81.5	-45.4	14.3447	3179.9	.016	-.21	165.426	839235.	-170.47	3.949
464.00	73825.	29.98	-65.29	494.1	-82.5	-45.3	14.3055	3179.9	.015	-.21	165.449	839210.	-170.48	3.882
466.00	72857.	29.98	-65.29	480.9	-83.4	-45.3	14.2189	3180.0	.014	-.20	165.469	839176.	-170.48	3.817
468.00	71913.	29.98	-65.29	468.4	-84.2	-45.2	14.1041	3180.0	.013	-.19	165.486	839136.	-170.49	3.753
470.00	70992.	29.98	-65.29	456.7	-84.9	-45.1	13.9756	3180.0	.012	-.17	165.501	839091.	-170.50	3.691
472.00	70093.	29.98	-65.29	445.7	-85.6	-45.0	13.8426	3180.0	.012	-.16	165.514	839041.	-170.50	3.630
474.00	69215.	29.98	-65.29	435.2	-86.2	-44.8	13.8161	3180.1	.011	-.16	165.524	838987.	-170.50	3.571
476.00	68356.	29.98	-65.29	425.0	-86.7	-44.7	13.7587	3180.1	.011	-.15	165.533	838931.	-170.51	3.513
478.00	67517.	29.98	-65.29	415.2	-87.2	-44.5	13.6765	3180.1	.010	-.15	165.541	838872.	-170.51	3.457
480.00	66697.	29.98	-65.29	405.9	-87.6	-44.3	13.5801	3180.1	.010	-.14	165.547	838812.	-170.51	3.402
482.00	65895.	29.98	-65.29	397.1	-87.9	-44.0	13.4786	3180.1	.009	-.13	165.553	838751.	-170.51	3.348
484.00	65109.	29.98	-65.29	389.0	-88.2	-43.7	13.3774	3180.2	.009	-.12	165.557	838689.	-170.52	3.295
486.00	64340.	29.98	-65.29	381.1	-88.5	-43.4	13.3625	3180.2	.008	-.12	165.561	838627.	-170.52	3.244
488.00	63585.	29.98	-65.29	373.4	-88.7	-43.0	13.3320	3180.2	.008	-.12	165.565	838565.	-170.52	3.193
490.00	62846.	29.98	-65.29	365.9	-88.9	-42.5	13.2773	3180.2	.008	-.11	165.567	838503.	-170.52	3.144
492.00	62122.	29.98	-65.29	358.8	-89.1	-42.0	13.2099	3180.2	.007	-.11	165.570	838442.	-170.52	3.094
494.00	61411.	29.98	-65.29	352.0	-89.2	-41.4	13.1377	3180.2	.007	-.10	165.572	838381.	-170.52	3.046
496.00	60713.	29.98	-65.29	345.6	-89.3	-40.6	13.0656	3180.3	.007	-.09	165.573	838321.	-170.52	2.998
498.00	60028.	29.98	-65.29	339.6	-89.4	-39.7	12.9957	3180.3	.006	-.09	165.575	838262.	-170.52	2.952
500.00	59355.	29.98	-65.29	333.8	-89.5	-38.7	13.0066	3180.3	.006	-.09	165.576	838204.	-170.52	2.906
502.00	58693.	29.98	-65.29	328.0	-89.6	-37.6	12.9927	3180.3	.006	-.09	165.577	838147.	-170.52	2.861
504.00	58043.	29.98	-65.29	322.3	-89.7	-36.2	12.9579	3180.3	.006	-.08	165.578	838091.	-170.52	2.817
506.00	57404.	29.98	-65.29	316.9	-89.7	-34.7	12.9132	3180.3	.005	-.08	165.579	838036.	-170.52	2.773
508.00	56775.	29.98	-65.29	311.7	-89.8	-33.0	12.8642	3180.3	.005	-.08	165.579	837982.	-170.52	2.730
510.00	56157.	29.98	-65.29	306.7	-89.8	-31.1	12.8143	3180.3	.005	-.07	165.580	837929.	-170.52	2.688
512.00	55548.	29.98	-65.29	302.1	-89.8	-28.9	12.7655	3180.3	.005	-.07	165.581	837877.	-170.52	2.647
514.00	54949.	29.98	-65.29	297.6	-89.8	-26.7	12.7254	3180.4	.005	-.06	165.581	837826.	-170.52	2.606
516.00	54358.	29.98	-65.29	293.3	-89.9	-24.3	12.7473	3180.4	.005	-.07	165.582	837776.	-170.52	2.565
518.00	53776.	29.98	-65.29	288.8	-89.9	-21.8	12.7417	3180.4	.004	-.07	165.582	837728.	-170.52	2.526
520.00	53202.	29.98	-65.29	284.5	-89.9	-19.3	12.7206	3180.4	.004	-.06	165.582	837680.	-170.52	2.487

TABLE XVIII

RFD-1 Reflector Springs No. 2 and 4 Trajectory

```
TTA7622 38-64  SNAP    000651  092463  SPR2                                  ATMOS= THEORETICAL ARDC 1959 ATMOSPHERE
CONTROLJIM AUG 28         DATA-A=                   DATA-B=RFDA REFRACTION  DATA-C=                         DATA-D=
OBSERVER     32.3467=LAT    -64.6538=LONG     0.0000=ORNT          64=ELEV        -64484=X .     -36074=Y.          -0=Z
  WT     CD   AREA       VI    GAMMAI         TAUI          LAT     LONG       VT     GAMMA       TAU
  12.0  1.00  1.00   21074. -7.13800 -41.83400  31.935400 -67.56  20123. -7.4773 -44.350
```

TIME	HITE	LAT	LONG	VT	GAMMA	TAU	Q	QC	DQC	AT	RANGE	SR	AZM	ELOBS
323.00	272248	31.94	-67.56	20123	-7.48	-44.3	4.70949	.00000	25.2	-.27	2.802-8	891003.	-96.931	16.48
324.00	269625	31.90	-67.51	20113	-7.51	-44.4	5.40395	26.037	27.0	-.32	3.23888	878888.	-98.011	16.57
326.00	264353	31.82	-67.42	20087	-7.57	-44.4	7.61674	85.094	31.9	-.51	9.71163	855563.	-100.26	16.73
328.00	259048	31.75	-67.33	20048	-7.63	-44.5	10.0048	153.36	36.4	-.71	16.1746	833534.	-102.64	16.86
330.00	253714	31.67	-67.24	19994	-7.69	-44.5	13.2153	231.47	41.6	-.97	22.6234	812909.	-105.13	16.97
332.00	248355	31.60	-67.15	19922	-7.75	-44.6	16.8834	319.71	46.6	-1.3	29.0522	793802.	-107.74	17.03
334.00	242975	31.52	-67.07	19828	-7.81	-44.7	21.6059	418.47	52.2	-1.7	35.4555	776318.	-110.47	17.06
336.00	237582	31.45	-66.98	19706	-7.87	-44.7	27.1908	528.44	57.8	-2.1	41.8248	760565.	-113.30	17.04
338.00	232182	31.37	-66.89	19551	-7.94	-44.8	33.7627	649.49	63.3	-2.7	48.1503	746638.	-116.21	16.97
340.00	226784	31.30	-66.80	19358	-8.01	-44.8	41.7166	781.56	68.8	-3.3	54.4206	734616.	-119.20	16.85
342.00	221399	31.22	-66.72	19121	-8.08	-44.9	50.2494	924.04	73.5	-4.1	60.6221	724560.	-122.24	16.68
344.00	216039	31.15	-66.63	18833	-8.16	-44.9	60.7143	1075.7	78.2	-4.9	66.7396	716500.	-125.31	16.44
346.00	210717	31.08	-66.55	18489	-8.24	-45.0	70.8939	1235.4	81.2	-5.8	72.7558	710436.	-128.38	16.16
348.00	205450	31.01	-66.47	18086	-8.32	-45.0	83.3660	1400.5	83.9	-6.8	78.6519	706328.	-131.42	15.82
350.00	200251	30.94	-66.39	17618	-8.42	-45.1	94.2172	1569.1	84.3	-7.7	84.4077	704100.	-134.40	15.43
352.00	195139	30.88	-66.31	17091	-8.52	-45.1	106.014	1737.3	83.7	-8.7	90.0031	703637.	-137.29	15.01
354.00	190129	30.81	-66.24	16501	-8.63	-45.2	117.309	1902.9	81.6	-9.6	95.4184	704788.	-140.08	14.57
356.00	185238	30.75	-66.17	15854	-8.76	-45.2	127.520	2062.8	78.1	-10.	100.634	707375.	-142.74	14.10
358.00	180481	30.69	-66.10	15156	-8.89	-45.2	136.150	2214.3	73.2	-11.	105.632	711198.	-145.25	13.61
360.00	175870	30.63	-66.04	14416	-9.05	-45.3	142.976	2355.0	67.3	-12.	110.397	716046.	-147.60	13.13
362.00	171419	30.58	-65.97	13641	-9.21	-45.3	150.095	2483.7	61.2	-12.	114.917	721706.	-149.80	12.65
364.00	167137	30.53	-65.92	12832	-9.40	-45.4	155.229	2599.6	54.6	-13.	119.180	727968.	-151.82	12.17
366.00	163035	30.48	-65.86	12002	-9.62	-45.4	157.587	2701.8	47.6	-13.	123.178	734630.	-153.68	11.72
368.00	159119	30.44	-65.81	11168	-9.85	-45.4	157.069	2790.2	40.7	-13.	126.905	741511.	-155.37	11.28
370.00	155392	30.40	-65.76	10343	-10.1	-45.4	154.164	2865.0	34.2	-13.	130.364	748453.	-156.91	10.87
372.00	151852	30.36	-65.72	9536.	-10.4	-45.5	151.209	2927.5	28.4	-12.	133.557	755325.	-158.30	10.48
374.00	148498	30.32	-65.68	8750.	-10.7	-45.5	145.665	2979.0	23.2	-12.	136.492	762017.	-159.55	10.11
376.00	145325	30.29	-65.65	8001.	-11.1	-45.5	138.040	3020.7	18.6	-11.	139.178	768446.	-160.67	9.770
378.00	142326	30.26	-65.61	7294.	-11.5	-45.6	130.315	3054.0	14.8	-11.	141.627	774553.	-161.68	9.452
380.00	139490	30.24	-65.58	6632.	-12.0	-45.6	120.785	3080.4	11.6	-9.9	143.853	780300.	-162.58	9.157
382.00	136808	30.21	-65.56	6023.	-12.5	-45.6	111.773	3101.0	9.09	-9.1	145.873	785668.	-163.38	8.883
384.00	134267	30.19	-65.53	5463.	-13.1	-45.6	102.155	3117.0	7.04	-8.3	147.702	790649.	-164.09	8.628
386.00	131855	30.17	-65.51	4954.	-13.7	-45.6	93.3219	3129.5	5.45	-7.5	149.357	795250.	-164.73	8.391
388.00	129559	30.15	-65.49	4493.	-14.4	-45.6	84.4157	3139.1	4.20	-6.8	150.854	799483.	-165.30	8.169
390.00	127368	30.14	-65.47	4077.	-15.2	-45.7	76.7689	3146.5	3.25	-6.1	152.208	803366.	-165.81	7.963
392.00	125271	30.12	-65.45	3703.	-16.1	-45.7	69.0526	3152.2	2.51	-5.5	153.432	806919.	-166.26	7.769
394.00	123256	30.11	-65.44	3369.	-17.1	-45.7	62.7394	3156.6	1.95	-4.9	154.539	810164.	-166.67	7.587
396.00	121314	30.10	-65.43	3068.	-18.1	-45.7	56.6408	3160.1	1.52	-4.4	155.542	813124.	-167.04	7.414
398.00	119436	30.09	-65.41	2800.	-19.3	-45.7	51.1761	3162.8	1.18	-3.9	156.451	815819.	-167.37	7.250
400.00	117616	30.08	-65.40	2559.	-20.5	-45.7	46.6014	3164.9	.931	-3.5	157.274	818273.	-167.66	7.094
402.00	115845	30.07	-65.39	2344.	-21.9	-45.7	42.2218	3166.5	.734	-3.2	158.022	820503.	-167.93	6.945
404.00	114118	30.06	-65.38	2153.	-23.4	-45.7	38.5328	3167.8	.583	-2.8	158.701	822530.	-168.17	6.803
406.00	112429	30.05	-65.37	1981.	-25.0	-45.7	35.3479	3168.9	.467	-2.5	159.318	824369.	-168.39	6.665
408.00	110774	30.05	-65.37	1827.	-26.7	-45.8	32.3411	3169.7	.375	-2.3	159.879	826037.	-168.59	6.533
410.00	109149	30.04	-65.36	1690.	-28.5	-45.8	29.8601	3170.4	.305	-2.0	160.389	827548.	-168.77	6.404
412.00	107550	30.03	-65.35	1567.	-30.4	-45.8	27.7436	3170.9	.250	-1.8	160.853	828916.	-168.93	6.280
414.00	105976	30.03	-65.35	1457.	-32.5	-45.8	25.7432	3171.4	.206	-1.6	161.275	830151.	-169.08	6.159
416.00	104423	30.02	-65.34	1358.	-34.6	-45.8	24.0610	3171.8	.171	-1.4	161.660	831265.	-169.21	6.041
418.00	102890	30.02	-65.34	1270.	-36.8	-45.8	22.7268	3172.1	.144	-1.3	162.009	832268.	-169.33	5.925
420.00	101377	30.02	-65.33	1191.	-39.2	-45.8	21.4439	3172.3	.122	-1.2	162.327	833168.	-169.44	5.813

TTA7622 3B-64 SNAP 000651 092463 SPR2 ATMOS= THEORETICAL ARDC 1959 ATMOSPHERE
CONTROLJIM AUG 28 DATA-A= DATA-B=RFDA REFRACTION DATA-C= DATA-D=
OBSERVER 32.3467=LAT -64.6538=LONG 0.0000=ORNT 64=ELEV -64484=X . -36074=Y. -0=Z

WT	CD	AREA	VI	GAMMAI	TAUI	LAT	LONG	VT	GAMMA	TAU
12.0	1.00	1.00	2138.9	-20.3291	-17.43351	30.012396	-65.33	1120.4	-41.548	-45.778

TIME	HITE	LAT	LONG	VT	GAMMA	TAU	Q	QC	DQC	AT	RANGE	SR	AZM	ELOBS
422.00	99882.	30.01	-65.33	1120.	-41.5	-45.8	20.2856	3172.6	.104	-1.0	162.615	833974.	-169.54	5.702
424.00	98404.	30.01	-65.33	1057.	-44.0	-45.8	19.5197	3172.8	.090	-.94	162.877	834694.	-169.63	5.594
426.00	96945.	30.01	-65.32	999.6	-46.5	-45.8	18.7482	3172.9	.078	-.84	163.115	835334.	-169.71	5.489
428.00	95505.	30.00	-65.32	948.2	-49.0	-45.8	18.0153	3173.1	.068	-.75	163.330	835901.	-169.78	5.385
430.00	94084.	30.00	-65.32	902.0	-51.5	-45.8	17.5254	3173.2	.061	-.68	163.524	836401.	-169.85	5.284
432.00	92682.	30.00	-65.32	859.8	-54.0	-45.8	17.1250	3173.3	.054	-.62	163.699	836838.	-169.91	5.185
434.00	91302.	30.00	-65.31	821.4	-56.5	-45.8	16.7058	3173.4	.048	-.57	163.856	837219.	-169.96	5.087
436.00	89944.	30.00	-65.31	786.7	-58.9	-45.8	16.3077	3173.5	.043	-.51	163.997	837548.	-170.01	4.992
438.00	88609.	29.99	-65.31	754.9	-61.2	-45.7	16.1727	3173.6	.040	-.48	164.124	837830.	-170.05	4.898
440.00	87298.	29.99	-65.31	725.2	-63.5	-45.7	15.9686	3173.7	.036	-.44	164.237	838069.	-170.09	4.807
442.00	86013.	29.99	-65.31	697.7	-65.7	-45.7	15.7322	3173.7	.033	-.41	164.337	838269.	-170.13	4.718
444.00	84755.	29.99	-65.31	672.5	-67.8	-45.7	15.5222	3173.8	.030	-.37	164.426	838433.	-170.16	4.631
446.00	83523.	29.99	-65.31	649.0	-69.8	-45.7	15.4453	3173.9	.028	-.36	164.505	838566.	-170.18	4.546
448.00	82319.	29.99	-65.30	626.7	-71.7	-45.7	15.3069	3173.9	.026	-.33	164.574	838670.	-170.21	4.463
450.00	81144.	29.99	-65.30	605.8	-73.4	-45.6	15.1323	3174.0	.024	-.31	164.635	838750.	-170.23	4.383
452.00	79996.	29.99	-65.30	586.6	-75.1	-45.6	14.9406	3174.0	.022	-.29	164.689	838807.	-170.24	4.304
454.00	78877.	29.99	-65.30	568.5	-76.6	-45.6	14.8816	3174.1	.021	-.27	164.735	838845.	-170.26	4.228
456.00	77784.	29.99	-65.30	551.2	-78.0	-45.5	14.7659	3174.1	.019	-.26	164.776	838865.	-170.27	4.153
458.00	76720.	29.99	-65.30	535.0	-79.3	-45.5	14.6206	3174.1	.018	-.24	164.811	838871.	-170.29	4.081
460.00	75681.	29.99	-65.30	519.8	-80.5	-45.5	14.4599	3174.2	.017	-.22	164.842	838864.	-170.30	4.010
462.00	74668.	29.99	-65.30	505.6	-81.6	-45.4	14.3406	3174.2	.016	-.21	164.868	838847.	-170.31	3.942
464.00	73680.	29.99	-65.30	492.1	-82.6	-45.3	14.2942	3174.2	.015	-.21	164.891	838820.	-170.31	3.875
466.00	72716.	29.99	-65.30	479.0	-83.5	-45.3	14.2020	3174.3	.014	-.20	164.910	838785.	-170.32	3.809
468.00	71776.	29.98	-65.30	466.6	-84.3	-45.2	14.0846	3174.3	.013	-.18	164.927	838744.	-170.33	3.746
470.00	70858.	29.98	-65.30	455.0	-85.0	-45.1	13.9553	3174.3	.012	-.17	164.941	838697.	-170.33	3.684
472.00	69962.	29.98	-65.30	444.1	-85.7	-44.9	13.8275	3174.3	.012	-.16	164.953	838646.	-170.33	3.623
474.00	69087.	29.98	-65.30	433.7	-86.3	-44.8	13.8111	3174.4	.011	-.16	164.964	838592.	-170.34	3.564
476.00	68231.	29.98	-65.30	423.5	-86.8	-44.6	13.7482	3174.4	.011	-.15	164.973	838535.	-170.34	3.507
478.00	67395.	29.98	-65.30	413.8	-87.2	-44.5	13.6635	3174.4	.010	-.15	164.980	838476.	-170.34	3.451
480.00	66578.	29.98	-65.30	404.6	-87.6	-44.2	13.5655	3174.4	.009	-.14	164.986	838416.	-170.35	3.396
482.00	65778.	29.98	-65.30	395.9	-88.0	-44.0	13.4637	3174.4	.009	-.13	164.992	838355.	-170.35	3.342
484.00	64995.	29.98	-65.30	387.8	-88.3	-43.7	13.3636	3174.5	.009	-.12	164.996	838293.	-170.35	3.290
486.00	64227.	29.98	-65.30	380.0	-88.5	-43.3	13.3647	3174.5	.008	-.12	165.000	838231.	-170.35	3.238
488.00	63475.	29.98	-65.30	372.3	-88.7	-42.9	13.3258	3174.5	.008	-.12	165.003	838169.	-170.35	3.188
490.00	62738.	29.98	-65.30	364.8	-88.9	-42.5	13.2682	3174.5	.008	-.11	165.006	838107.	-170.35	3.138
492.00	62016.	29.98	-65.30	357.7	-89.1	-41.9	13.1999	3174.5	.007	-.10	165.008	838046.	-170.35	3.089
494.00	61307.	29.98	-65.30	351.0	-89.2	-41.3	13.1274	3174.5	.007	-.10	165.010	837985.	-170.35	3.041
496.00	60611.	29.98	-65.30	344.7	-89.3	-40.5	13.0553	3174.5	.007	-.09	165.012	837925.	-170.36	2.993
498.00	59928.	29.98	-65.30	338.8	-89.4	-39.6	12.9947	3174.6	.006	-.09	165.013	837866.	-170.36	2.947
500.00	59256.	29.98	-65.30	333.0	-89.5	-38.6	13.0084	3174.6	.006	-.09	165.014	837808.	-170.36	2.901
502.00	58596.	29.98	-65.30	327.1	-89.6	-37.4	12.9878	3174.6	.006	-.09	165.015	837751.	-170.36	2.856
504.00	57948.	29.98	-65.30	321.5	-89.7	-36.0	12.9513	3174.6	.006	-.08	165.016	837695.	-170.36	2.812
506.00	57310.	29.98	-65.30	316.1	-89.7	-34.5	12.9058	3174.6	.005	-.08	165.017	837640.	-170.36	2.768
508.00	56683.	29.98	-65.30	310.9	-89.8	-32.7	12.8566	3174.6	.005	-.08	165.018	837586.	-170.36	2.726
510.00	56067.	29.98	-65.30	306.0	-89.8	-30.8	12.8068	3174.6	.005	-.07	165.018	837534.	-170.36	2.684
512.00	55459.	29.98	-65.30	301.4	-89.8	-28.6	12.7584	3174.6	.005	-.07	165.019	837482.	-170.36	2.642
514.00	54861.	29.98	-65.30	297.0	-89.8	-26.3	12.7290	3174.6	.005	-.06	165.019	837431.	-170.36	2.601
516.00	54271.	29.98	-65.30	292.6	-89.9	-23.9	12.7494	3174.7	.005	-.07	165.020	837382.	-170.36	2.561
518.00	53690.	29.98	-65.30	288.2	-89.9	-21.4	12.7400	3174.7	.004	-.07	165.020	837333.	-170.36	2.522
520.00	53118.	29.98	-65.30	283.9	-89.9	-19.0	12.7171	3174.7	.004	-.06	165.021	837285.	-170.36	2.483

TABLE XIX

RFD-1 Reflector No. 1 Trajectory

TTA7622 38-64 SNAP 000655 092463 RFL1 ATMOS= THEORETICAL ARDC 1959 ATMOSPHERE
CONTROLJIM AUG 28 DATA-A= DATA-B=RFDA REFRACTION DATA-C= DATA-D=
OBSERVER 32.3467=LAT -64.6538=LONG 0.0000=ORNT 64=ELEV -64484=X . -36074=Y. -0=Z

WT	CD	AREA	VI	GAMMAI	TAUI	LAT	LONG	VT	GAMMA	TAU
8.69	1.00	1.00	21074.	-7.11700	-41.83400	31.935400	-67.56	20123.	-7.4553	-44.350

TIME	HITE	LAT	LONG	VT	GAMMA	TAU	Q	QC	DQC	AT	RANGE	SR	AZM	ELOBS
323.00	272248	31.94	-67.56	20123	-7.46	-44.3	4.70946	.00000	25.2	-.42	2.802-8	891003.	-96.931	16.48
324.00	269633	31.90	-67.51	20108	-7.48	-44.4	5.39778	26.024	26.9	-.50	3.23862	878891.	-98.011	16.57
326.00	264379	31.82	-67.42	20068	-7.54	-44.4	7.59174	84.941	31.8	-.75	9.70801	855583.	-100.26	16.73
328.00	259096	31.75	-67.33	20012	-7.60	-44.5	9.93932	152.85	36.2	-1.0	16.1626	833585.	-102.63	16.86
330.00	253789	31.67	-67.24	19935	-7.66	-44.5	13.0915	230.25	41.1	-1.4	22.5966	813009.	-105.12	16.97
332.00	248464	31.60	-67.15	19833	-7.73	-44.6	16.6347	317.25	45.9	-1.8	29.0020	793967.	-107.72	17.04
334.00	243126	31.52	-67.07	19702	-7.79	-44.7	21.1988	414.04	51.0	-2.3	35.3713	776564.	-110.43	17.07
336.00	237784	31.45	-66.98	19535	-7.86	-44.7	26.4595	521.02	55.9	-2.9	41.6933	760902.	-113.24	17.05
338.00	232448	31.37	-66.89	19325	-7.93	-44.8	32.6487	637.67	60.7	-3.6	47.9553	747073.	-116.12	16.98
340.00	227130	31.30	-66.81	19066	-8.00	-44.8	39.8569	763.50	65.1	-4.5	54.1424	735145.	-119.07	16.87
342.00	221842	31.23	-66.72	18752	-8.08	-44.9	47.5724	897.36	68.6	-5.3	60.2377	725163.	-122.05	16.70
344.00	216599	31.16	-66.64	18376	-8.16	-44.9	56.5158	1037.6	71.6	-6.4	66.2223	717142.	-125.05	16.47
346.00	211418	31.09	-66.56	17934	-8.25	-45.0	65.1699	1182.3	72.9	-7.4	72.0754	711058.	-128.03	16.20
348.00	206316	31.02	-66.48	17425	-8.34	-45.0	74.9276	1328.8	73.4	-8.5	77.7753	706848.	-130.96	15.88
350.00	201310	30.96	-66.41	16848	-8.45	-45.1	83.3451	1474.6	72.0	-9.4	83.3002	704409.	-133.82	15.52
352.00	196419	30.89	-66.33	16210	-8.57	-45.1	91.4199	1616.2	69.4	-10.	88.6286	703603.	-136.58	15.12
354.00	191657	30.83	-66.26	15515	-8.70	-45.1	98.7015	1751.4	65.6	-11.	93.7417	704259.	-139.22	14.71
356.00	187040	30.77	-66.20	14771	-8.84	-45.2	104.524	1877.9	60.7	-12.	98.6220	706185.	-141.72	14.27
358.00	182580	30.72	-66.13	13991	-9.00	-45.2	108.600	1993.8	55.1	-12.	103.256	709177.	-144.06	13.83
360.00	178286	30.67	-66.07	13187	-9.18	-45.3	110.832	2097.9	49.0	-13.	107.633	713028.	-146.24	13.39
362.00	174164	30.62	-66.02	12373	-9.38	-45.3	111.691	2189.7	42.8	-13.	111.747	717540.	-148.26	12.96
364.00	170218	30.57	-65.96	11554	-9.61	-45.3	112.178	2269.5	37.0	-13.	115.597	722526.	-150.12	12.53
366.00	166451	30.53	-65.92	10736	-9.86	-45.4	111.331	2338.0	31.5	-13.	119.182	727817.	-151.82	12.12
368.00	162865	30.49	-65.87	9932.	-10.1	-45.4	108.588	2395.8	26.3	-12.	122.504	733262.	-153.37	11.73
370.00	159457	30.45	-65.83	9154.	-10.5	-45.4	104.162	2443.6	21.6	-12.	125.568	738736.	-154.77	11.36
372.00	156220	30.42	-65.79	8413.	-10.8	-45.4	99.1374	2482.7	17.6	-11.	128.386	744139.	-156.03	11.01
374.00	153148	30.39	-65.76	7710.	-11.2	-45.5	93.8937	2514.4	14.2	-11.	130.970	749394.	-157.18	10.68
376.00	150232	30.36	-65.72	7050.	-11.6	-45.5	87.8230	2539.8	11.3	-9.9	133.331	754441.	-158.20	10.37
378.00	147464	30.34	-65.70	6433.	-12.1	-45.5	82.1676	2560.0	8.99	-9.2	135.485	759240.	-159.12	10.08
380.00	144833	30.31	-65.67	5862.	-12.6	-45.5	75.5800	2576.0	7.06	-8.5	137.446	763764.	-159.95	9.804
382.00	142329	30.29	-65.64	5339.	-13.2	-45.5	69.8123	2588.5	5.55	-7.8	139.229	768000.	-160.69	9.549
384.00	139941	30.27	-65.62	4860.	-13.9	-45.6	63.5110	2598.3	4.32	-7.1	140.847	771945.	-161.36	9.311
386.00	137659	30.25	-65.60	4425.	-14.6	-45.6	58.2544	2606.0	3.38	-6.5	142.317	775600.	-161.96	9.087
388.00	135473	30.24	-65.59	4030.	-15.4	-45.6	52.7686	2612.0	2.63	-5.8	143.651	778976.	-162.49	8.877
390.00	133371	30.22	-65.57	3675.	-16.3	-45.6	48.1260	2616.7	2.06	-5.3	144.862	782084.	-162.97	8.678
392.00	131347	30.21	-65.55	3353.	-17.3	-45.6	43.6577	2620.3	1.61	-4.7	145.961	784938.	-163.41	8.489
394.00	129390	30.20	-65.54	3065.	-18.3	-45.6	39.5953	2623.2	1.27	-4.2	146.959	787554.	-163.80	8.311
396.00	127494	30.19	-65.53	2805.	-19.5	-45.6	36.1394	2625.4	.999	-3.8	147.867	789948.	-164.15	8.141
398.00	125650	30.18	-65.52	2572.	-20.7	-45.7	32.7985	2627.2	.790	-3.4	148.692	792135.	-164.47	7.978
400.00	123854	30.17	-65.51	2363.	-22.1	-45.7	30.0159	2628.6	.629	-3.1	149.443	794130.	-164.76	7.823
402.00	122100	30.16	-65.50	2174.	-23.5	-45.7	27.5138	2629.7	.504	-2.8	150.127	795949.	-165.02	7.674
404.00	120382	30.15	-65.49	2006.	-25.1	-45.7	25.1507	2630.6	.405	-2.5	150.750	797603.	-165.26	7.530
406.00	118697	30.15	-65.48	1854.	-26.8	-45.7	23.2701	2631.4	.329	-2.2	151.318	799107.	-165.47	7.390
408.00	117041	30.14	-65.48	1718.	-28.6	-45.7	21.5432	2632.0	.269	-2.0	151.836	800472.	-165.67	7.255
410.00	115411	30.14	-65.47	1596.	-30.4	-45.7	19.9212	2632.5	.220	-1.8	152.307	801708.	-165.84	7.124
412.00	113805	30.13	-65.46	1486.	-32.5	-45.7	18.6580	2632.9	.183	-1.6	152.738	802825.	-166.00	6.996
414.00	112221	30.13	-65.46	1388.	-34.5	-45.7	17.5136	2633.2	.153	-1.5	153.130	803834.	-166.15	6.871
416.00	110657	30.12	-65.45	1299.	-36.7	-45.7	16.4328	2633.5	.129	-1.3	153.488	804742.	-166.28	6.750
418.00	109112	30.12	-65.45	1220.	-39.0	-45.7	15.5846	2633.7	.109	-1.2	153.813	805557.	-166.40	6.631
420.00	107586	30.11	-65.44	1148.	-41.3	-45.7	14.8699	2633.9	.094	-1.1	154.110	806286.	-166.51	6.514

TTA7622 38-64 SNAP 000655 092463 RFL1 ATMOS= THEORETICAL ARDC 1959 ATMOSPHERE
CONTROLJIM AUG 28 DATA-A= DATA-B=RFDA REFRACTION DATA-C= DATA-D=
OBSERVER 32.3467=LAT -64.6538=LONG 0.0000=ORNT 64=ELEV -64484=X . -36074=Y. -0=Z

WT	CD	AREA	VI	GAMMAI	TAUI	LAT	LONG	VT	GAMMA	TAU
8.69	1.00	1.00	2094.9	-20.9527	-16.64581	30.110838	-65.44	1083.5	-43.740	-45.715

TIME	HITE	LAT	LONG	VT	GAMMA	TAU	Q	QC	DQC	AT	RANGE	SR	AZM	ELOBS
422.00	106078	30.11	-65.44	1084.	-43.7	-45.7	14.1797	2634.1	.081	-.95	154.379	806936.	-166.61	6.400
424.00	104589	30.11	-65.44	1026.	-46.2	-45.7	13.5987	2634.2	.070	-.85	154.623	807513.	-166.70	6.289
426.00	103119	30.11	-65.43	973.4	-48.6	-45.7	13.1981	2634.4	.062	-.78	154.845	808023.	-166.78	6.179
428.00	101668	30.10	-65.43	925.8	-51.1	-45.7	12.7881	2634.5	.055	-.70	155.046	808471.	-166.85	6.072
430.00	100237	30.10	-65.43	883.0	-53.5	-45.7	12.3922	2634.6	.049	-.63	155.227	808861.	-166.92	5.966
432.00	98828.	30.10	-65.43	844.1	-56.0	-45.7	12.1803	2634.7	.044	-.58	155.391	809200.	-166.98	5.863
434.00	97440.	30.10	-65.43	808.2	-58.3	-45.7	11.9682	2634.8	.040	-.53	155.538	809490.	-167.03	5.762
436.00	96076.	30.10	-65.42	775.3	-60.7	-45.7	11.7395	2634.8	.036	-.49	155.670	809737.	-167.08	5.663
438.00	94736.	30.09	-65.42	745.2	-62.9	-45.7	11.5443	2634.9	.033	-.45	155.788	809943.	-167.13	5.566
440.00	93422.	30.09	-65.42	717.3	-65.1	-45.7	11.4768	2635.0	.030	-.42	155.893	810114.	-167.16	5.472
442.00	92135.	30.09	-65.42	690.9	-67.2	-45.6	11.3609	2635.0	.027	-.39	155.987	810251.	-167.20	5.380
444.00	90875.	30.09	-65.42	666.5	-69.2	-45.6	11.2172	2635.1	.025	-.36	156.070	810359.	-167.23	5.290
446.00	89643.	30.09	-65.42	643.7	-71.1	-45.6	11.1083	2635.1	.023	-.34	156.143	810441.	-167.25	5.203
448.00	88439.	30.09	-65.42	622.2	-72.8	-45.6	11.0845	2635.2	.022	-.33	156.208	810500.	-167.28	5.118
450.00	87265.	30.09	-65.42	601.5	-74.5	-45.6	11.0056	2635.2	.020	-.31	156.265	810538.	-167.30	5.035
452.00	86121.	30.09	-65.42	582.1	-76.1	-45.5	10.6934	2635.2	.019	-.29	156.314	810557.	-167.32	4.954
454.00	85005.	30.09	-65.41	563.9	-77.5	-45.5	10.7632	2635.3	.017	-.27	156.357	810561.	-167.33	4.875
456.00	83918.	30.09	-65.41	546.8	-78.8	-45.5	10.7395	2635.3	.016	-.26	156.395	810551.	-167.35	4.799
458.00	82860.	30.09	-65.41	530.2	-80.1	-45.4	10.6655	2635.3	.015	-.25	156.428	810529.	-167.36	4.724
460.00	81829.	30.09	-65.41	514.5	-81.2	-45.4	10.5642	2635.4	.014	-.23	156.456	810497.	-167.37	4.652
462.00	80826.	30.09	-65.41	499.7	-82.2	-45.3	10.4481	2635.4	.013	-.22	156.480	810457.	-167.38	4.581
464.00	79848.	30.09	-65.41	486.0	-83.2	-45.2	10.3394	2635.4	.012	-.20	156.501	810409.	-167.39	4.513
466.00	78895.	30.09	-65.41	473.1	-84.0	-45.1	10.2928	2635.5	.012	-.20	156.519	810356.	-167.39	4.446
468.00	77966.	30.09	-65.41	460.6	-84.8	-45.0	10.2184	2635.5	.011	-.19	156.534	810297.	-167.40	4.381
470.00	77060.	30.09	-65.41	448.6	-85.4	-44.9	10.1287	2635.5	.010	-.17	156.547	810235.	-167.40	4.318
472.00	76176.	30.08	-65.41	437.7	-86.0	-44.8	10.0329	2635.5	.010	-.16	156.558	810170.	-167.41	4.256
474.00	75313.	30.08	-65.41	427.5	-86.6	-44.7	9.93657	2635.5	.009	-.15	156.568	810103.	-167.41	4.196
476.00	74469.	30.08	-65.41	417.8	-87.0	-44.5	9.89331	2635.6	.009	-.15	156.576	810034.	-167.41	4.137
478.00	73644.	30.08	-65.41	408.4	-87.5	-44.3	9.86290	2635.6	.008	-.14	156.583	809964.	-167.42	4.079
480.00	72837.	30.08	-65.41	399.3	-87.8	-44.0	9.81156	2635.6	.008	-.14	156.588	809894.	-167.42	4.023
482.00	72048.	30.08	-65.41	390.6	-88.1	-43.8	9.74788	2635.6	.007	-.13	156.593	809823.	-167.42	3.968
484.00	71275.	30.08	-65.41	382.5	-88.4	-43.4	9.68141	2635.6	.007	-.12	156.597	809752.	-167.42	3.914
486.00	70518.	30.08	-65.41	374.8	-88.6	-43.1	9.61481	2635.6	.007	-.11	156.601	809681.	-167.42	3.861
488.00	69776.	30.08	-65.41	367.6	-88.8	-42.6	9.57060	2635.6	.006	-.11	156.604	809611.	-167.42	3.809
490.00	69048.	30.08	-65.41	360.6	-89.0	-42.1	9.56739	2635.7	.006	-.11	156.606	809541.	-167.42	3.758
492.00	68333.	30.08	-65.41	353.7	-89.2	-41.5	9.54044	2635.7	.006	-.10	156.608	809473.	-167.42	3.708
494.00	67633.	30.08	-65.41	347.0	-89.3	-40.8	9.50244	2635.7	.006	-.10	156.610	809405.	-167.43	3.659
496.00	66945.	30.08	-65.41	340.7	-89.4	-39.9	9.45852	2635.7	.005	-.09	156.611	809339.	-167.43	3.612
498.00	66270.	30.08	-65.41	334.7	-89.5	-39.0	9.41245	2635.7	.005	-.09	156.613	809273.	-167.43	3.565
500.00	65606.	30.08	-65.41	329.0	-89.6	-37.9	9.36700	2635.7	.005	-.08	156.614	809209.	-167.43	3.519
502.00	64954.	30.08	-65.41	323.6	-89.6	-36.6	9.32746	2635.7	.005	-.08	156.615	809146.	-167.43	3.473
504.00	64312.	30.08	-65.41	318.4	-89.7	-35.1	9.33918	2635.7	.005	-.08	156.616	809084.	-167.43	3.429
506.00	63680.	30.08	-65.41	313.1	-89.7	-33.4	9.32977	2635.7	.005	-.08	156.616	809023.	-167.43	3.385
508.00	63059.	30.08	-65.41	308.0	-89.8	-31.6	9.30835	2635.8	.004	-.08	156.617	808963.	-167.43	3.342
510.00	62448.	30.08	-65.41	303.0	-89.8	-29.5	9.28040	2635.8	.004	-.07	156.617	808905.	-167.43	3.299
512.00	61847.	30.08	-65.41	298.3	-89.8	-27.3	9.24951	2635.8	.004	-.07	156.618	808848.	-167.43	3.257
514.00	61255.	30.08	-65.41	293.8	-89.9	-25.0	9.21802	2635.8	.004	-.07	156.618	808792.	-167.43	3.216
516.00	60672.	30.08	-65.41	289.5	-89.9	-22.5	9.18725	2635.8	.004	-.06	156.619	808737.	-167.43	3.176
518.00	60097.	30.08	-65.41	285.5	-89.9	-20.0	9.15792	2635.8	.004	-.06	156.619	808684.	-167.43	3.136
520.00	59530.	30.08	-65.41	281.6	-89.9	-17.6	9.16913	2635.8	.004	-.06	156.620	808631.	-167.43	3.096

TABLE XX

RFD-1 Reflector No. 2 Trajectory

```
TTA7622 3B-64  SNAP    000656  092463  RFL2                                     ATMOS= THEORETICAL ARDC 1959 ATMOSPHERE
CONTROLJIM AUG 28         DATA-A=                     DATA-B=RFDA REFRACTION  DATA-C=                  DATA-D=
OBSERVER    32.3467=LAT    -64.6538=LONG    0.0000=ORNT         64=ELEV      -64484=X .    -36074=Y.       -0=Z
   WT    CD  AREA        VI   GAMMAI        TAUI          LAT   LONG      VT   GAMMA      TAU
 8.69  1.00  1.00  21074. -7.11700 -41.83400  31.940000 -67.56  20123. -7.4553 -44.350
```

TIME	HITE	LAT	LONG	VT	GAMMA	TAU	Q	QC	DQC	AT	RANGE	SH	AZM	ELOBS
323.00	272248	31.94	-67.56	20123	-7.46	-44.3	4.70949	.00000	25.2	-.42	.000000	890857.	-96.818	16.48
324.00	269633	31.90	-67.51	20108	-7.48	-44.4	5.39780	26.024	26.9	-.50	3.23863	878715.	-97.897	16.57
326.00	264379	31.83	-67.42	20068	-7.54	-44.4	7.59177	84.942	31.8	-.75	9.70804	855345.	-100.14	16.74
328.00	259096	31.75	-67.33	20012	-7.60	-44.5	9.93937	152.85	36.2	-1.0	16.1627	833282.	-102.51	16.87
330.00	253789	31.68	-67.24	19935	-7.66	-44.5	13.0916	230.25	41.1	-1.4	22.5967	812638.	-105.00	16.98
332.00	248464	31.60	-67.16	19833	-7.73	-44.6	16.6348	317.25	45.9	-1.8	29.0020	793525.	-107.60	17.05
334.00	243126	31.53	-67.07	19702	-7.79	-44.7	21.1989	414.05	51.0	-2.3	35.3714	776050.	-110.31	17.08
336.00	237784	31.45	-66.98	19535	-7.86	-44.7	26.4596	521.03	55.9	-2.9	41.6934	760315.	-113.11	17.07
338.00	232448	31.38	-66.89	19325	-7.93	-44.8	32.6488	637.67	60.7	-3.6	47.9554	746411.	-116.00	17.00
340.00	227130	31.30	-66.81	19066	-8.00	-44.8	39.8571	763.51	65.1	-4.5	54.1426	734408.	-118.95	16.89
342.00	221842	31.23	-66.72	18752	-8.08	-44.9	47.5726	897.36	68.6	-5.3	60.2379	724353.	-121.93	16.72
344.00	216599	31.16	-66.64	18376	-8.16	-44.9	56.5160	1037.6	71.6	-6.4	66.2224	716260.	-124.93	16.50
346.00	211418	31.09	-66.56	17934	-8.25	-45.0	65.1701	1182.3	72.9	-7.4	72.0755	710106.	-127.92	16.22
348.00	206316	31.03	-66.48	17425	-8.34	-45.0	74.9279	1328.8	73.4	-8.5	77.7755	705829.	-130.85	15.90
350.00	201310	30.96	-66.41	16848	-8.45	-45.1	83.3455	1474.6	72.0	-9.4	83.3004	703328.	-133.72	15.54
352.00	196419	30.90	-66.33	16210	-8.57	-45.1	91.4202	1616.2	69.4	-10.	88.6288	702463.	-136.48	15.15
354.00	191657	30.84	-66.26	15515	-8.70	-45.1	98.7018	1751.4	65.6	-11.	93.7419	703065.	-139.12	14.74
356.00	187040	30.78	-66.20	14771	-8.84	-45.2	104.525	1877.9	60.7	-12.	98.6223	704942.	-141.63	14.30
358.00	182580	30.72	-66.13	13991	-9.00	-45.2	108.600	1993.8	55.1	-12.	103.256	707890.	-143.97	13.86
360.00	178286	30.67	-66.07	13187	-9.18	-45.3	110.832	2097.9	49.0	-13.	107.633	711702.	-146.16	13.42
362.00	174164	30.62	-66.02	12373	-9.38	-45.3	111.691	2189.7	42.8	-13.	111.748	716179.	-148.19	12.98
364.00	170218	30.58	-65.97	11554	-9.61	-45.3	112.178	2269.5	37.0	-13.	115.598	721134.	-150.05	12.56
366.00	166451	30.54	-65.92	10736	-9.86	-45.4	111.331	2338.0	31.5	-13.	119.182	726398.	-151.75	12.15
368.00	162865	30.50	-65.87	9932.	-10.1	-45.4	108.588	2395.8	26.3	-12.	122.504	731820.	-153.30	11.76
370.00	159457	30.46	-65.83	9154.	-10.5	-45.4	104.162	2443.6	21.6	-12.	125.569	737273.	-154.71	11.38
372.00	156220	30.43	-65.79	8413.	-10.8	-45.4	99.1376	2482.7	17.6	-11.	128.387	742658.	-155.98	11.03
374.00	153148	30.39	-65.76	7710.	-11.2	-45.5	93.8938	2514.4	14.2	-11.	130.970	747897.	-157.12	10.70
376.00	150232	30.37	-65.72	7050.	-11.6	-45.5	87.8231	2539.8	11.3	-9.9	133.332	752931.	-158.15	10.39
378.00	147464	30.34	-65.70	6433.	-12.1	-45.5	82.1677	2560.0	8.99	-9.2	135.486	757718.	-159.07	10.10
380.00	144833	30.32	-65.67	5862.	-12.6	-45.5	75.5800	2576.0	7.06	-8.5	137.447	762233.	-159.90	9.828
382.00	142329	30.30	-65.65	5339.	-13.2	-45.5	69.8123	2588.5	5.55	-7.8	139.229	766460.	-160.65	9.573
384.00	139941	30.28	-65.62	4860.	-13.9	-45.6	63.5111	2598.4	4.32	-7.1	140.848	770396.	-161.31	9.334
386.00	137659	30.26	-65.60	4425.	-14.6	-45.6	58.2545	2606.0	3.38	-6.5	142.317	774045.	-161.91	9.110
388.00	135473	30.24	-65.59	4030.	-15.4	-45.6	52.7686	2612.0	2.63	-5.8	143.651	777415.	-162.45	8.899
390.00	133372	30.23	-65.57	3675.	-16.3	-45.6	48.1260	2616.7	2.06	-5.3	144.862	780517.	-162.93	8.700
392.00	131347	30.22	-65.55	3353.	-17.3	-45.6	43.6577	2620.3	1.61	-4.7	145.961	783367.	-163.37	8.511
394.00	129390	30.20	-65.54	3065.	-18.3	-45.6	39.5954	2623.2	1.27	-4.2	146.960	785978.	-163.76	8.332
396.00	127494	30.19	-65.53	2805.	-19.5	-45.6	36.1394	2625.4	.999	-3.8	147.867	788368.	-164.12	8.161
398.00	125650	30.18	-65.52	2572.	-20.7	-45.7	32.7985	2627.2	.790	-3.4	148.693	790552.	-164.43	7.999
400.00	123854	30.17	-65.51	2363.	-22.1	-45.7	30.0159	2628.6	.629	-3.1	149.444	792544.	-164.72	7.843
402.00	122100	30.17	-65.50	2174.	-23.5	-45.7	27.5138	2629.7	.504	-2.8	150.128	794360.	-164.99	7.694
404.00	120382	30.16	-65.49	2006.	-25.1	-45.7	25.1507	2630.7	.405	-2.5	150.750	796012.	-165.22	7.549
406.00	118697	30.15	-65.48	1854.	-26.8	-45.7	23.2702	2631.4	.329	-2.2	151.318	797513.	-165.44	7.410
408.00	117041	30.15	-65.48	1718.	-28.6	-45.7	21.5432	2632.0	.269	-2.0	151.836	798876.	-165.63	7.274
410.00	115411	30.14	-65.47	1596.	-30.4	-45.7	19.9213	2632.5	.220	-1.8	152.308	800110.	-165.81	7.142
412.00	113805	30.14	-65.46	1486.	-32.5	-45.7	18.6580	2632.9	.183	-1.6	152.738	801226.	-165.97	7.014
414.00	112221	30.13	-65.46	1388.	-34.5	-45.7	17.5136	2633.2	.153	-1.5	153.130	802234.	-166.12	6.889
416.00	110657	30.13	-65.45	1299.	-36.7	-45.7	16.4328	2633.5	.129	-1.3	153.488	803140.	-166.25	6.768
418.00	109112	30.12	-65.45	1220.	-39.0	-45.7	15.5846	2633.7	.109	-1.2	153.814	803954.	-166.37	6.648
420.00	107586	30.12	-65.44	1148.	-41.3	-45.7	14.8700	2633.9	.094	-1.1	154.110	804682.	-166.48	6.532

TTA7622 3B-64 SNAP 000656 092463 RFL2 ATMOS= THEORETICAL ARDC 1959 ATMOSPHERE
CONTROLJIM AUG 28 DATA-A= DATA-B=RFDA REFRACTION DATA-C= DATA-D=
OBSERVER 32.3467=LAT -64.6538=LONG 0.0000=ORNT 64=ELEV -64484=X . -36074=Y. -0=Z

WT	CD	AREA	VI	GAMMAI	TAUI	LAT	LONG	VT	GAMMA	TAU
8.69	1.00	1.00	2094.9	-20.9533	-16.64638	30.115436	-65.44	1083.5	-43.740	-45.715

TIME	HITE	LAT	LONG	VT	GAMMA	TAU	Q	QC	DQC	AT	RANGE	SR	AZM	ELOBS
422.00	106078	30.12	-65.44	1084.	-43.7	-45.7	14.1797	2634.1	.081	-.95	154.379	805331.	-166.58	6.417
424.00	104589	30.11	-65.44	1026.	-46.2	-45.7	13.5987	2634.2	.070	-.85	154.624	805907.	-166.67	6.305
426.00	103119	30.11	-65.44	973.4	-48.6	-45.7	13.1981	2634.4	.062	-.78	154.846	806415.	-166.75	6.196
428.00	101668	30.11	-65.43	925.8	-51.1	-45.7	12.7881	2634.5	.055	-.70	155.046	806862.	-166.82	6.088
430.00	100237	30.11	-65.43	883.0	-53.5	-45.7	12.3922	2634.6	.049	-.63	155.228	807252.	-166.89	5.982
432.00	98828.	30.10	-65.43	844.1	-56.0	-45.7	12.1804	2634.7	.044	-.58	155.391	807590.	-166.95	5.879
434.00	97440.	30.10	-65.43	808.2	-58.3	-45.7	11.9682	2634.8	.040	-.53	155.538	807879.	-167.00	5.778
436.00	96076.	30.10	-65.42	775.3	-60.7	-45.7	11.7395	2634.8	.036	-.49	155.670	808125.	-167.05	5.678
438.00	94736.	30.10	-65.42	745.2	-62.9	-45.7	11.5443	2634.9	.033	-.45	155.788	808331.	-167.10	5.582
440.00	93422.	30.10	-65.42	717.3	-65.1	-45.7	11.4768	2635.0	.030	-.42	155.894	808501.	-167.13	5.487
442.00	92135.	30.10	-65.42	690.9	-67.2	-45.6	11.3609	2635.0	.027	-.39	155.987	808638.	-167.17	5.395
444.00	90875.	30.10	-65.42	666.5	-69.2	-45.6	11.2172	2635.1	.025	-.36	156.070	808746.	-167.20	5.305
446.00	89643.	30.09	-65.42	643.7	-71.1	-45.6	11.1083	2635.1	.023	-.34	156.144	808827.	-167.23	5.218
448.00	88439.	30.09	-65.42	622.2	-72.8	-45.6	11.0845	2635.2	.022	-.33	156.208	808886.	-167.25	5.132
450.00	87265.	30.09	-65.42	601.5	-74.5	-45.6	11.0056	2635.2	.020	-.31	156.265	808923.	-167.27	5.049
452.00	86121.	30.09	-65.42	582.1	-76.1	-45.5	10.8934	2635.3	.019	-.29	156.315	808942.	-167.29	4.968
454.00	85005.	30.09	-65.41	563.9	-77.5	-45.5	10.7632	2635.3	.017	-.27	156.358	808946.	-167.30	4.889
456.00	83918.	30.09	-65.41	546.8	-78.8	-45.5	10.7395	2635.3	.016	-.26	156.395	808935.	-167.32	4.812
458.00	82860.	30.09	-65.41	530.2	-80.1	-45.4	10.6655	2635.4	.015	-.25	156.428	808913.	-167.33	4.738
460.00	81829.	30.09	-65.41	514.5	-81.2	-45.4	10.5642	2635.4	.014	-.23	156.456	808881.	-167.34	4.665
462.00	80826.	30.09	-65.41	499.7	-82.2	-45.3	10.4481	2635.4	.013	-.22	156.481	808840.	-167.35	4.595
464.00	79848.	30.09	-65.41	486.0	-83.2	-45.2	10.3394	2635.4	.012	-.20	156.501	808792.	-167.36	4.526
466.00	78895.	30.09	-65.41	473.1	-84.0	-45.1	10.2928	2635.5	.012	-.20	156.519	808739.	-167.36	4.459
468.00	77966.	30.09	-65.41	460.6	-84.8	-45.0	10.2184	2635.5	.011	-.19	156.535	808681.	-167.37	4.394
470.00	77060.	30.09	-65.41	448.8	-85.4	-44.9	10.1287	2635.5	.010	-.17	156.548	808618.	-167.37	4.330
472.00	76176.	30.09	-65.41	437.7	-86.0	-44.8	10.0329	2635.5	.010	-.16	156.559	808553.	-167.38	4.269
474.00	75313.	30.09	-65.41	427.5	-86.6	-44.7	9.93657	2635.6	.009	-.15	156.568	808486.	-167.38	4.208
476.00	74469.	30.09	-65.41	417.8	-87.0	-44.5	9.89331	2635.6	.009	-.15	156.576	808417.	-167.38	4.149
478.00	73644.	30.09	-65.41	408.4	-87.5	-44.3	9.86290	2635.6	.008	-.14	156.583	808347.	-167.39	4.091
480.00	72837.	30.09	-65.41	399.3	-87.8	-44.0	9.81156	2635.6	.008	-.14	156.589	808276.	-167.39	4.035
482.00	72048.	30.09	-65.41	390.6	-88.1	-43.8	9.74788	2635.6	.007	-.13	156.594	808205.	-167.39	3.980
484.00	71275.	30.09	-65.41	382.5	-88.4	-43.4	9.68142	2635.6	.007	-.12	156.598	808134.	-167.39	3.926
486.00	70518.	30.09	-65.41	374.8	-88.6	-43.1	9.61482	2635.6	.007	-.11	156.601	808063.	-167.39	3.873
488.00	69776.	30.09	-65.41	367.6	-88.8	-42.6	9.57061	2635.7	.006	-.11	156.604	807993.	-167.39	3.821
490.00	69048.	30.09	-65.41	360.6	-89.0	-42.1	9.56739	2635.7	.006	-.11	156.606	807923.	-167.39	3.770
492.00	68333.	30.09	-65.41	353.7	-89.2	-41.5	9.54045	2635.7	.006	-.10	156.609	807854.	-167.40	3.720
494.00	67633.	30.09	-65.41	347.0	-89.3	-40.8	9.50244	2635.7	.006	-.10	156.610	807787.	-167.40	3.671
496.00	66945.	30.09	-65.41	340.7	-89.4	-39.9	9.45853	2635.7	.005	-.09	156.612	807720.	-167.40	3.623
498.00	66270.	30.09	-65.41	334.7	-89.5	-39.0	9.41245	2635.7	.005	-.09	156.613	807654.	-167.40	3.576
500.00	65606.	30.09	-65.41	329.0	-89.6	-37.9	9.36700	2635.7	.005	-.08	156.614	807590.	-167.40	3.530
502.00	64954.	30.09	-65.41	323.6	-89.6	-36.6	9.32746	2635.7	.005	-.08	156.615	807527.	-167.40	3.484
504.00	64312.	30.09	-65.41	318.4	-89.7	-35.1	9.33918	2635.7	.005	-.08	156.616	807465.	-167.40	3.440
506.00	63680.	30.09	-65.41	313.1	-89.7	-33.4	9.32978	2635.8	.005	-.08	156.617	807404.	-167.40	3.396
508.00	63059.	30.09	-65.41	308.0	-89.8	-31.6	9.30835	2635.8	.004	-.08	156.617	807344.	-167.40	3.352
510.00	62448.	30.09	-65.41	303.0	-89.8	-29.5	9.28040	2635.8	.004	-.07	156.618	807286.	-167.40	3.310
512.00	61847.	30.09	-65.41	298.3	-89.8	-27.3	9.24952	2635.8	.004	-.07	156.618	807229.	-167.40	3.268
514.00	61255.	30.09	-65.41	293.8	-89.9	-25.0	9.21802	2635.8	.004	-.07	156.619	807173.	-167.40	3.227
516.00	60672.	30.09	-65.41	289.5	-89.9	-22.5	9.18725	2635.8	.004	-.06	156.619	807118.	-167.40	3.186
518.00	60097.	30.09	-65.41	285.5	-89.9	-20.0	9.15792	2635.8	.004	-.06	156.620	807064.	-167.40	3.146
520.00	59530.	30.09	-65.41	281.6	-89.9	-17.6	9.16913	2635.8	.004	-.06	156.620	807011.	-167.40	3.106

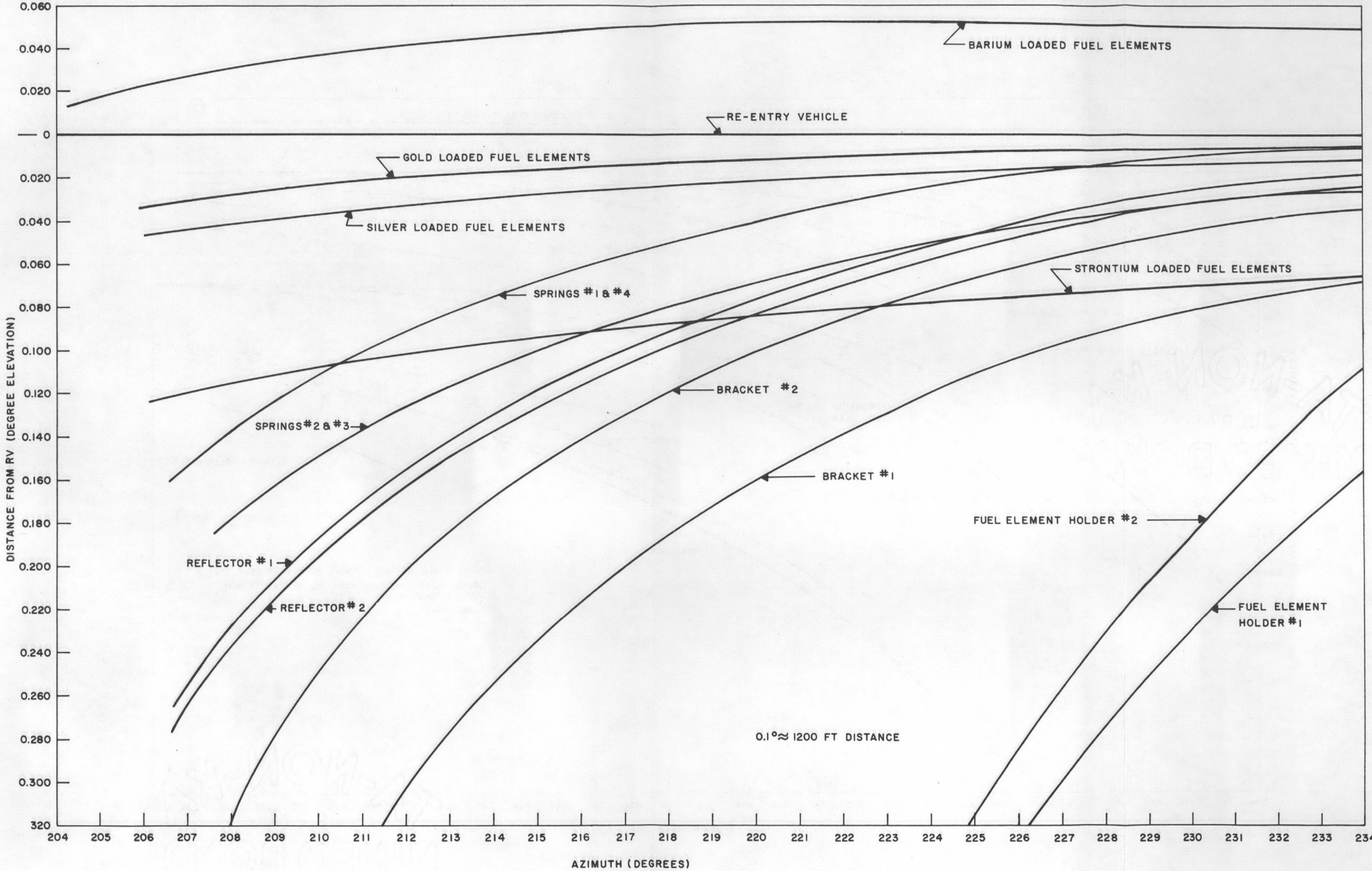

Figure 31. Plot of theoretical re-entry trajectories for RFD-1 components

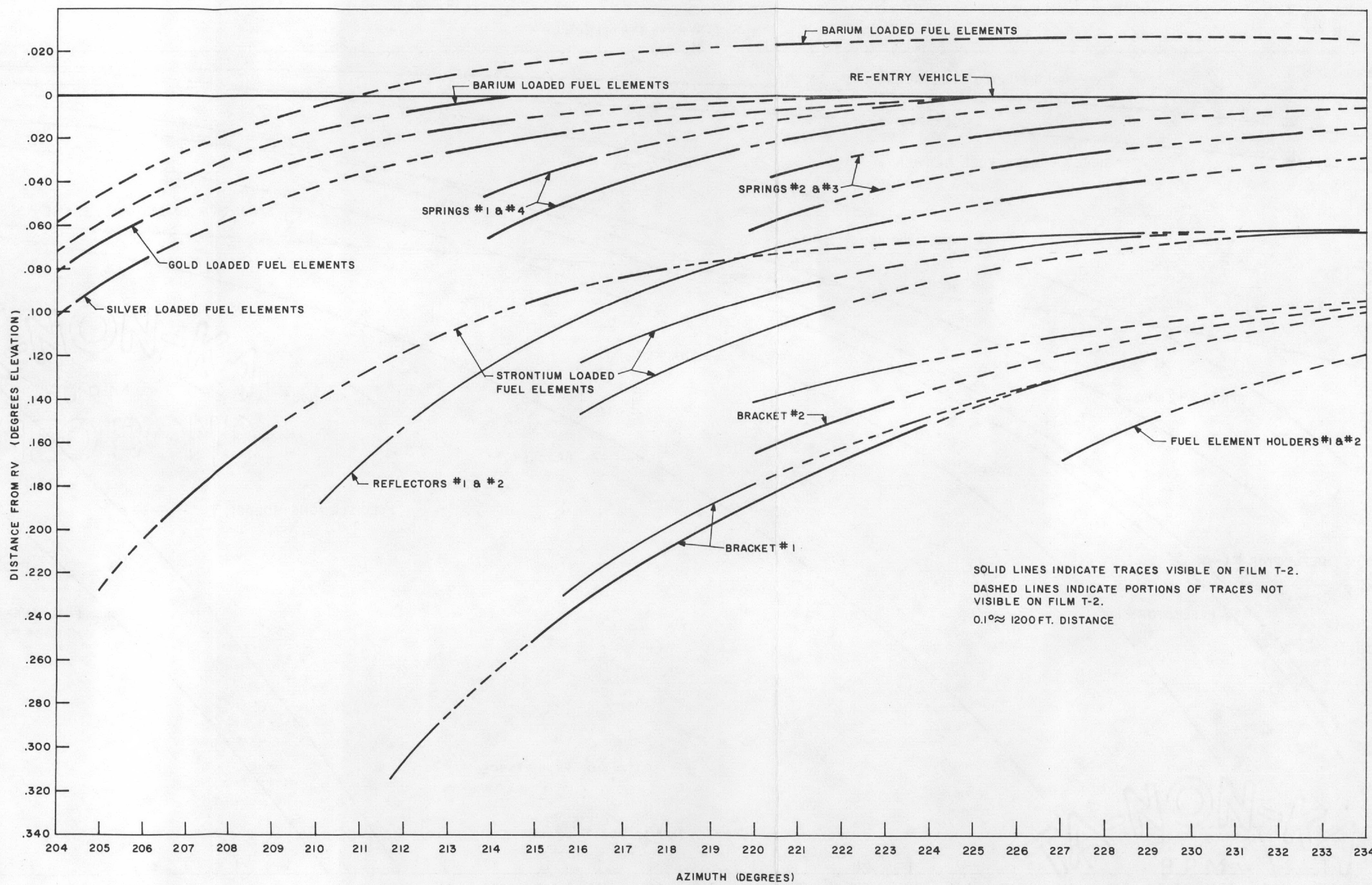

Figure 32. Plot of observed re-entry trajectories for RFD-1 components

Visual inspection of the plate-camera films shows the timing chops and distinctive events (see Figures 48A and 48B, p. 107). The two re-entry trails identified as the strontium-loaded and barium-loaded rods pulsate and flare very brightly in comparison with the other trails. The flares are caused by the tracers. The RV appears as a steady, fairly intense streak, as do the brackets. The remainder of the re-entry items are dimmer and have much less distinctive trails.

Confirmation of the plate-camera film evaluation by other portions of the data reduction is discussed on pages 104 to 114.

NASA Plate-Camera Films

Figures 33 and 34 were taken from NASA aircraft plate cameras AC-36 and AC-38. The films from the four NASA plate cameras were used to confirm and supplement data from the Sandia plate cameras. Many of the re-entry events (such as flares) were evident on both films. Also, the angles of view, due to the different locations of the cameras (see Figure 13), afforded essentially two different pictures of the same events. Several re-entry trails and events not clear on one film were obvious on the other. However, reduction of the NASA plates by the same procedure employed to reduce the Sandia plates was impossible for the following reasons:

1. The timing chopper on the NASA camera failed to operate. Consequently, the camera plates could not be correlated with the data from the other cameras except by means of distinctive events.

2. The position, turn rate, and bank angle of the aircraft could not be accurately determined (this aircraft was not tracked by the verlort radar). As a result, the plates could not be measured, nor could theoretical calculations of azimuth and elevation be made.

Spectral Data

The spectrographic-photometric data on RFD-1 were collected in a variety of ways. Unfortunately, most of the data suffered limitations of one kind or another. The most severe limitations were imposed by the re-entry conditions themselves: that is, the distances between the re-entering objects and the optical instrumentation. The distance to the objects, plus the attenuation of the intervening atmosphere, resulted in drastic reduction in the light intensity at the instrumentation. Since all the spectral instruments were light detectors of some description, the low light level resulted in no data collection in some instances, and in borderline data in others. However, low light levels at the instruments had been expected, and the instruments had been designed to cope with the problem, within the time and money restrictions of the experiment. An unexpected limitation making data reduction difficult was the loss of timing on several instruments and the relatively poor time resolution on others. In addition, the LA-24 tracking telescope was not tracking the proper objects for part of the time, so the data it might have obtained were lost.

Reduction of the spectrographic data required much cross-referencing between data in order to correlate events. Most of the optical data were recorded photographically. The best timing seemed to be on framing-camera film, so events that occurred on a spectrographic plate or film (nonframing) were associated with events on framing camera records whenever possible. Approximate timing was often determined by comparing chopped plate-camera data with spectral-camera data. Spectral films and plates were often underexposed; if an event could be located on one film, it was sometimes possible, knowing what to look for, to locate the same event on the less exposed films and plates. The less exposed film then could be used as corroborative evidence for the data first found. Also, the less exposed films sometimes had time, while the better exposed did not, and a comparison of the two made it possible to determine the time of an event.

Before reduction of the spectral data began, an effort was made to collect material specifications on all re-entering objects. This information was needed as an aid in identifying the spectra recorded and in associating spectra with specific objects.

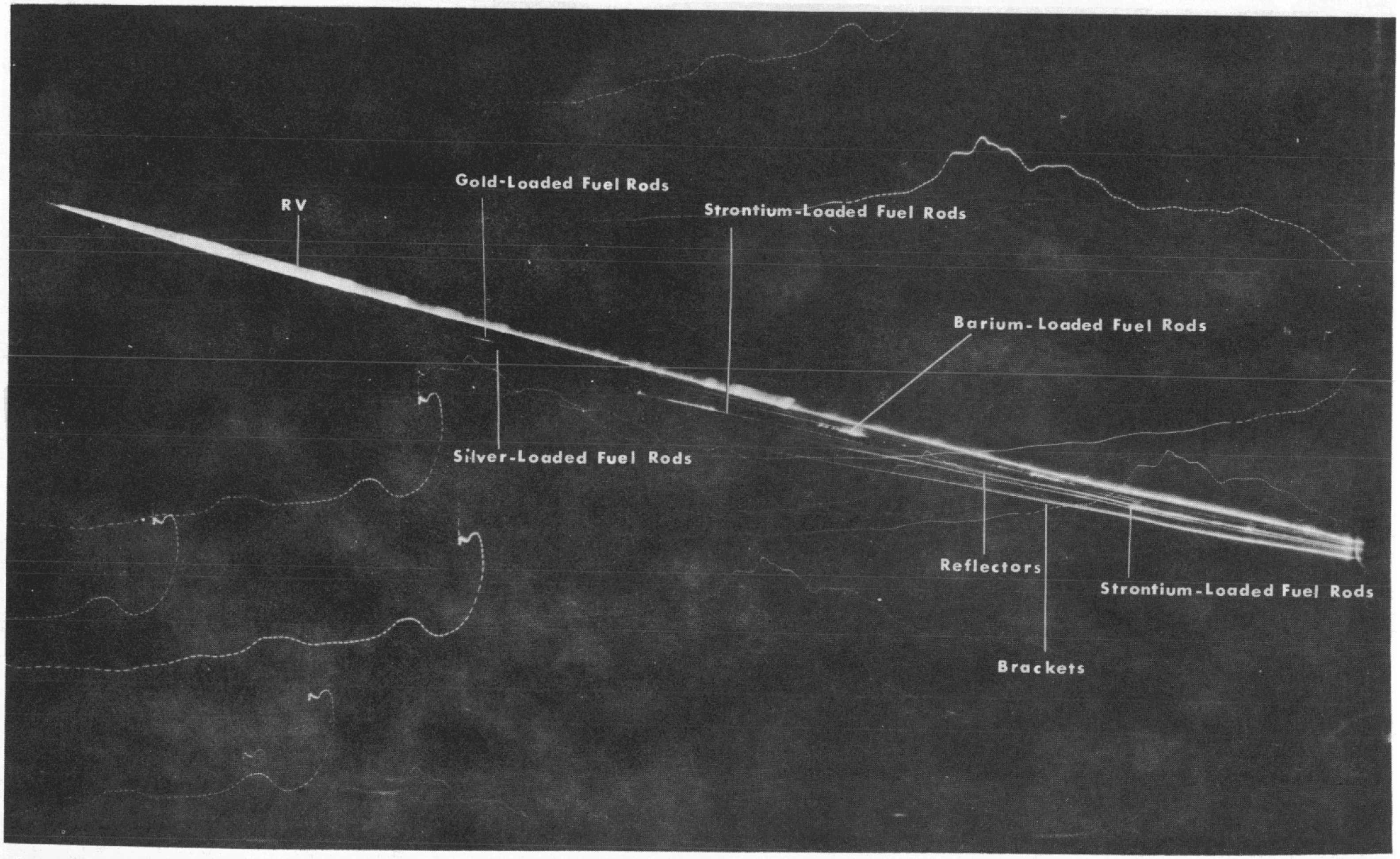

Figure 33. Re-entry trajectories for RFD-1 components (from Camera AC-80)

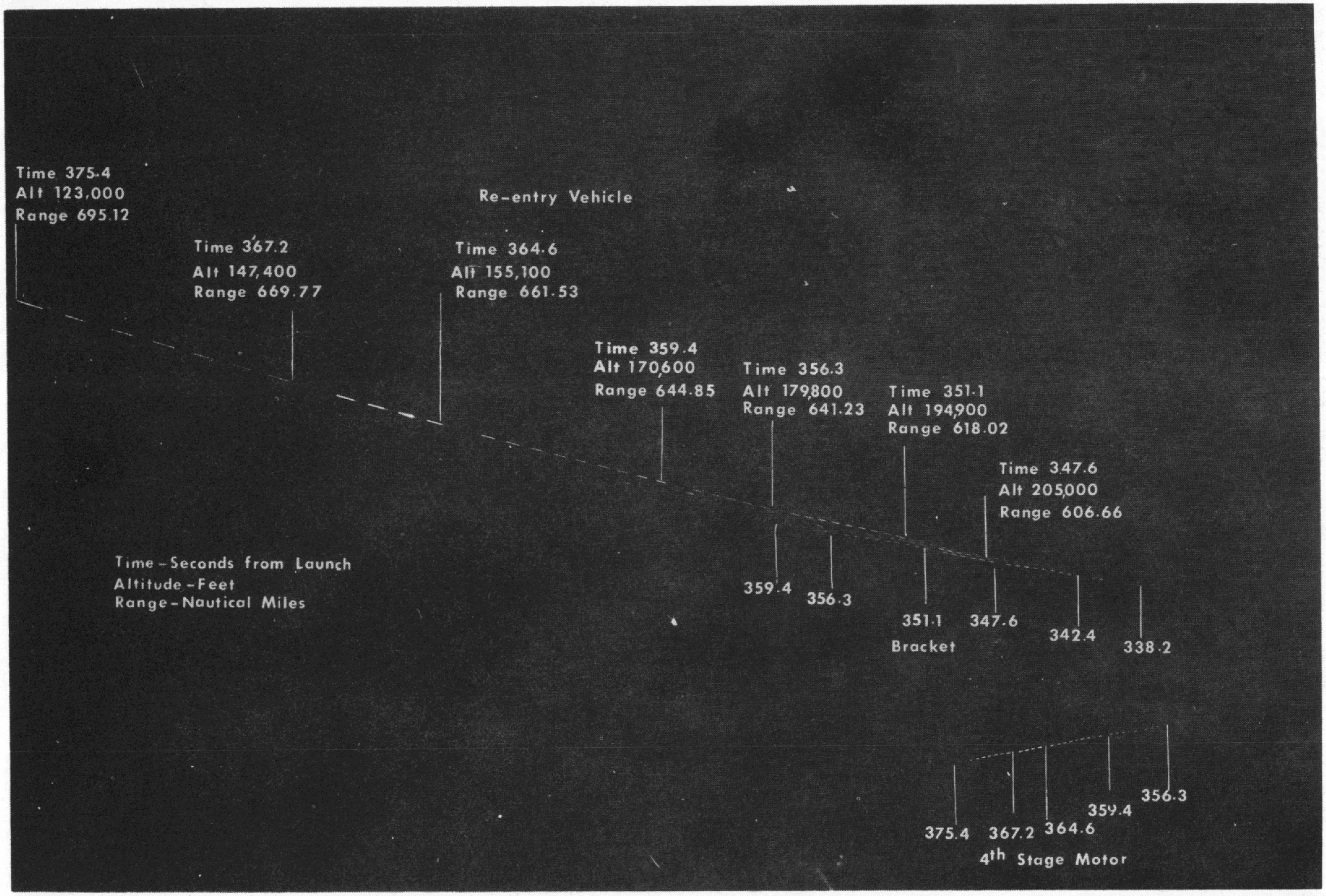

Figure 34. RFD-1 re-entry (from Camera AC-1)

An early accumulation of materials and their specifications proved to be incomplete, and in many instances the specifications provided by a manufacturer proved to be incomplete and/or in error. Extensive laboratory spectral analyses were carried out during the data reduction. Many times such analyses were of a disjunctive nature: that is, either a material contained a particular element or it did not. In other instances, quantitative or semiquantitative analyses were requested and obtained. Some of the analyses and the results obtained are listed in Table XXI. Sodium, which was associated with several re-entry objects, is a common impurity and one easily detected spectrally because of its electronic configuration. If any significant amount were present during the re-entry, it should be easily detectable. Sodium investigations were conducted when some discrepancies arose between specifications and laboratory analyses. The fiberglass-filled covering used on the brackets and on the re-entry vehicle case were supposed to contain only trace amounts of sodium or a few parts per million, but analysis of this material indicated that it contained from 0.5 to 5 percent sodium.

TABLE XXI

Material Analyses

Item	Percentage of Element Detected							
	Ca	Na	Li	Mg	Al	Si	K	Pb
1. Large plastic sheet[1]	1-10	0.5-5	ND*	>10	>10	>10	ND	ND
2. Rubber sample[2]	0.1-1	ND	ND	>10	<1	<1	ND	ND
3. Heat paper[3]	0.1-1	ND	0.1	<1	1-10	<1	ND	ND
4. Potting material[3]	<0.1	ND	<0.1	>10	>10	>10	1-10	<1
5. Plastic inner liner (1)[3]	0.1-1	1-10	<0.1	>10	<1	<1	1-10	<1
6. Plastic inner liner (2)[3]	0.1-1	1-10	0.1-1	1-10	<1	<1	1-10	<1
7. Electrolyte pad[3]	1-10	0.1-1	>10	>10	>10	>10	>10	1-10
8. Fiberglass-filled material[4]	0.1-1	ND	ND	1-10	<1	>10	ND	ND
9. Fiberglass-filled material[5]	1-10	0.1-1	ND	1-10	>10	>10	ND	ND
10. Fiberglass-filled material[6]	1-10	ND	ND	>10	>10	>10	ND	ND
11. Fiberglass-filled material[7]	1-10	ND	ND	1-10	>10	>10	ND	ND

*ND = not detected.

NOTES:
1. The fiberglass-filled ablating material covering the fuel-rod brackets and parts of the RV.
2. A rubber cushion between the fuel-rod brackets and the RV.
3. Components of the MC1192 battery.
4. Fiberglass-filled material from the forward flare of the RV.
5. Fiberglass-filled material from the access door of the RV.
6. Fiberglass-filled material from the front flange of the RV, to which the reactor was bolted.
7. Fiberglass-filled material from the aft flare of the RV.

Table XXII lists materials exposed to re-entry heating during the RFD-1 flight test.

TABLE XXII

Materials Exposed to RFD-1 Re-entry Heating

Item	Materials Included
Reactor	
Reflectors	Aluminum (6061)
Reflector springs	Rene 41
Reflector band	Stainless steel (316)
Fins	Aluminum (6061)
Core vessel and tubing	Stainless steel (316)
Pump	Stainless steel (316)
Re-entry Vehicle	
Ablation-material (heat shield)	Fiberglass with phenolic resin
Antenna window (heat shield)	Teflon
Collar (ballast)	Tungsten, nickel, copper
Fixed fuel rods	Al_2O_3, graphite
Standoffs	Titanium
Experimental Fuel Elements	
Strontium-loaded rod	UZrH, strontium, lead, Al_2O_3, Fiberfrax insulation, Hastelloy N
Barium-loaded rod	UZrH, barium, lead, Al_2O_3, Fiberfrax insulation, Hastelloy N
Silver-loaded rod	UZrH, silver, Fiberfrax insulation, Hastelloy N
Gold-loaded rod	UZrH, gold, Fiberfrax insulation, Hastelloy N
Brackets	Aluminum (6061), fiberglass, Almag 35, MC1192 battery (see Table XXI)
Rod holders	Almag 35
Guillotine	Stainless steel
Fourth-Stage Motor	
Case	Fiberglass
Adapter	Magnesium
Retro-rockets	Stainless steel
Rocket brackets	Aluminum
Battery	MC1192 (similar to bracket battery)
Propellant gases	Arcite 362

As mentioned previously, the objective of the experiment was to monitor fuel-rod ablation. Rate and volume of fuel-rod ablation were to be monitored by detecting flare materials inside the fuel rods and determining when and where in the trajectory these flare materials were exposed. The flare materials chosen were ones not likely to be present as part of or as impurities in the re-entering objects. Furthermore, they were materials with physical properties expected to be compatible with the re-entry environment, including: (1) vapor pressures such that the fuel rods would not be ruptured before ablation down to the tracer material, (2) moderate refractoriness, so as not to resist vaporization altogether and so preclude spectral excitation, and (3) spectral characteristics such as to be relatively easily detected, even in small abundances. Since Item (3) was obviously very important to the success of the experiment, excitation energies required for specific spectral lines, and the transition probabilities for these lines (the best available transition probabilities, whether theoretical or empirical) were carefully considered. The elements finally chosen for tracers were barium, strontium, silver, and gold.

Figures 35, 36, 37, and 38 show diagrams of the most intense lines of the spectrum of each of the four tracers. The intensities are those listed in Wallace Brode, Chemical Spectroscopy, 2nd ed. (published by John Wiley and Sons). The intensity values listed in this book have the same value as those listed in the MIT tables (compiled by George Harrison, published by John Wiley and Sons), but they are more convenient to use for the present problem. The intensities listed are almost certainly at variance with those under re-entry conditions. Thermal excitation is believed to be the primary mode of excitation during re-entry, with electron excitation and collisions of the second kind being secondary. If thermal excitation is predominant and some sort of thermal equilibrium exists, the number of atoms in an excited state, E_n, is proportional to the Boltzman factor $e[\exp(-E_n/kT)]$ where k is the Boltzman factor, T is the temperature in degrees Kelvin, and E_n is the energy of the excited state. The intensity of a line radiated from this excited level can be written as $I_{nm} = A_{nm}N_n h\nu_{nm}$, where A_{nm} is the Einstein transition probability, N_n is the number of atoms in the nth state, h is Planck's Constant, and ν_{nm} is the frequency of the emitted radiation. N_n can be written as

$$\left(\frac{Ng_n}{Z}\right)\left(e^{(-E_n/kT)}\right),$$

where N is the total number of a species (atom or molecule in a particular state of ionization) present, g_n is the statistical weight of the levels, and Z is the partition function.

$$Z = \sum_i g_i \left(e^{(-E_i/kT)}\right)$$

for the species under investigation.

One can see from even this simplified description how dependent the number of atoms or molecules in a particular state of excitation is upon the energy value of the state, through the exponential function. Higher excitation energies result in lower intensities. To calculate absolute intensities under re-entry conditions would be virtually impossible. Even under laboratory conditions, and with only one or two species involved, calculations are difficult. In some cases, wave mechanics can be used to calculate realistic transition probabilities; in others, the transition probabilities can be determined experimentally to varying degrees of accuracy. In many instances, partition function can only be approximated. If electron collision excitation becomes significant, the exponential dependence falls out and thermal equilibrium no longer exists (see Atomic Spectra and Atomic Structure (C. Herzberg), page 160, Dover Publications). Many of the intensities listed in the literature are probably derived from combinations of thermally excited and electron-excited spectra, and so should be used only as rough guide lines.

Collected from four stations, three airborne and one on the ground, the data will be discussed by site category. The ground station was High Point, and the airborne stations were the NASA DC-4 (238) and the two AFSWC C-54's (461 and 521). The instrumentation on the NASA plane was provided by NASA, which graciously gave Sandia the original data acquired. The instrumentation on the AFSWC C-54's was provided partially by Sandia Corporation and partially by AFSWC. AFSWC also very graciously made its original data available. In addition, Mr. David Mick of AFSWC made a special effort to help interpret the timing records and to provide other helpful information.

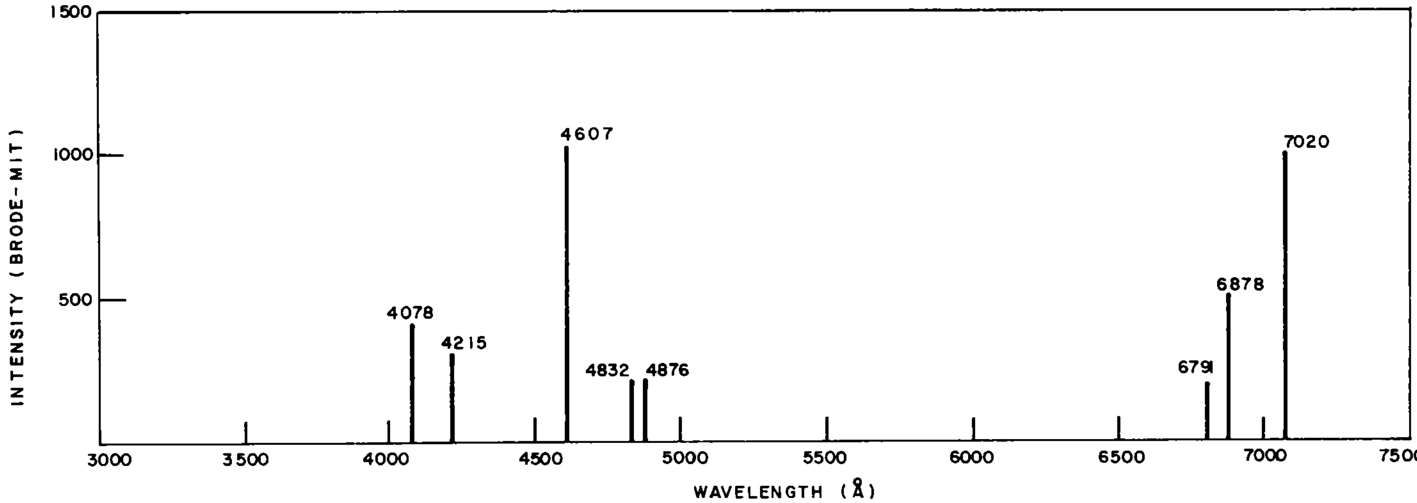

Figure 35
Most intense spectral
lines for strontium

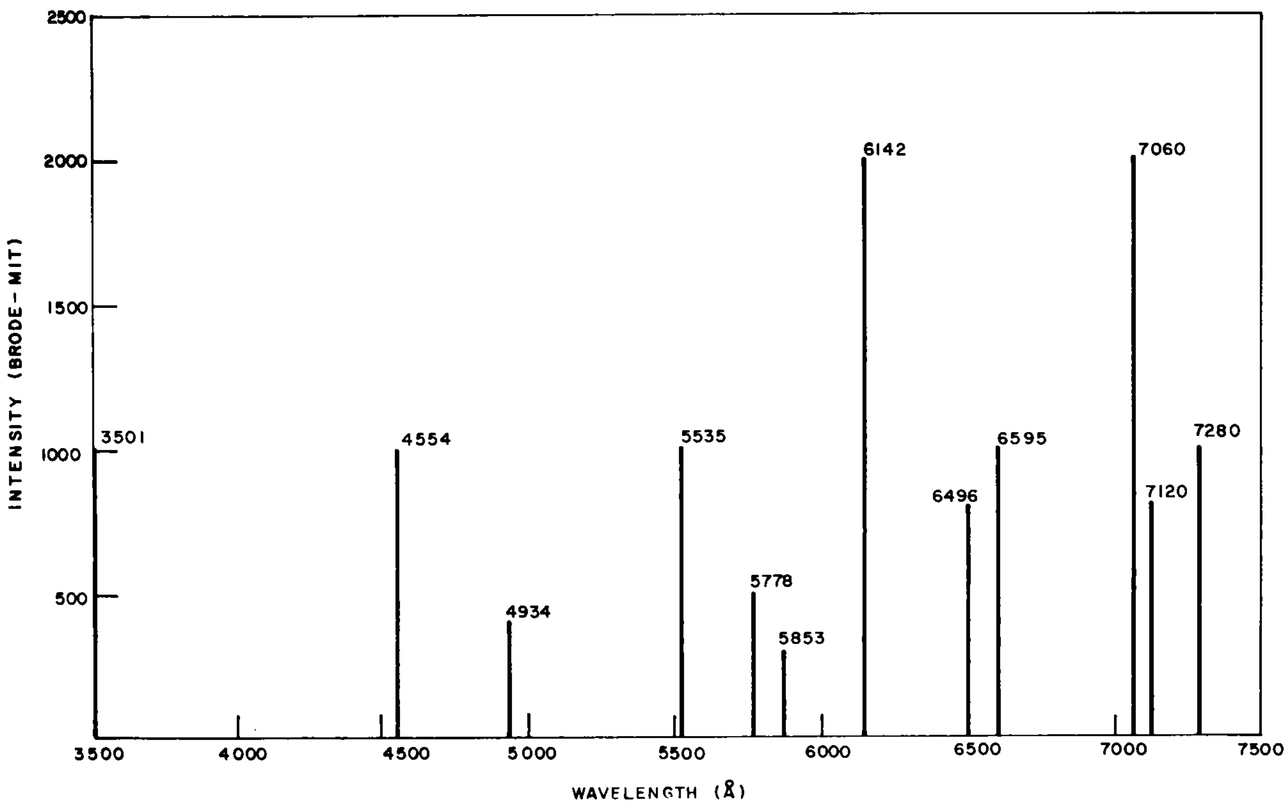

Figure 36
Most intense spectral lines
for barium

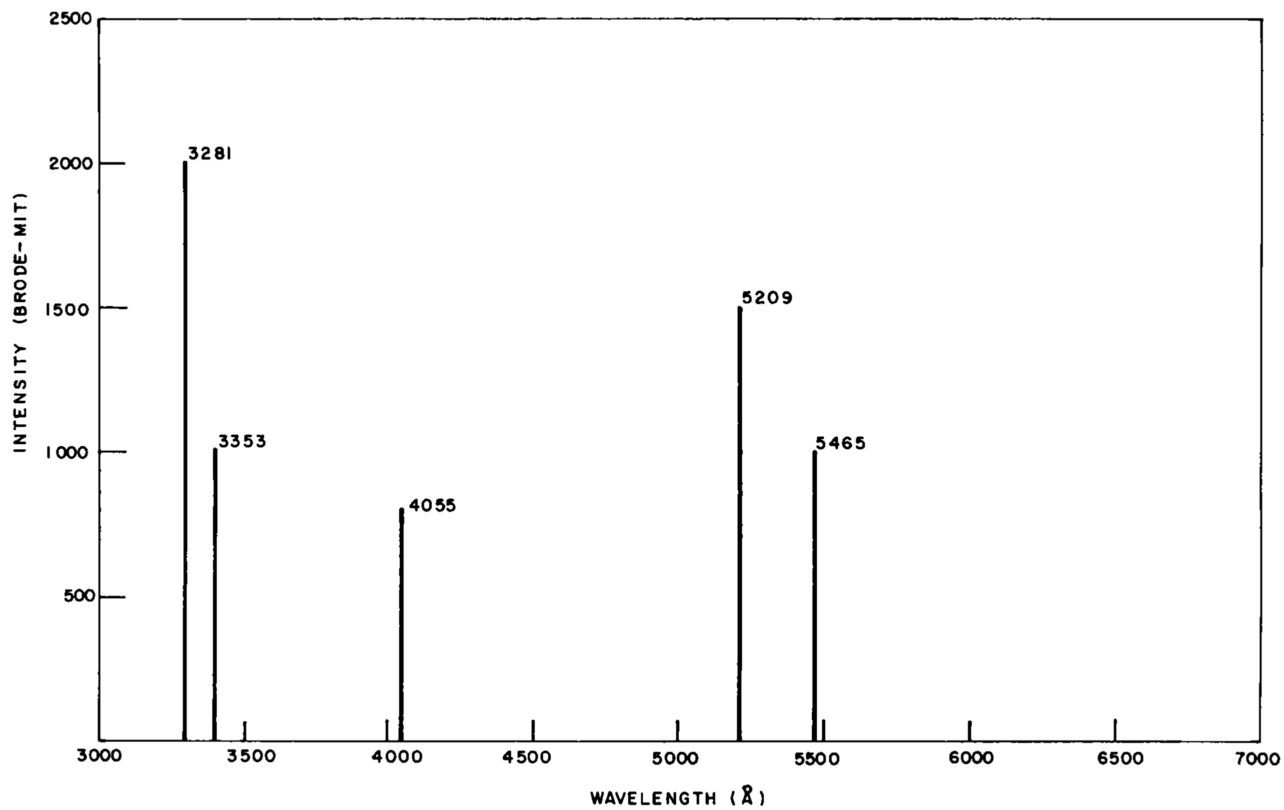

Figure 37. Most intense spectral lines for silver

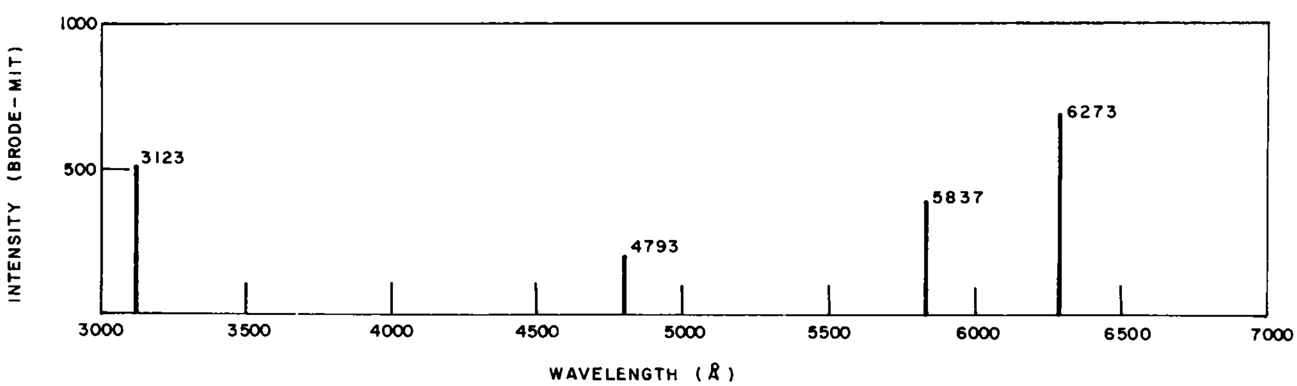

Figure 38. Most intense spectral lines for gold

Data from Ground-Based Spectral Instruments

Spectral instrumentation at High Point consisted of a cinespectrograph, six plate spectrographs, an LA-24 TRSS mounted on and utilizing the 24-inch optics of the LA-24 tracking telescope, and a photometer, also mounted on the LA-24.

Cinespectrograph -- The cinespectrograph was a hand-tracked Photosonics 10A 70-mm framing camera operated at 10 frames/sec. The camera had a 4-inch-f.l., f/1.9 lens and a 600-lines/mm grating. The film used was Kodak Linagraph Shellburst. BRT was clearly visible on this film. The only exposures of the re-entry sequences recorded were a few underexposed frames at 364.75 seconds, which coincides with a large flare up of the RV, which was supposedly being tracked by this instrument. No usable data were acquired, since the optical aperture on this instrument was too small to collect enough light to record, and exposures were too weak to determine much about the quality of the focus.

Plate Spectrographs -- The plate spectrographs were all Sandia-built instruments with 12-inch-f.l., f/2.5 Kodak Aeroektar lenses and 600-lines/mm transmission gratings. The gratings were placed in front of the lenses, with their dispersion perpendicular to the predicted trajectory and their blaze oriented to enhance the first-order spectra. The photographic plates on which the data were recorded were 10 x 12 inches, with Kodak 103-F emulsion. This emulsion proved to have much better sensitivity in the red region from 6300 to 6900 Å than did the Royal-X Pan used by NASA and AFSWC. Spectrographs S-1, S-2, and S-3 were tilted up so as to put their zero orders at the upper edge of the plate; S-4, S-5, and S-6 were tilted down to place their zero orders at the lower edge of the plate. These spectrograph positions were chosen so that at least one set of instruments would cover the trajectory even if it went either higher or lower than predicted. Cameras S-1, S-2, and S-3 were rotated in azimuth with respect to one another so as to cover the trajectory in azimuth. Cameras S-4, S-5, and S-6 were also rotated with respect to one another to cover the trajectory. Some of these instruments were not in as sharp a focus as would have been desirable. Also, when used off axis and at full aperture, these lenses are subject to distortions which create fuzzy off-axis images. The plate spectrographs all suffered from lack of light intensity, but usable data were collected.

The data from plate spectrographs, S-1 through S-6, will be discussed, instrument by instrument. Events referred to can be seen in Figures 48A and 48B, which were reproduced from the trajectory-camera data.

The spectra will be discussed in terms of the zero-order, first-order, and sometimes second-order spectra. The zero order is the undiffracted light that passes through the grating and the lens and then is imaged on the film or plate just as though the grating were removed (except that its intensity is reduced). The first-order spectrum is the one displayed with the greatest intensity because of the gratings chosen, and the second-order spectrum is the one recorded with less intensity and twice the dispersion of the first-order spectrum. The second order is further displaced from the zero order than the first is. Events will be referred to in terms of their spectral characteristics. For instance, RV flareup or burnup will signify that the materials believed to make up the reactor on the RV were undergoing re-entry heating, either on or off the RV, which was sufficient to vaporize them. For chromium or chromium-oxide spectra or other atomic or molecular spectra to exist under re-entry conditions means that the atoms or molecules were free at the moment they radiated their characteristic radiation.

S-1 Camera: This camera recorded only about 2 inches of the zero order of the radiation from the fourth stage of the launch vehicle. The image is fuzzy, because of an out-of-focus condition or because of lens aberrations. The image is close to the edge of the plate. The fourth-stage image broadens as it progresses in time, which is consistent with other data indicating that the fourth stage broke into two objects. There are no spectra on this plate. Either the light level was too low to expose the plate, or, more likely, the spectra were off the photosensitive surface as a consequence of the camera orientation. The fourth stage was considerably below the actual and predicted trajectory of the re-entry objects of primary interest.

S-2 Camera: The data on this camera were the best of any of the plate spectrographs. Focus was sharp over the entire format, including star trails, zero-order images, and spectral lines. The zero order of the fourth stage and of the several objects in the "flare" or "fuel-rod" region (i.e., that interval between about 336 and 361 seconds) are recorded, as are the spectra of some of these objects. The object with the lowest trajectory, with the exception of the fourth stage, has a strong sodium spectrum associated with it, as is attested by correspondence between the sodium spectrum and intensity variations in the zero order of that object. The sodium lines at 5890 and 5896 Å are present from about 341 until about 349 seconds. This same object has magnesium lines at 5167, 5172, and 5183 Å associated with it from 342.5 until 345 seconds. The magnesium lines have intensity fluctuations corresponding to those of the zero order and sodium spectrum, and they end with an intensity burst like that associated with a sodium intensity burst. Four intensity flareups quite definitely identified as strontium are visible in the zero order. The spectral bands associated with these flares are just detectable on this plate. The times that have been assigned to these flares by correlating the framing-camera data and chopped trajectory plate-camera data with the spectral data are 350.72, 352.00, 353.88, and 355.98 seconds. A number of other flares were visible in the zero order of the "flare" region, but they were not intense enough to produce identifiable spectra. The fourth stage was quite intensely exposed and a spectrum was recorded. The zero order of the fourth stage clearly separates into two objects. Strong components in the fourth-stage spectrum on this plate are the sodium lines at 5890 and 5896 Å and the lithium line at 6707 Å.

S-3 Camera: This camera covered the latter part of the trajectory. The zero order attributed to the RV is visible from 359 to 383.5 seconds. The zero order is not a sharp image, but the spectra and star trails in the center of the plate are in fairly good focus. The only measurable and identifiable spectra are associated with an intensity flareup at 365 seconds. In this region, sodium is present in low amounts and lithium is barely detectable. Chromium lines at 5204, 5206, 5208, 5296, 5328, 5345, and 5348 Å, plus strong chromium oxide bands with heads at 5794, 6051, and 6394 Å clearly indicate that chromium was undergoing re-entry burnup at this time.

S-4 Camera: This camera covered the early part of the re-entry. The only visible record is of the fourth stage. The zero order and spectra from this source are not sharp. The lithium line at 6707 Å, and the sodium lines at 5890 and 5896 Å (associated with the fourth stage), are visible. The doubling of the zero-order image is not obvious. This may be a result of underexposure or of relatively poor image quality--again caused, perhaps, by focus or by lens aberration.

S-5 Camera: This camera was aimed to cover approximately the same portion of the trajectory as the S-2. However, the focus (or chromatic lens aberration) was worse on this camera than it was on the S-2, and the spectral lines are not as well exposed or resolved. More of the re-entry vehicle flareup is recorded on this plate than on the one from the S-2. The spectra early in the flare region have the sodium 5890 and 5896 Å lines associated with the bottom object in the "flare" region. However, the zero order for this sodium doublet is off the plate. The spectra are present because of the angle at which the grating was oriented. The RV flareup at 365 seconds has the same general features as it had in the plate from the S-3, except that it is fainter. For some reason, perhaps the angle of the camera axis, the band structures associated with the strontium flares on the S-2 at 350.72, 352.00, 353.88, and 355.98 seconds are more distinct on this plate than on the S-2.

S-6 Camera: This camera covered the latter part of the trajectory, as did the S-3. Its focus seems to have been better than the focus of the S-3 (the zero order of the re-entry vehicle is sharper), but the spectra are less distinct. The chrome-oxide bands associated with the re-entry vehicle flareup at 365 seconds are visible for about 1 or 2 seconds.

None of the pertinent data from the preceding films was distinct enough for reproduction and presentation in this report.

LA-24 Time-Resolved Streak Spectrograph -- The best-exposed film was that recorded with the LA-24 TRSS. The basic reason for this was that the LA-24 primary optics have a 24-inch-aperture light-gathering system. A secondary reason for the good record was that the focus on the film plane was sharp. Unfortunately, the LA-24 was tracking the fourth stage at the time this record was obtained; in addition, the time system failed on this spectrograph. However, the photometer was aligned so that its optical axis was essentially parallel with the optical axis of the LA-24 primary, and they were pointed at the same point in space. By comparing the C.E.C. record of the photometer output with the LA-24 TRSS spectrogram, it was possible to determine approximate timing for the TRSS spectrogram. The conclusion that the LA-24 was tracking the fourth stage was based on a number of data. Even before chopped trajectory plate-camera data were received from NASA, the object being tracked was identified as the fourth stage from the spectral characteristics of the radiation. Intense aluminum-oxide molecular bands were present in the fourth-stage spectra and were only weak or not present elsewhere. In addition, the intensity fluctuations in the radiation from the fourth stage as recorded on other instruments corresponds with that recorded on the LA-24 instruments. Also, an intense lithium line at 6707 Å was present in the fourth-stage data and not (or only faintly) elsewhere. Finally, the fourth stage was clearly seen to separate into two objects on the LA-24 TRSS data, as it was on several of the other plates and films. The time of the fourth-stage radiation and its intensity variation in time are shown in Figure 34.

Before Sandia received these data (shown in Figure 34), it was believed that the fourth-stage intensity maximum occurred much earlier, so it had been hard to reconcile the data. (As it turned out, both the RV and the fourth stage had their maximum intensity at about the same time, 365 seconds.) The reason so much effort was put into the LA-24 TRSS data was the possibility that the data were of re-entry objects of primary interest. But the fourth-stage data recorded on the photometer have the same duration and character as on all other data, including the data from NASA. Since these data have been reduced and are of peripheral interest, the spectrogram is shown in Figure 39, with the lines and bands identified. Note how the sodium and lithium lines split in two. The zero order also shows this splitting. The waviness of the spectral lines was caused by variations in tracking. Another reason for showing these data is that they illustrate the effectiveness of this method, even when the spectral source is over 100 miles away.

LA-24 Photometer -- This instrument operated very well, and if it had been tracking the proper objects it probably would have provided valuable data. The technique of filling a chamber around the photomultiplier with CO_2 from a fire extinguisher, and so cooling the photomultiplier, reduced the noise level of the tube to a very satisfactory level. The filter wheel (operating at 600 rpm) was so well balanced and designed that vibration effects were negligible.

The band pass of the filters used was to have been 10-Å wide and were to monitor two intense lines per flare material and two regions about 50 Å away from each of the spectral lines of interest. This was so that background radiation could be subtracted. The spectral line filters and background filters were chosen so as not to encompass other strong line radiation in their band pass. As it turned out, however, some strong radiation that had not been anticipated occurred during the re-entry, partly a consequence of the fact that the photometer was tracking the fourth stage. The photometer detected radiation from about 346 to 373 seconds, with relatively high-to-high intensity occurring from 358.5 to 371 seconds. One of the filters had been chosen to monitor the silver line at 5209 Å. This filter's band pass covered the chromium lines at 5204, 5206, and 5208 Å, thus becoming a "chromium filter." The chromium radiation received by the photometer was successfully discriminated against the background radiations.

In some cases, the filters proved to have wider band passes than the specified 10 Å. After the RFD-1 flight test, Dr. Fred Roesler of the University of Wisconsin evaluated some of the filters with instrumentation he had designed for mapping the band passes of filters. Time limitations had not permitted earlier evaluation. The filters appeared to have 10-Å band passes, but the peak transmission varied up to 30 Å across a filter, creating an effective band pass of 30 to 40 Å. This cut down the transmitted light at any chosen wavelength and passed undesirable wavelengths. The peak transmission wavelengths of the 24 filters follow: gold lines 6278 and 5837 Å with gold lines background 6228, 6328, 5787, and 5877 Å; silver lines 5209 and 5465 Å with silver lines background 5159, 5259, 5415,

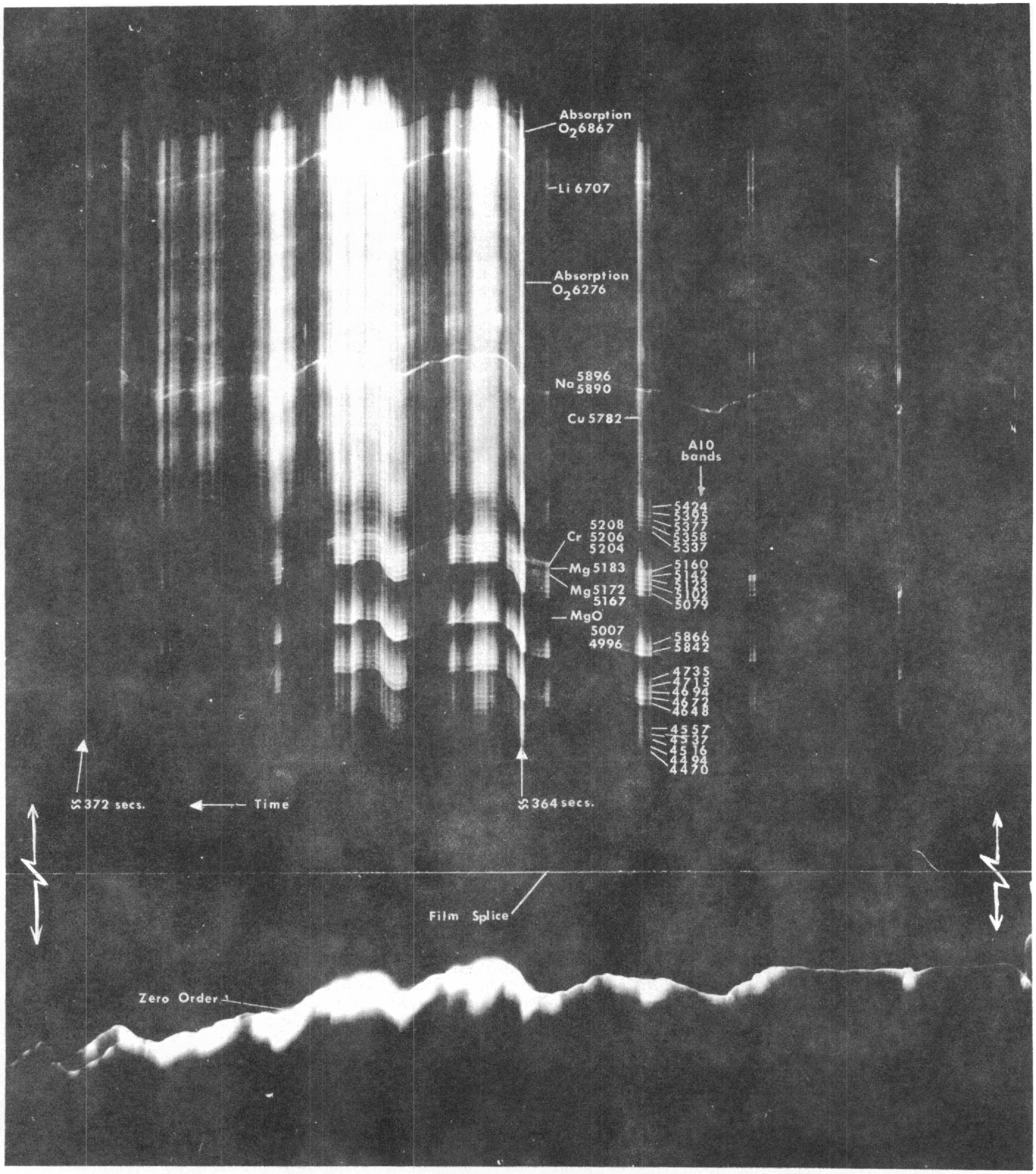

Figure 39. Spectrogram of RFD-1 re-entry
(from Camera LA-24-1)

and 5515 Å; strontium lines 4607 and 6878 Å with strontium lines background 4555, 4657, 6828, and 6928 Å; barium lines 5535 and 6142 Å with barium lines background 5486, 5586, 6142, and 6228 Å. The lines chosen and their relative intensities were shown in Figures 35, 36, 37, and 38. Neither gold nor silver lines were seen on any of the data. (Theoretical predictions had indicated that these tracer elements would not be exposed.) The relatively high excitation energies required for gold, the very small amount of gold in the fuel rods, and the intensities of the other lines indicate that the gold lines would have been very faint and possibly not detectable even if the gold had been exposed.

Other references used in estimating line intensities and interfering lines were NBS Monograph 32 (Part 1), Tables of Spectral Line Intensities - Arranged by Elements (United States Department of Commerce, and NBS Circular 467, Atomic Energy Levels (United States Department of Commerce).

Data from Sandia Airborne Spectral Instruments

The TRSS's in AFSWC-461 and AFSWC-521 detected radiation throughout the re-entry. These instruments were both in sharp focus and, because of the movement of the film and their relatively narrow field of view (about 3 degrees), they did not suffer much from overlapping spectra from different objects. These instruments were hand-tracked.

The film was to be pulled at 3/16-in./sec past a 3/4-inch slot so time resolution was to be about 4 seconds. BRT was to have been imprinted on the film, but it failed on the TRSS aboard AFSWC-461. Time on this film was estimated from film-transport rate, associating events with other data. On the TRSS aboard AFSWC-461, the film-pull rate was actually about twice as fast as had been intended. Since variable-speed DC motors were used to drive the cameras, it was difficult to achieve a desired speed; when this TRSS was airborne, the friction between the film and the plate against which it was held (by a vacuum pump) varied from what it had been at ground level.

AFSWC-461 was off to the side of the trajectory, about even with the "flare region" where flare materials were expected to be exposed. Much good data were collected, but better data would have been recorded if the film rate had been 3/16 in./sec. AFSWC-521 was stationed farther along the trajectory and looking upstream, but even so, good data were recorded in the flare region and good exposures of the RV burnup were recorded.

The roll of the airplanes and effects of hand-tracking from an unstable platform are visible in the data. The hydraulic autopilot in AFSWC-521 was not as good as the electronic one in AFSWC-461. The results of the greater roll of AFSWC-521 are noticeable in the plate-camera data as well as in the hand-tracked TRSS records. A disadvantage of tracked instruments is that one has a record of what is being detected with respect to time (if time is operational) but not of the location of the events in space, so the data must be correlated with other data. A good timing record was obtained on the TRSS aboard AFSWC-521.

AFSWC-521 Time-Resolved Streak Spectrograph -- The data obtained from the TRSS aboard AFSWC-521 were first recorded at 339.5 seconds, and were made possible by a mistrack that resulted in light integration on the film. It is believed that data were recorded somewhat earlier by the TRSS aboard AFSWC-461, because of the relative positions of the two aircraft. The TRSS in AFSWC-521 tracked the rods, or objects in the "flare" region, until 357 seconds, and then had a period with no record. At about 374 seconds, the tracker apparently started tracking the RV, and this was tracked until 392 seconds, with the intensity much diminished after 385 seconds. This last-tracked object is believed to have been the re-entry vehicle, since no other data show any other object with intensity enough to record at this late time in the trajectory.

At 345 seconds an intensity integration due to mistrack allows spectra to be identified. These spectral lines follow: magnesium lines at 5183, 5172, and 5167 Å; lead line at 4058 Å or potassium lines at 4044 and 4047 Å; aluminum lines at 3944 and 3961 Å, and more magnesium lines at 3829, 3832, and 3838 Å. Another intensity integration at 347.5 seconds has the same general characteristics as the one at 345 seconds, except that some radiation at about 4319 Å is quite intense. This could be the strong iron lines at 4308 and 4326 Å, but since the two lines are not resolved, because of movement of the camera, the identification is tentative. At 351 seconds occurs a flare with the band structure of what has been identified as strontium. There is also a line at the correct position to be the strong strontium line at 4607 Å. The flare at 351 seconds is believed to be the same one identified as strontium at 350.72 seconds on the framing-camera color film. Another flare occurring at 357 seconds is believed to be a strontium flare (the one at 355.98 seconds from framing-camera data).

The several-second time resolution on the TRSS films allows only approximate determination of time. The prominent spectra on this spectrogram are sodium. Sodium spectral lines 5890 and 5896 Å were visible from 339.5 until 353 seconds, and again from 374 until 385 seconds. Lithium is not present in the spectra from 339.5 until 353 seconds, but it is barely detectable from 374 until 382 seconds. The RV is the probable source for the latter spectra. The lithium does not appear as intense, in comparison with the sodium lines, as in the fourth-stage spectra. Furthermore, the intense aluminum-oxide bands associated with the fourth stage are completely absent here. Chromium and iron were undergoing re-entry burnup during this time. Lines detected follow: chromium lines at 4254, 4274, 4289, 5204, 5206, 5208, and 5264 Å including nearby iron lines, 5298 Å including nearby iron lines, and 5345 Å; and a combination iron line composed of iron lines 5324 and 5328 Å.

<u>AFSWC-461 Time-Resolved Streak Spectrograph</u> -- As mentioned previously, there were no timing marks on the film from the AFSWC-461 TRSS. A calculation based on the total time anything was being tracked allows an estimate of 3/8 in./sec. All times given for these data will be based on this somewhat arbitrary estimate. Sodium lines at 5890 and 5896 Å were visible from 341 to 350 seconds. Little or no sodium and no lithium are detectable on this record from 376.9 until 392 seconds. There are two intensity increases or intensity integrations at 343.6 seconds and at 344.3 seconds, and these have the same spectra. Spectral lines identified follow: sodium at 5890 and 5896 Å; magnesium at 5183, 5172, 5167, 3838, 3823, and 3829 Å; chromium at 4289, 4274, and 4254 Å; lead at 4058 Å <u>or</u> potassium at 4044 and 4047 Å; and aluminum at 3944 and 3961 Å.

An intense flare at 350 seconds has the band structure associated with the strontium flares, and a line identified as the strontium line at 4607 Å. This flare was recorded better on this film than on any other. If it is the same flare identified as the most intense "strontium" flare on other data, its true time is probably 350.72 seconds. Another strontium-type flare occurs at 352.6 seconds, and yet another flare without such definite strontium characteristics occurs at 356.4 seconds. These may be the flares identified as strontium on other data at 352.00 and 355.98 seconds. If so, only the "strontium" flare at 353.88 was not detected. The zero order is multiple in the "flare" region, indicating that more than one object was being tracked; but it is single and sharp from 376.9 until 388.4 seconds, when the RV was the probable object being tracked. The spectra from the RV region are fuzzy and not well exposed. However, chromium lines and chromium-oxide bands appear to be present, and this agrees with other RV data. It must be emphasized that the timing was relatively uncertain on the TRSS on AFSWC-461. The last spectra from the RV probably were not after 384 seconds, or the end of the large reactor-RV flareup.

<u>AFSWC-521 Photometer</u> -- The photometer on AFSWC-521 was hand-tracked on the same mount as the TRSS. This photometer collected no usable data. Its field of view was only 24 minutes of angle, so the difficulties of hand-tracking a heavy assembly, compounded by the poor autopilot on this aircraft, caused the only detectable signal to appear as the photometer field of view passed over a re-entry object. Except for very brief intervals, there were only two periods when signals were recorded. These were 0.2 second at 380 seconds, and 0.05 second at 376.5 seconds. During the longer interval, the photometer was reading high on the silver 5209-Å filter, which was probably monitoring the chromium lines at 5204, 5206, and 5208 Å. This would be consistent with the other data for this time. The brief intervals of record indicate that the photometer functioned properly within its field-of-view limitations. The C.E.C. recorder provided excellent time resolution.

<u>Data from AFSWC Spectral Instruments</u>

On AFSWC-521, spectral data were collected on Z-1, Z-2, and Z-10, which were the K-24 spectral cameras discussed in Section III and Tables III and V. The Hulcher 70-mm cinespectrograph on AFSWC-521 did not collect any usable data. The timing did not record satisfactorily, and exposures believed to be of the RV re-entry are underexposed and poorly resolved. The camera may have been out of focus. Timing was somewhat uncertain on the K-24 spectral cameras, which were supposed to cycle 2.5 seconds open and 1.5 seconds shut while the film was being pulled. In reality, the signals from the camera to the timing record show open times from 7 to 8 seconds down to zero. Since it was not possible to definitely relate one timing signal to a certain frame, the relation was arrived at deductively.

Z-1 Spectral Camera: The deduced times for the two exposed frames on the Z-1 camera were from 371.3 to 378 seconds, and from 378.6 to 380.8 seconds. This camera was aimed aft, and so should have been looking at the RV-burnup region in space; the spectrogram reproduced in Figure 40 agrees with the other data on RV burnup, and the timing agrees approximately with other data on RV intensity brightness. The intensity fluctuations in time seem to indicate that the timing may be off by several seconds. Since the spectrum lines and bands are identified in Figure 40, their identification will not be discussed further here.

The second spectrogram from the Z-1 camera has the same features as the one reproduced. Camera vibration and motion are signified by the waviness of the lines. This camera was in sharp focus and probably provides the clearest identification of lines arising from burnup of the RV.

Z-2 Spectral Camera: Camera Z-2 was the center camera of the three spectral K-24's. Three of its frames acquired data that appear to be of the same event recorded on the Z-1; therefore the data must be of the RV burnup. Since these data were not as good as those from Camera Z-1, and since they apparently had no features not contained in those from the Z-1, the data were not reduced further.

Z-10 Spectral Camera: Camera Z-10, aimed forward, covered the "flare" region. The focus on this instrument was only fair and the film was underexposed. Data were collected on three frames. The underexposure is lamentable, because this camera was operated with an f stop of f/5.6 when it could have been opened up to f/2.5 for a fivefold or sixfold increase in exposure. An event identified as a strontium flare on the AFSWC-521 TRSS record, at what is called 350.72 seconds from the motion-picture data, was identified on the Z-10 data. The line identified as the strontium line at 4607 Å is visible. The film indicates that a wide-open camera would have acquired excellent data. Timing of the frames was not exactly determined, since the time record was bad. The spectral characteristics indicate that the exposed frames were of the "fuel-rod flare" region. The sodium lines at 5890 and 5896 Å associated with the "bottom" object in the flare region were recorded, and chromium lines were recorded as well.

On AFSWC-461, none of the AFSWC-provided spectral instrumentation recorded data. Orientation of cameras on the aircraft may be the explanation.

Data From NASA Airborne Spectral Instruments

The NASA aircraft was located well downrange. As a result, its optical instrumentation was viewing the trajectory somewhat end on. Most of the trajectory could be covered with single, fixed cameras; however, the aircraft position was far enough to the side to resolve events along the trajectory with the open plate trajectory and the spectral plate cameras. NASA instrumented the NASA aircraft completely. The data from the chopped trajectory plate camera AC-1 (see Figure 34) have been valuable in determining time for different events. The chops on this plate were coded and had a 0.25-second open shutter and a 0.25-second closed shutter. NASA had three spectral cameras (KG-24's) with gratings as indicated in Table IV. The NASA spectral cameras used Royal-X Pan film, as did the AFSWC cameras, and they suffered the same cutoff in the red region of the spectrum above 6300 Å.

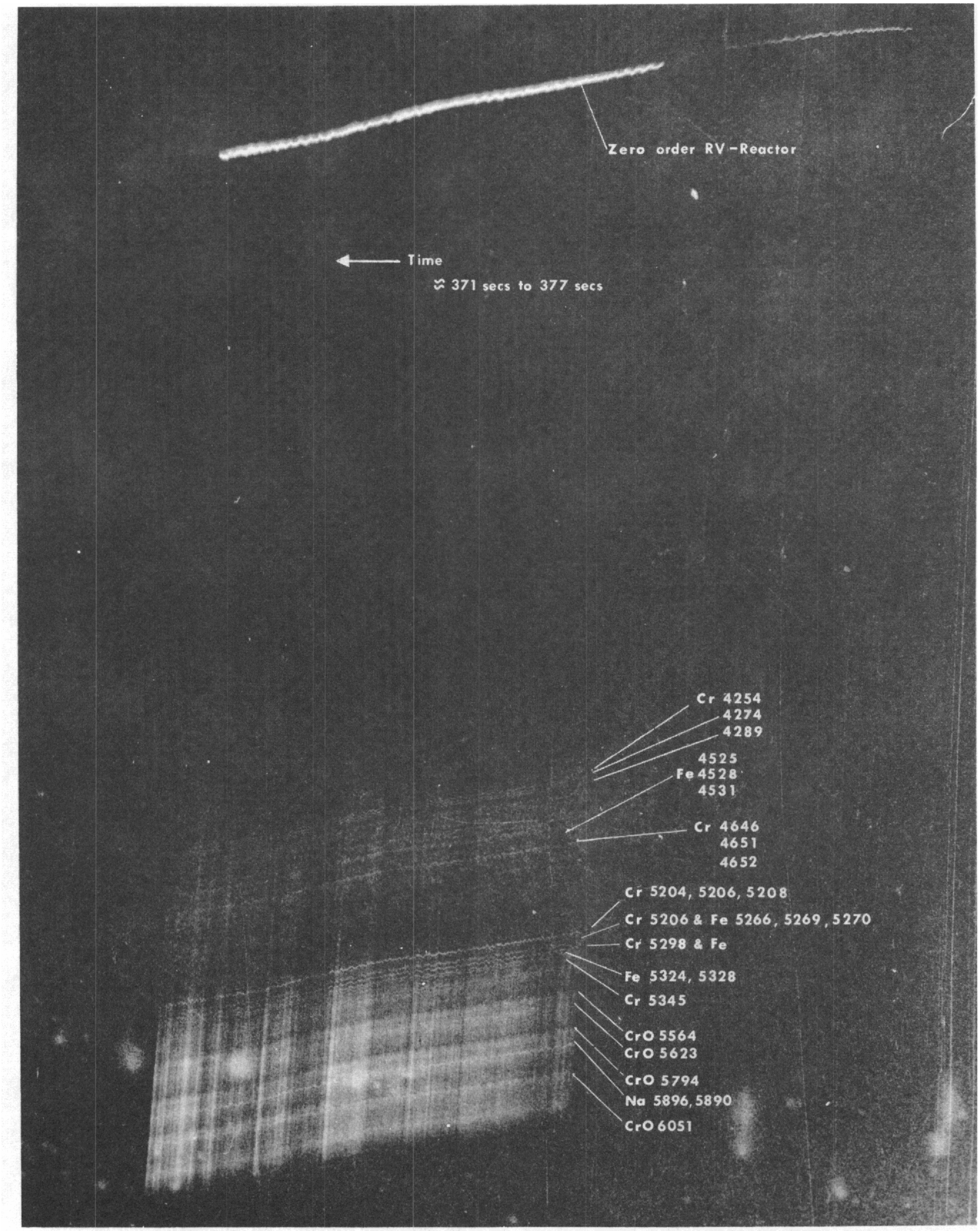

Figure 40. RFD-1 RV-reactor spectra
(from Z-1)

AC-37 Spectral Camera -- Spectral Camera AC-37 used a 600-lines/mm grating, and had a dispersion on the film of about 93 Å/mm. Although this camera was not in sharp focus, the images were fairly good. The field of view covered the latter part of the "fuel-rod flare" region and the RV flareups in the zero order. The spectra from the fourth stage were on the plate, although the zero order was not. The aluminum-oxide molecular bands, and the sodium lines at 5890 and 5896 Å associated with the fourth stage, are very evident and compare well with the data recorded on the LA-24 TRSS. Because of the red-end cutoff of the film, the lithium line at 6707 Å is not seen. Spectra arising from the RV flareups are not sharp and well resolved. These spectra are not as intense as would be expected, because they arise from the unblazed side of the grating and thus have much less intensity than those arising from the blazed side. In this instance these spectra were off the format. However, the spectra from the RV burnup are obviously the same as those in the data recorded by the other instruments in which the details were more distinct and have been or will be discussed. Therefore, AC-37 data will not be pursued further.

AC-85 Spectral Camera -- Spectral Camera AC-85 utilized a 400-lines/mm grating, giving a dispersion on the film of about 136 Å/mm. The data recorded by this instrument were the most comprehensive and distinct recorded by any single instrument. The focus was sharp, the regions of interest in space were well covered, and lines were, relatively speaking, well resolved (Figure 41). The NASA cameras all seemed to suffer much less from aircraft vibration than did the instruments in the AFSWC C-54's.

The regions in space covered by the zero order of AC-85 were from the middle of the "fuel-rod flare" region through the RV flareups, or from about 351 seconds until after 386 seconds. Spectra from the entire "fuel-rod flare" region are on the film due to the angle of the grating lines. In addition to the first-order spectrum of the fuel-rod region, there are some second-order spectra from the RV flareup, some first-order spectra of the fourth stage, and some first-order spectra of the RV flareup from the unblazed side of the grating. AC-85 was the only camera or instrument to record indications of barium flares. Barium lines arising from the "fuel-rod region" occur from about 350.5 until 353.5 seconds, and again at 359.37 seconds. The flare observed at 356.62 seconds is possibly barium. The barium lines seen in the flare at 350.5 to 353.5 seconds are the strong line at 5535 Å and the weaker line at 4554 Å. A line that could be the barium line at 6142 Å tends to confirm the identification. The barium line at 5535 Å was the only barium line identified in the flare at 359.37 seconds. The strontium flares identified on the other spectral data are recognizable on this spectrogram and are labeled on the spectrogram.

In addition to the lines labeled on the spectrogram shown in Figure 41, other lines from the RV flareup were also identified. They will be listed, although they add little to the picture previously drawn by the other data. The lines and bands follow: chromium oxide band heads at 5564 and 5794 Å; a combination line made up of iron lines at 5265, 5266, 5269, 5281, and 5283 Å, and chromium lines at 5264 and 5265 Å; a combination line made up of iron lines at 5324, 5328, 5329, 5332, and 5339 Å, and chromium lines at 5345 and 5409 Å. At the very right edge of the spectrogram are some short magnesium lines at 5167, 5172, and 5183 Å. The bright line in the spectrum at the right of the picture that then trails to the left and down across the other spectra is the strong sodium doublet associated with the "bottom" object or objects. The sodium doublet is also visible in the RV spectra. In the trajectory cameras the bottom trace is seen to separate into two traces. The sodium spectrum is seen to fuzz out (in time), indicating that two sources of sodium radiation could be present.

AC-84 Spectral Camera -- Spectral Camera AC-84 was aimed somewhat more upstream than were AC-37 and AC-85 (see Figure 42). The zero order of the entire "fuel-rod region," the first RV flareup, and the fourth stage were recorded. This instrument used a 75-lines/mm grating, so the dispersion was only about 740 Å/mm on the film. Because of the small dispersion and somewhat fuzzy focus, relatively poor resolution was present in the first order. However, the second-order spectra of the fourth stage and some of the fuel-rod region are exposed well enough to be usable at its higher dispersion of 370 Å/mm. There are even some third-order spectra arising from the fourth stage. The falling off in intensity of spectra with increasing order is one reason for using low-dispersion gratings. In cases where the first-order spectrum is overexposed, the second or third are very unlikely to be. In addition to the lines labeled on the spectrogram, a line identified as

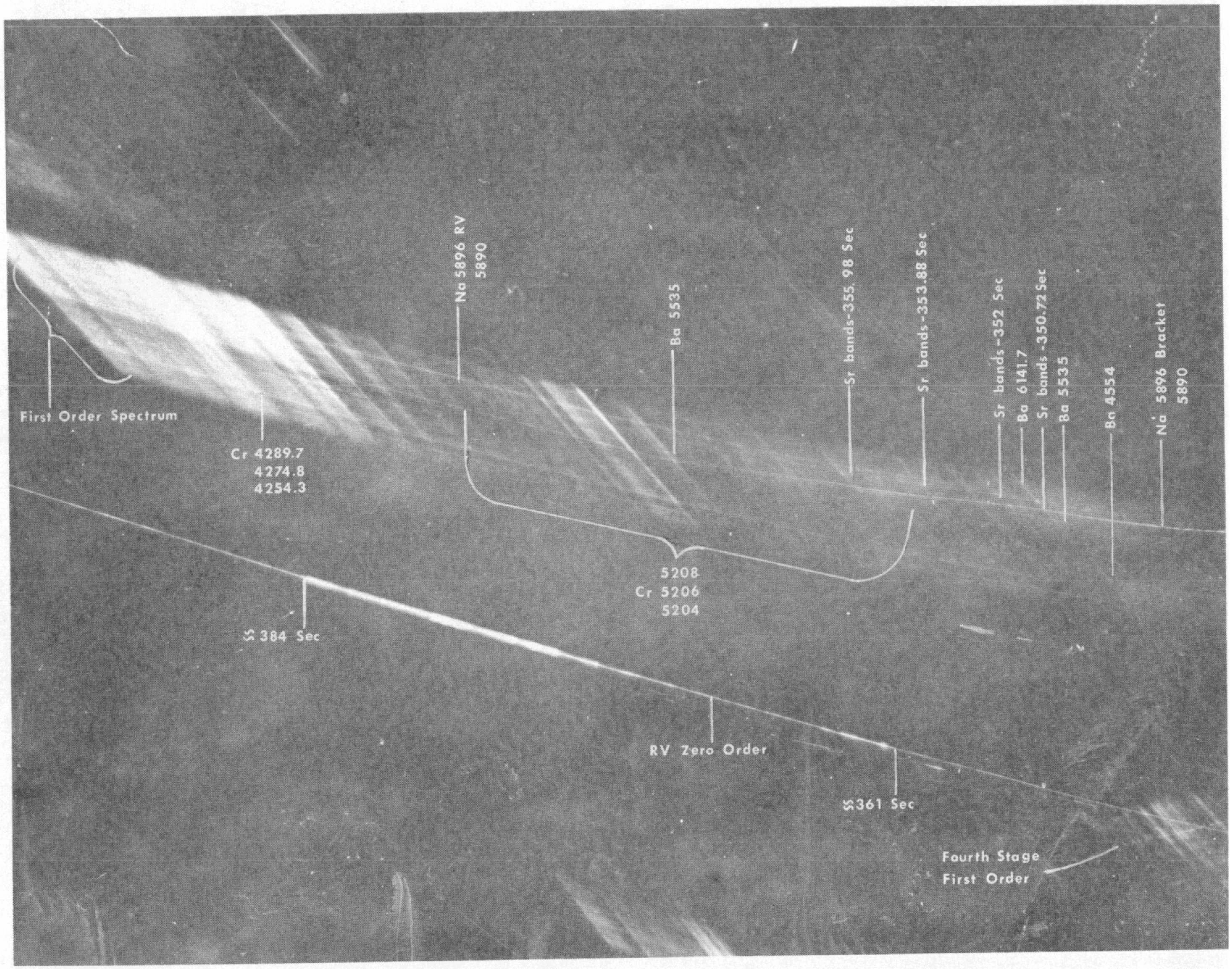

Figure 41. RFD-1 re-entry spectra (from Camera AC-85)

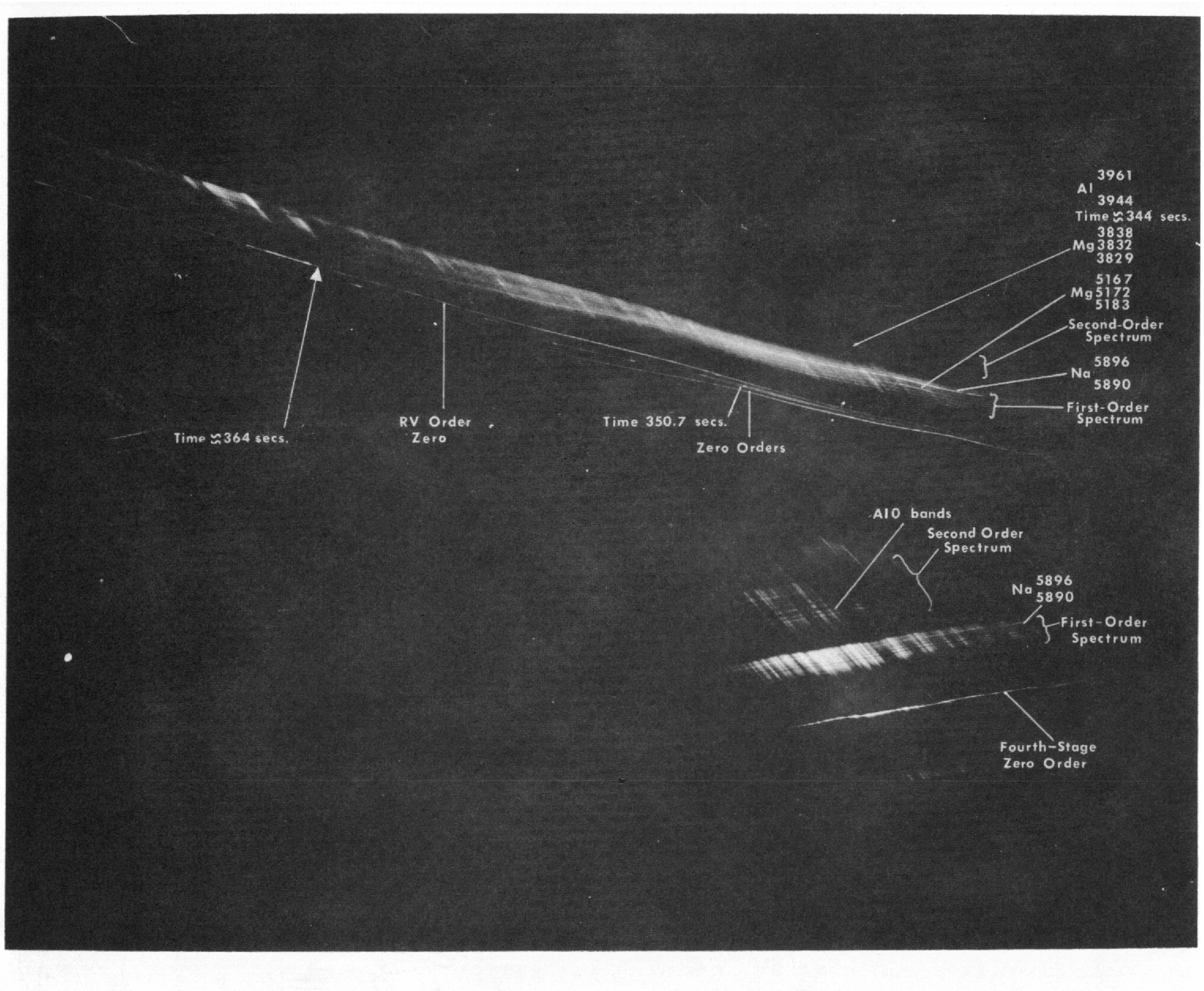

Figure 42. RFD-1 re-entry spectra (from Camera AC-84)

either potassium lines 4044 and 4047 Å or the lead line at 4058 Å arises from the "bottom" object which has the strong sodium doublet associated with it. The strontium flares with their typical spectral bands are recognizable but could not be identified from the spectrogram alone. The aluminum-oxide bands and the sodium doublet are again pronounced spectral structures of the fourth-stage spectra.

Motion-Picture Data

As explained in Table V, Section III, most of the framing-camera films were underexposed. Three films, however, did record usable information. These included:

1. The color films from Sandia ME-16-1 (35-mm Mitchell motion-picture camera with 18-inch-f.l., f/3.0 Paxar lens).
2. The black-and-white film from NASA AC-101 (35-mm Flight Research motion-picture camera with 10-inch-f.l., f/4.5 Bell and Howell Eyeman lens).
3. The color film from NASA 113 (16-mm Cine Kodak motion-picture camera with 2-inch-f.l., f/2.0 Kodak Anastigmat lens).

Reduction of these three films constituted the motion-picture evaluation of the re-entry. A discussion of their analysis follows:

Four of the re-entry objects are quite evident on the motion-picture films. Several others are just visible but too faint and blurred for identification or analysis. A complete tabulation of the observed events from the films versus time is given in Tables XXIII to XXVI. BRT, which is accurate to 0.01 second, was recorded on the border of the films. The small discrepancies in times from the three films are due to several factors. For example, since the frame rates of the two NASA films were 10 and 16 frames/sec, while the Sandia camera frame rate was 96 frames/sec, the NASA cameras could have missed some of the faster events. In addition, the Sandia camera was closer to the early portion of the re-entry flight path, while the NASA cameras were closer to the latter portion (see Figure 13). The Sandia camera could have missed some of the less intense flares due to its faster frame rate. Neither NASA Cameras AC-101 nor Sandia Camera ME-16-2 tracked the fuel rods to the completion of burnup, but NASA Camera 113 did. Even though the timing on the films was accurate to 0.01 second, determination of the precise times of flare beginning, peaks, and end was difficult. The times agree closely enough to permit correlation with other films and records. No determination of altitude or location in space is directly possible from these films. However, a comparison of the motion-picture times with the plate films and theoretical trajectories furnishes this information.

Figure 43 is a black-and-white reproduction of one frame from the 35-mm color motion-picture film taken by Sandia Camera ME-16. Time of the events shown was 351.62 seconds. The lower object was identified as a strontium flare, and the upper object is believed to be a barium flare.

Figure 44 is an enlargement of one frame from the 35-mm black-and-white motion-picture film taken by NASA Camera AC-101. Time of the events shown was 352.00 seconds. The objects included are, from left to right: the re-entry vehicle, strontium and barium flares, and the fuel-rod brackets.

Re-entry Vehicle

Identification of the RV on the motion-picture films was easily made because of its size, brightness, and behavior during re-entry. Disassembly of the simulated SNAP-10A reactor was visible on the films (see Table XXVI and Figure 45). These events correlated well with the predicted, telemetered disassembly and spectral data. Reactor disassembly is discussed in SC-RR-64-515.

TABLE XXIII

Fuel-Rod Flare Times Recorded by NASA Camera AC-101

Time from Launch (sec)			Intensity			
Flare Start	Flare Peak	Flare Out	Bright	Med.	Dim	Remarks
342.17	342.37	342.57		x		Not fuel-rod flares
342.27	342.37	342.47		x		Bottom, strontium flare
344.70	344.80	345.10		x		Bottom, strontium flare
345.20	345.20	345.20		x		Bottom, strontium flare
345.30	345.41	345.51			x	Bottom, strontium flare
345.51	345.51	345.51			x	Not fuel-rod flares
346.11	346.21	346.31	x			Bottom, strontium flare
346.21	346.31	346.41	x			Bottom, strontium flare
346.72	346.92	347.12			x	Bottom, strontium flare
348.13	348.13	348.13			x	Bottom, strontium flare
348.63	348.73	348.83		x		Bottom, strontium flare
348.64	348.94	349.45		x		Bottom, strontium flare
349.55	349.65	349.85		x		Bottom, strontium flare
349.65	349.85	349.95		x		Bottom, strontium flare
349.95	350.05	350.15		x		Bottom, strontium flare
350.15	350.25	350.46		x		Bottom, strontium flare
350.15	350.35	350.46		x		Bottom, strontium flare
350.15	350.35	350.55	xx			Bottom, strontium flare
350.15	350.35	350.55	xx			Bottom, strontium flare
350.55	350.75	350.85	xx			Bottom, strontium flare
351.46	351.66	352.16	xx			Bottom, strontium flare
350.25	350.75	352.26	xx			Top, barium flare
352.77	352.77	352.87	xx			Top, barium flare
352.87	352.87	352.87		x		Top, barium flare
352.87	352.87	352.87		x		Bottom, strontium flare
352.97	352.97	352.97			x	Top, barium flare
352.97	352.97	352.97			x	Bottom, strontium flare
353.28	353.28	353.28			x	Bottom, strontium flare
353.58	353.88	354.39	x			Bottom, strontium flare
354.39	354.49	354.79	x			Bottom, strontium flare
354.79	354.99	Dim, not out	x			Bottom, strontium flare
	355.29	Dim, not out	x			Bottom, strontium flare
	355.90	356.00	x			Bottom, strontium flare
356.90	356.90	356.90			x	Top, barium flare
357.10	357.20	357.52	x			Top, barium flare
	358.00					Off edge of film

TABLE XXIV

Fuel-Rod Flare Times Recorded by Sandia Camera ME-16-2

Time from Launch (sec)			Intensity			
Flare Start	Flare Peak	Flare Out	Bright	Med.	Dim	Remarks
344.75						Rods show
	345.25			x		Bottom, strontium flare
	349.33			x		Bottom, strontium flare
	349.83		x			Bottom, strontium flare
	350.49				x	Bottom, strontium flare
350.59	350.62	350.75	x			Bottom, strontium flare at 350.72 breaks into 2 parts
351.83	351.87	351.96	x			Bottom, strontium flare
351.98	352.00	352.13	x			Bottom, strontium flare
350.59	350.75	350.88	x			Top, barium flare
351.30	351.40	351.50	x			Top, barium flare
351.53	351.86	351.96	x			Top, barium flare
	353.70			x		Bottom, strontium flare
	353.75			x		Bottom, strontium flare
	353.79				x	Bottom, strontium double flare
	353.88		x			Bottom, strontium double flare
	355.33				x	Bottom, strontium flare
	355.98		x			Bottom, strontium flare
	356.00		x			Off edge of film

NOTE: Color of top (barium) flares was yellow-white. Color of bottom (strontium) flares was red.

TABLE XXV

Fuel-Rod Flare Times Recorded by NASA Camera 113

Time from Launch (sec)			Intensity			
Flare Start	Flare Peak	Flare Out	Bright	Med.	Dim	Remarks
345.18	345.24	345.43		x		Strontium flare
345.74	345.74	345.87		x		Strontium flare
346.10	346.12	346.21		x		Not fuel-rod flares
346.61	346.62	346.72		x		Not fuel-rod flares
348.75	348.94	349.00		x		Strontium flare
349.00	349.25	349.37		x		Strontium flare
349.44	349.44	349.56		x		Strontium flare
349.62	349.69	349.81		x		Strontium flare
350.00	350.13	350.25			x	Strontium flare
350.31	350.31	350.38		x		Bottom, strontium flare
350.31	350.38	350.44		x		Top, barium flare
350.44	350.44	350.56	xx			Bottom, strontium flare
350.50	351.31	351.94	x			Top, barium flare
350.63	350.69	350.75			x	Bottom, strontium flare
350.94	351.50	351.75	x			Bottom, strontium flare
352.32	352.38	352.38			x	Bottom, strontium flare
352.51	352.57	352.63			x	Bottom, strontium flare
352.56	352.56	352.62			x	Top, barium flare
352.76	352.82	352.88		x		Bottom, strontium flare
353.01	352.32	353.70	x			Bottom, strontium flare
353.76	353.76	353.82		x		Bottom, strontium flare
353.88	353.88	353.95		x		Bottom, strontium flare
354.01	354.01	354.07		x		Bottom, strontium flare
354.14	354.57	354.82		x		Bottom, strontium flare
354.89	355.08	355.20	xx			Bottom, strontium flare
356.18	356.18	356.25			x	Top, barium flare
356.31	356.62	356.81	x			Top, barium flare
357.01	357.01	357.01			xx	Bottom, strontium flare
357.14	357.14	357.14			xx	Bottom, strontium flare
359.12	359.37	359.56	x			Top, barium flare
359.68	359.74	359.87			x	Top, barium flare
360.83	361.14	361.45		x		Top, barium flare
361.76	361.83	361.89		x		Top, barium flare

NOTE: Color of top (barium) flares was yellow-white.
Color of bottom (strontium) flares was red.

TABLE XXVI

RV Event Times Recorded by NASA Camera AC-101

Time from Launch (sec)	Event	Remarks
340.38	Brackets show	Tumbling
342.64	RV shows	
343.64	RV and reflectors brighter	
344.64	Object off RV	
346.04	RV bright and object off	
348.00	Object off	
352.43	Object off	
352.62	RV flat face on front of flare	Coning
352.82	Stable	Coning
352.94	RV front of flare slanted	Coning
353.04	RV front of flare slanted opposite	Coning
353.15	RV front of flare slanted	Coning
353.25	Stable	Coning
353.35	Very flat face - object off	Coning
354.45	Two objects from previous object off	
354.85	Rear object breaks into 2 parts - RV stable	
356.06	Object off	
357.67	Severe coning starts	Coning
359.07	RV bright	Coning
359.47	RV appears to be canted - large - bright	Coning
359.67	RV stable	Coning
362.50	Object off	
363.71	RV very bright	Overexposed frame
364.41	Object off	
365.00	Many objects off	Reactor disassembly
366.02	Object off	
366.72	Rear objects break up	
371.86	Off edge of film	

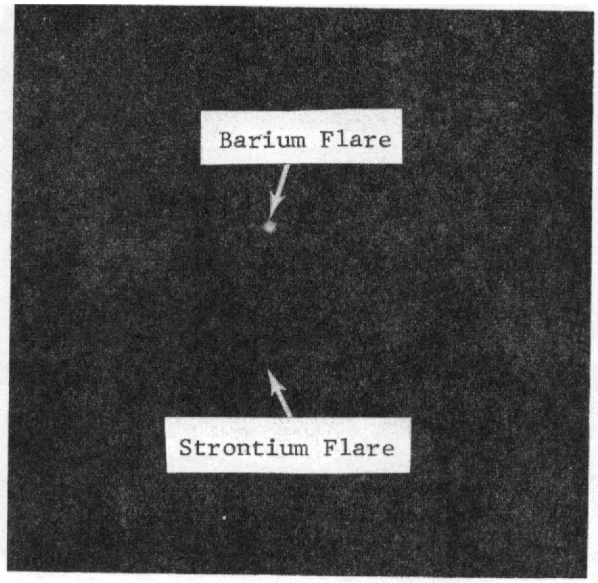

Figure 43. Strontium and barium flares during re-entry (351.62 seconds)

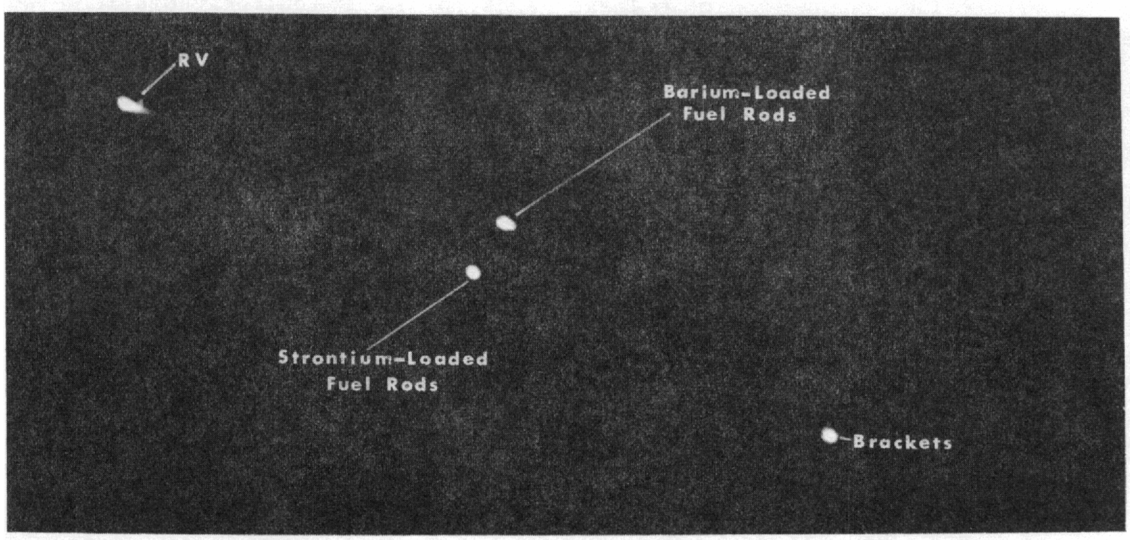

Figure 44. RFD-1 re-entry at 352 seconds (blown up from 35-mm motion-picture film, Camera AC-101)

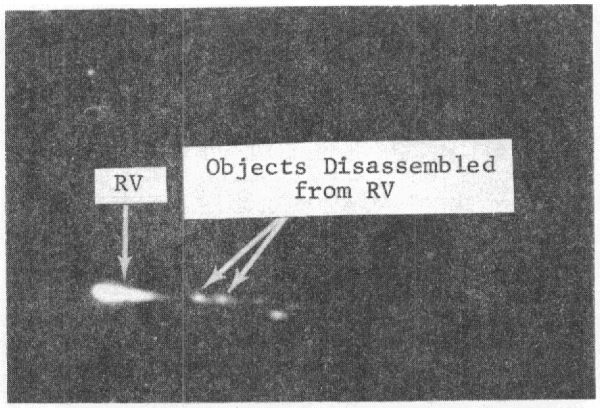

Figure 45. RFD-1 re-entry at 366.9 seconds (blown up from 35-mm motion-picture film, Camera AC-101)

External Fuel Rods

Identification of the strontium and barium tracers on the motion-picture films was determined from the flare colors and from the pattern of pulsations. This analysis is thought to be conclusive for the following reasons:

1. When strontium is excited in an air atmosphere, the predominance of radiation from it is in the red spectral region (6000 to 7000 Å). This is a consequence of heavy molecular bands plus some atomic lines in that region. Barium appears as a white light with a yellow-pink cast. The white light results from an even distribution of lines over the spectrum from 4000 to 7000 Å. Strong barium-oxide molecular bands exist in the yellow-orange region. These bands, plus atomic line radiation in the orange region, contribute to the yellow-pink cast. Comparison of colors in the color photoprints from which Figure 12 (preflight electric-arc tunnel tests) and Figure 43 (ME-16-2) were reproduced suggests that the two flares were strontium and barium. The top flare of Figure 43 was noted pulsating 10 times from 350.25 seconds (198,000 feet) to 357.52 seconds (178,000 feet) on framing-camera films. The bottom flare pulsed 28 times from 342.27 seconds (220,125 feet) to 361.83 seconds (165,400 feet). Color film does not always depict true colors, because of overexposure, underexposure, atmospheric effects, film emulsion, and processing. However, the flare colors recorded on the films remained essentially the same through many cycles of varying intensity, pulsating from very bright to not visible. This lends some validity to the color comparisons. As previously mentioned the spectral data corroborates these conclusions.

2. The pattern of flare occurrence on the motion-picture films is similar to that noted in the electric-arc tunnel preflight ablation tests. During these tests, even though the specimens were rotating, a hot spot invariably caused excessive ablation at one or two locations. This resulted in a hole or holes through the rod wall, which exposed the tracer. As rotation and ablation continued, the flare from the tracer pulsated in an irregular pattern of intensity similar to the one mentioned above. The irregular flare pattern from the fuel-rod tracers on the flight-test motion-picture films was thought to be caused by intermittent exposure of the tracers. This was probably due to tumbling and to uneven ablation of the rods. It should be noted that the

re-entry trails from the RV and brackets were essentially steady and continuous streaks. These phenomena are also very evident on the plate-camera films.

<u>Fuel-Rod Brackets</u>

Even though Bracket No. 1 was the first visible re-entry object, and among the brightest, identification of the fuel-rod brackets from the motion-picture films was not possible. Identification was initially determined from the spectral films and theoretical trajectories. It was first visible on the motion-picture films at 340.38 seconds (227,000 feet) and appeared to have a tumbling motion. Peak intensity was reached at 343.64 seconds (218,000 feet). However, the light from this object was essentially continuous and did not pulsate or flare appreciably. From peak intensity to 364.50 seconds (173,000 feet), it grew steadily dimmer, and it was not visible after that time. The brightness of Bracket No. 1 was believed caused by the sodium content of the fiberglass shield and the contents of the battery it supported. Bracket No. 2 did not include a battery and was therefore not as bright on the motion-picture films.

The rest of the re-entry items are faintly visible in Figure 46. They do not, however, present any positive characteristics to allow identification.

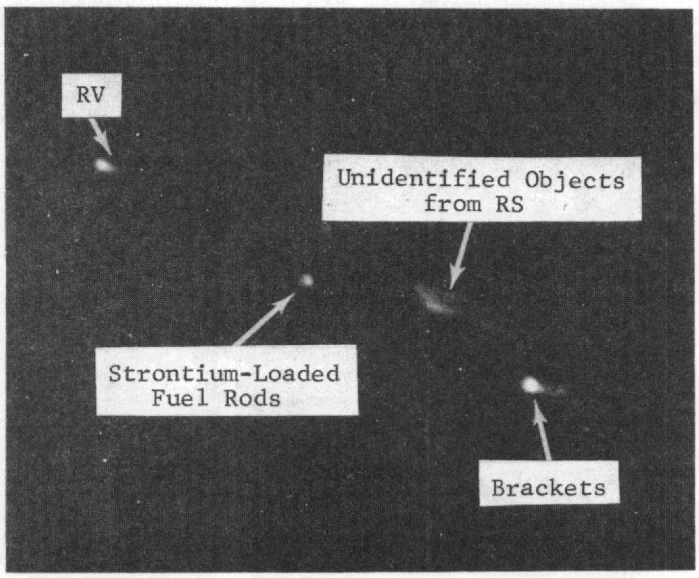

Figure 46. RFD-1 re-entry at 348.9 seconds (blown up from 35-mm motion-picture film, Camera AC-101)

Identification of the re-entry objects from the motion-picture films should not be construed as final proof. Confirmation of these observations by the spectral and plate-camera films and by the theoretical trajectories is discussed on pp. 106 to 114.

Summary of Optical Data Reduction

Reduction of the RFD-1 films and records to establish re-entry events and object identification was pursued according to individual type of film or record involved. The three major types included plate-camera films, spectral data, and motion-picture films. This method was employed because each type displayed the information in varying manners and required different procedures for analysis.

Generally, each record revealed information about the re-entry that by itself was not absolute. However, coincidental agreement of the three data categories on almost every conclusion appears to verify and confirm those conclusions. For clarity, discussion of the data correlations will be according to individual re-entry objects. Time is considered as the common dimension of comparison. Figures 47-50 summarize the finding discussed in this section.

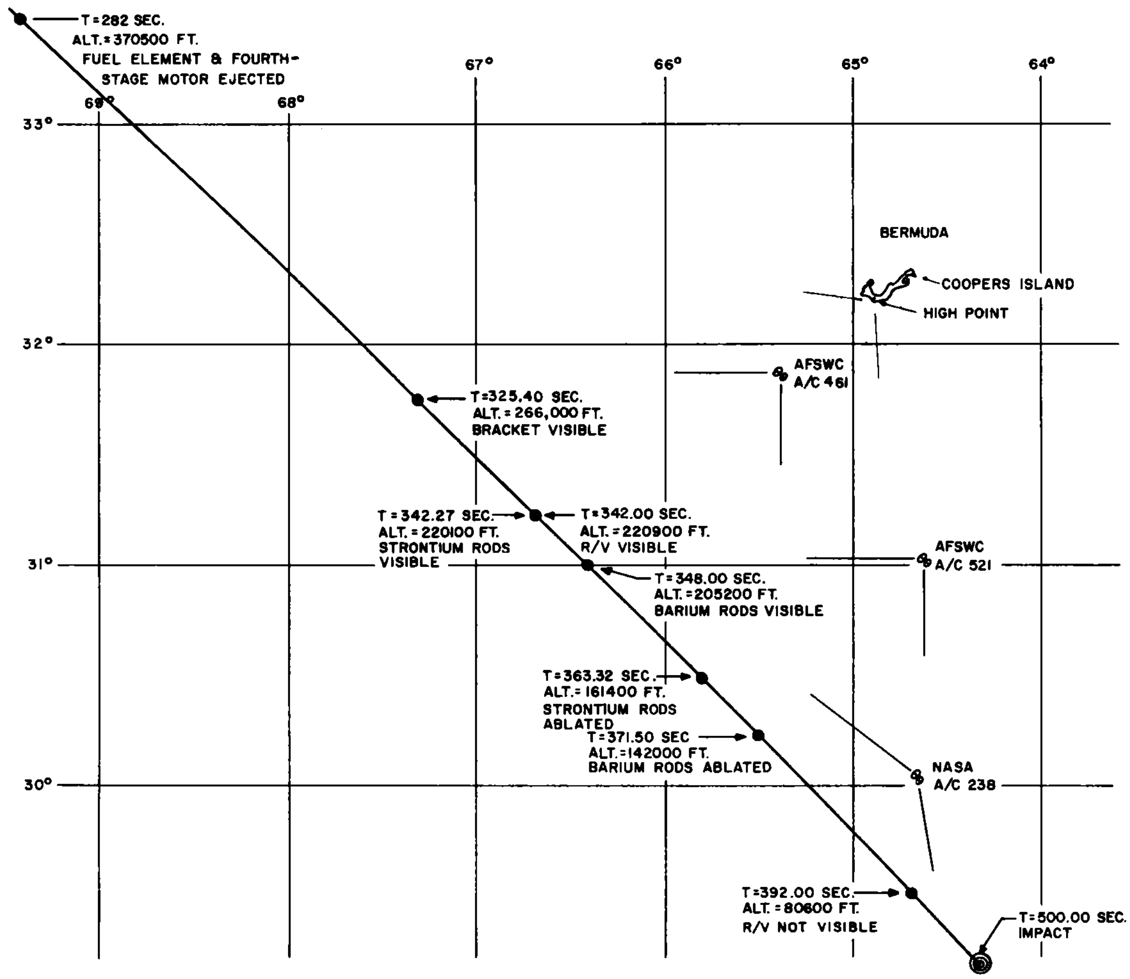

Figure 47. Summary of RFD-1 re-entry events

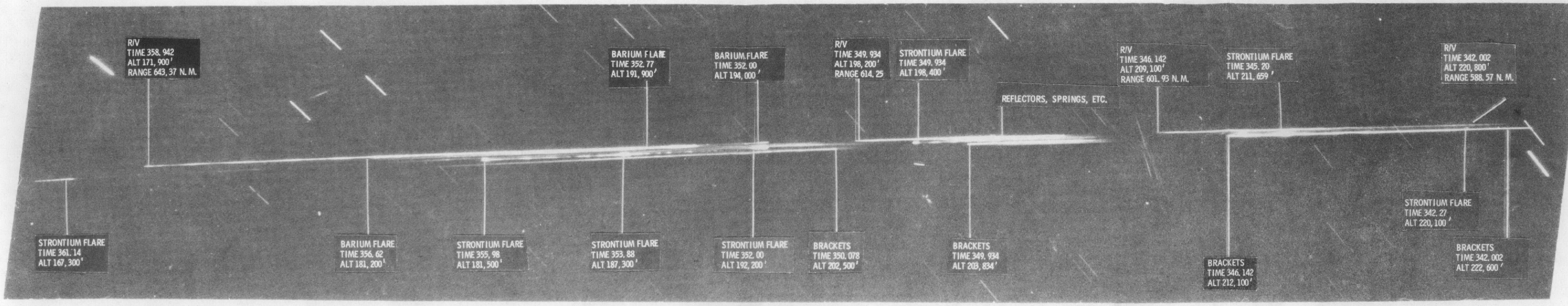

A. From Plate Camera T-2

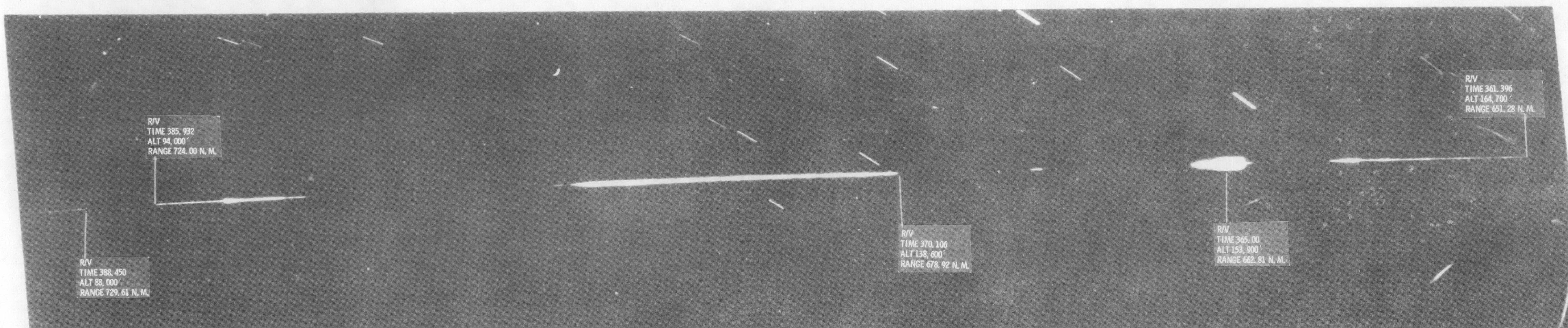

B. From Plate Camera T-3

Figure 48. Summary of RFD-1 re-entry events (0.1" ≈ 2800')

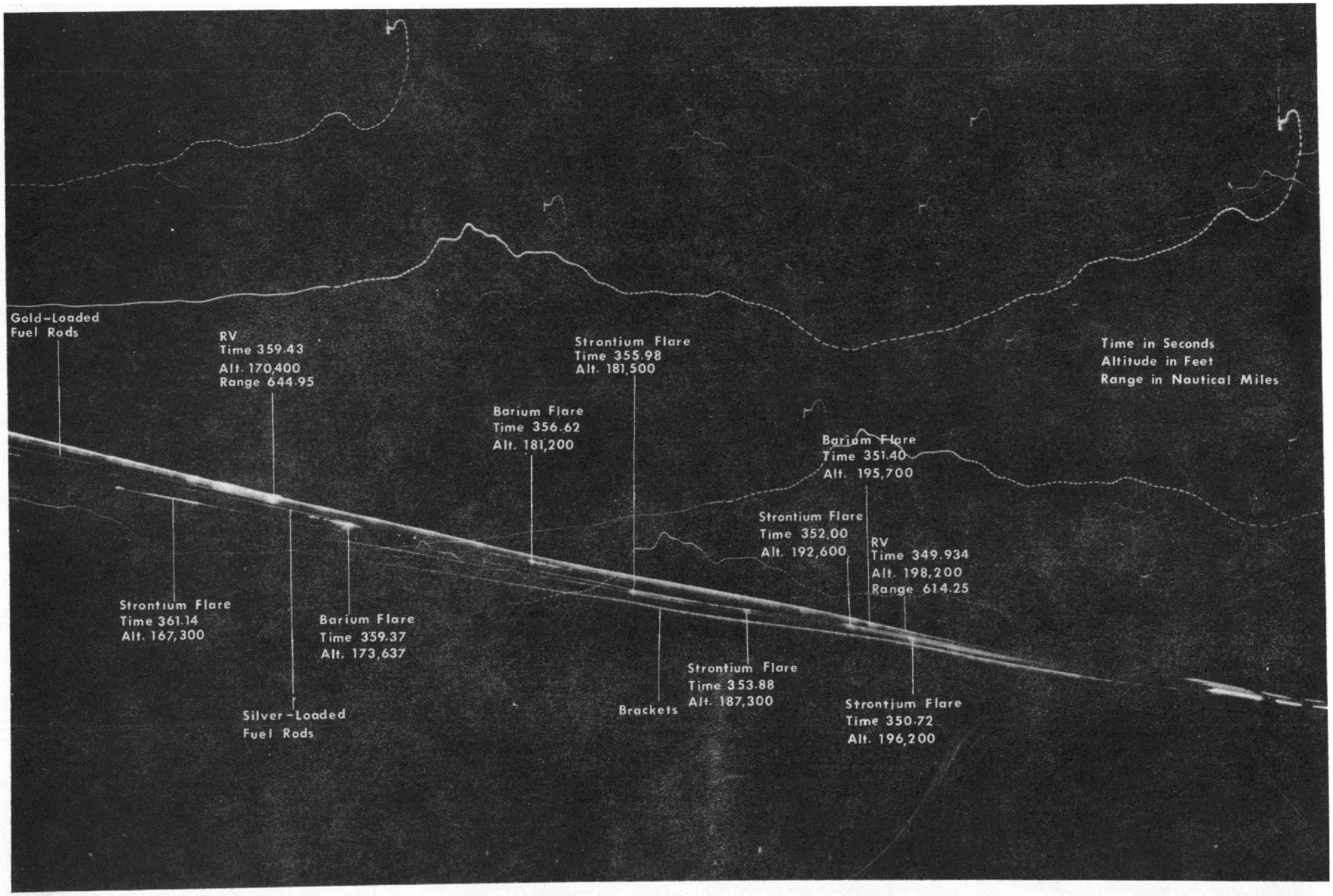

Figure 49. Summary of RFD-1 re-entry events (from Camera AC-34)

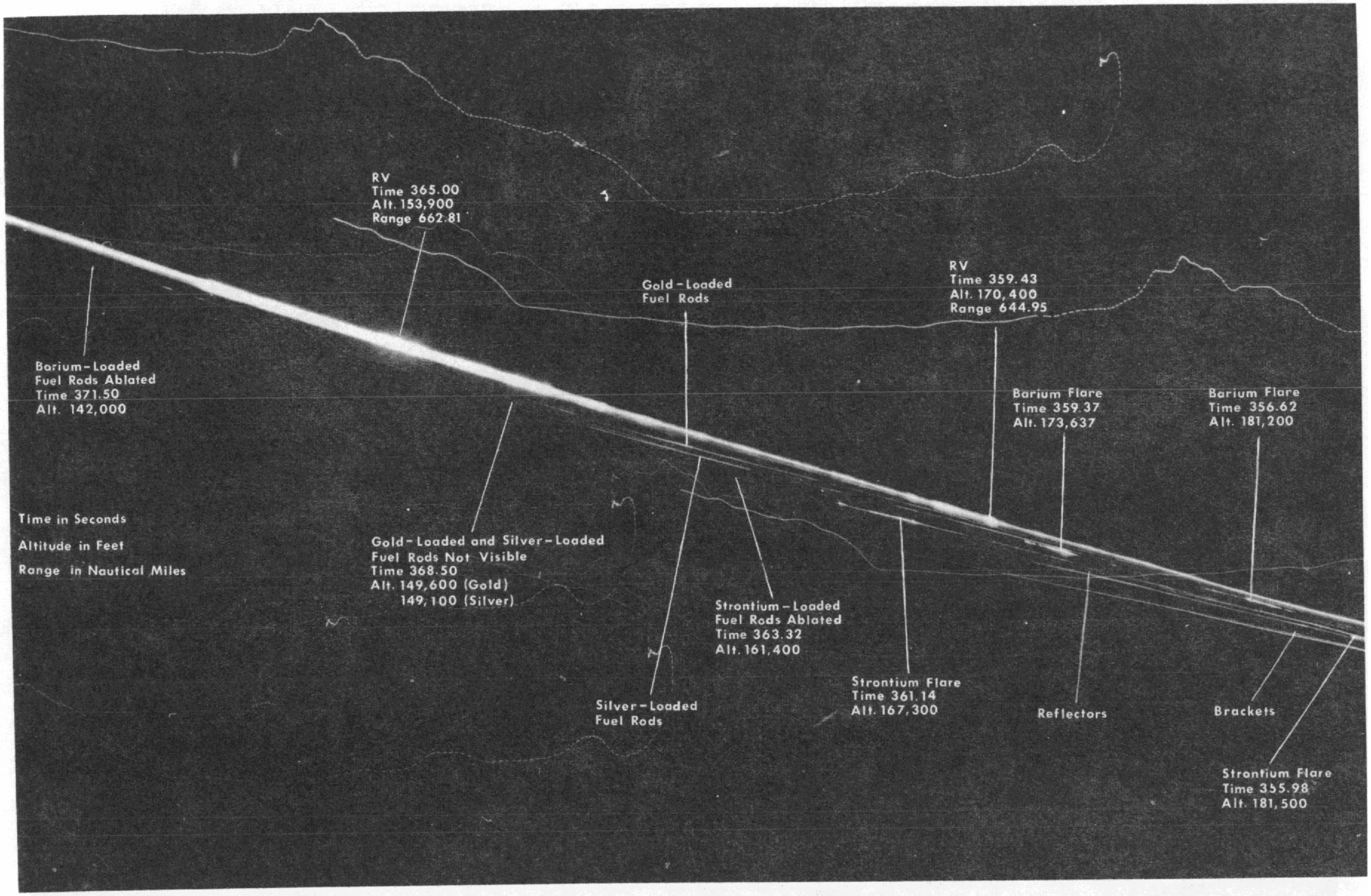

Figure 50. Summary of RFD-1 re-entry events (from Camera AC-38)

Reactor and Re-entry Vehicle

Identification of the reactor and RV from the films was obvious, especially when compared with visual observation of the actual re-entry. They were the leading object in the re-entry sequence (as predicted by the preflight trajectory). They were also much larger and brighter than all other items except the fourth-stage motor. The fourth-stage motor, however, was far enough removed from the re-entry area so as not to interfere with their identification.

The theoretical RV trajectory discussed previously (pp. 46-79) agreed to within 300 feet with the measured FPS-16 radar trajectory, from approximately 167 seconds (450,000 feet) to 360 seconds (168,800 feet). This theoretical trajectory also agreed to within 400 feet with the measured plate-camera trajectory, from 325.4 seconds (266,000 feet) to 392.1 seconds (80,400 feet). At this altitude, the velocity of the RV and reactor was slow enough to cause cooling below the temperature which permitted them to be self-luminous.

Spectral films from the TRSS on AFSWC 521 indicated the presence of aluminum at 345 seconds (212,000 feet) and 347.5 seconds (205,000 feet). The TRSS on AFSWC 461 showed aluminum at 343.6 seconds (218,200 feet) and 344.3 seconds (214,000 feet). These times and altitudes compare with the indicated melting time of 336 seconds (237,500 feet) to 342 seconds (220,400 feet) of the aluminum fins on the reactor, as telemetered from the thermocouples. However, these spectra cannot be definitely confirmed as having radiated from the zero-order streak known to be the RV-reactor. Aluminum brackets and reflectors were also melting in this vicinity at the same time, and could have contributed at least part of the aluminum spectra.

Chrome and iron lines were continuously evident (with intermittent variations in intensity) between 343.6 seconds (218,200 feet) and 388.4 seconds (87,300 feet) on most of the spectral films. Many of the lines were directly associated with the zero-order trail of the RV-reactor. Both chrome and iron are constituents of stainless steel, and all the reactor components, except the aluminum fins, were constructed of stainless steel. The strongest indication of stainless steel occurred from 365 seconds (153,900 feet) to 388.4 seconds (87,300 feet). This was the period of very intense reactor flaring. Additional discussion of the reactor disassembly and spectral verifications can be found in SC-RR-64-515.

Sodium spectra associated with the zero-order RV-reactor streak is also continuously in evidence between 343.6 seconds (218,200 feet) and 385 seconds (96,300 feet). This element was found in the fiberglass ablative material from the RV. Although the specification for that material specifies only trace amounts of sodium (which probably would not have been very prominent spectrally), laboratory spectral analysis of an actual RFD-1 specimen revealed greater than 1 percent sodium content. This amount can be readily seen under the re-entry condition of RFD-1. It was noted that all objects containing fiberglass (the RV, the fourth-stage motor, and the fuel-rod brackets) appeared very intense on all the plate, spectral, and framing-camera films.

Motion-picture data confirm the RV-reactor identification and the reactor disassembly. Figure 45 shows a typical reactor-object separation event. This photograph was enlarged from the film in NASA framing-camera AC-101. The time of this particular event was 366.9 seconds. Table XXVI tabulated all the RV-reactor re-entry events from that film. Approximately 12 objects can be seen separating from the reactor between 344.6 seconds (213,500 feet) and 371.9 seconds (133,600 feet). These events and times agree reasonably well with the thermocouple and spectral data.

Strontium-Loaded Fuel Rods

From 342.60 seconds (218,600 feet) to 361.90 seconds (165,200 feet), the theoretical trajectory for the strontium-loaded fuel rods compared closely with the trajectory as measured from the plate-camera film. However, at 348.64 seconds (202,000 feet), the measured trajectory separated into two streaks, with the lower one following a somewhat steeper trajectory to 355.98 seconds (181,500 feet), when it disappeared. Both of these trails are known to be the strontium-loaded rods because of the bright flares identified as strontium on the spectral films. The discrepancy in the latter portion of the trajectory is thought to be due to the final stages of ablation, breakup of the rods, and melting of the strontium tracer. As can be seen on the plate-camera films, the strontium-loaded rods pulsated and flared from 342.27 seconds (220,100 feet) to 361.83 seconds (165,400 feet). This long period of intermittent strontium flares was probably caused by molten strontium spilling out of the rods through the vent holes and/or ablated areas. There were five major flares during this time, three in the upper strontium streak and two in the lower. The lower strontium streak flared at 353.88 seconds (187,300 feet) and 355.98 seconds (181,500 feet). The lower trail definitely ended at this flare, with no further evidence of either strontium or the UZrH fuel rod. The upper trail flared at 350.72 seconds (196,200 feet), 352.00 seconds (192,200 feet), and 361.83 seconds (165,400 feet). A faint streak assumed to be caused by final consumption of the UZrH fuel element continued to approximately 363.32 seconds (161,400 feet) on the NASA plate-camera films. This point is considered as the time and altitude of burnup for purposes of calculating heat input versus volume consumed (see Figure 50).

Four of the major flares in the re-entry trails mentioned above were identified as strontium on the spectral films. They were evident on spectral films from Cameras S2, S5, TRSS 521, TRSS 461, AC-84, and AC-85. The first-order spectra of the strontium bands were definitely associated with the flares shown in the zero order. It was also obvious that these flares were the same flares shown on the plate-camera films. The last flare in this group, at 361.83 seconds, was evident in the zero order of the plate-camera film but could not be identified as strontium in any of the first-order spectra. This was thought to be caused by lack of intensity. Even the four flares that were identified were extremely faint on the films.

The motion-picture films discussed on pp. 98 to 105 also identified the strontium flares. As shown in Table XXIII, the strontium flares were first visible at 342.27 seconds (220,100 feet). They were intermittently visible, pulsating from not visible to very bright, down to 361.83 seconds (165,400 feet). These pulsations can definitely be matched to the flares shown in the plate-camera and spectral films. Also, as explained on p. 104 and 105, the flare colors on the films compare with the color for strontium extremely well.

<u>Barium-Loaded Fuel Rods</u>

Identification of the barium-loaded rods was not as positive as the identification of the strontium-loaded rods. However, enough corroborative evidence was extracted from the films to strongly imply their presence and ablation altitudes.

The theoretical and measured trajectories for the barium-loaded rods agreed almost exactly for the entire re-entry sequence. Their patterns of behavior were very similar. Also, no other theoretical trajectory for the remaining re-entry objects showed above the RV as did the barium rods (see Figure 31). Sandia plate-camera film T-2 and P-2 indicate some of the barium flares above the RV from 348.00 seconds (205,200 feet) to 352.77 seconds (191,900 feet). After that time, the barium is superimposed on the RV trail until 356.62 seconds (181,200 feet), then slightly below the RV to 359.37 seconds (173,600 feet). Bright flares are noted at 356.62 seconds (181,200 feet) and 359.37 seconds (173,600 feet). The change in trajectory of the barium-loaded rods from above to below the RV is explainable. The barium-loaded rods were ejected up when released at 282.09 seconds. However, their W/C_DA was 44.4 as compared with 259.4 for the RV. This caused the steeper trajectory for the rods to eventually fall below the RV trajectory. Also, in the latter portion of the re-entry, the barium-loaded rods were ablating and breaking up, as were the strontium-loaded rods. Another reason could have been separation of the three rods into slightly different trajectory altitudes. The NASA plate films from AC-36 and AC-38, taken much closer to the trajectory and at a different angle, show these same streaks and flares very clearly, and they are not superimposed on the RV streak (see Figures 49 and 50). After the last barium flare on the NASA plate-camera films at 359.37 seconds (173,600 feet), a faint trail continued down to approximately 371.50 seconds (142,000 feet). This was assumed to be the altitude of final burnup of the barium-loaded rods.

Only one spectral film (NASA AC-85) indicated the presence of barium. This was probably because the barium flares were not so intense as the strontium flares and because they occurred closer to the NASA aircraft Camera AC-85 than to the other stations. However, the zero-order events producing the spectral lines were the same events identified as barium from the plate and framing cameras. Since the NASA AC-85 film was not time-chopped, all times were assigned to the barium flares from the NASA and Sandia framing cameras and the Sandia chopped-trajectory camera.

The framing-camera films showed the pulsating barium flares from 350.25 seconds (198,900 feet) to 357.52 seconds (178,000 feet). Evidently the barium tracer, like the strontium tracer, was prematurely exposed. The times and durations of the flares (see Tables XXIII-XXV) agree with the plate and spectral films. The strongest indication from the motion-picture film that these were the barium-loaded rods was their pulsating pattern, and the color of the flares which matched those of movies made of laboratory tests under simulated re-entry conditions.

Gold- and Silver-Loaded Fuel Rods

The theoretical trajectories for the gold- and silver-loaded fuel rods correlated with two re-entry trails on the plate cameras (see Figures 31 and 32). Both groups of rods were superimposed on the RV trail until 355.5 seconds (184,000 feet), when their trajectories fell below the RV. They were dim compared with the barium and strontium fuel-rod trails. The extreme brightness of the strontium- and barium-loaded rods was due to the strontium and barium, not the UZrH. Since the gold and silver tracers were not exposed, only the radiation from the UZrH was visible. These trails can be traced down to 368.00 seconds (149,000 feet) where they apparently were no longer luminous. There was no evidence of either gold or silver on the spectral films. The framing-camera films also furnished no indication of the gold- or silver-loaded fuel rods.

Fuel-Rod Brackets

Identification of the remaining re-entry objects was completed only so that they could be eliminated from consideration and not be mistaken for re-entering fuel rods. However, since the fuel-rod brackets were so strongly in evidence on the plate, spectral, and framing-camera films, an explanation of their reduction is in order.

The complete fuel-rod mount consisted of two brackets (see Figure 10B). One of the brackets included an MC1192 battery for initiation of the explosive bolts. Both brackets were made of aluminum and magnesium, and included a fiberglass heat shield on the front surface. Theoretical trajectories indicated that the lower re-entry trail on the plate-camera films was Bracket No. 1. The trail of Bracket No. 2 was somewhat higher as a consequence of ejection perturbations. However, these ejection conditions could not be measured accurately and, therefore, the theoretical trajectories are not necessarily positive proof of exact actual altitudes. Their main function was to duplicate re-entry patterns. Spectral films S-2, S-5, TRSS 521, TRSS 461 and AC-84 all revealed the presence of aluminum, magnesium, potassium, lead, and sodium. These spectral lines radiated from the zero order of the bottom re-entry trail. All these elements are ingredients of some part of the bracket, battery, or fiberglass shield. The zero order on the spectral film shows two objects in this bottom trail. The plate-camera and framing-camera films confirm this observation. Consequently, it was concluded that the bottom re-entry streak was from the two fuel-rod brackets. These objects are also very bright on the motion-picture films, but cannot be individually identified.

Fourth-Stage Motor

The fourth-stage motor was retro-rocketed away from the flight path after ejection from the re-entry vehicle at 282.09 seconds. This perturbation was included as a reduction in the velocity of the initial conditions of the theoretical trajectory. Several unsuccessful attempts were made to compute a theoretical trajectory which would match the measured fourth-stage trajectory from the plate films. It was concluded that unknowns such as pitch angle and residual thrust at ejection made comparison impossible.

Spectral reduction of the combination LA-24 TRSS and photometer indicated that this instrument tracked the fourth-stage motor. This observation was based on the presence of sodium, lithium, and aluminum-oxide spectra. Cameras S-2, S-4, AC-37, and AC-84 confirmed their presence and also showed the same band structure and intensity pattern. In addition, on those data having timing, the timing agreed. This was discussed previously on pp. 89 to 91.

The fourth-stage motor was not tracked by any of the motion-picture cameras because it was out of the fields of view of all cameras except the LA-24 framing camera, which did not function.

Fuel-Rod Ablation Analysis

The trajectory actually followed by the fuel rods was somewhat different from the preflight nominal prediction. The theoretical aerodynamic heating associated with the actual flight of the strontium-, barium-, silver-, and gold-loaded rods is given in Figures 51 to 54. An analysis of the response of the fuel rods to this heating will be made in this section, together with predictions of the resulting burnup altitudes.

The temperatures of the materials within the insulation were measured in neither the qualification nor the flight tests. Since some heat will be conducted through the insulation to the flares, an iterative process must be used together with theoretically predicted temperatures to estimate and evaluate this effect. The reduction of data from the qualification tests is presented in detail in Sandia Corporation report SCDR 124-63. The calculated aerodynamic heat absorbed by the UZrH is given below for convenience. No calculation was made of possible oxidation heating effects, since the initial model conditions and the surface temperature response were not known.

Qualification Test Results

Tracer	Q_T (BTU/lb)
Strontium	749
Silver	761
Solid UZrH	639

This analysis of the specimens also neglected any heat conducted through the insulation. This heat was neglected because the insulation presented a rather severe resistance to heat flow as compared to that absorbed by the UZrH. For purposes of thoroughness, it seems advisable to neglect this heat in an initial analysis of the rods during the re-entry, and to include it in a later analysis so as to provide a limiting comparison of the internal effects.

The models used in the qualification tests were similar in cross section to the re-entry rods, except that the cladding was not included on the tunnel-test models. For purposes of predicting for the re-entry, the required heat is that determined from the qualification tests to ablate the UZrH, plus that necessary to heat and melt the cladding on the outside of the rods. This may be written as

$$Q_r = (WC\Delta T)_c + (WH)_c + MQ_T \ , \qquad (1)$$

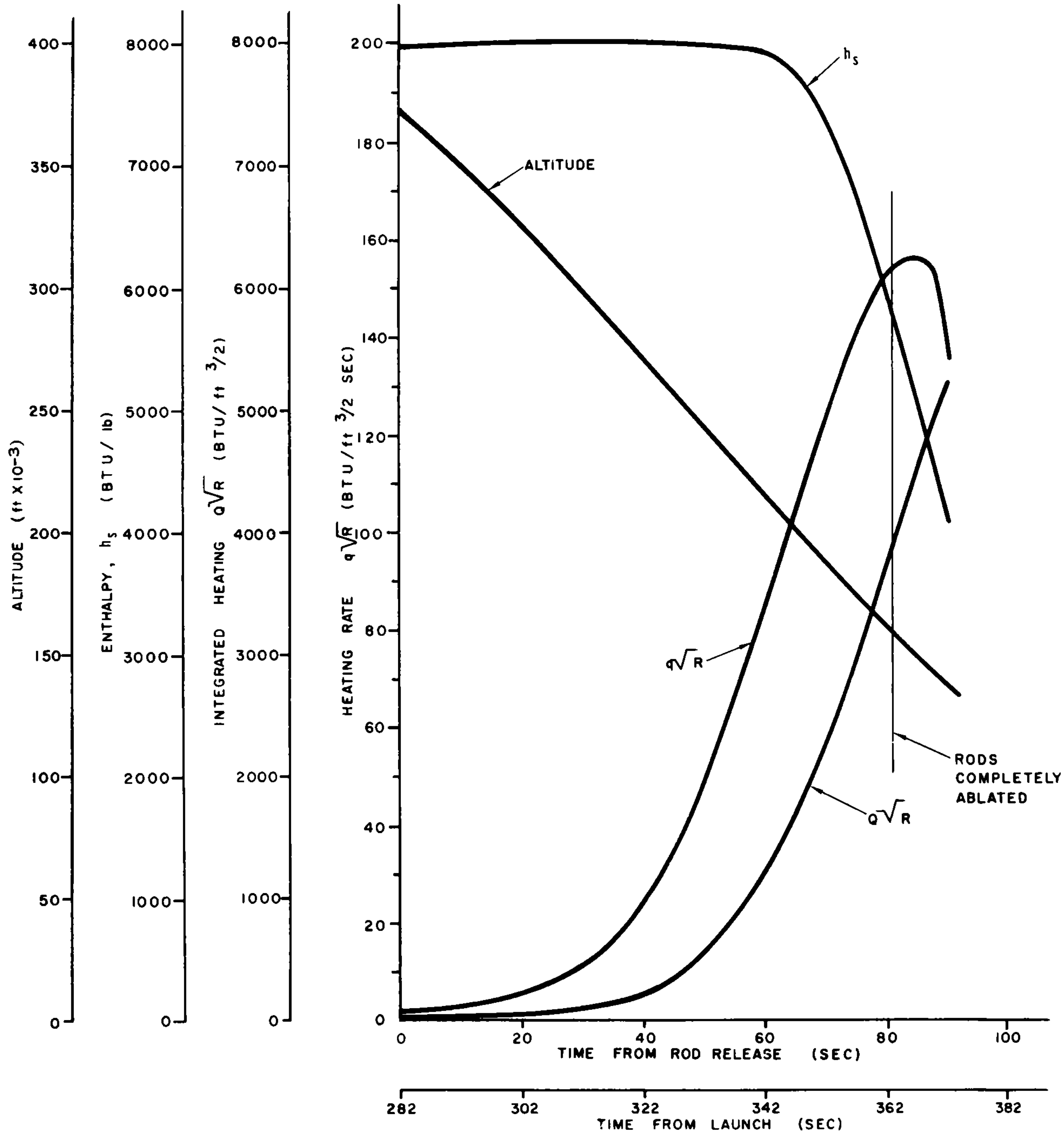

Figure 51. Actual trajectory and heating for strontium-loaded rods

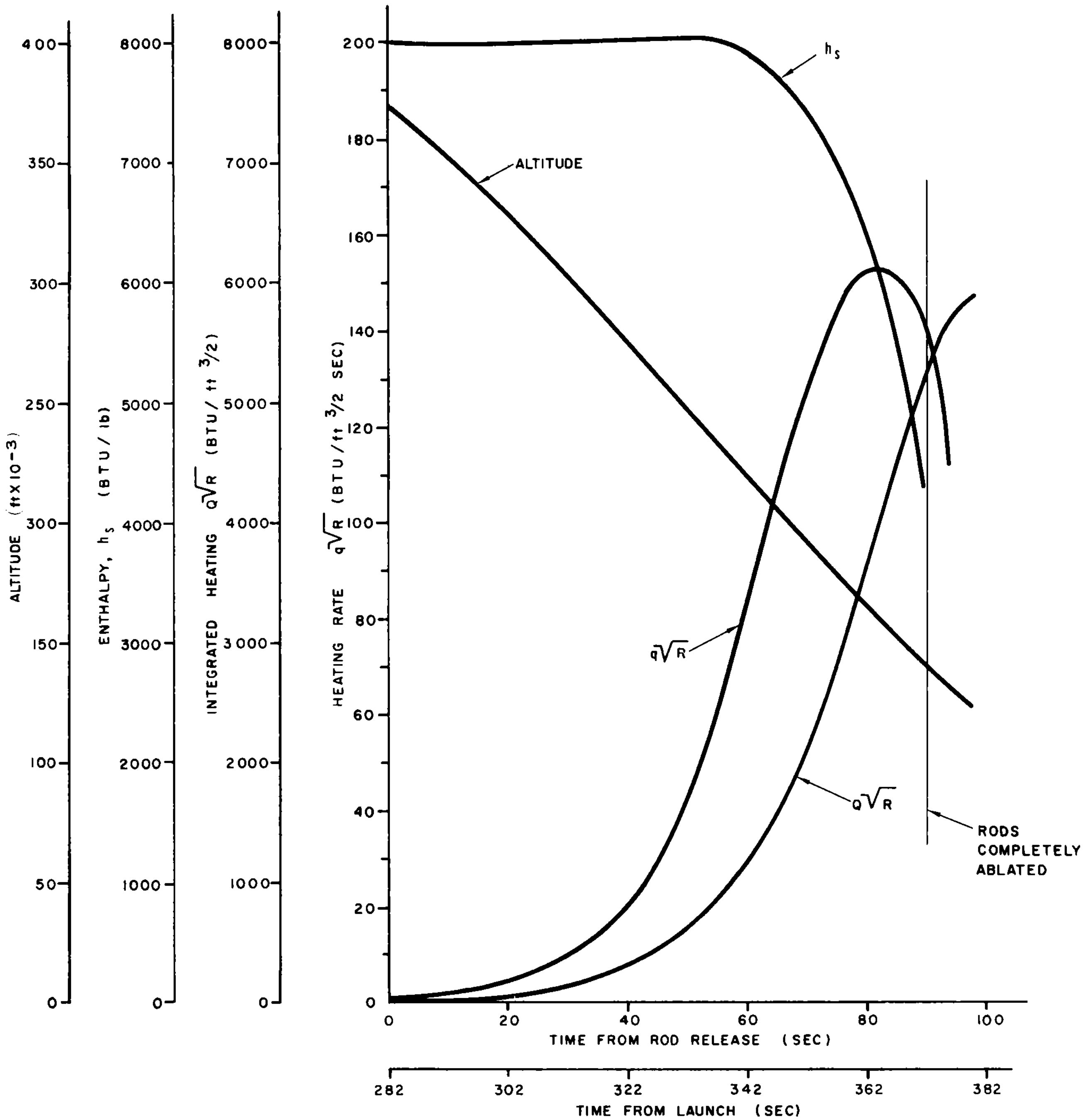

Figure 52. Actual trajectory and heating for barium-loaded rods

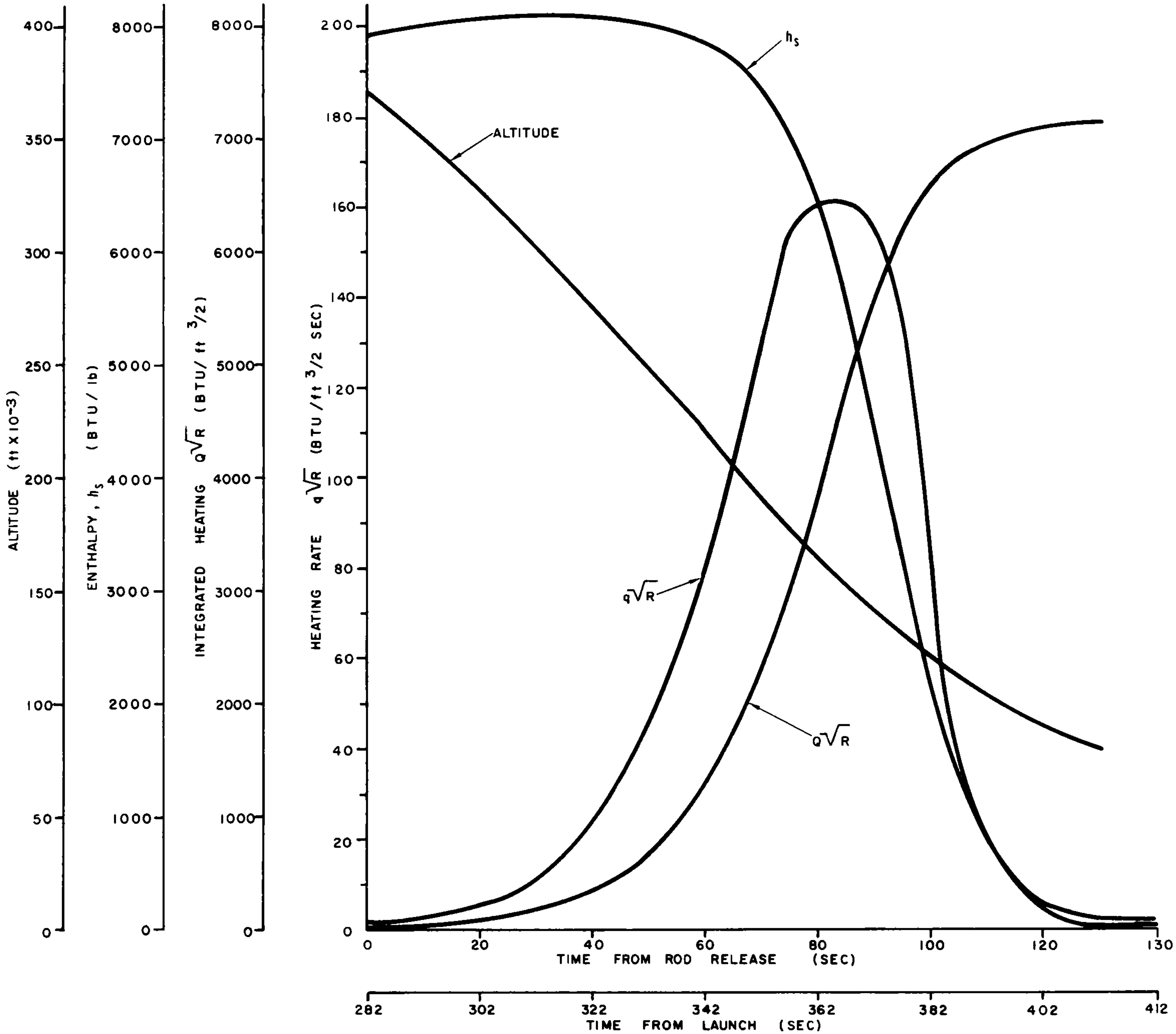

Figure 53. Actual trajectory and heating for silver-loaded rods

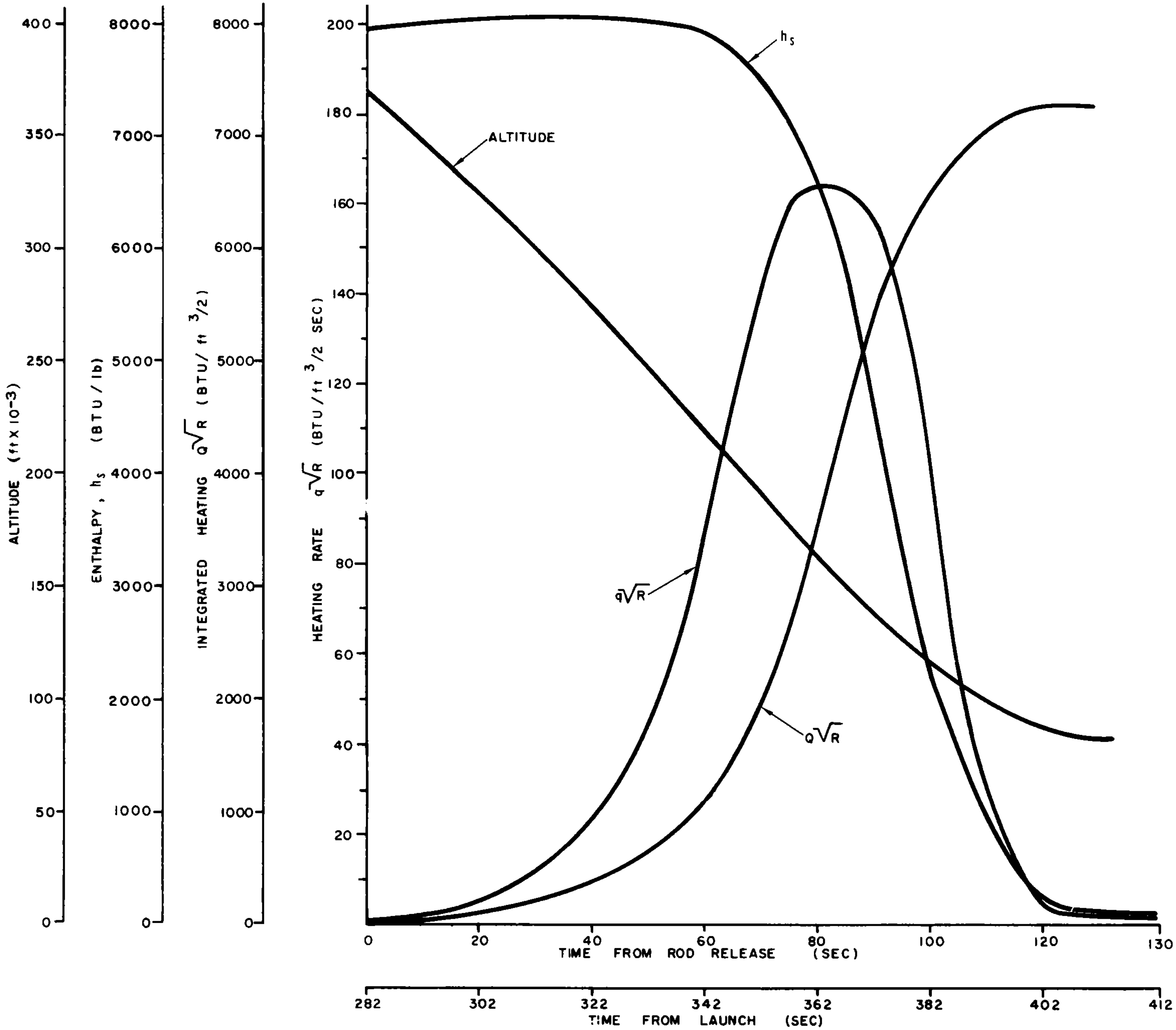

Figure 54. Actual trajectory and heating for gold-loaded rods

where

Q_r = calculated aerodynamic heat required, BTU

$(WC\Delta T)_c$ = heat required to raise temperature of cladding, BTU

$(WH)_c$ = heat required to melt cladding, BTU

MQ_T = heat required for UZrH from tests, BTU

For the strontium-loaded rod, the heat required for complete ablation is

$$Q_r = (0.336)(0.095)(2350) + (0.336)(130) + (0.995)Q_T = 118.69 + 0.955\ Q_T\ .$$

Using the values obtained in the tunnel tests,

$$Q_r = 118.69 + (0.955)(761) = 845.44 \text{ BTU} \qquad (1a)$$

$$Q'_r = 118.69 + (0.955)(749) = 854 \text{ BTU} \qquad (1b)$$

$$Q''_r = 118.69 + (0.955)(639) = 729 \text{ BTU} \qquad (1c)$$

(In all cases, three values of heat and an altitude range will be calculated, since it is not obvious which one of the results from the tunnel tests is more nearly correct.)

The cold-wall stagnation-point heat flux taken from the theoretical trajectory is adjusted for radiation from the surface and for the effect of increasing surface temperature on the enthalpy gradient across the boundary layer. The net heat available is

$$\dot{q}_{net} = FA\ \dot{q}_{cw}\left(1 - \frac{h_w}{h_s}\right) - Aq_{rad}\ , \qquad (2)$$

where

q_{net} = available heat into the fuel rod for purposes of material ablation, BTU/sec

$\dot{q}_{cw}$ = cold-wall stagnation heat flux, BTU/ft²-sec

h_w = C_pT_W = gas enthalpy evaluated at the wall temperature, BTU/lb

h_s = free-stream stagnation enthalpy, BTU/lb

$\dot{q}_{rad}$ = $\epsilon\sigma Tw^4$ = radiation loss, BTU/ft²-sec

A = fuel-rod surface area = 0.327 ft²

F = 0.179 = $0.167 + \frac{0.242}{2(L/D)}$ = factor to reflect stagnation heating on a hemisphere to average value on tumbling cylinder

Then for the re-entry

$$Q_a = \int_{\theta_1}^{\theta_2} \dot{q}_{net} \, d\theta \qquad (3)$$

where

Q_a = total heat available at time θ, BTU

θ = time, seconds.

It is necessary in this analysis to know the fuel-rod surface temperature as a function of time during the re-entry. For this purpose a theoretical study was performed on both a "thermalog" analog computer and a CDC 1604 digital computer. The results of this study, which will be discussed in detail in a later part of this section, are presented in Figures 55 to 58. These surface-temperature responses are used to calculate radiation loss from the rods for the type of analysis being discussed in this section.

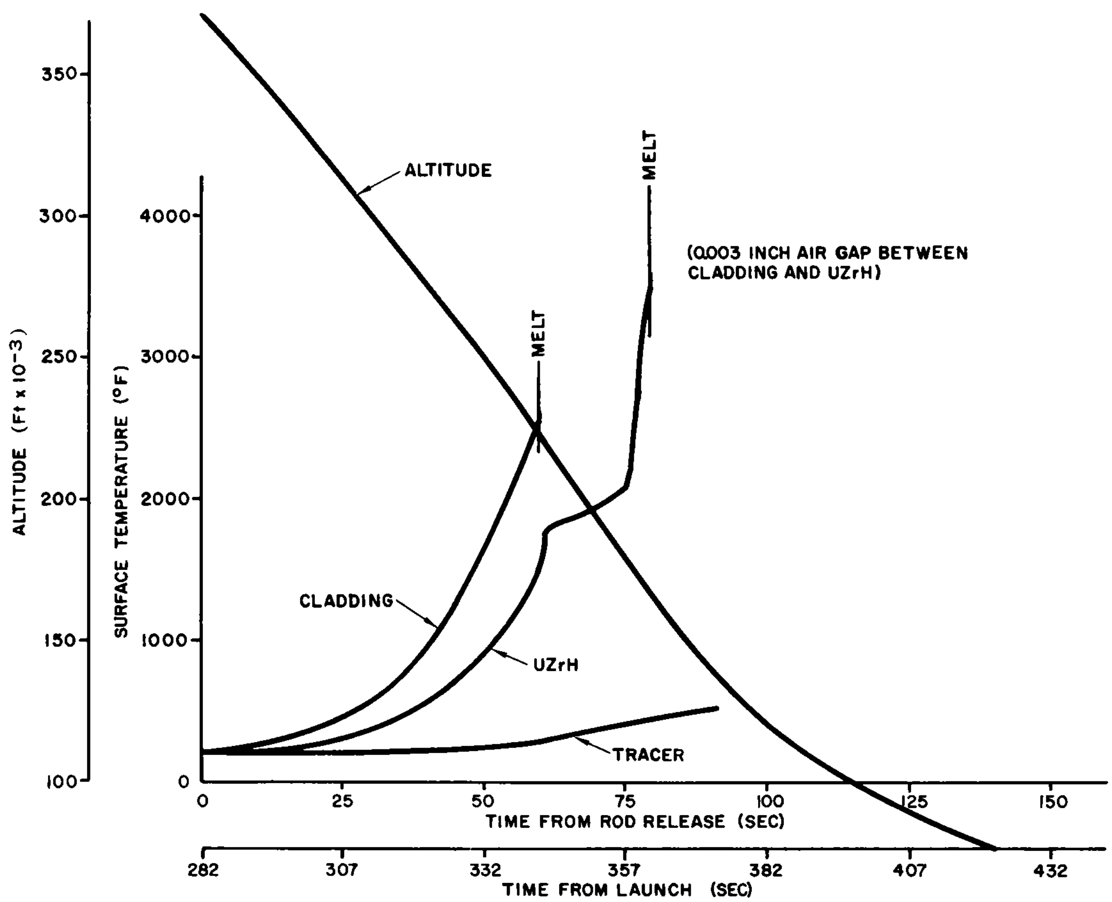

Figure 55. Predicted temperatures for strontium-loaded rods

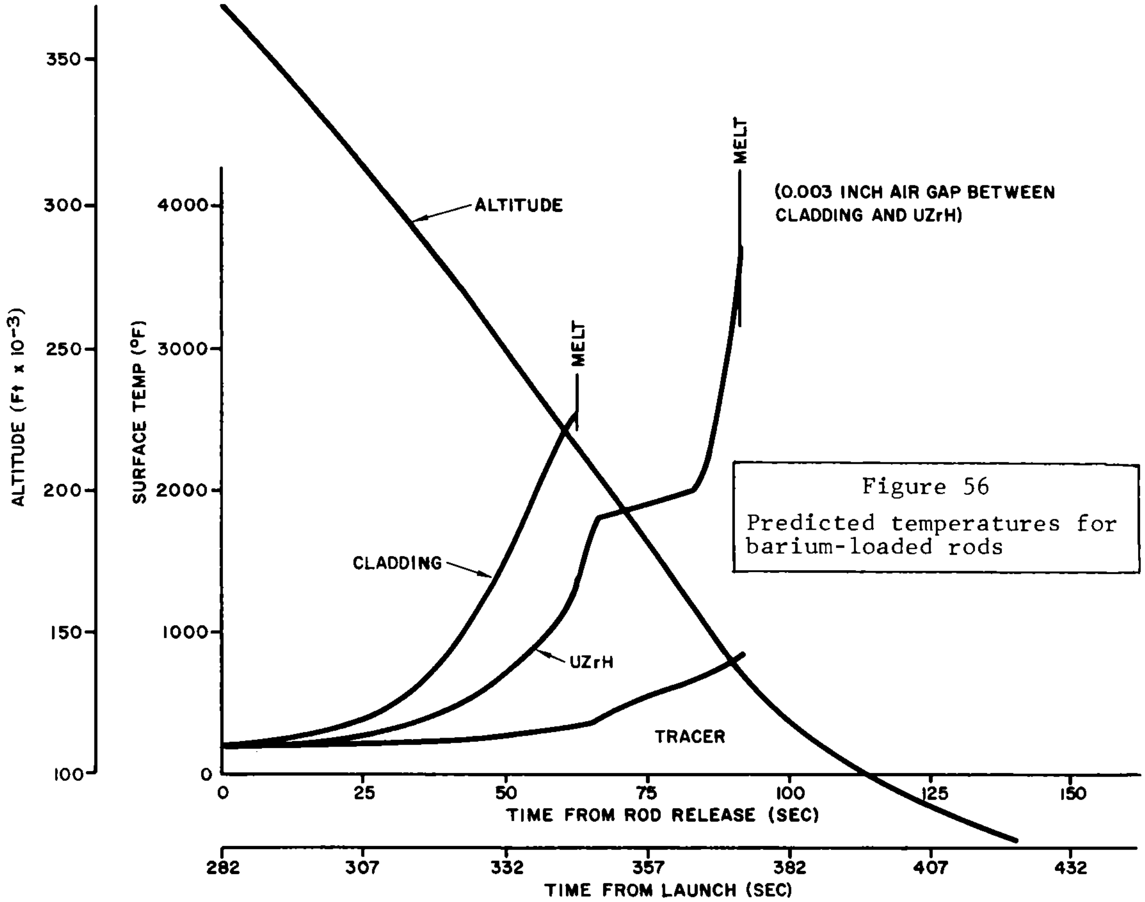

Figure 56
Predicted temperatures for barium-loaded rods

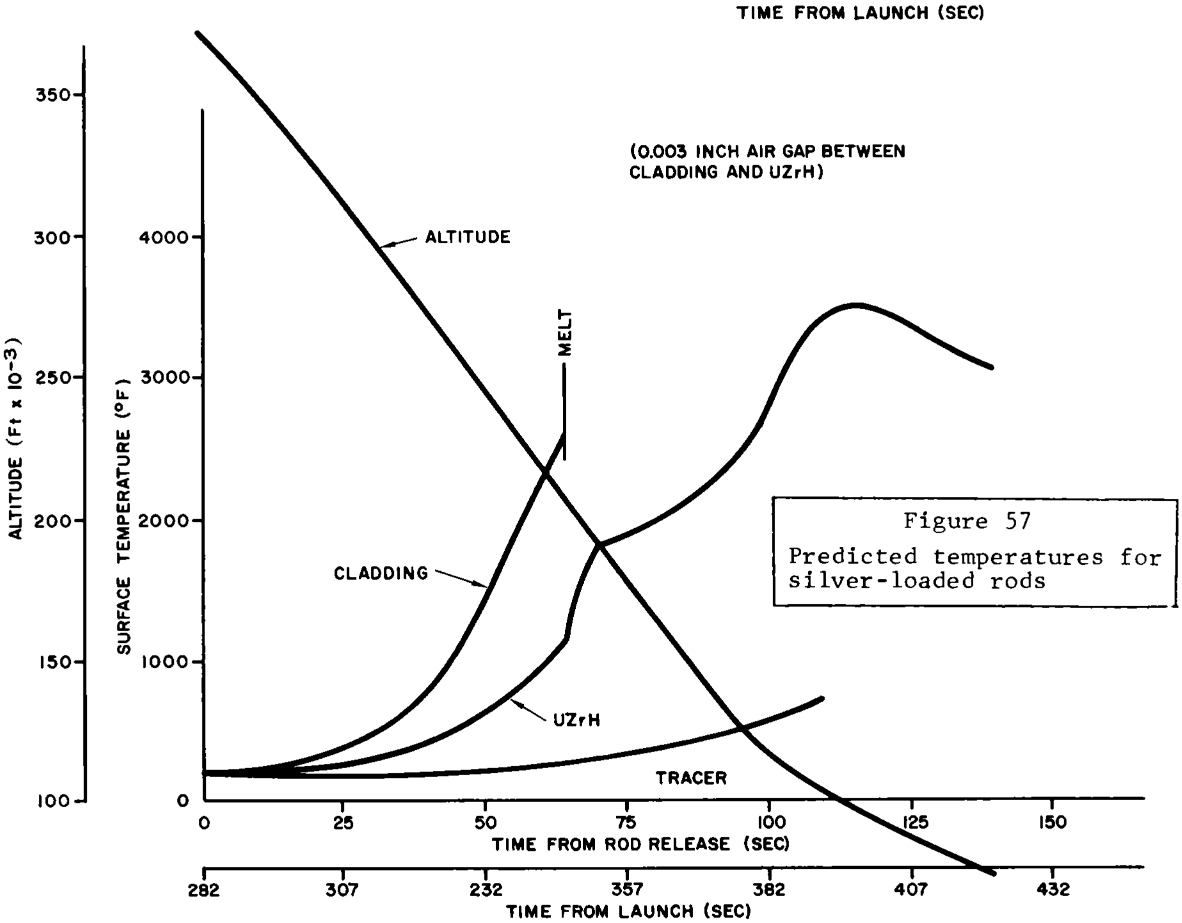

Figure 57
Predicted temperatures for silver-loaded rods

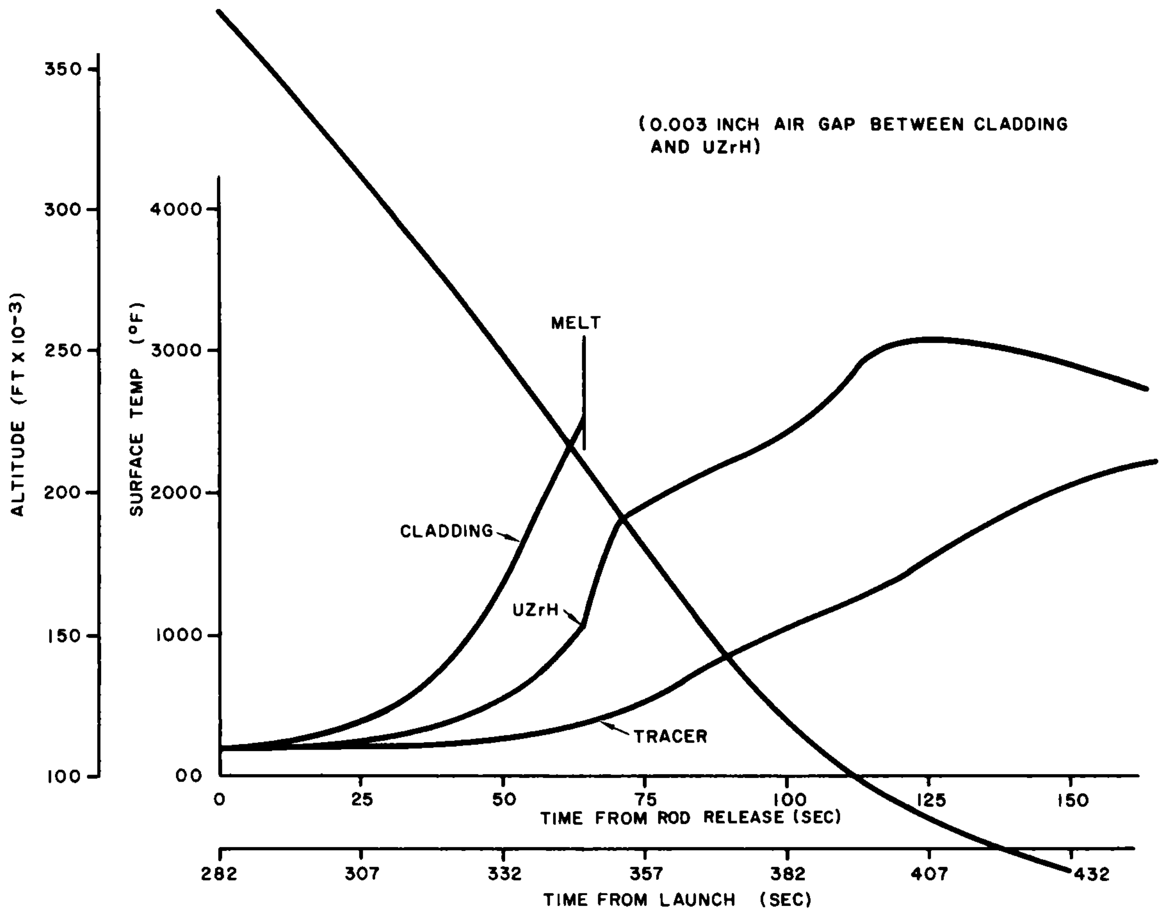

Figure 58. Predicted temperatures for gold-loaded rods

The net total aerodynamic heat available to the rods during the re-entry for purposes of ablating the UZrH, as computed from Eq. (3), is shown in Figures 59 to 62. With values for the heat required as computed from Eq. (1), one can predict the range of altitude burnup of the strontium-loaded rod as given below. Following the same analysis for the rod containing the barium tracer, the predicted range of burnup altitude is also given below. The same type of analysis performed on the silver- and gold-loaded rods indicates that insufficient heat is available to ablate the UZrH and expose the tracer. Further analysis of the silver- and gold-loaded rods will not be pursued in this report.

Tracer	Predicted Burnup Altitude (ft)
Strontium	152,000 to 167,000
Barium	120,000 to 136,000

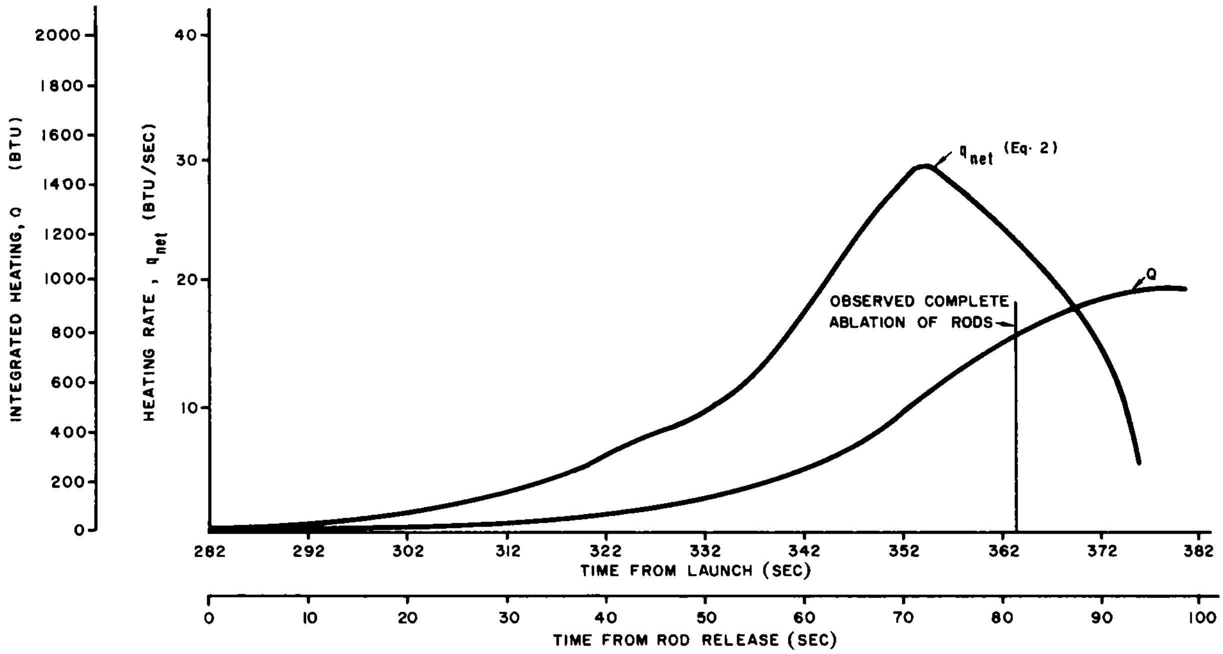

Figure 59. Net aerodynamic heating for strontium-loaded rods

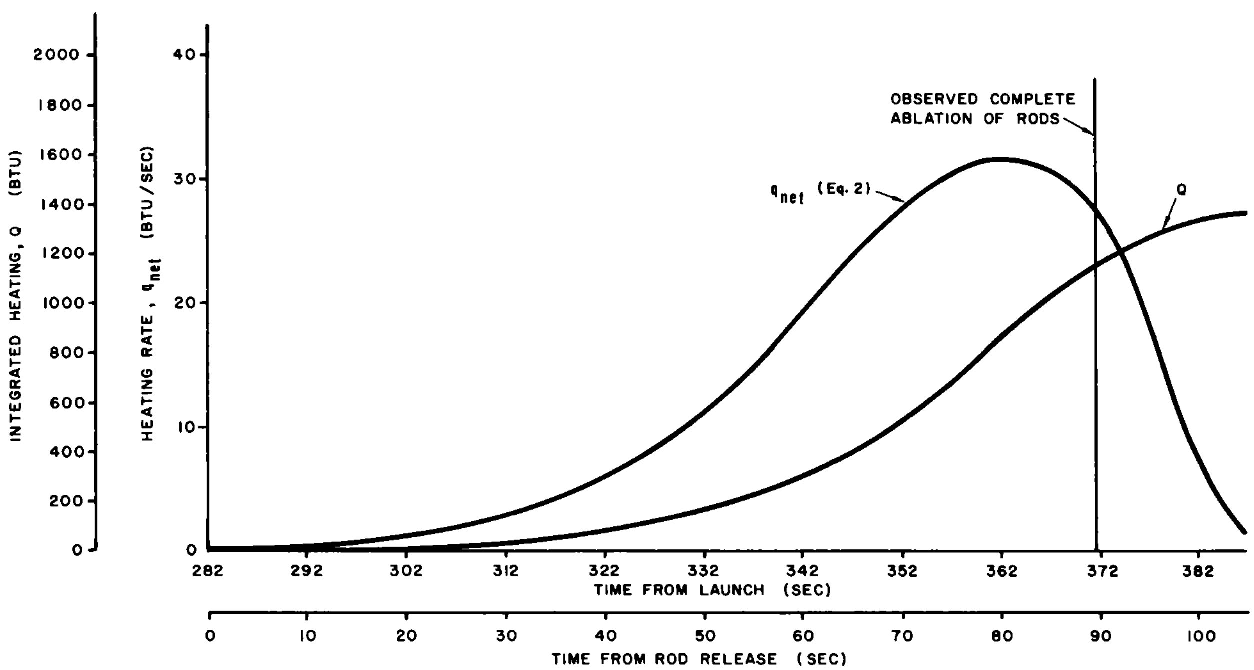

Figure 60. Net aerodynamic heating for barium-loaded rods

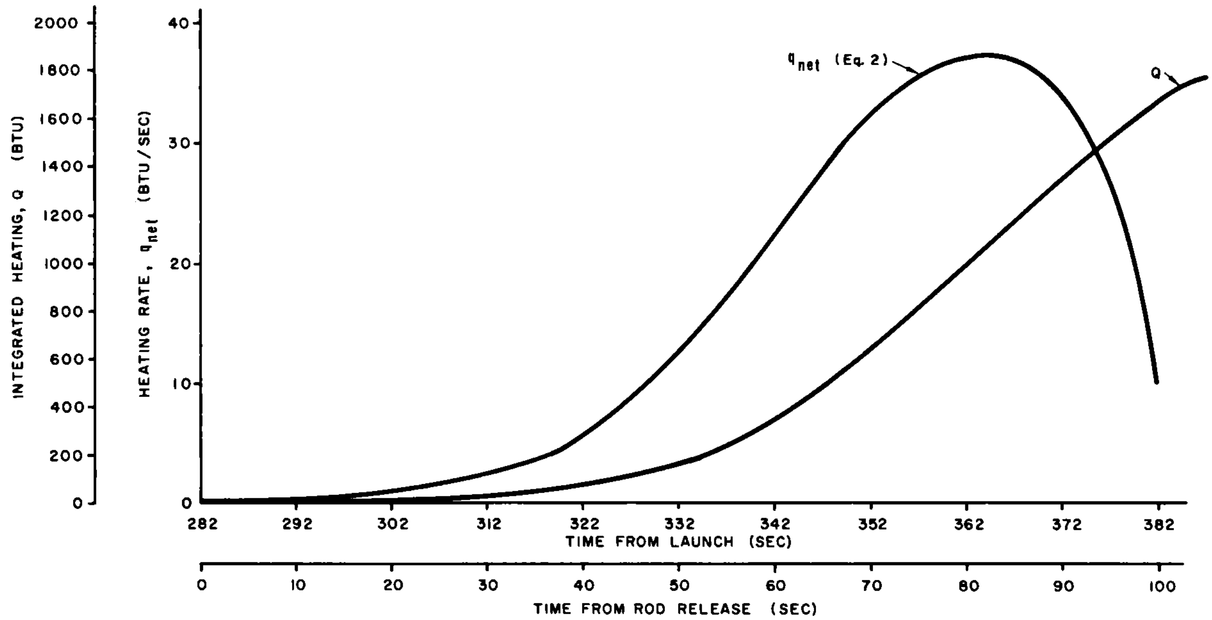

Figure 61. Net aerodynamic heating for silver-loaded rods

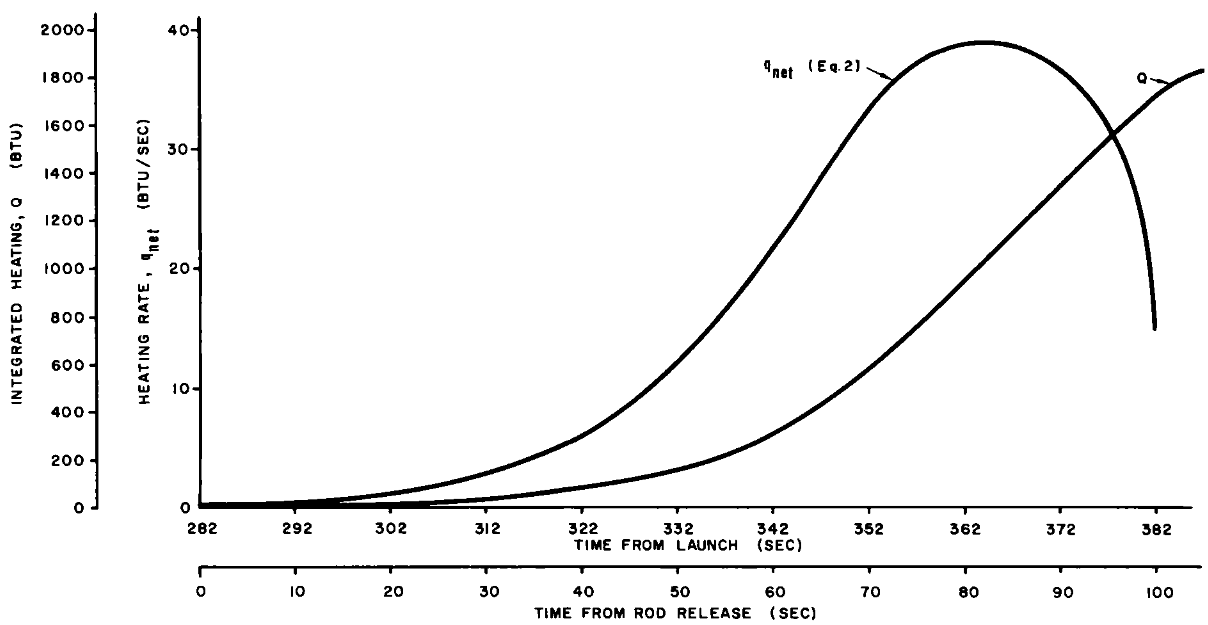

Figure 62. Net aerodynamic heating for gold-loaded rods

The preceding calculation neglects any heat conducted into the tracer, and, as such, it presents an upper limit on the altitudes of tracer exposure predicted by means of this analysis. Computer analyses indicate that quantities of heat which may not be negligible are conducted through the insulation during the re-entry period. Estimates of this quantity of heat are made utilizing computer-predicted temperatures for the qualification tests, as shown in Figures 63 and 64.

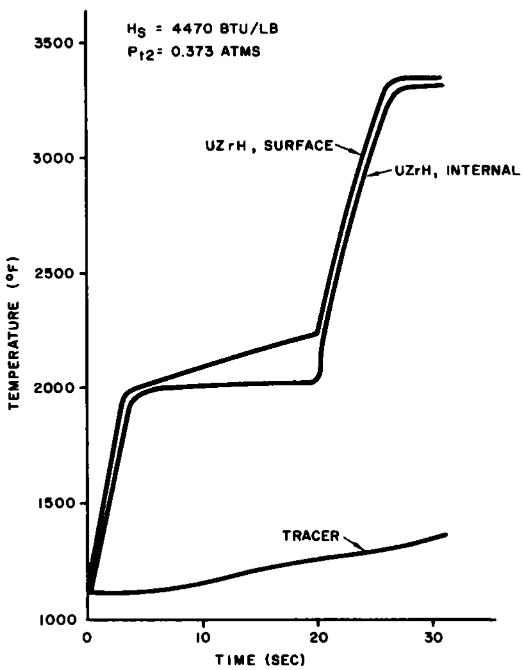

Figure 63

Predicted temperature response of strontium-loaded rod in qualification tests

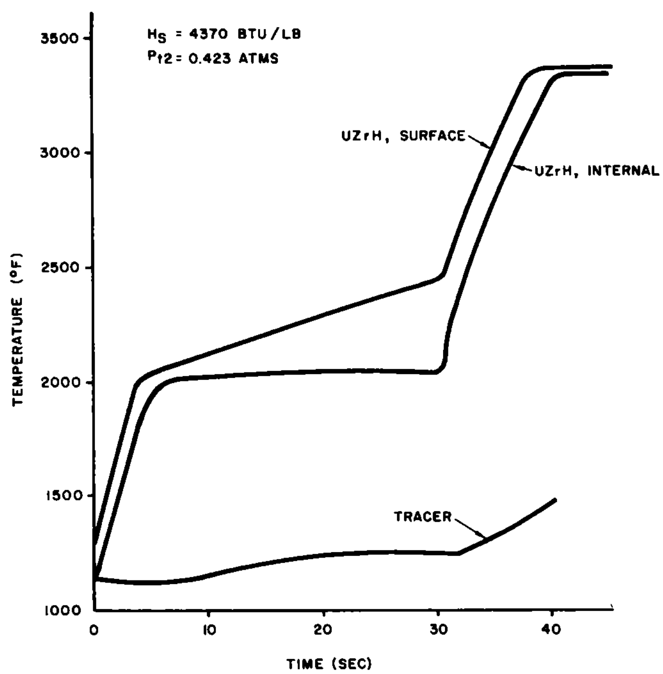

Figure 64

Predicted temperature response of barium-loaded rod in qualification tests

It is convenient to compute heat conducted through the insulation on a unit-length basis. The computation should include the heat required to raise the temperature of the flare, the lead ballast, and the insulation to their predicted values. For the tunnel tests, the aerodynamic heat remaining in the UZrH to cause its ablation may be expressed as

$$Q_{UZrH} = Q_T - (WC\Delta T)_T - (WC\Delta T)_B - (WC\Delta T)_I \ . \qquad (4)$$

where

$(WC\Delta T)_T$ = heat absorbed by tracer, BTU/inch

$(WC\Delta T)_B$ = heat absorbed by ballast, BTU/inch

$(WC\Delta T)_I$ = heat absorbed by insulation, BTU/inch.

For the strontium-loaded rod in the qualification test, this equation results in

$$Q_{UZrH} = 59.62 - 1.532 - 3.98 = 54.11 \text{ BTU/inch} \qquad (4a)$$

or

$$Q_{UZrH} = \frac{54.11}{0.0796} = 680 \text{ BTU/lb} \ .$$

Likewise, for the silver-loaded rod this calculates as

$$Q_{UZrH} = 146.87 - (3.36 + 1.33) = 142.18 \text{ BTU/inch} \qquad (4b)$$

or

$$Q_{UZrH} = \frac{142.18}{0.193} - 736.7 \text{ BTU/lb} \ .$$

Of course the solid rod had no internal flare, so the required heat for ablation remains

$$Q_{UZrH} = 639 \text{ BTU/lb} \ .$$

Using the estimates of altitudes and time of flare exposure made previously, and the computer surface-temperature predictions shown in Figures 55 and 56, it is possible to calculate the heat absorbed by the tracer, ballast, and insulation during the flight test. The total heat necessary for ablation of the rod under these conditions is

$$Q_F = Q_{UZrH} + (WC\Delta T)_T + (WC\Delta T + WH)_B + (WC\Delta T)_I + (WC\Delta T + WH)_C \ . \qquad (5)$$

For the strontium-loaded rod, using the calculated net values of heat required in the qualification tests for the UZrH, this results in

$$Q_F = 894 \text{ BTU} \qquad (5a)$$

$$Q'_F = 944 \text{ BTU}$$

$$Q''_F = 988 \text{ BTU} \ .$$

From Figure 59 (the net input into the strontium-loaded rod during re-entry), the predicted altitudes of burnup may be made as shown below. Likewise, calculations for the barium-loaded rod result in the predicted altitudes of flare exposure as shown below. Similar calculations on the remaining two types of rods indicated that those flares would not be exposed.

Tracer	Predicted Exposure Altitude (ft)
Strontium	144,000 to 129,000
Barium	110,000

As discussed in other portions of this report, optical instrumentation employed to record the events of the fuel-rod re-entry resulted in the following observed altitudes of complete burnup of the various tracers.

Tracer	Observed Burnup Altitude (ft)
Strontium	161,400
Barium	142,000

Since these altitudes are somewhat higher than the predicted values for the trajectory, some investigative analysis is warranted. Figures 51 and 52 show the cold-wall heat flux and total heat of this trajectory, together with the times of tracer burnup. A reasonable estimate of the net total aerodynamic heat input to the rod may be made with Eq. (3), and these values are shown in Figures 59 and 60. From these curves, values of aerodynamic heat associated with the rods at the time of burnup may be determined as:

Tracer	Aerodynamic Heat Absorbed (BTU)
Strontium	770
Barium	980

It is apparent that these values are somewhat smaller than the corresponding values predicted with data from the qualification tests. Again, analyses may be made by (1) calculating the heat absorbed by the UZrH and the cladding, while neglecting any heat conducted through the insulation, and (2) estimating the heat absorbed by the internal components and considering it as absorbing a portion of the input. The first of these operations may be performed as follows:

$$Q_a = Q_{UZrH} + (WC\Delta T)_C + (WH)_C \ . \qquad (6)$$

Applying this expression to the strontium-loaded rod, the amount of aerodynamic heating absorbed by the UZrH at the time of tracer exposure as recorded during re-entry is

$$Q_{UZrH} = \frac{Q_a - (WC\Delta T + WH)_C}{0.955} = 673 \text{ BTU/lb} \ . \qquad (6a)$$

Likewise, the calculation for the barium-loaded rod is

$$Q_{UZrH} = \frac{Q_a - (WC\Delta T + WH)_C}{1.543} = 554 \text{ BTU/lb} \ . \qquad (6b)$$

The second of the analyses may be performed with Eq. (5). Using theoretical predictions of the internal temperatures at the time of exposure yields

$$Q_{UZrH} = \frac{580}{0.955} = 608 \text{ BTU/lb} . \tag{5b}$$

A similar calculation for the barium-loaded rod results in

$$Q_{UZrH} = \frac{831}{1.543} = 538 \text{ BTU/lb} . \tag{5c}$$

The table below gives the calculated and observed values for the aerodynamic heat absorbed by the rods to cause flare exposure that results from the different assumptions in the analyses. The calculated values are based on the results of the hyperthermal tunnel tests, while the observed values are based on the actual RFD-I data reduction. It is apparent from this table that the calculated and observed values of heat required are not very different, especially for the strontium-loaded rod.

	Aerodynamic Heat Absorbed (BTU)		
	Calculated		
Tracer	Neglect Tracer	Consider Tracer	Observed
Strontium	729 to 854	894 to 988	770
Barium	1107 to 1293	1350	1150

In an attempt to better correlate all the results, an investigation of oxidation contributions was undertaken.

An examination of possible contributions to heating made by oxidation may be conducted on the RFD-1 fuel rods in the following manner. The total heating rate on the rod after the UZrH surface is exposed to the high-enthalpy flow may be expressed as

$$\dot{q}_t = \dot{q}_c + \dot{q}_{ox} \tag{7}$$

where

$\dot{q}_t$ = total surface heat rate, BTU/ft^2-sec

$\dot{q}_c$ = convective heat rate, BTU/ft^2-sec

$\dot{q}_{ox}$ = effective oxidation heat rate, BTU/ft^2-sec.

The convection heat rate is available from the trajectory, and the oxidation heating rate may be evaluated as

$$\dot{q}_{ox} = W_o H_{ox} \tag{8}$$

where

W_o = effective rate of surface oxygen flux, lb/ft^2-sec

H_{ox} = heat of oxidation, BTU/lb-oxygen.

The rate of oxygen flux to the surface is

$$W_o = 0.215\ W_A \tag{9}$$

where

W_A = effective rate which air diffuses to the body surface, lb/ft^2-sec.

The mass-flow rate of the air immediately ahead of the re-entering body and its associated shock is based on a unit area, $\dot{M} = \rho V$. Also, the local cold-wall heat-transfer rate to a body may be defined as

$$\dot{q}_{cw} = C_H\ \rho V\ h_s \tag{10}$$

where

C_H = Stanton number

ρ = gas density, lb/ft^2

V = gas velocity, ft/sec

h_s = gas enthalpy, BTU/lb.

The rate at which the air molecules actually strike the surface of the material and release their energy to the body depends on the particle transfer within the boundary layer, and is defined as

$$W_A = C_H\ \dot{M} = C_H\ \rho V\ . \tag{11}$$

Equations (9), (10), and (11) may be combined to yield

$$W_o = 0.215\ \frac{\dot{q}_{cw}}{h_s}\ . \tag{12}$$

The process assumed to account for the significant portion of any heat of oxidation released is

$$Zr + O_2 \longrightarrow ZrO_2 + \text{energy}\ . \tag{13}$$

For each mole of Zr and O_2, one mole of ZrO_2 is formed, so that the heat of oxidation is

$$H_{ox} = 2815\ \frac{(\text{Mol. wt})_{Zr}}{(\text{Mol. wt})_O} \tag{14}$$

or

$$H_{ox} = 8.0245 \frac{CAL}{MG - O_2} = 14,350 \text{ BTU/lb-}O_2 \ .$$

Combining Eqs. (12), (13), and (14) produces an expression for the total surface heating due to convection and oxidation as follows:

$$\dot{q}_T = \dot{q}_C + 0.215 \frac{\dot{q}_C}{\bar{h}_s} (14,350) \ ,$$

or

$$\dot{q}_T = \dot{q}_C \left(1 + \frac{3085}{\bar{h}_s}\right) \text{BTU/ft}^2\text{-sec} \ . \qquad (15)$$

This equation may be evaluated from the information available on the theoretical trajectories. It is shown in Figures 65 and 66 for the strontium-loaded and the barium-loaded rods.

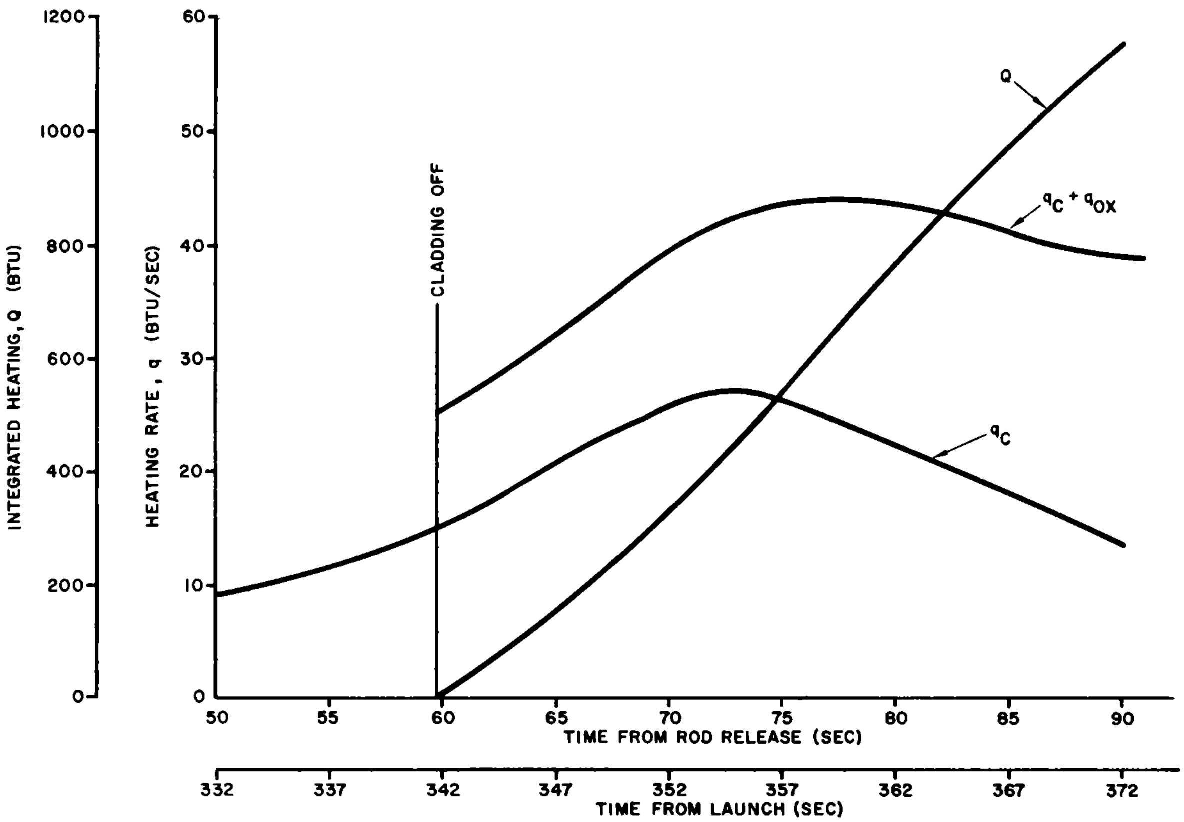

Figure 65. Net re-entry aerodynamic and oxidation heating to strontium-loaded rods

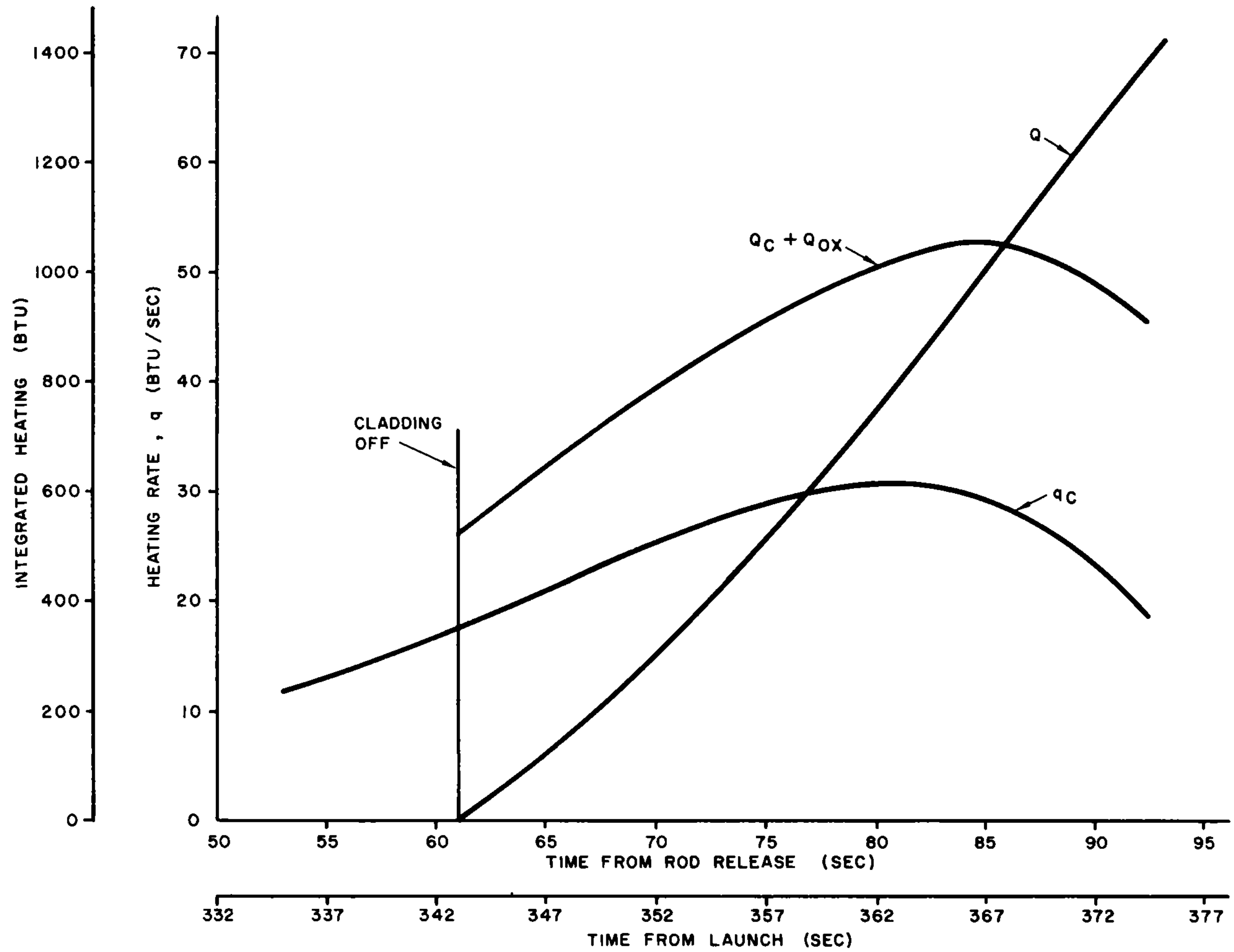

Figure 66. Net re-entry aerodynamic and oxidation heating to barium-loaded rods

The computer study mentioned earlier included the predicted effects of oxidation heating after the cladding material was removed. From the initial ejection of the rods from the RV until the cladding reached its melting temperature, the heating was assumed to be aerodynamic only, as given by Figures 59 and 60. The temperatures shown on Figures 55 and 56 resulted from the assumption that a 0.003-inch air gap existed between the cladding and the UZrH material. There is reason to believe that this assumption is reasonable and, in fact, that real effects such as local hot spots, internal pressure, and shear may cause the UZrH to be exposed to the flow even earlier than this calculation indicates. Once the cladding is removed, the total heat input was assumed to be convection- and oxidation-induced. It was calculated for the re-entry using Eq. (15). The computer program includes the nonhomogeneous cross section and also the surface radiation. No effects of hydrogen combustion or injection in the boundary layer are included in the calculated heat input.

These calculations indicate that the rods containing strontium and those containing barium should reach their melting temperature, while those containing the silver and those containing the gold would not reach sufficient temperature to cause ablation. The predicted burnup altitude from this analysis is

Tracer	Predicted Burnup Altitude (ft)
Strontium	167,000
Barium	138,000

The temperature data from these analyses are used in the oxidation analysis to determine the temperature of the UZrH at the time of the cladding removal.

The energy required to ablate the UZrH from this condition is as shown in Eq. (16), with the temperature T_o equal to the UZrH temperature at the time of cladding melt, as given on Figures 55 and 56:

$$Q = WC(T_m - T_o) + WD - WM \qquad (16)$$

where

Q = heat to complete ablation, BTU

W = UZrH weight, lb

C = UZrH specific heat BTU/lb-°F

D = heat to dissociate the hydrogen, BTU/lb

M = UZrH heat of fusion, BTU/lb

T_m = temperature of UZrH melt, °F.

For the strontium-loaded rod, this may be evaluated as

$$Q = (0.9548)(0.1)(3400\text{-}1600) + (0.9548)(650) + (0.9548)(56.5)$$

$$Q = 846 \text{ BTU} . \qquad (16a)$$

Likewise, for the barium-loaded rod, is obtained:

$$Q = (1.543)(0.1)(3400\text{-}1600) + (1.543)(650) + (1.543)(56.5)$$

$$Q = 278 + 1003 + 87$$

$$Q = 1368 \text{ BTU} . \qquad (16b)$$

Corrections (Eq. 2) were made as described previously for the surface-radiation loss and the effect of the hot wall on the boundary-layer enthalpy gradient on the convection heating, and this was added to the oxidation heating. The net total heat into the model is calculated as

$$Q_T = \int_{\theta_1}^{\theta_2} (\dot{q}_c + \dot{q}_{ox})\, d\theta . \qquad (17)$$

Figures 65 and 66 present this calculation for the strontium- and barium-loaded rods.

With the values of heat required to ablate the rod as shown in Eq. (16a) and (16b), the predicted altitudes of burnup and the corresponding aerodynamic heat absorbed are:

Tracer	Altitude (ft)	Aerodynamic Heat Absorbed (BTU)
Strontium	158,000	795
Barium	135,000	1215

Discussion

The analysis and correlation of the flight-test results, the qualification-test results, and the oxidation presentation were performed in two ways: (1) a total aerodynamic heat calculation to the time at which a significant event occurred, and (2) a computer analysis to describe the transient surface-temperature response. Each of these two methods has certain advantages, but the results of both are shown in the analysis for completeness. First, the total-heat method allows correlation between the varying pulse of re-entry heating and the constant hyperthermal input of tunnel heating, and second, the various thermo-chemical surface effects of the ionized gases are not sufficiently known to allow them to be included in a satisfactory computer program. Evaluation of these effects and incorporation of them into a computer program is presently an object of effort, but the work is incomplete. As a result, calculations of the transient temperature of a material such as UZrH, showing melting and/or ablation, are not completely satisfactory.

For the fuel-rod heating analysis, several assumptions were made which somewhat affect the results. As a summary of these results, the following table is presented:

Conditions	Resulting Predicted or Observed Altitude for Flare Exposure (ft)	
	Strontium	Barium
Based on RFD-1 fuel-rod qualification tests; neglects heat conducted into tracer	152,000 to 167,000	120,000 to 136,000
Based on RFD-1 fuel-rod qualification tests; estimates heat conducted into tracer	129,000 to 144,000	110,000
Computer program; includes oxidation after Hastelloy is removed	167,000	138,000
Oxidation analysis based on total heat available	158,000	135,000
Observed on RFD-1 re-entry	161,400	142,000

Comparing observed values with the predictions made under the different assumptions shows that, in general, good agreement exists. However, assumptions were necessary for each of these analyses (and in fact cause the different predicted values), and these should be examined for their validity.

The basic assumption necessary in using data from the hyperthermal tunnel tests in the re-entry analysis is that a material responds to a particular tunnel environment in the same manner that it would to the same environment during re-entry. This is obviously a major assumption, but computer analyses and the observed data from the re-entry indicate that, at least in this instance, the assumption is adequate. The total heat which had to be applied in the constant environment of the hyperthermal tunnel to result in complete model ablation is assumed to be the total necessary to cause a similar model to completely ablate in the varying re-entry environment.

Only estimates of the heat conducted through the insulation into the tracer materials could be made in the qualification tests, flight test, and the oxidation analysis. The estimates were based on computer analyses and, as has been explained, these analyses are not exact. It is obvious from the preceding table immediately above that the analysis with estimations made for the heat conducted into the tracers resulted in predicted altitudes which are the farthest from agreement with the observed conditions. These are included for completeness, but in view of the manner in which the heat conduction was assumed, they should probably be regarded as the least meaningful data in the analyses.

The corrections applied to the cold-wall heating taken from the trajectory were functions of the surface temperature, which were in turn determined from a computer. To neglect this correction completely results in an error of only a few percent (from 5 to 10 percent), but this, of course is enough to account for some of the difference between predicted and actual values. Assumed properties of the material are also factors that could affect predictions of burnup; but until material properties are known that are typical of the materials in re-entry, little would be gained by merely changing the material properties so as to have a particular program give data that correlate with a known result.

In summary, the method used to predict burnup conditions and to reduce data from the tests is thought to be satisfactory. From the table on the previous page it can be seen that the several analyses employed produced burnup altitudes not significantly different from the observed conditions. The inclusion of all the analyses in this report serves to illustrate the gross data correlation between the actual re-entry, empirical data from the hyperthermal tunnel, and analytical analyses employing a computer.

One manner in which a tracer might be exposed in a manner different from the one assumed in this analysis would be either a structural failure of the rods or a re-entry in which the rods stabilized in either end-on or stationary cross-flow attitudes. Either of these would cause tracer exposures at a higher altitude than the one at which they would be exposed as a result of tumbling re-entry. It is not thought likely that either of these occurred, however, since either would result in continued traces of the UZrH remaining after the tracer was exposed. The altitudes given for observed burnup are those at which a given identified trace was determined to have completely stopped, whereas traces of the remaining rods continued. As a matter of fact, the paths of the rods containing the silver and gold tracers were identified during the re-entry. These traces could be seen to grow more dim during the latter part of the re-entry, and this agrees with the predictions of insufficient heat to ablate the UZrH and expose the tracer.

In summary, it can be said that the data resulting from the re-entry tracer exposures can be correlated fairly satisfactorily with predictions both from the hyperthermal tunnel tests and from the computer analyses. The agreement is gross in nature, since many transient effects can be postulated which cannot at present be evaluated. Since factors which affect and contribute to sources of heat other than convective heating cannot be evaluated, no attempt is made in this report to extrapolate to an orbital-decay re-entry environment. It is not recommended at this time that net values of aerodynamic heat as observed in the RFD-1 re-entry be used as the effective aerodynamic heating necessary to cause ablation of UZrH in other environments. Partial agreements, as mentioned previously, indicate that the flight-test data may be accurate, but the factors which result in partial agreement and cause the variations between the flight-test values and those predicted both from hyperthermal tunnel tests and oxidation analysis render problematical the question of how an orbital-decay environment would actually affect the aerodynamic heating required. This suggests that further studies, both experimental and analytical, must be done before one can predict the fate of UZrH in a wide range of re-entry conditions with any degree of analytical certainty. Data on the topic are being accumulated from several sources. Additional studies are being made of oxidation, combustion, environmental effects, and other factors.

SECTION V -- CONCLUSIONS

Accurate monitoring of the ablation of UZrH fuel elements is difficult even under laboratory conditions. An attempt to measure the rate and volume of UZrH ablation at a distance of from 100 to 200 miles with spectral tracers and optical instrumentation therefore had a marginal chance of success. This was recognized from the initial concept of the RFD-1 fuel-rod experiment. Also, there was little information on such an experimental method to provide guidance. It was realized that, at best, only gross information on the ablation of the fuel rods would be obtained. However, even gross information was considered valuable enough to justify including the external fuel-rod experiment on RFD-1. Monitoring the reactor disassembly was a more straightforward operation. Optical coverage was utilized to supplement the TM data from the RV.

Most of the optical data obtained on the RFD-1 flight test were somewhat circumstantial. No attempt was made in this report to rationalize or mitigate any of the uncertainties involved in reduction of the films. However, coincidental agreement among the data from the various films and records indicated that the results are positive enough to justify interpretation and acceptance of them. If the data and results presented in this report are accepted as valid, the following conclusions can be drawn:

1. The strontium-loaded group of RFD-1 experimental fuel rods was completely ablated away at 363.32 seconds (161,400 feet). The average weight and volume of UZrH in each rod was 0.955 pound and 4.30 cubic inches. The total aerodynamic heat input to each rod at 363.32 seconds was 770 BTU. Therefore, a total of 806 BTU/lb (aerodynamic heating) was required to complete the ablation at the observed altitude. The predicted time and altitude of complete ablation, based on theoretical calculations and experimental data, and assuming aerodynamic plus oxidation heating, was approximately 364.3 seconds (158,000 feet) (see p. 133). The calculated average BTU/lb (aerodynamic heating) required for ablation was 843.

2. The barium-loaded group of RFD-1 experimental fuel rods was completely ablated away at 371.50 seconds (142,000 feet). The average weight and volume of UZrH in each rod was 1.543 pounds and 7.10 cubic inches. The total aerodynamic heat input to each rod at 371.50 seconds was 980 BTU. Therefore, a total of 635 BTU/lb (aerodynamic heating) was required to complete the ablation at the observed altitude. The predicted time and altitude of complete ablation, based on theoretical calculations and experimental data, and assuming aerodynamic plus oxidation heating, was approximately 374.6 seconds (135,000 feet) (see p. 133). The calculated average BTU/lb (aerodynamic heating) required for ablation was 787.

3. The silver-loaded rods did not ablate enough to expose the silver tracer. The UZrH glow was not visible after 368.00 seconds (149,100 feet). Calculations indicate that the silver-loaded rods would have reached a maximum surface temperature of 3500°F at 397.0 seconds (96,000 feet). This corresponds to 1375 BTU, or 595 BTU/lb aerodynamic heat input. This is not enough total heat to complete ablation.

4. The gold-loaded rods did not ablate enough to expose the gold tracer. The UZrH glow was not visible after 368.00 seconds (149,600 feet). Calculations indicate that the gold-loaded rods would have reached a maximum surface temperature of 3000°F at 408.0 seconds (85,100 feet). This corresponds to 1325 BTU, or 485 BTU/lb aerodynamic heat input. This is not enough total heat to complete ablation.

5. The discrepancy between the observed and calculated ablation is considered to be within the accuracy of the overall experiment. However, the apparently higher observed ablation rate could be due to (a) oxidation heating effects greater than had been predicted, (b) possible exothermic effects of nitrogen, and/or (c) effects of hydrogen combustion.

   The observed disappearance of the silver- and gold-loaded rods before disappearance of the barium-loaded rods is not explainable. However, several possible reasons are offered: (a) runaway exothermic reaction of the barium due to higher BTU/lb heat input, and (b) increased heat input to the barium-loaded rods due to increased velocity caused by breakup and subsequent higher W/C_DA. It is conceivable that the two traces identified as the silver- and gold-loaded rods were not actually made by these rods. The only identification of these objects was made from a comparison of the theoretical trajectories with the measured trajectories from the plate films. The strontium- and barium-loaded rods were identified from the spectral and framing-camera films as well as from the trajectory comparisons, which makes their identification much more positive.

6. The volume of ablated material was as stated. However, the rate of ablation is not constant enough to be defined.

7. The final sizes of the ablated particles from the RFD-1 external fuel rods is not known.

8. Disassembly events of the reactor were observed (see SC-RR-64-515 for times, altitudes, and final conclusions).

SECTION VI -- RECOMMENDATIONS FOR FUTURE FLIGHT TESTS

Considering the factors involved, optical coverage and reduction of the films and records from RFD-1 were highly successful. The experience gained in this operation should not be underestimated. During the design of the experiment and of the optical instrumentation, as well as during data acquisition, computation of theoretical trajectories, and data evaluation, many possible modifications and refinements which would improve the quality of the data obtained in future similar efforts became apparent. The extreme importance of some instruments and operational procedures in acquisition and reduction of the data emerged clearly. In what follows, these features are discussed so that their value can be realized and so that they may be used even more efficiently in future flight tests. Where possible, these recommendations have already been incorporated into the plan for RFD-2.

Radar

The FPS-16 radar was extremely important to the RFD-1 operation and data reduction. The FPS-16 directed the ME-16 and LA-24 cameras to the re-entry, indicated the correct starting time for the cameras, and recorded the re-entry trajectory of the RV. This record was used to confirm the theoretical trajectory for identification of the remaining objects. The theoretical trajectory program has since been modified to compute the position of the RV in terms of spatial coordinates, which will eliminate the need to convert the plate-camera films to terms of azimuth and elevation. The FPS-16 radar is necessary to establish the basic trajectory used in computing these coordinates. It is considered crucial enough to the program to warrant radar redundancy to assure tracking of the RV. Raw (uncorrected) data from the radar track should be furnished for data reduction, since the present TTA program includes built-in correction factors.

The verlort radar is also very necessary. To reduce the films from the aircraft cameras, the position, heading, turn rate, and bank angle of the aircraft, versus time, must be known. Film from the NASA aircraft would have been much more useful if that aircraft had been tracked by radar. Conceivably, however, the verlort radar could be switched between the RV and the aircraft during re-entry, so that spot checks of the positions of the RV and aircraft would be available.

Re-entry Objects

The number of extraneous objects re-entering the atmosphere along with objects from the primary experiments should be kept to a minimum. Items such as brackets, bolts, and bands interfere with the identification of the primary objects and events of the experiment. Of course, most of the items are necessary, but where possible, vertical separation of the re-entering parts should be attempted by means of ejection or retro-rockets. This would lessen the effects of superposition of the plate-camera film streaks.

Ejection Measurements

Monitoring the orientation of the RV when objects are ejected is essential, since the directions of ejection are applied as perturbations to the initial conditions for computing the theoretical trajectories of individual objects. The accuracy, or lag, of the roll-stable gyro system should be determined before the flight test.

Velocities of all ejected objects should be measured during development of the test unit in the laboratory. Framing cameras furnished an accurate history of the ejection velocities and directions of the RFD-1 external fuel rods and brackets during preflight tests. Calculation of the velocities and directions is not accurate enough, because objects do not release instantaneously.

Tracers

Tracer elements should be carefully selected on the basis of special criteria. The most important of these criteria are low excitation energies for intense lines (see pp. 84 to 86).

Identification of Materials

During reduction of the RFD-1 spectral films, many elements were identified as present in very small amounts in the RV, fourth-stage motor, brackets, and fuel rods. This indicates the possibility of identifying many objects, in addition to the tracer materials, by spectral means. The specifications of all materials included in any of the re-entry items should be recorded for use in postflight data reduction. In addition, specimens of the actual materials should be retained for laboratory spectral analysis. Often, impurities or elements not listed in the specification but present in the materials can be identified in the laboratory.

Aircraft

Airborne optical instrumentation has both advantages and disadvantages for re-entry investigations. The disadvantages of vibration, power limitations, lack of availability when needed, window restrictions, and other problems warrant concentrated efforts at solution.

Among the advantages, the positions of the stations are flexible: they can be located anywhere along the trajectory, and, if desired, the trajectory and stations can even be moved to another part of the world. In addition, such stations can be above clouds or ground-level haze. However, by far the biggest advantage of aircraft stations is the lesser atmospheric attenuation of the radiation reaching the detectors, even under clear-sky conditions. An approximate calculation based on the tables for a tropical maritime atmosphere, taken from Edgerton, Germeshausen and Grier, Inc., Report No. B-2621, November 15, 1963, Spectral Transmission of Slant Paths Through the Atmosphere, Vol. II, will exemplify the problem existing for distance objects, particularly at the shorter wavelengths. These calculations neglect the familiar R^2 falloff of intensity, which adds to the problem when a distant, point-source object is involved. At 4000 Å and a slant range of 50 nautical miles from a sea-level detector to a source object at 50,000 feet, about 0.35 percent of the radiation is transmitted. At 4000 Å and a slant range of 50 nautical miles from a detector at 10,000 feet to a source object at 50,000 feet, about 9.3 percent of the radiation is transmitted. At 6000 Å and a slant range of 50 nautical miles from a detector at sea level to a source object at 50,000 feet, about 3.0 percent of the radiation is transmitted. At 6000 Å and a slant range of 50 nautical miles from a detector at 10,000 feet to a source object at 50,000 feet, about 43.5 percent of the radiation is transmitted.

If the atmospheric conditions were poorer than "very clear," the results would be even more exaggerated. Assumptions and calculations based on aerosol and Rayleigh scattering are discussed in the cited report. The examples were not worked out for slant ranges greater than 50 nautical miles, because it was believed that the additional range and higher altitude involved in RFD-1-type re-entry experiments would reduce the atmospheric transmission by about the same amount for a ground station as for a station at 10,000 feet altitude.

The value of different optical stations was apparent during the RFD-1 data reduction. Trajectories that lay in the line of sight from one station were seen as different trajectories from other stations. Downrange stations, such as the NASA aircraft, were able to cover the entire portion of the flight path of prime optical interest. Two or more airborne stations would be preferrable, if most of the optical instruments have fixed axes, because if one aircraft should be off course for any reason, all coverage by that station would be lost. Two or more aircraft are desirable, even if they do not cover the same region in space, because they can then be positioned closer to the flight path. The light intensity reaching the cameras would then be increased by both the distance-squared effect and the atmospheric-attenuation effect. The advantages of different view angles, atmospheric-attenuation factors, and general redundancy in data acquisition favor having two or more airborne optical stations. Aircraft mobility, of advantage in data acquisition, becomes a distinct disadvantage in the reduction of the plate-camera films. To accurately identify the spatial position of the re-entry objects, the exact position and orientation of the observer (cameras) must be known. Consequently, tracking of the aircraft by the verlort radar during the time of picture taking is essential in order to locate the latitude and longitude of the aircraft. In addition to the location of the aircraft, its heading, turn rate, bank angle and velocity, versus time, must be known. A flight recorder is excellent for the purpose.

Orientation (azimuth and elevation) of the cameras with reference to the aircraft also enters into the reduction of the data. This can be measured either before or after the flight, since orientation is not variable with time. However, one method proposed for accurate measurement is to align the aircraft on the ground in a known direction and then photograph a distant object of known azimuth and elevation (such as a mountain range or building) with all the cameras. Reduction of these films would furnish a complete picture of the relative orientation of all the cameras for later reference. Aircraft cameras must be mounted to minimize all effects of aircraft vibration. Vibration causes the plate-camera film details to be blurred and superimposed; several of the RFD-1 films were unusable because of this.

Photometer and Filters

The quality of the filters used in the photometers on RFD-1 must be upgraded for future experiments. The effective band passes of the filters used on RFD-1 were too wide to yield conclusive information. Narrow band-pass filters with high transmission are a necessity for experiments similar to RFD-1 if the shorter wavelengths are of interest. The filters should be checked in the laboratory to determine the precise peak of their transmission maxima at the temperature at which they will be used, since the transmission peak shifts with temperature. The band pass of the filters should also be checked.

Atmospheric attenuation is such that the photometer is probably the only ground-based instrument with sensitivity enough to be able to detect radiation in the blue and ultraviolet region of the spectrum. When the ultraviolet is of interest, ultraviolet-transmitting optics must be used. The advantages of aircraft for the short wavelengths have been discussed, and must again be emphasized. Many elements have their most intense spectral lines in the ultraviolet, and use of this spectral region would increase the available information on spectral events during re-entry. To adequately investigate the ultraviolet would require obtaining, or designing and building, special instruments in addition to the photometers.

Film

Color film was used for most motion-picture coverage of the RFD-1 re-entry. The color rendition seemed to be quite good, and it aided in flare identification. However, with time as the only reference, it was often difficult to determine just what was being tracked with any of the tracked instruments. The color-film exposures indicated that the emulsion was quite fast. In the past, people have often used black-and-white film to maximize exposure, but the color film used seemed to have good sensitivity. The underexposures which occurred are attributable to shutter speed and aperture problems. Color film for some of the open-plate trajectory cameras would provide another means of identifying objects which emit characteristic colors. The black-and-white trajectory plates on RFD-1 were good, so the use of color plates in some cameras should be considered as an addition to, rather than a substitution for, black-and-white emulsions. Some of the emulsions used for RFD-1 proved to have limitations, particularly for the spectral cameras. The Royal-X Pan (RXP) film used by NASA and AFSWC lacks the requisite sensitivity in the red region of the spectrum beyond about 6350 Å. This meant that none of the cameras using RXP detected the lithium line at 6707 Å or any other radiation in the red region. RXP seemed very satisfactory as far as speed and graininess were concerned. In general, the 103-F or Aero-Recon Tri-X used by Sandia on RFD-1 would be preferable when the red region is of interest. The range of some of the limited-range films has supposedly been extended. If use of these new emulsions is contemplated, they should be laboratory-tested first for sensitivity and wavelength range. Faster, finer-grained emulsions with greater wavelengths would be desirable if they can be obtained.

After events on the framing cameras had been viewed and evaluated, it was often difficult and time-consuming to find, later, the particular frames of interest. The printing of sequencing numbers on the edge of these films would be a very valuable aid in reducing the data from them.

Focus

The focus on several instruments was not quite as good as it should have been. If possible, all cameras should have complete focusing runs under operating conditions as close to the actual ones as possible. Camera bodies, lenses, and backs should be considered one unit after alignment. Gratings should all be checked for quality before they are used. Reports from other investigators indicate that gratings are sometimes not up to specifications and could create poor images.

Frame Rates - Focal Length and Exposure

Shutter speeds were too high on most of the framing cameras to give adequate exposures for RFD-1. NASA cameras operated at lower frame rates than did Sandia cameras, and their exposures were better. On the other hand, in case intensities should be higher than expected, not all cameras should be operated at very low frame rates. More exposure can also be obtained by using optics of larger aperture. Higher frame rates allow more frames of an event to be recorded if the event has a duration of a goodly portion of a second; higher rates thus reduce the difficulty of distinguishing between film imperfections and actual exposure. Also, in the case of short-duration events, the length of camera "dead time" between any two frames is reduced. The preferred method would seem to be to run most cameras at slow framing rates, but to run those with large-aperture optics which are tracking objects expected to be bright at frame rates up to 100 frames/sec. The cinespectrograph data were radically underexposed, so this instrument should have larger-aperture optics and a slower frame rate. If it were not for the better time resolution of the cinespectrograph, it would be better to replace it with a streak spectrograph. Two-thirds of the cinespectrograph's operating time is "dead time." The best solution is to use both instruments and obtain the advantages of both.

Reduction of data from the trajectory camera was difficult because of the absence of separation between the traces recorded by different re-entry objects. The separation of two traces on the photographic plate is proportional to the focal length of the recording camera, so it is advisable to have lenses with focal lengths as long as possible while still remaining compatible with the other restrictions imposed by longer focal lengths. Objects at a distance of from 100 to 200 miles can be regarded as point sources. Since recording rate along the plate is doubled when the focal length is doubled, maintaining the same exposure requires doubling the aperture. However, large lenses of good quality are expensive.

Low-Rate Framing Cameras

Plate-trajectory cameras with short-duration timing chop are essential for accurate data reduction. However, such cameras do have limitations, for they show the various re-entry streaks superimposed on one another. Not only are the timing marks somewhat obliterated as a result, but also the individual objects are difficult to distinguish. A low-rate framing camera (such as a modified K-37) would be free of some of these problems. By exposing each frame for only a short time (1 to 4 seconds), the problem of overlap, except from immediately adjacent objects, would be lessened. Since the framing pulses could be recorded, a measure of time could be obtained for correlation with other films. If two alternating cameras were employed, "dead time" between frames would be eliminated. This system would work equally well for spectral cameras.

Camera Orientation

Camera orientation should be carefully considered for nontracked instruments both on the ground and in aircraft. The spectral and open-plate-trajectory camera should have overlapping fields. When gratings are in front of the lenses and light intensity is expected to be a problem, vignetting by the grating should be minimized. If light intensities are expected to vary over a larger range, a grating with reduced dispersion should be considered, since it would allow both first-order and second-order spectra to record. Such a grating would enable two intensity levels to be recorded and hence would increase the probability of proper exposure, but it would have as a disadvantage the fact that the lens behind the grating would be operating farther off axis. If lens aberrations were a problem, these distortions could become serious.

Tracking Cameras

Power scopes should be included on all hand-tracked cameras as well as on the ME-16 and LA-24 tracking telescopes, since visual acquisition of items as small as the external fuel rods is difficult. The 12 external rods in the RFD-1 re-entry were individually visible through the 5.6- and 32-power scopes.

A tape recorder for the optical trackers on ME-16 and LA-24 tracking telescopes to permit verbal recording of the re-entry picture by the operators during the re-entry would be advisable. Recalling the entire re-entry sequence after the conclusion of the test is difficult, and accounts frequently conflict.

Data Reduction

The reduction of data from a large number of optical instruments creates a heavy work load. An effort should be made to computer-program as much of the data reduction as possible. In any case, computer reduction of data is usually more thorough and accurate than manual reduction. The theoretical trajectory program is one example already in operation. Other aspects of the data reduction which are adaptable to computerization are the photometer records and the plate, trajectory, and spectral films (by densitometry). Some records, such as the framing-camera films, are not adaptable to computer programs. However, their reduction can be made more accurate and efficient through the use of analyzing projectors, film editors, and edge-numbered films.

A record of the ME-16 and LA-24 tracking mount azimuth and elevations versus time would be of benefit in the data reduction. Motion-picture films furnish no indication of the position in space of the objects being tracked. Correlation of their azimuths, elevations, and time with those of the other films would provide a more complete picture of the re-entry sequence for preliminary and final reduction. This would also aid in relating the various films to one another. If azimuths and elevations versus time had been known for the LA-24 during RFD-1, a positive identification of what it had tracked would be available.

Inclusion of a barometer and thermometer at the High Point site is suggested. These would provide a measure of pressure and temperature during the re-entry, permitting atmospheric-refraction corrections to be made in preliminary reduction of the data until the reduced meteorological data are received. High-altitude radiosonde weather balloon soundings would provide adequate atmospheric data during the re-entry. Atmospheric conditions above 100,000 feet are reasonably stable. The standard 1959 atmosphere was very similar to the measured RFD-1 atmosphere.

The members of the data-reduction group who will be charged with reducing the flight-test data should be consulted about the design of the experiment during development of the instrumentation and flight-test details. Preparations for data reduction should be initiated before the test and included in the design.

Handling and use of the original films from the test should be kept to a minimum. Whenever possible, analysis and reduction should be done with prints of the original. No cutting or modification to the films should be allowed, since some reduction techniques utilize the frame dimensions as pseudo-fiducials. In the event of damage or breakage of the framing-camera film, repairs should be made so that the original length is maintained. Interpolation between timing marks is often necessary. Recording of the timing, camera functions, and photometer pulses would be better done on magnetic tape than on oscillograph paper, since playback of a tape can be condensed or expanded to the optimum scale for any given data of interest, and since tapes can be digitized for computer reduction of the data.

Timing

The lack of timing on some RFD-1 data proved to be a serious limitation. Redundant timing systems would be desirable. In addition, more accurate time resolution would make it easier to correlate events recorded on various instruments.

Chopped-trajectory plate-camera films should employ a chopping code which allows a long exposure time relative to closed-shutter time. The RFD-1 chopping code included 7 seconds exposure time versus 2 seconds closed-shutter time. This ratio was adequate, but the long exposure time made interpolation of event times inaccurate, and the long closed-shutter time made completion of the chopped-out portion extremely difficult.

The RFD-1 unchopped plate-camera films furnished no indication of camera orientation, because the position of the star trail background versus time was not known. Consequently, corrections for atmospheric refraction and lens distortion were difficult to make, and accurate correlation with other data was not possible. It has been suggested that in future similar tests, these cameras be uncapped for a short time before and/or after the re-entry. The exact times of these operations should be recorded on the tape or oscillograph in terms of WWV or BRT. This would allow the star trail background to be used in reduction of the films.

Micro-Densitometer

The theoretical trajectory program has been modified to furnish positions of the re-entry objects in terms of film coordinates. Employment of a micro-densitometer to read the plate films in terms of a two-dimensional coordinate system would expedite and improve the quality of the data reduction. The resolution of the densitometer is much finer in distinguishing superimposed objects than that of the Mann Comparator, and it also provides a measure of the intensity of the streaks. This instrument could be digitized to furnish the data in a tabulated form for direct comparison with the theoretical trajectory. Experiments using the micro-densitometer on RFD-1 plate films have indicated its usefulness; it may also have possibilities for the analysis of spectral plates. This will be investigated further before the RFD-2 flight test.

Weather Versus Launch

The decision to launch RFD-1 was delayed several weeks because of clouds and haze in the re-entry area. To determine the amount of haze and clouds in the area of the re-entry trajectory just before launch is extremely difficult. It has been suggested that an optical instrument be developed to scan the re-entry envelope to determine the probable attenuation of the re-entry light due to the atmospheric conditions. The equitorial telescope located at High Point, Bermuda, could be employed for this purpose. With the telescope, the brightness of known stars in the re-entry envelope could be measured periodically. The decision to launch could then be based on a comparison of star brightness with a predetermined brightness required for adequate optical coverage of the re-entry.

DISTRIBUTION:
TID-4500 (35th Ed.), UC-36 (481)
J. A. Lieberman, Asst. Director for Nuclear Safety, Div. of Reactor Development, USAEC, Washington D. C.
F. K. Pittman, Director, Div. of Reactor Development, USAEC, Washington 25, D.C.
H. G. Hembree, Safety Eng. & Test Branch, Div. of Reactor Development, USAEC, Washington 25, D.C.
Lt. Col. W. K. Kern, Aerospace Safety Section, Eng. & Test Branch, Div. of Reactor Development, USAEC, Washington 25, D.C. (6)
R. L. Kirk, SNAP Program Director, Div. of Reactor Development, USAEC, Washington 25, D.C.
Robert Lowenstein, Director, Div. of Licensing & Regulation, USAEC, Washington 25, D.C.
Brig. Gen. D. L. Crowson, USAEC/DMA, Washington 25, D.C.
L. Otoski, Area Manager, AEC Albuquerque Opr. Office, P. O. Box 5400, Albuquerque, N. Mex. (2)
S. A. Upson, Director, Reactor Opr. Div., AEC Albuquerque Opr. Office, P. O. Box 5400, Albuquerque, N. Mex. (3)
J. V. Levy, Area Mgr., USAEC, Canoga Park Area Office, P. O. Box 591, Canoga Park, California (2)
I. A. Peltier, Idaho Operations Office, Idaho Falls, Idaho
C. A. Keller, USAEC, Oak Ridge Opr. Office, P. O. Box E, Oak Ridge, Tenn.
T. R. Wilson, Phillips Petroleum Company, Idaho Falls, Idaho
Col. I. J. Russell, Air Force Weapons Lab (WLRB), Kirtland Air Force Base, N. Mex.
Col. R. A. Gilbert, Air Force Weapons Lab (WLG), Kirtland Air Force Base, N. Mex.
Lt. Col. J. W. Talley, Air Force Weapons Lab (WLDN), Kirtland Air Force Base, N. Mex.
Col. D. C. Jameson, Nuclear Safety (AFINS-R), Adm. & Security, Kirtland Air Force Base, N. Mex.
R. L. Detterman, AI, P. O. Box 309, Canoga Park, California (4)
NASA Langley Research Center, Langley Station, Hampton, Va., Attn: E. D. Schult (5)
T. B. Kerr, RNS, NASA Headquarters, Washington 25, D.C.
R. D. Ginter, NASA Headquarters, Washington 25, D.C.
W. A. Guild, NASA Headquarters, Washington 25, D.C.
J. Whitfield, Asst. Br. Mgr., Hypervelocity Br., VonKarman Gas Dynamics Facility, Arnold Engr. Div. Center, Arnold AFB, Tenn.
S. P. Schwartz, 1
R. W. Henderson, 100
E. H. Draper, 1000
C. F. Bild, 1100, Attn: E. R. Frye, 1112
R. R. Sowell, 1110
J. C. Russell, 1114
M. M. Robertson, 1114-2 (6)
W. M. O'Neill, 1120
L. D. Hopkins, 1300, Attn: J. P. Cody, 1320
G. I. Hildebrandt, 1330
J. H. Findlay, 1400, Attn: J. P. Shoup, 1430
G. W. Rodgers, 1420
J. M. Wiesen, 1440
W. A. Gardner, 1500, Attn: D. M. Olson, 1530
S. A. Moore, 1540
R. T. Othmer, 1541-2, Attn: P. L. Class, 1541-2
L. D. Smith, 1600
R. A. Bice, 2000
L. J. Heilman, 2100
H. E. Lenander, 2500
R. B. Powell, 3000
K. A. Smith, 3100
D. S. Tarbox, 3200
S. P. Bliss, 3300
M. K. Linn, 3400
C. W. Campbell, 4000
R. J. Hansen, 4200
K. S. Spoon, 4300
T. T. Robertson, 4400, Attn: F. F. Eichert, 4410
R. E. Hopper, 4500
R. C. Fletcher, 5000
R. S. Claassen, 5100

DISTRIBUTION (cont):
Director, 5300
T. B. Cook, 5400, Attn: B. F. Murphey, 5410
J. D. Shreve, 5414
F. C. Cheston, 6000
G. A. Fowler, 7000
L. E. Hollingsworth, 7200, Attn: H. E. Viney, 7210
W. T. Moffat, 7220
D. Beatson, 7223-5
R. D. Statler, 7224
D. Parsons, 7224-1
G. E. Hansche, 7240
H. S. North, 7241
L. H. Ivy, 7241-3
J. C. Eckhart, 7250
L. E. Lamkin, 7300
R. H. Schultz, 7320
J. W. Pearce, 7330
D. B. Shuster, 7400
V. E. Blake, 7410
H. E. Hansen, 7411 (6)
B. W. Marshall, 7411 (2)
I. B. White, 7411 (6)
A. J. Clark, Jr., 7412 (6)
H. J. Gay, 7412-2
H. K. Togami, 7412-2
R. D. Klett, 7412-3
H. R. Spahr, 7412-3
A. E. Bentz, 7413 (6)
C. E. Erickson, 7413-1
A. Y. Pope, 7420 (3)
M. L. Kramm, 7430
W. C. Scrivner, 7600
J. L. Tischhauser, 7620
A. R. Iacoletti, 7622
J. A. Allensworth, 7622
B. S. Biggs, 8000
L. Gutierrez, 8100
D. R. Cotter, 9100
E. A. Paxton, 8232-1
B. R. Allen, 3421
M. G. Randle, 3428-1, Bldg. 836
M. G. Randle, 3428-1, Bldg. 880
J. L. Fife, 3412 (2)
R. C. Smelich, 3427-3 (50)
L. D. Patterson, 3411-1 (2)